

THE ROLE OF ALTERED CILIARY MUSCLE MORPHOLOGY IN REFRACTIVE ERROR
AND ACCOMMODATIVE FUNCTION

RICHA NAOMI SAIGAL

Doctor of Philosophy

ASTON UNIVERSITY

June 2016

© Richa Naomi Saigal, 2016

Richa Naomi Saigal asserts her moral right to be identified as the author of this thesis

This copy of the thesis has been supplied on condition that anyone who consults it is understood to recognise that its copyright rests with its author and that no quotation from the thesis and no information derived from it may be published without proper acknowledgement.

ASTON UNIVERSITY

**THE ROLE OF ALTERED CILIARY MUSCLE MORPHOLOGY IN REFRACTIVE ERROR
AND ACCOMMODATIVE FUNCTION**

RICHA NAOMI SAIGAL

Doctor of Philosophy

June 2016

Summary

The primary theme of this thesis was to investigate *in vivo* ciliary muscle morphology in refractive error, and how ciliary muscle parameters are linked with accommodative function in a young adult population. Anterior segment optical coherence tomography was utilised for all ciliary muscle image acquisition to examine morphological differences between eyes.

High levels of inter-ocular ciliary muscle symmetry were shown in emmetropes and myopes. Whilst the myopic ciliary muscle was longer and thicker than in emmetropes for both eyes, ciliary muscle length and thickness were linked with axial length in both cohorts. In amblyopes and anisometropes, high levels of inter-eye ciliary muscle symmetry were observed. The ciliary muscle in amblyopic eyes appear to grow in accordance with the axial length of the non-amblyopic eye ($P = 0.022$, $r^2 = 0.438$).

The possibility of diurnal variation in accommodative axial elongation and accommodative error was explored in emmetropes and myopes. Daily stability in these accommodative functions were shown, and between groups there was no difference in accommodative axial elongation ($P = 0.884$) or accommodative error ($P = 0.098$). It was demonstrated that ciliary muscle morphology is not linked with accommodative function, disputing the theory that the thickened ciliary muscle has reduced contractility, which initiates hyperopic defocus in myopigenesis.

In emmetropes, males had significantly longer ciliary muscle lengths ($P = 0.031$) and axial length ($P = 0.001$) compared with females. Novel parameters to analyse the ciliary muscle were investigated; both inner apical angle and ciliary muscle cross-sectional area measures were linked to axial length, as were the area and apical angle. Both measures are highly effective ciliary muscle analysis parameters which demonstrated high repeatability.

The studies detailed demonstrated normal ciliary muscle growth with ocular development in myopia, and indicated that the ciliary muscle is not a crucial causative myopigenesis factor.

Keywords: ciliary muscle, accommodation, refractive error, myopia

ACKNOWLEDGEMENTS

I would firstly like to express my gratitude to my supervisors Dr Amy Sheppard and Dr Leon Davies for their continual support, vast expertise and guidance over the last three years. Additionally, I am grateful to Dr Benjamin Colderick for creating the bespoke semi- objective ciliary muscle analysis software.

I wish to also thank the College of Optometrists for the award of a 3-year Postgraduate Research Scholarship to fund of this body of research and support my postgraduate studies.

Many thanks to all my study participants for their involvement, and my appreciation is extended to my postgraduate friends and staff at Aston University, who have provided me with advice and encouragement throughout my PhD.

Finally, I wish to warmly thank my family and friends, particularly my parents, brothers and Pry for their belief, encouragement and support.

CONTENTS

	Page
SUMMARY	2
ACKNOWLEDGEMENTS	3
CONTENTS	4
LIST OF TABLES	9
LIST OF FIGURES	10
CHAPTER 1 Ciliary muscle morphology in refractive error and accommodation	
1.1 Introduction	13
1.1.1 Accommodative structures	15
1.1.2 Human ciliary body	15
1.1.3 Crystalline lens	19
1.1.4 Capsule	20
1.1.5 Zonules	21
1.2 Mechanisms of accommodation	23
1.3 Components of accommodation	26
1.3.1 Reflex accommodation	26
1.3.2 Proximal accommodation	27
1.3.3 Tonic accommodation	27
1.3.4 Convergence accommodation	27
1.4 Ciliary muscle <i>in vivo</i> imaging	27
1.4.1 Ultrasound biomicroscopy	28
1.4.2 Magnetic resonance imaging	28
1.4.3 Time-domain and spectral-domain optical coherence tomography	29
1.4.4 Anterior segment optical coherence tomography	31
1.4.5 <i>Visante</i> AS-OCT and ciliary muscle imaging	33
1.5 Ciliary muscle morphology	35
1.5.1 Ciliary muscle morphology and refractive error	39
1.6 Theories of myopia development relating to the ciliary muscle	45
1.6.1 The hyperopic defocus model	45
1.6.2 Hyperopic defocus and accommodative lag	46
1.6.3 Accommodative microfluctuations and refractive error	49
1.6.4 Ciliary muscle and accommodative microfluctuations	51
1.6.5 Accommodative axial length changes	52
1.6.6 Ciliary muscle and accommodative axial length changes	56

1.7 Ciliary muscle morphology in amblyopia and anisometropia	58
1.8 Instrumentation and techniques	60
1.8.1 Grand Seiko WAM-5500 auto ref/keratometer	60
1.8.2 Distance refractive error measurement technique	62
1.8.3 Stimulus- response accommodative error measurement technique	62
1.8.4 Analysis of stimulus- response accommodation data	63
1.8.5 Measure of accommodative axial length changes	65
1.8.6 Badal modification of the <i>Lenstar LS 900</i>	66
1.8.7 IOLMaster	69
1.8.8 Ciliary muscle image acquisition	70
1.8.9 Ciliary muscle image analysis	72
1.8.10 Validation of bespoke ciliary muscle analysis software	73
1.9 Summary	76
1.10 Aims of this thesis	77
CHAPTER 2 Diurnal stability of accommodative accuracy and axial length change with accommodation	
2.1 Introduction	79
2.2 Methods	82
2.2.1 Subjects	82
2.2.2 Measurements	83
2.2.3 Analysis	84
2.3 Results	85
2.4 Discussion	88
2.5 Conclusion	90
CHAPTER 3 Ciliary muscle morphology and ocular biometric correlates in emmetropia	
3.1 Introduction	91
3.2 Methods	92
3.2.1 Subjects	92
3.2.2 Measurements	92
3.2.3 Ciliary muscle acquisition and analysis	93
3.3 Statistical analysis	93
3.4 Results	94
3.4.1 Ciliary muscle length parameters and ocular biometric correlates	96

3.4.2 Gender differences in ciliary muscle length and ocular biometric correlates	96
3.4.3 Ciliary muscle thickness parameters and ocular biometry	98
3.4.4 Gender differences in ciliary muscle thickness	98
3.5 Discussion	99
3.6 Conclusion	102

CHAPTER 4 Inter- eye ciliary muscle symmetry and morphological variation with refractive error

4.1 Introduction	103
4.2 Methods	106
4.2.1 Subjects	106
4.2.2 Measurements	107
4.2.3 Ciliary muscle image acquisition and analysis	107
4.2.4 Statistical analysis	108
4.3 Results	108
4.3.1 Ciliary muscle length and symmetry	110
4.3.2 Ciliary muscle thickness and symmetry	112
4.4 Discussion	114
4.5 Conclusion	116

CHAPTER 5 Ciliary muscle morphology and associated accommodative function

5.1 Introduction	117
5.2 Methods	121
5.2.1 Subjects	121
5.2.2 Measurements	122
5.2.3 Ciliary muscle acquisition and analysis	123
5.2.4 Statistical analysis	124
5.3 Results	124
5.3.1 Accommodative error index	125
5.3.2 Transient accommodative axial length change	128
5.4 Discussion	129
5.5 Conclusion	133

CHAPTER 6 Ciliary muscle morphology in amblyopia and anisometropia

6.1 Introduction	134
6.2 Methods	137

6.2.1 Subjects	137
6.2.2 Measurements	137
6.2.3 Ciliary muscle image acquisition and analysis	137
6.2.4 Statistical analysis	138
6.3 Results	
6.3.1 Amblyopes	138
6.3.2 Anisometropes	141
6.4 Discussion	142
6.5 Conclusion	144
CHAPTER 7 Additional parameters for analysis of ciliary muscle morphology	
7.1 Introduction	145
7.2 Methods	148
7.2.1 Subjects	148
7.2.2 Measurements	148
7.2.3 Repeatability	152
7.2.4 Statistical analysis	152
7.3 Results	152
7.3.1 Repeatability	152
7.3.2 Ciliary muscle parameters	154
7.3.3 Ciliary muscle area	154
7.3.4 Ciliary muscle inner apical angle	155
7.4 Discussion	156
7.5 Conclusion	158
CHAPTER 8 Conclusions and potential future research	
8.1 General conclusions	159
8.2. Evaluation of experimental work: suggestions for improvement and plans for future research	161
8.3 Concluding statement	163
REFERENCES	164
Appendices	192
A1 Ethical Approval	192
A2 Participant information and consent for project 548 (main study)	195

A3 Participant information and consent for project 548 (diurnal study)	201
A4 Participant information and consent for project 548 (amblyopia study)	207

LIST OF TABLES

Table	Page(s)
1.1 Layers of the ciliary body with respective functions	17
2.1 Key findings from accommodative axial length change studies in emmetropes and myopes	81-82
2.2 Summary characteristics of emmetropic and myopic participants, including the grouped means of biometric data across the 4 measurement session	86
2.3 Mean AXL change with accommodation (corrected values) and AEI values at each measurement session for emmetropic and myopic refractive groups and for the whole cohort	86
3.1 Summary characteristics of the RE of emmetropic participants	94
3.2 Mean ciliary muscle parameters across the emmetropic cohort	95
4.1 Key findings from <i>in vivo</i> studies of human ciliary muscle morphology and refractive error	105
4.2 Summary characteristics of emmetropic and myopic participants	108
4.3 Mean ciliary muscle parameters in emmetropic and myopic participants	109
5.1 Mean pupil size and associated accommodative demand levels	125
5.2 AEI values for emmetropes, myopes and the whole cohort	125
5.3 Summary biometric characteristics and AXL changes with accommodation in emmetropic and myopic participants	129
6.1 Characteristics of amblyopic participants	139
6.2 Nasal ciliary muscle morphological characteristics of amblyopic participants	139
6.3 Characteristics of anisometric participants	141
6.4 Nasal ciliary muscle characteristics across both eyes of anisometropes	141
7.1 Repeatability of ImageJ analysis technique on cross sectional area and inner apical angle, from a single ciliary muscle image analysed ten times	153
7.2 The effect of varying PVL locations on the cross- sectional area of the ciliary muscle	153
7.3 Mean results for ciliary muscle cross- sectional area and inner apical angle measures for 2 different examiners, through ImageJ ciliary muscle image analysis of 10 participants	154
7.4 Summary characteristics of emmetropic and myopic participants	154

LIST OF FIGURES

Figure	Page
1.1 Conventional classification of muscle fibres within the ciliary muscle, based on fibre orientation	18
1.2 Illustration showing the definition of anterior and overall length of the ciliary muscle	19
1.3 AS-OCT image of the crystalline lens of a 26 year old participant	21
1.4 Schematic diagram of the human accommodative apparatus showing the arrangement of both anterior and posterior (vitreous) zonules	23
1.5 Illustration of Hemholtzian mechanism of accommodation	24
1.6 <i>Visante</i> stand-alone AS-OCT	32
1.7 AS-OCT image of the anterior segment with distortion corrected for by the <i>Vistane</i> , utilising the <i>anterior segment single</i> mode	35
1.8 Images demonstrating the noticeable difference in temporal ciliary muscle morphology between an axial myopic eye and an emmetropic eye	36
1.9 Calliper measurements of ciliary muscle width	37
1.10 Representation of fixed width ciliary muscle thickness measurements	38
1.11 Comparison of temporal ciliary muscle of an emmetropic eye with the temporal ciliary muscle of a myopic eye	41
1.12 The relationship between mean sphere equivalent refractive error and axial length	43
1.13 Illustration of theory of myopia development due to interruption to lens thinning	44
1.14 Hyperopic defocus model	46
1.15 Accommodative response sample showing microfluctuations from a PowerRefractor measurement using -4.00 D stimulus demand	49
1.16 Magnitude of mean transient axial elongation in emmetropes and myopes at 2 D, 4 D and 6 D	54
1.17 The Grand Seiko <i>WAM-5500</i> Auto Ref/Keratometer (Grand Seiko Co. Ltd., Hiroshima, Japan)	61
1.18 Photograph of Grand Seiko <i>WAM 5500</i> with Badal lens system	63
1.19 A mean accommodative stimulus- response curve for 100 pre-presbyopic subjects	64

1.20A Schematic diagram of experimental setup for accommodative axial length changes using the <i>Lenstar LS 900</i>	67
1.20B Photograph of the <i>Lenstar LS 900</i> and bespoke attachment	68
1.21 Photograph of the <i>IOLMaster 500</i>	70
1.22 Photograph of AS-OCT with external fixation target	71
1.23 AS-OCT image of a temporal ciliary muscle with associated parameters	72
1.24 Schematic diagram of two rigid gas-permeable lenses designed to simulate the sclera and ciliary muscle, and associated diameters of lenses	74
1.25 Arrangement of ciliary muscle lens in direct contact with, and centred on sclera lens	75
1.26 Setup of simulated ciliary muscle image acquisition	76
2.1 AXL change with accommodation throughout the day in emmetropes and myopes	87
2.2 Accommodative error throughout the day in emmetropes and myopes	88
3.1 Relationship between AXL and temporal CML in male emmetropes and female emmetropes	97
3.2 Relationship between AXL and nasal CML in male emmetropes and female emmetropes	97
3.3 Sample images comparing male emmetropic ciliary muscle to female emmetropic ciliary muscle and associated depiction of ciliary muscle width analysis techniques	101
4.1a Relationship of RE nasal and temporal CML with AXL in emmetropes	110
4.1b Relationship of RE nasal and temporal CML and AXL in myopes	111
4.2a Relationship of RE nasal and temporal CM3 with AXL in myopes	113
4.2b Relationship of LE nasal and temporal CM3 with AXL in myopes	113
5.1 Image of display screen of Grand Seiko <i>WAM 5500</i> , showing the pupil diameter measurement	123
5.2 A mean accommodative stimulus- response curve for emmetropic and myopic subjects	126
5.3 Relationship between temporal CM50 and AEI	127
5.4 Relationship between temporal CM2 and AEI	127
5.5 Relationship between nasal CM1 and AEI	128

6.1 Relationship between axial length and nasal ciliary muscle length in the non-amblyopic eye of the amblyopic cohort	140
6.2 Relationship between axial length and nasal ciliary muscle length in the amblyopic eye	140
7.1 Photograph of user controlled in-built callipers of the <i>Visante</i> AS-OCT, superimposed on the acquired ciliary muscle image to provide morphological ciliary muscle data for the designated parameters	146
7.2 ImageJ analysis of the ciliary muscle area, extending from the scleral spur to the posterior visible limit, showing an accepted area outline image for analysis	150
7.3 Apical angle of the temporal ciliary muscle in the right eye, outlined by the angle tool of ImageJ	151
7.4 The straight line tool extending from the scleral spur to the posterior visible limit	151
7.5 Relationship between ciliary muscle area and axial length	155
7.6 Relationship between axial length and ciliary muscle inner apical angle	156

Chapter 1

Ciliary muscle morphology in refractive error and accommodation

1.1 Introduction

Myopia, a major health concern is one of the foremost reasons for visual impairment worldwide. The refractive condition can significantly hinder quality of life, ranging from being a simple visual inconvenience with financial cost to sufferers, to a predisposition to sight threatening pathological conditions such as glaucoma, cataract, retinal detachment and chorioretinal degeneration (Lin *et al.*, 2016 Woodman *et al.*, 2011; Ghosh *et al.*, 2014).

An increased lag of accommodation has been documented in myopic eyes, but there is dispute as to whether this occurs before or after myopia onset (Gwiazda *et al.*, 2005; Mutti *et al.*, 2006). The ciliary body supplies the musculature for controlling accommodation and significantly, recent findings have discovered a link between refractive error and ciliary muscle morphology (Bailey *et al.*, 2008; Sheppard and Davies, 2010b; Buckhurst *et al.*, 2013; Pucker *et al.*, 2013). The findings are based on non-invasive imaging of the ciliary muscle through the sclera, by utilising anterior segment optical coherence tomography (AS-OCT). Several studies have reported thicker ciliary muscles in myopic eyes; it has been hypothesised that an altered physiological response in myopes may be responsible for a thickened, hypertrophic ciliary muscle which could display a reduced contractile response, resulting in the reported accommodative lag (Bailey *et al.*, 2008). Relating the altered ciliary muscle morphology to the aetiology of myopia is unclear, though it has been suggested that the thickened ciliary muscle may mechanically restrict equatorial expansion required for maintenance of emmetropia. Whilst ciliary muscle morphology in terms of both length and thickness appears to be altered in myopic eyes, there still remains ambiguity between findings of previous studies, and the relevance of these observations is not fully understood.

Previous *in vivo* studies on human ciliary muscle have typically investigated only one eye, and/ or just one aspect (e.g. just the temporal side; Bailey *et al.*, 2008). As such, laterality and symmetry of the ciliary muscle which could be relevant to refractive error development, is not well understood. The authors of a relatively recent investigation have discovered asymmetry in the laterality of globe profile in myopia development and the results indicate that binocular growth may be synchronised by processes operating past the optic chiasm (Gilmartin *et al.*, 2013). It is not known whether ciliary muscle morphology displays similar properties between the refractive error groups or if such asymmetry in myopia development may translate to the ciliary muscle, and this matter is investigated for the first time.

Accommodation is known to produce a temporary elongation of the eye and results indicate that myopic eyes may demonstrate the largest expandability during, and immediately following an accommodative task (Mallen *et al.*, 2006; Woodman *et al.*, 2010; Woodman *et al.*, 2012). Findings again denote that there may be discrepancies between myopes and emmetropes in the morphology of the ciliary body, causing ciliary muscle forces to be transmitted differentially to the choroid and sclera amid these different refractive groups and thereby resulting in differences in the magnitude of transient elongation (Mallen *et al.*, 2006; Ghosh *et al.*, 2014). Such information will help benefit our understanding of whether altered ciliary muscle morphology impacts on this other element of accommodation.

Whilst information relating to ocular biometric data in amblyopia has been investigated, there have been no reports of ciliary muscle morphology in amblyopia. Since amblyopic eyes have a reduced visual output and accommodation (Ciuffreda and Rumpf, 1985; Maheshwari *et al.*, 2011), it would intuitively be thought that ciliary muscle morphology should be altered in the amblyopic eye and asymmetry of the ciliary muscle across both eyes may be expected where amblyopia has been present for most of an adult's life. The impact of any altered ciliary muscle morphology is not currently known and may be relevant to the aetiology of amblyopia. Paediatric investigations of amblyopia indicate that reduced axial length is present in some amblyopias (Kugelberg *et al.*, 1996; Cass and Tromans, 2008). An investigation that studied the ocular parameters and their relationship in both strabismic and anisometropic amblyopic eyes (Cass and Tromans, 2008) reported that the components of the amblyopic eye differ physically from their fellow non-amblyopic eye across both amblyopic groups. Whilst the anisometropic amblyopic eye seemed to be a proportionally smaller version of the fellow eye largely due to a greater magnitude of hyperopia, the strabismic amblyopic eye was found to have a disproportionately greater degree of anterior chamber reduction and crystalline lens thickness, a reduced vitreous chamber depth and therefore total axial length (Cass and Tromans, 2008); the authors suggested that the strabismic eye may be under-developed, with a delay of emmetropisation in the infantile phase, though it has not been ascertained whether the reported biometric characteristics are a consequence or cause of amblyopia.

The overall objectives of this thesis are to provide new *in vivo* data regarding ciliary muscle morphology and biometric parameters with refractive error, and linking such anatomical parameters with accommodative function, for the first time. The experimental chapters within this thesis explore the morphology of the ciliary muscle and ocular biometric correlates in emmetropia on a large scale and compare such data across refractive error. The possibility of diurnal variation in accommodative function is studied, as well as the methods to measure ciliary muscle parameters *in vivo*. The research involved application of relatively new high-resolution imaging and biometric techniques that permitted visualisation of the ciliary muscle

in vivo and accurately measure ocular parameters, respectively. Full details of the instrumentation used and validation of techniques is given in following chapters. Previous experimental work has provided great insight into ciliary muscle morphology with refractive error but many findings remain ambiguous. The thesis therefore aims to clarify several related questions.

The anatomy and function of the accommodative apparatus and theories of the mechanism of accommodation are discussed in this chapter as well as instrumentation and measurement techniques. Methods of ciliary muscle imaging and a discussion of current morphological ciliary muscle findings are included, as well as current theories of myopia development in relation to the ciliary muscle.

1.1.1 Accommodative structures

An appreciation of the anatomy and functions of the accommodative apparatus is needed to comprehend in detail the conventional and controversial theories relating to human accommodation, and the background to the investigations carried out. The following section considers in detail the anatomy of the ciliary body, crystalline lens, lenticular capsule and zonules.

1.1.2 Human Ciliary Body

The ciliary body is a circumferential structure largely comprised of the ciliary muscle. It embodies the anterior continuance of the choroid and retina and is approximately triangular in cross-section (Tamm and Lütjen-Drecoll, 1996; Remington, 2005). Aside from (fundamentally) supplying the musculature of accommodation, other ciliary body key functions include aqueous humour production, zonular fibre secretion and support, and providing crystalline lens nourishment (Aiello *et al.*, 1992; Atchison, 1995; Tamm and Lütjen-Drecoll, 1996; Snell and Lemp, 1998).

The posterior part of the ciliary body is the relatively even, smooth surfaced pars plana (*orbicularis ciliaris*), which contacts the vitreous and is comprised of zonular fibres oriented longitudinally (Tamm and Lütjen-Drecoll, 1996). The most posterior portion of the pars plana is covered by posterior zonular fibres creating a broad sheet connected to the ciliary body internal limiting membrane (ILM), which is continuous with the retinal ILM (Atchison, 1995). The wider, anterior region of the ciliary body is the pars plicata (*corona ciliaris*), continuous with the posterior surface of the iris. The pars plicata is characterised by approximately 70 to

80 densely vascularised radiating ridges, the ciliary processes, which unlike the pars plana are not covered by zonular fibres, but protrude freely into the posterior chamber. In the depressions between ciliary processes, the zonular fibres are firmly attached to the ciliary epithelium in order to join the pars plicata surface. Aqueous humour is produced by a two-fold method of ultrafiltration of fluid from the ciliary process vasculature into the adjacent stroma, followed by an active secretion by the ciliary epithelium into the posterior chamber of the eye from the ciliary processes (Tamm and Lütjen-Drecoll, 1996). *In vitro* methods have shown the antero-posterior ciliary body in adults is longest temporally, with a mean of approximately 5.76 mm, in contrast with approximately 4.79 mm nasally (Aiello *et al.*, 1992).

The ciliary body consists of six layers, from the outer (scleral) to the inner (vitreous) phase: the supraciliary lamina, ciliary muscle, stroma, basal lamina, epithelium and ILM (Aiello *et al.*, 1992; Tamm and Lütjen-Drecoll, 1996); see table 1.1 for a summary of these layers and their respective functions. The outermost layer, the supraciliary (or suprachoroidal) lamina is a thin layer of sparse collagen fibres, fibroblasts and melanocytes; this loose connective tissue facilitates movement of the ciliary muscle against the sclera (Atchison, 1995; Tamm and Lütjen-Drecoll, 1996). The three innermost layers are all relatively thin; the basal lamina is the continuation of the chorio-retinal Bruch's membrane (Tamm and Lütjen-Drecoll, 1996); the epithelial layer is made up of two single epithelial linings, the inner of which is non-pigmented and continuous with the posterior iris epithelium and neural retina, whilst the outer lining is pigmented heavily and continuous with the anterior iris epithelium and retinal pigment epithelium; the ILM of the ciliary body is secreted by the non-pigmented epithelial layer and is continuous with the retinal ILM. The stroma of the ciliary body has rich vascularity and is comprised of loose connective tissue and melanocytes (Mafee *et al.*, 2005). The stroma of the ciliary processes is also highly vascular, consisting of a vast number of capillaries to deliver the water and metabolites necessary for aqueous production, yet does not contain the elastic fibres present in ciliary body stroma (Tamm and Lütjen-Drecoll, 1996).

	Ciliary Body Layer	Key Functions
Outer  Inner	Supraciliary Lamina	A very thin layer connecting the ciliary body to the sclera. It allows motion between the ciliary body and the sclera. Detachments occur at this point.
	Ciliary Muscle	Contracts to reduce tension on the zonules to form a more convex crystalline lens in the process of accommodation, whilst its relaxation pulls the zonules taught to create less convex lens in disaccommodation.
	Stroma	Highly vascular, thereby providing blood supply to the ciliary body and constituents required for aqueous humour production.
	Basal Lamina	The site at which zonular fibrils attach
	Epithelium	Consists of an inner (non-pigmented) layer which is a continuation of the posterior iris epithelium and neural retina. The outer (pigmented) epithelium layer secretes the ILM of the ciliary body.
	Inner Limiting Membrane	The basement membrane of the six layers, and forms an organised scaffold to provide structural support to the tissue.

Table 1.1 Layers of the ciliary body with respective functions

Much of the mass of the ciliary body is comprised of the ciliary muscle, underneath ciliary processes (Pardue and Sivak, 2000; Glasser *et al.*, 2001). Innervated by the autonomic nervous system, the human ciliary muscle is classified as a rapid, multi-unit smooth muscle (Bozler, 1948). Conventionally, the muscle has been organised into three distinct regions which relate to the orientation of smooth muscle bundles (Figure 1.1): the longitudinal fibres, attached anteriorly to the scleral spur and trabecular meshwork, running longitudinally along the inner scleral surface; radial fibres which bundle in a fan-like arrangement from the anterior chamber angle towards the ciliary processes, and finally the circular fibres, whose bundles run around the globe, parallel with the limbus (Tamm and Lütjen-Drecoll, 1996; Pardue and Sivak, 2000). However, detailed *in vitro* analysis of the muscle has revealed that these regions are not truly distinct, and during accommodation there is reorganisation of the muscle fibres, with a relative increase in circular fibres with a decrease in the relative proportion of longitudinal fibres (Pardue and Sivak, 2000). During the reorganisation of fibres, it is believed that the longitudinal fibres act as a syncytium and change orientation; there is an increase in

the relative proportion of circular fibres to create an internal protuberance (Pardue and Sivak, 2000), which explains the accommodative movement of the ciliary muscle, considered to shorten longitudinally and thicken anteriorly. The choroid is drawn forward, pulling the ciliary body closer to the crystalline lens by the sphincter-like action of the circular fibres (Duke-Elder, 1961; Strenk *et al.*, 1999). The crystalline lens equator is situated approximately 1- 1.5 mm centrally from the ciliary processes (Atchison, 1995; Tamm and Lütjen-Drecoll, 1996). In terms of mass, longitudinal fibres always constitute the greatest proportion (41- 69 %), followed respectively by the radial fibres (25- 47 %) and circular fibres (4- 24 %) (Pardue and Sivak, 2000).

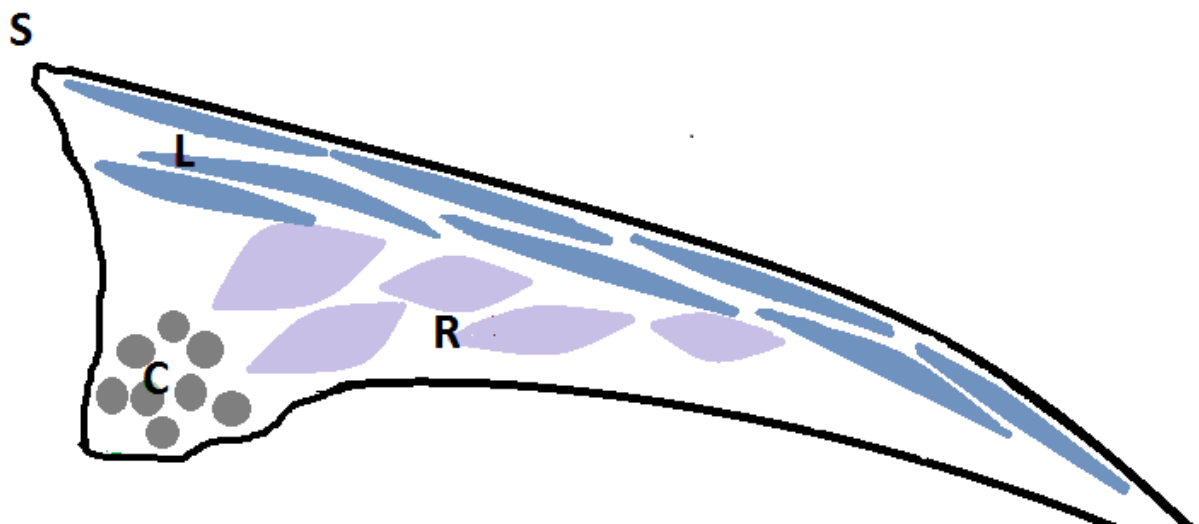


Figure 1.1. Conventional classification of muscle fibres within the ciliary muscle, based on fibre orientation. The longitudinal fibres (L) run along the inner aspect of the sclera and terminate at the scleral spur (S). The radial fibres (R) form a fan-like arrangement and connect the longitudinal fibres to the circular fibres (C), which form bundles around the globe.

Age-dependent histological and morphological alterations in human ciliary muscle have been described by several previous authors using *in vitro* methods (e.g. Lutjen, 1966; Nishida and Mizutani, 1992; Tamm *et al.*, 1992a; Tamm and Lütjen-Drecoll, 1996; Pardue and Sivak, 2000). Neonatal eyes show a uniform distribution of singular fibres, with a lack of connective tissue. With increasing age, these individual fibres form bundles within their own fibre type. Increasing masses of connective tissue segregate these bundles, predominantly in the circular and radial areas, of which has been suggested to account for why fibre type orientation was more defined in older ciliary muscle (Pardue and Sivak, 2000). The relative proportion of the muscle fibre orientations also varies with increasing age (Nishida and Mizutani, 1992; Tamm *et al.*, 1992a; Pardue and Sivak, 2000). The radial fibres show a significant increase in percentage with age, the longitudinal fibres show a significant decrease, whilst the circular fibres maintain a stable proportion (Pardue and Sivak, 2000).

Morphologically, there is a decrease in both the overall length and anterior length (distance from the point of maximum muscle thickness to the anterior tip) of the ciliary muscle, whilst there is a tendency for maximum width to increase with increasing age (Tamm *et al.*, 1992a; Pardue and Sivak, 2000). Figure 1.2 illustrates definitions of overall ciliary muscle length and anterior length. Together with the age-dependent shortening and thickening, the distance from the scleral spur to the inner apex of the muscle is lessened, signifying that a more antero-inward position is adopted in the ageing human ciliary muscle, comparable to that of the young, accommodating muscle (Tamm *et al.*, 1992a).

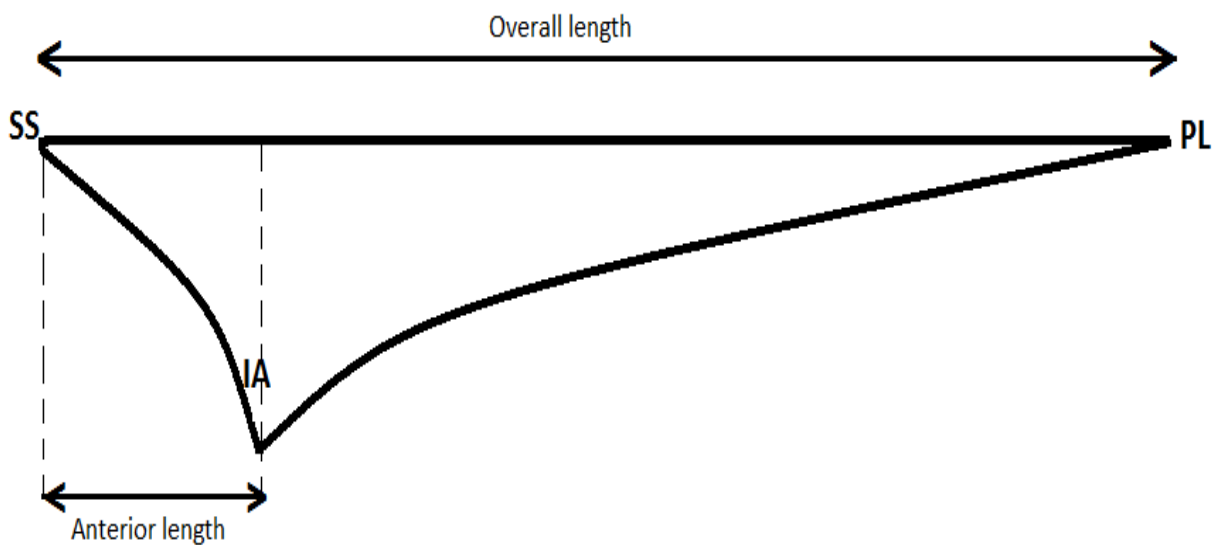


Figure 1.2. Illustration showing the definition of anterior and overall length of the ciliary muscle. The overall length of the ciliary muscle is measured in mm from the scleral spur (SS) to the posterior limit (point where no more thinning of the muscle occurs, PL). The anterior length is taken from the scleral spur to the point of maximum thickness of the muscle. IA represents the inner apex.

1.1.3 Crystalline Lens

The human crystalline lens is an elaborate and transparent refractive structure, which shows continuous growth and maturation (Brown, 1974; Koretz *et al.*, 1989; Weale, 1989; Pierscionek and Weale, 1995; Strenk *et al.*, 2004). Contrasting to skin cells, where the oldest are ultimately shed, accumulation of newly differentiated cells on the lens surface occurs with lenticular growth. The lens fibres originate from the continual differentiation of the anterior lens surface epithelial cells, with morphological alterations occurring primarily near the lens equator (Kaufman and Alm, 2003). As the new lens fibre cells continually advance and overlay their predecessors (which consequently displace inwardly) sphericity of the lens is lost as its form becomes more ellipsoidal. The lens nucleus, the large central portion (see figure 1.3), consists of the oldest fibres (Fisher and Pettet, 1973; Brown, 1974) and is the

region of highest refractive index due to peak protein concentration of approximately 36 % (Fisher and Pettet, 1973). Such lifelong growth of the lens would be expected to result in an age-dependent increase in lenticular optical power, and hence a myopic shift in refractive error (Hemenger *et al.*, 1995). Conversely, the lens actually becomes dioptrically weaker with age- a contradiction known as Brown's lens paradox (Brown, 1973; Brown, 1974; Dubbleman *et al.*, 2003). Alterations in the lenticular refractive index distribution are considered to counteract the propensity for myopia induced by lens growth (Gilmartin, 1995; Koretz *et al.*, 2004). A gradient protein concentration and therefore, gradient refractive index (GRIN) occurs within the crystalline lens. The increase in axial lens thickness during accommodation is primarily due to the shape alteration of the lens nucleus whereas the axial cortical thickness remains constant (Hermans *et al.*, 2007).

Despite its high protein concentration and cellular structure, the young human lens exceptionally transmits nearly all the incident light, with optical homogeneity being essential for efficient light transmission (Patel and Bron, 2002; Truscott, 2009). To maintain lens transparency, the nuclei, organelles and any internal cytoplasmic structure large enough to scatter light are shed from the fibre cells whilst nuclei-containing newer fibres are situated in the equatorial region, obscured by the iris (Strenk *et al.*, 2005; Truscott, 2009). So that the crystalline lens provides an effective refractive contribution, it must maintain a higher refractive index than its surrounding media (aqueous and vitreous humours), achieved through internal fibre cell protein concentrations greater than 300 mg/ml (Strenk *et al.*, 2005); this mechanism ensures that the maintenance of transparency is independent of lens curvature, shape and size (Koretz *et al.*, 1994; Yaroslavsky *et al.*, 1994; Zhao and Bettelheim, 1995).

1.1.4 Capsule

Enclosing the entire crystalline lens is the capsule (see figure 1.3), an elastic basement membrane that is essential for moulding the crystalline lens during accommodation (Snell and Lemp, 1998; Strenk *et al.*, 2005). Electron microscopy reveals the capsule to be a lamellar structure that is composed of collagen filament layers (Stafford, 2001), while this lamellar arrangement of filaments is responsible for the highly elastic nature of the capsule. The outer capsular layer is denser and consists of zonular microfibrils amongst collagen (Atchison, 1995). The posterior capsule maintains a relatively constant thickness over time, at about 5 μm (Krag and Andreassen, 2003). In contrast, the anterior portion of the capsule continually thickens throughout life (up to approximately 25 μm) due to the production of anterior epithelium, and in order for the capsule to continue mirroring the growing size of the crystalline lens (Remington, 2005). In terms of the capsular equatorial region, here zonular fibres insert,

joining the lens to the ciliary processes, thereby suspending the lens and permitting contractile alterations of the ciliary muscle to be transmitted to the lens mass (Snell and Lemp,1998).

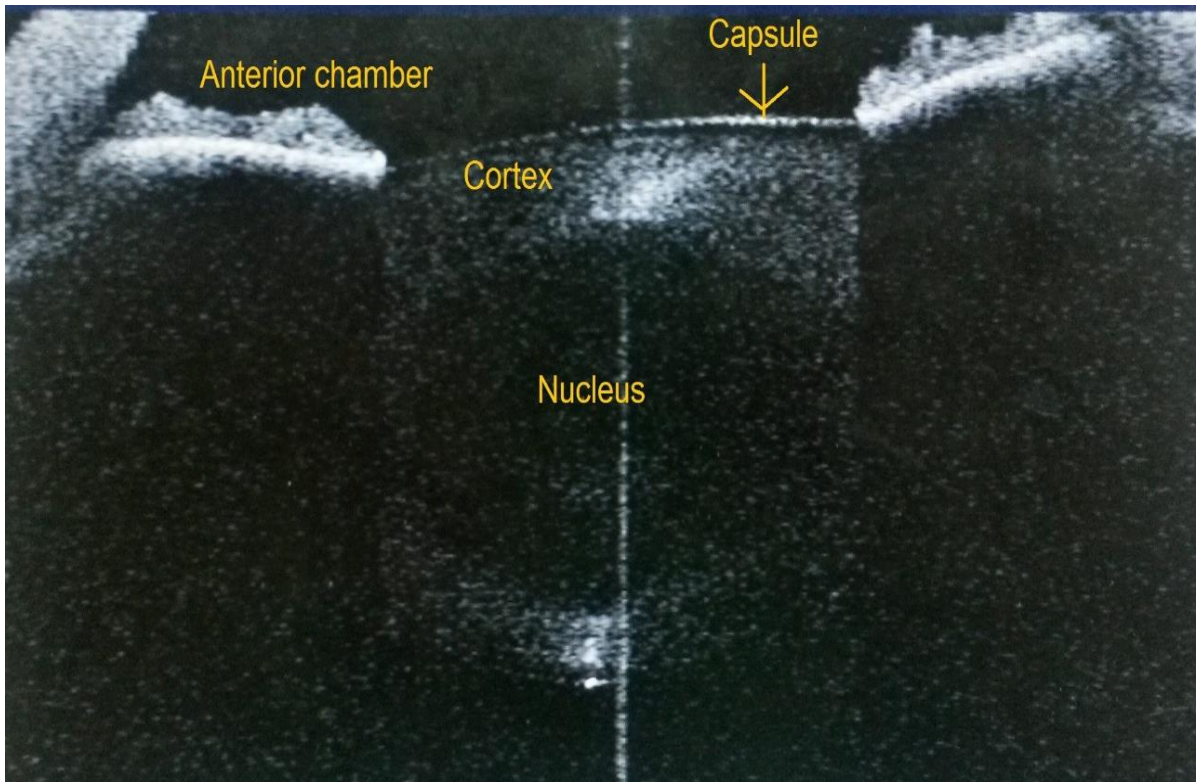


Figure 1.3. AS-OCT image of the crystalline lens of a 26 year old participant. The nucleus, cortex and capsule can be easily distinguished.

1.1.5 Zonules

The zonular fibres are responsible for suspending the crystalline lens and supplementing accommodation (Rohen, 1979; Croft *et al.*, 2013). The zonules are delicate structures composed of intricate meshworks of fibrils (Kaufman and Alm, 2003) and have been separated into two categories: the main fibres (anterior and posterior/ vitreous) and the spanning/ tension fibres (Rohen, 1979).

The lens is supported by the anterior zonules, running from the ciliary processes of the anterior portion of the ciliary body, traversing the circumferential space and implanting into the equatorial area of the capsule, with crossover of many fibres occurring (Glasser and Campbell, 1999; Charman, 2008) (see figure 1.4). Lengthier, posterior/ vitreous zonular fibres run from the ora serrata towards the ciliary process valleys (Glasser, 2008; Lutjen-Drecoll *et al.*, 2010; Croft *et al.*, 2013). Furthermore, both anterior and posterior arrangements are connected by shorter, intermediate, tension fibres that inject into the ciliary epithelium within the valleys of the ciliary processes (Rohen, 1979). The precise role of these tensile fibres is

unclear, but they may act as a fulcrum, supplying specific leverage to allow rapid and precise amendments to the amount of accommodation (Rohen, 1979; Gilmartin, 1995; Charman, 2008).

Gradual alterations to the geometry of zonular insertions into the capsule occur due to ongoing lens growth, such that there is an age-dependent forward shift of the zonular fibres away from the equator of the lens (Farnsworth and Burke, 1977; Farnsworth and Shyne, 1979; Sakabe *et al.*, 1998). Whilst there is lifelong variation of the zonular attachment geometry, the extensile characteristics of the zonules are stable between the ages of 15- 45 years (Fisher, 1986). The role of the vitreous zonules in the mechanism of accommodation has been a topic of recent research interest. A key investigation (on primate and human eyes) used scanning electron microscopy and ultrasound biomicroscopy techniques to image the anterior, intermediate, and posterior vitreous zonules and their connections to the ciliary body, lens capsule, vitreous membrane, and ora serrata, characterising their age-related alterations and relating them with loss of ciliary body accommodative forward movement (Lutjen-Drecoll *et al.*, 2010). It was suggested that the vitreous zonules could facilitate smooth translation of the ciliary muscle driving forces of accommodation and disaccommodation to the lens, whilst protecting the lens capsule and ora serrata from acute tractional forces, and sustaining visual focus (Lutjen-Drecoll *et al.*, 2010). A further study also using rhesus monkeys and human subjects discovered that the anterior zonule only relaxes at or near maximal accommodation (Croft *et al.*, 2013). It was also indicated that the role of the vitreous zonule may be to prevent shear between the retina and vitreous and/ or to assist ocular ability to smoothly pursue the movement of objects, without distortions within the field of view (Croft *et al.*, 2013).

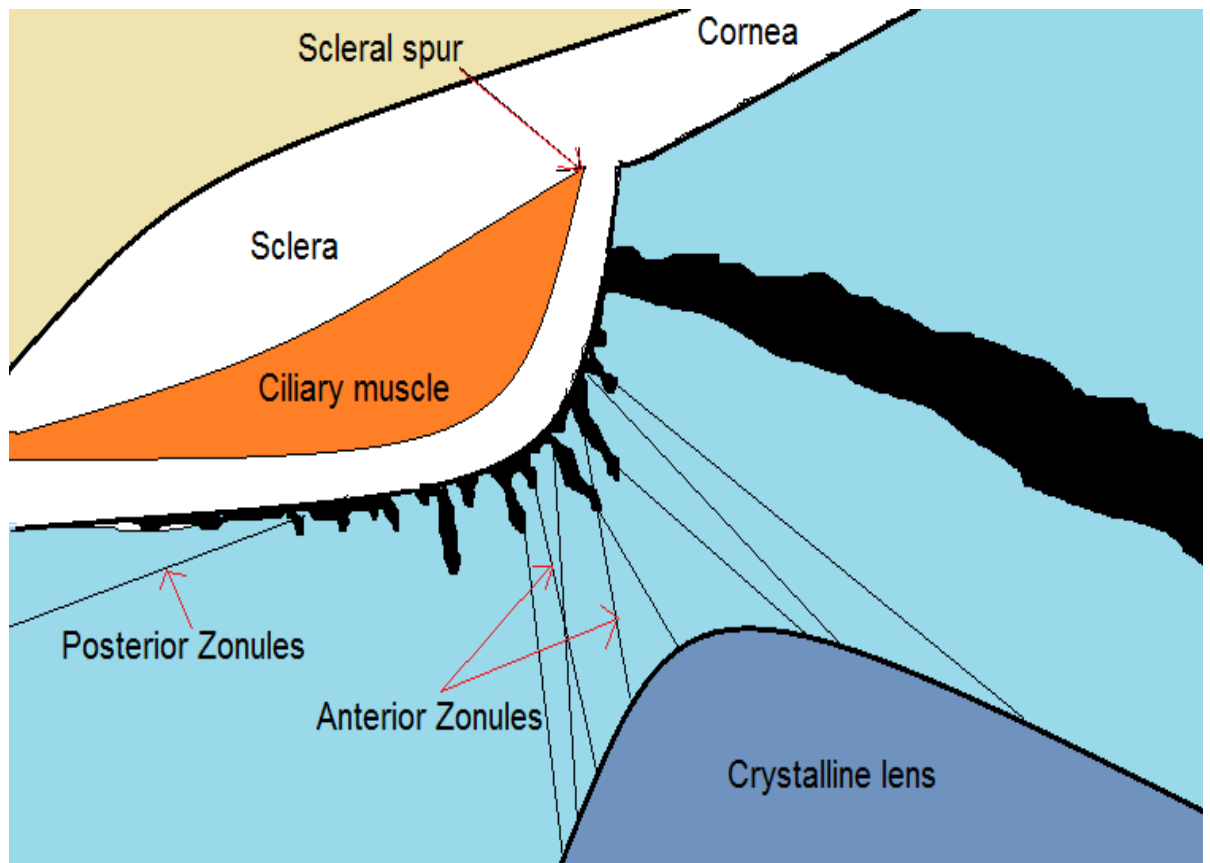


Figure 1.4. Schematic diagram of the human accommodative apparatus showing the arrangement of both anterior and posterior (vitreous) zonules. During accommodation as the ciliary muscle contracts anteriorly and inwards, tension on the anterior zonules is reduced, allowing the elastic capsule to mould the crystalline lens into a more convex form.

1.2 Mechanism of accommodation

Ocular accommodation is the alteration in shape of the crystalline lens to allow focus of near-objects (Dubbelman *et al.*, 2005; Kasthurirangan *et al.*, 2011), a process instigated by ciliary muscle contraction through parasympathetic innervation. In the unaccommodated state where the ciliary muscle is relaxed, the lens is held relatively flat by the taught zonules such that a low dioptric power is achieved to allow the focus to correspond with the far point of the eye. There is a shift in the mass of the ciliary muscle as it contracts during accommodation, sliding anteriorly and fundamentally, inwards, towards the optical axis, producing a reduction in the ciliary muscle collar diameter (Gilmartin, 1995; Strenk *et al.*, 1999; Croft *et al.*, 2001; Zhonga *et al.*, 2014). As a result, zonular tension is lessened, permitting the elastic lens capsule to mould the youthful lens into a more convex form with greater dioptric power (Charman, 2008; Glasser, 2008); this Helmholtzian mechanism (Figure 1.5) is the basis of our modern understanding of accommodation and is almost universally accepted, with a vast amount of research to support the theory (Strenk *et al.*, 1999; Hermans *et al.*, 2007; Jones *et*

al., 2007; Hermans *et al.*, 2009; Reilly and Ravi, 2010; Kasthurirangan *et al.*, 2011; Sheppard *et al.*, 2011b)

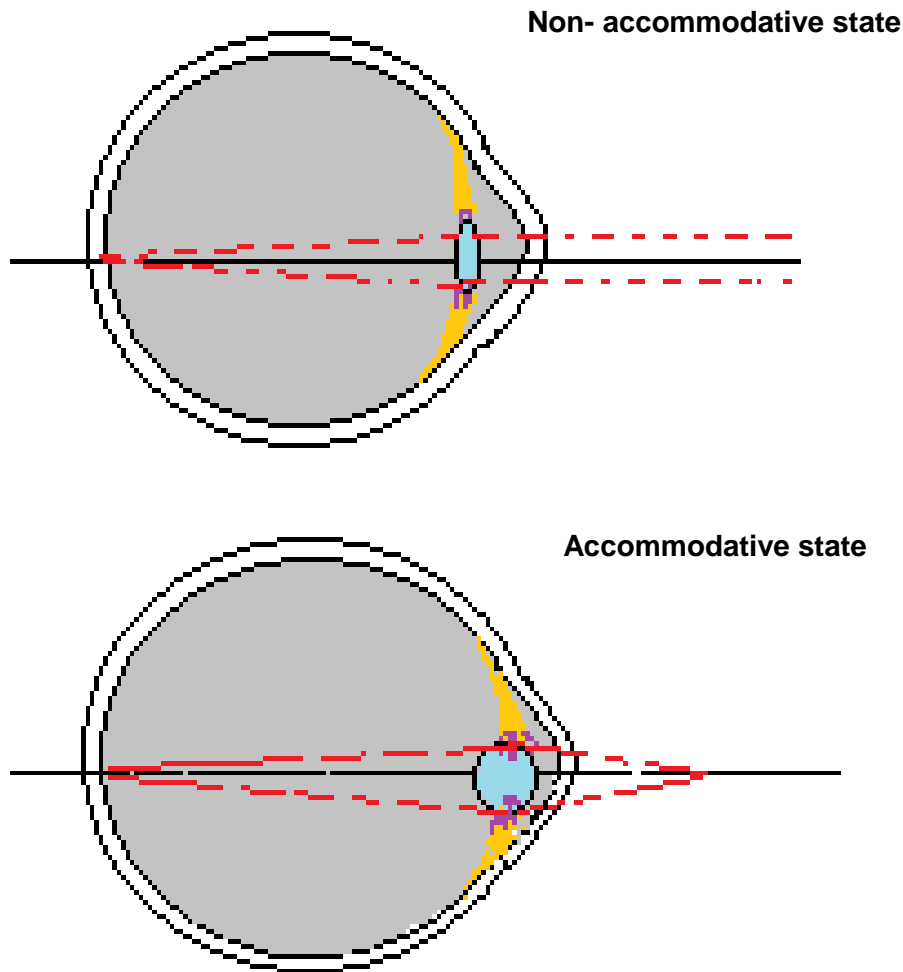


Figure 1.5. Illustration of Hemholtzian mechanism of accommodation. The top image represents the non-accommodative state when the eye is focused on a distant object; light rays (red dotted line) enter at parallel and are focussed on the retina through the crystalline lens (blue), which is held flat by the taugh zonules (purple), via relaxation of the ciliary muscle (orange). The bottom image illustrates the accommodative state; divergent light rays from a near object are focused on the retina by the crystalline lens entering a more dioptrically powerful, convex form through the contraction of the ciliary muscle releasing the tension on the zonules.

In both the accommodated and the unaccommodated states, the posterior lens surface is more steeply curved than the anterior lens surface (ALS). Although during accommodation both surface curvatures increase in convexity, the anterior does so more significantly, undergoing the greatest increase in curvature and axial movement, though its steepness never exceeds that of the posterior surface (Koretz *et al.*, 2004). The discrepancy during accommodative response between these two crystalline lens surfaces may be due to the

thicker anterior capsule applying more elastic force to the crystalline lens substance and greater tensional forces affecting the anterior zonules. Moreover, vitreous body resistance could oppose posterior movement of the posterior lens surface (Charman, 2008). The behaviour of these surface curvatures are mimicked by the internal curvatures (Dubbleman *et al.*, 2003); this structural change in the anterior lens surface results in a shallower anterior chamber during accommodation (Atchison, 1995; Drexler *et al.*, 1997; Croft *et al.*, 2001). Overall, and due to these combined alterations, the lens thickens axially, there is a small bulge in the central lenticular mass anteriorly, and equatorial diameter reduces during accommodation (Patnaik, 1967; Brown, 1973a; Drexler *et al.*, 1997; Wilson, 1997; Strenk *et al.*, 1999; Croft *et al.*, 2001; Jones *et al.*, 2007; Charman, 2008; Croft *et al.*, 2013). The closer proximity between the cornea and anterior lens surface together with the greater lens convexity and thickness, increases the dioptric power of the eye (von Helmholtz, 1855).

Additionally, the potential roles of the iris and vitreous body in the mechanism of ocular accommodation have been debated. The iris sphincter has been suggested to facilitate accommodation by pulling the ciliary body further forward and inwards to allow increased lenticular convexity (Crawford *et al.*, 1990), and vitreous pressure variations during accommodation could aid movement of the anterior lens surface forward to augment the accommodative response (Koretz and Handelman, 1982; Coleman, 1986). Still, accommodation has been observed in both aniridic subjects (Fincham, 1937) and those with empty vitreous chambers (Fisher, 1982; Fisher, 1983) so any involvement from these structures is unlikely to be substantial.

The process that commences when cessation of ciliary muscle contraction occurs is often referred to as disaccommodation (Croft *et al.*, 2001; Glasser, 2008). It involves the reversal of the actions occurring with accommodation; the elastic choroid operates as a restorative force as the ciliary muscle is pulled posteriorly and away from the optical axis, along the inner scleral surface, into its relaxed and unaccommodated arrangement again (Strenk *et al.*, 1999; Croft *et al.*, 2001). The swiftly increased zonular tension manipulates the lens capsule, pulling the lens into a flatter form and shifting the anterior lens surface posteriorly away from the cornea, such that anterior chamber depth increases. Likewise, a small returning movement of the posterior lens surface occurs anteriorly, thus deepening the vitreous chamber. The flattening of lenticular surface curvatures causes a reduced dioptric power of the eye (Croft *et al.*, 2001; Glasser, 2008; Davies *et al.*, 2010).

Nonconformist opinions of the mechanism of accommodation remain, particularly the notion of a Tscherning-type system, whereby there is greater zonular tension (specifically the

equatorial zonules) during accommodation, resulting in the outward movement of the lens equator towards the sclera, with the crystalline lens steepening centrally and flattening peripherally (Schachar, 2006; Schachar and Koivula, 2008). Controversially, this theory suggests that anterior and posterior zonules (inserting into the lens capsule) solely supply suspension for the lens, whilst the equatorial zonules respond to ciliary muscle activity and thereby initiate alterations to lens shape. Despite its controversial nature, various investigations have findings which are in agreement with the theory (Sa *et al.*, 2005; Schachar and Koivula, 2008); an investigation utilised OCT imagery to observe the alteration in reflected light intensity from the ALS in both the accommodated and non-accommodated state. The investigative findings were on the basis that a greater surface strain leads to the surface being smoother, and therefore a greater amount of light reflectance will occur (compared with increased light scatter occurring with a rough surface) (Federici *et al.*, 1999; Schachar and Koivula, 2008). In accordance with the nonconformist Schachar theory, the data indicated that the ALS was more stretched in the accommodated state (Schachar and Koivula, 2008).

In summary, ocular accommodation involves the coordination of various anatomical structures, including the ciliary muscle, crystalline lens and zonules. The ciliary muscle is a circumferential multi-unit smooth muscle which rapidly contracts anteriorly and inwards, causing a release of zonular tension on the crystalline lens such that it enters a more dioptrically powerful, convex form (von Helmholtz, 1855).

1.3. Components of accommodation

Physiologically, the accommodative response is a dynamic process that involves several components (Ni *et al.*, 2013). Four components of accommodation have been differentiated, specifically reflex, proximal, tonic and convergence (Heath, 1956).

1.3.1. Reflex accommodation

Reflex accommodation is known as the automatic modification of the refractive ocular power (over approximately a 2 D range) in response to a blurred stimulus, in order to sustain a clear retinal image (Charman, 2008). It has been suggested that reflex accommodation is the only accommodative component to be manipulated by retinal image quality (Heath, 1956)

1.3.2. Proximal accommodation

Belief of the distance of an object, or awareness of its proximity produces proximal accommodation (Heath, 1956; Rosenfield and Ciuffreda, 1991); the mere presentation of a near object may initiate the accommodative response, or when employing a device such as

a closed-view autorefractor (instrument myopia). Because simply “thinking near” can induce a response, voluntary accommodation may be deemed a type of proximal accommodation (Provine and Enoch, 1975; Rosenfield and Ciuffreda, 1991).

1.3.3. Tonic accommodation

The accommodative mechanism adopts an intermediate state of approximately 1 D (Heath, 1956; Millodot, 2008), producing a mild myopic state which arises when there is inadequate visual stimulus e.g. a structureless/ empty field (Schor *et al.*, 1986) or darkness (Gilmartin *et al.*, 1984), poor visual acuity (Heath, 1956) or a low spatial frequency target (Kotulak and Schor, 1987). This phenomenon was initially termed tonic accommodation as it was thought to stem from the dual innervation of the ciliary muscle; an intermediate dioptric power would be established without presence of accommodative stimulation (Rosenfield *et al.*, 1993). However, the term is likely to be somewhat inaccurate, as a feasible explanation of this accommodative response is multifactoral, including non-optical features, such as visual imagination, auditory and vestibular input (Rosenfield *et al.*, 1993).

1.3.4. Convergence accommodation

Convergence accommodation outlines the accommodative mechanism automatically stimulated by a change in convergence; the convergence accommodation (CA)/ convergence (C), (CA/ C) ratio, governs the magnitude of this response. The near triad consists of convergence, accommodation and pupil miosis, and synkinesis of these processes is due to their neural connection (Charman, 2008).

1.4 Ciliary muscle *in vivo* imaging

Historically, information regarding the ciliary muscle was extracted from *in vitro* studies. Whilst such investigations have advanced our understanding of primate and human accommodative physiology (Aiello *et al.*, 1992; Tamm *et al.*, 1992; Poyer *et al.*, 1993), *in vitro* findings may be modified by post mortem chemical tissue changes, (Weale, 1999; Kasthurirangan *et al.*, 2008) along with handling and storage processes; the extent of these changes cannot be known (Strenk *et al.*, 2004; Werner *et al.*, 2008; Sheppard and Davies, 2010b). *In vitro* methods involve dissection of accommodative structures (Lutjen-Drecoll *et al.*, 2010), and this introduces uncertainty as to whether the accommodative structures under investigation are behaving as they would in the intact accommodative system. Furthermore, ischaemic effects may modify the ciliary muscle response to the application of topical pharmacological agents (Pardue and Sivak, 2000; Sheppard and Davies, 2010b). Hence the ability to view the active human ciliary muscle *in vivo* is highly beneficial. The use of *in vivo* imaging techniques allows

an enhanced comprehension of the anatomical and physiological ocular structures and the processes involved in ocular accommodation. The key *in vivo* techniques are ultrasound biomicroscopy (UBM), magnetic resonance imaging (MRI) and optical coherence tomography (OCT) due to their wide use in research, clinically acceptable resolution, speed of imaging and availability.

1.4.1 Ultrasound biomicroscopy

UBM is a type of ophthalmic ultrasound imaging based on high frequency acoustic pulses being reflected; the sound waves are generated by piezoelectric constituents, (Wolffsohn and Davies, 2007) and are reflected from ocular tissue interfaces. An A-scan is created from the subsequent detection of these reflected acoustic pulses (Konstantopoulos *et al.*, 2007). UBM for use in anterior segment imaging has been utilised since the early 1990s (Pavlin *et al.*, 1992) and employs a transducer of approximately 50 MHz (contrasting to 10- 20 MHz for entire-globe ultrasonography), allowing visualisation behind opaque corneas, for the imaging of ocular structures. Although high frequency UBM permits tissue penetration to just 4- 5 mm, resolution is improved compared to low frequency UBM; transverse resolution is approximately 25 μm and axial resolution around 50 μm with the high frequency (Nolan, 2008).

The chief disadvantage of UBM is that the technique requires the patient to remain supine because the eye is submerged in saline, using an eye cup directly placed onto the globe. Furthermore, the contact nature of the technique may cause discomfort for the subject whilst also potentially distorting angle structures (Konstantopoulos *et al.*, 2007). Because the probe is in contact with and occludes the eye being studied, this may cause potential precision problems in accommodation studies as binocular vision is obstructed and only the fellow eye can view the accommodative stimulus. UBM has been used in the analysis of the relationship between ciliary body thickness and refractive error, e.g. Olivera *et al.* (2005) described thicker ciliary muscles in myopic eyes. Whilst resolution of the ciliary muscle with UBM is inferior to AS-OCT, it does however permit visualisation of structures posterior to the iris such as the ciliary body and posterior zonules (Oliveira *et al.*, 2005a; Croft *et al.*, 2013). High frequency UBM has been utilised in investigations to study the movement of implanted IOLs (Stachs *et al.*, 2002; Muftuoglu *et al.*, 2009).

1.4.2 Magnetic resonance imaging

Because MRI is a non-optical (and non-invasive) imaging method (Strenk *et al.*, 1999; Gilmartin *et al.*, 2013), it is not obstructed by the iris. It provides unparalleled soft tissue contrast that offers visualisation of the anterior segment in any required plane with no optical

distortion (Jones *et al.*, 2007; Strenk *et al.*, 2010). MRI is utilised primarily in clinical applications for the diagnosis of ocular diseases including space- occupying lesions (Ben Simon *et al.*, 2005), soft tissue injury (Kolk *et al.*, 2005) and congenital disorders (Chaudhry *et al.*, 2007) as well as extraocular muscle investigation (Sa *et al.*, 2005). However, due to the technical difficulties of imaging small volumes and the relative expense and inaccessibility of the method, use in anterior segment research is limited (Singh *et al.*, 2006; Strenk *et al.*, 2006; Wolffsohn and Davies, 2007; Strenk *et al.*, 2010).

The strength of the magnetic field in an MRI system is measured in Tesla units, which helps govern image resolution. In recent years image resolution has improved. Previously high resolution- MRI scanners typically scanned at 1.5 Tesla (Strenk *et al.*, 2006), though resolution is now less of an issue with newer scanners that permit ultra-high field 7.1- Tesla MRI imaging of ocular structures (Richdale *et al.*, 2009; Langner *et al.*, 2010).

MRI employs the basis of nuclear magnetic resonance to image the internal bodily structures (Wolffsohn and Davies, 2007). Typically the proton nuclear spins in tissues have no stable orientation, though when within a prevailing magnetic field, for instance, an MRI scanner, the nuclear spins become oriented along the field (Hornak, 2008). The proton spins are flipped out of their longitudinal plane into the transverse plane with the application of a 90° radiofrequency (RF) pulse of a precise frequency (Liney, 2005). Such linear alterations to the magnetic field permit construction of an image for visualisation, as the RF coil is able to detect a spatially localised signal.

Investigations using MRI reported that ciliary ring diameter decreases as a function of age and accommodation (Strenk *et al.*, 1999; Strenk *et al.*, 2004). In addition to ciliary muscle investigations, MRI has provided much information on the morphological and optical and alterations in the crystalline lens with accommodation. Procedures to map the lenticular refractive index distribution have been developed (Moffat *et al.*, 2002a; Moffat *et al.*, 2002b; Jones and Pope, 2004) and applied to human eyes and *in vivo* (Jones *et al.*, 2007; Kasthurirangan *et al.*, 2008), and *in vitro* (Jones *et al.*, 2005). MRI has also been utilised to explore globe shape with refractive error (Atchison *et al.*, 2004; Gilmartin *et al.*, 2013), which is discussed in further detail in section 1.4.2.

1.4.3 Time-domain and spectral-domain optical coherence tomography

Becoming commercially available in 1995, OCT has been used widely for retinal disease assessment (Drexler and Fujimoto, 2007). Fundus examination using OCT is useful in age

related macular degeneration (Pieroni *et al.*, 2006) macular hole (Bakri *et al.*, 2007) and diabetic retinopathy (Polito *et al.*, 2006), as the technique permits segmenting through the retinal layers (Wolffsohn, 2008). OCT provides very high resolution, with a penetration of 2 - 20 mm, making it advantageous in imaging and quantifying small ocular structures (Ramos *et al.*, 2009).

Two different OCT systems have been established: time domain (TD) and Fourier- domain (FD). With time-domain (TD) OCT, the reference mirror is moveable in order to create the A-scans, thus yielding a reflectivity profile corresponding to depth and thereby limiting the speed at which the image is acquired (Kiernan *et al.*, 2010). Fourier-domain (FD) OCT has an immobilised reference mirror so can operate much more rapidly, and the interference between the sample and reference reflections is detected as a spectrum (Yaqoob *et al.*, 2005; Ramos *et al.*, 2009). A Fourier transformation algorithm of the spectral interferogram generates the A-scan, creating increased sensitivity and faster image acquisition compared with traditional TD-OCT systems (Asrani *et al.*, 2008; Ramos *et al.*, 2009; Kiernan *et al.*, 2010) which rely on the mechanical locomotion of a reference mirror to measure the reflectivity of the tissues; therefore the speed of this approach is restricted by the mechanical cycle time of the reference mirror driver (Ramos *et al.*, 2009).

The greater sensitivity of FD-OCT systems has been utilised to image at high scan rates without intensifying the optical exposure or losing image brightness (Asrani *et al.*, 2008) as signals are not detected from the entire depth range just serially, but in parallel (Ramos *et al.*, 2009; Rodrigues *et al.*, 2012). Nonetheless, FD-OCT devices functioning with a long wavelength superluminescent diode have been restricted in effective imaging depths to less than 3- 4 mm, preventing useful ocular anterior segment imaging (Huber *et al.*, 2006; Christopoulos *et al.*, 2007; Asrani *et al.*, 2008). In current ophthalmic FD-OCT versions, the detector arm of the interferometer encompasses the spectrometer (Ramos *et al.*, 2009). Swept-source OCT (SD- OCT) is a further implementation of FD-OCT where the source is a rapidly tunable, narrowband scanning laser (Yaqoob *et al.*, 2005) that is more detection sensitive and has lower signal-to-noise ratios at greater scanning depths, compared with traditional FD-OCT devices (Lim *et al.*, 2014). As wider range swept-source wavelength provides greater depth resolution, and rapid wavelength tuning of the source permits faster image acquisition, the design and operation of a tunable source is an essential aspect in the swept-source FD-OCT performance; several ~ 1300 nm laser designs have been utilised (Yaqoob *et al.*, 2005) and the high speed tuning of the light source are founded on three major concepts: the first is based on a diffraction grating on a mechanically resonant galvanometer scanning mirror (Yun *et al.*, 2003a; Yun *et al.*, 2004; Yaqoob *et al.*, 2005), the

second is a polygonal rapidly rotating mirror (Yun *et al.*, 2003a; Yun *et al.*, 2003b; Gora *et al.*, 2009), and thirdly a tunable Fabry-Perot cavity (Choma *et al.*, 2003; Yaqoob *et al.*, 2005; Gora *et al.*, 2009). The details of these concepts are beyond this thesis and will not be discussed in further detail.

The most rapid TD-OCT system is the *Visante* AS-OCT (Carl Zeiss Meditec, Inc., Dublin, CA), no longer commercially available and which acquires 2,000 A-scans per second. The *RTVue* (Optovue, Inc., Fremont, CA) and the *Cirrus* (Carl Zeiss Meditec) are SD-OCT systems that can provide either retinal or anterior segment imaging (the latter requires a corneal adaptor module (CAM)) whose spectrometers encompass high speed line cameras that capture A-scans thirteen times faster than the *Visante* per second, at 26,000- 27,000 scans (Ramos *et al.*, 2009; Ostrin *et al.*, 2015). Despite the rapid speed of the *Cirrus* and *RTVue* which reduces motion artefacts to provide a higher definition from a greater quantity of A-scans per image (Gora *et al.*, 2009; Ramos *et al.*, 2009), their shorter wavelength (830 and 840nm for *RTVue* and *Cirrus*, respectively, compared with 1310 nm *Visante*) cannot penetrate as deep through the sclera and iris, whereas the *Visante*'s 16 mm scan width and approximately 6 mm scan depth in tissue are effective for anterior segment biometry. However, the *RTVue* and *Cirrus* feature a depth resolution that is over three times greater (5 mm) than the *Visante*, whose depth resolution in tissue is approximately 17 mm (Ramos *et al.*, 2009). A swept source SD-OCT system, the DRI *Triton* (Topcon) has recently become available which alike to the previous 2012 model *Atlantis*, utilises a 1050 nm wavelength to provide increased penetration through the sclera and iris compared with traditional SD-OCT systems, and boasts the fastest current scanning speed at 100,000 A-scans per second (Miki *et al.*, 2015). Like the *Cirrus* and *RTVue*, the *Triton* utilises a CAM for anterior segment imaging. The *Triton* has a scan depth of 9 mm, surpassing that of the *Visante*, though its scan width is 12 mm and comprises of additional features such as fundus photography and Fluorescein Angiography.

Whilst each OCT system has distinct advantages and which is defined as a better instrument depends on the precise application, there is a scarcity of literature relating to which OCT is ideal for imaging the ciliary muscle.

1.4.4 Anterior segment optical coherence tomography

A more recent development is anterior segment OCT, first devised in 1994 (Izatt *et al.*, 1994) and available since 2001, when a high speed AS-OCT supplying images of good resolution, was obtainable. Clinical use of the AS-OCT is wide- spread, including evaluation of anterior chamber depth (Baikoff *et al.*, 2004; Baikoff, 2006), anterior segment tumours (Huang *et al.*,

2004), corneal thickness (Li *et al.*, 2006b) and corneal grafts (Ardiemand *et al.*, 2007), precise measurements of phakic IOLs (Goldsmith *et al.*, 2005), assessment of IOL implantation (Wirbelauer *et al.*, 2005; Baikoff, 2006) and the detection of closed-angle glaucoma (Radhakrishnan *et al.*, 2005; Nolan *et al.*, 2007).

There are presently very limited dedicated AS-OCT instruments commercially available (Nolan, 2008): The slit-lamp OCT (Heidelberg Engineering, GmbH, Heidelberg, Germany) combines a slit-lamp and AS-OCT. The *Visante* stand-alone OCT (Carl Zeiss Meditec Inc., Dublin, CA, USA) shown in Figure 1.6 is no longer commercially available though it has been used in several human ciliary muscle studies (Bailey *et al.*, 2008; Sheppard and Davies, 2011; Pucker *et al.*, 2013).



Figure 1.6. *Visante* stand-alone AS-OCT, used in the Ophthalmic Research Group laboratories of Aston University.

AS-OCT technology employs a light source of which wavelength varies depending on the type of OCT system (830 - 1310 nm). Resolution is governed by the wavelength and the spectral bandwidth of the light source, with wider bandwidths and shorter wavelengths

providing better resolution (Ramos *et al.*, 2009). The employment of the long wavelength light source (opposed to 830 nm used for retinal imaging) enables enhanced scleral penetration, a light scattering tissue, hence the ciliary body can be visualised (Konstantopoulos *et al.*, 2007; Ramos *et al.*, 2009). The light source is divided by a beamsplitter into a measurement beam, which is reflected by the ocular structures and a reference beam that is reflected by a mirror (Yaqoob *et al.*, 2005; Wolffsohn, 2008). Coherent interference occurs if light from both the measurement and reference beam travel identical optical distances prior to their recombination (Wolffsohn and Davies, 2007). An A-scan is built up through the determination of the axial depth of tissues by altering the reference path optical length at each scanning point. This scanning point travels across the eye laterally, and the alignment of many A-scans are utilised to develop a two-dimensional cross-sectional image. AS-OCT has greater sensitivity than other imaging techniques utilising a similar principle, because photodetection at the interferometer output comprises of multiplying the two optical waves together. As such, the weak signal in the object arm, transmitted or back-scattered through the tissue, is intensified by the powerful signal in the reference arm, permitting the OCT to detect reflected signals as small as one part in 10^{-10} of the incident power (Ramos *et al.*, 2009). Previously, imaging of the ciliary muscle had been difficult due to the anatomical position of the pigmented iris obstructing the view of the ciliary apparatus, leading to a lack of complete understanding of ciliary muscle morphology in accommodation and myopia (Lewis *et al.*, 2012). OCT is advantageous over MRI and UMB as it is relatively inexpensive, a natural head position can be maintained by the subject, the technique is non- contact and images can be captured rapidly.

1.4.5 Visante AS-OCT and ciliary muscle imaging

As with all methods consisting of light or acoustic waves bypassing curved-surfaced media and altering refractive indices, optical distortion results (Wolffsohn, 2008), and AS-OCT is no exemption. However, the distortion is decreased by the incorporated *Visante* software (versions 1.0 or 2.0) which uses edge detection algorithms to locate the corneal surfaces, consequently assigning the fitting refractive indices to each image section; for the portion anterior to the cornea, a refractive index of 1.000 (air) is employed; the portion within the corneal margins has 1.338 index (cornea) applied; and 1.343 index (aqueous humour) for anatomy posterior to the cornea, is implemented. Whilst the software provides increased accuracy compared with using uncorrected images for assessing the ocular components, some inaccuracy still resides. An investigation that utilised physical model eyes in the *anterior segment single* mode with recognised dimensions ascertained, found for instance, that anterior chamber depth may be overestimated by approximately 88 μm with the AS-OCT

software (Dunne *et al.*, 2007). A range of corneal radii, lens radii, anterior chamber depths, and lens thicknesses were used, while each model corneal thicknesses was fixed at 0.8 mm. Distortion correction factors with the *Visante* instrument have been developed to decrease errors of axial distance measurements and a scheme established to permit surface curvature measurement with a higher level of accuracy (Dunne *et al.*, 2007).

More recently OCT has been utilised in the evaluation of ciliary muscle morphology (Bailey *et al.*, 2008; Sheppard and Davies, 2010b; Sheppard and Davies, 2011; Buckhurst *et al.*, 2013) and contraction (Sheppard and Davies, 2010b; Lossing *et al.*, 2012). Rather than the internal target of the AS-OCT, the ciliary muscle can be visualised with the patient instructed to fixate on an eccentric target, thereby avoiding iris pigmentation and imaging the ciliary muscle through the sclera. The imaging mode frequently used to visualise the ciliary muscle is *high resolution corneal*, and the anterior segment can be imaged as a single image (see figure 1.7) with the patient fixating on the internal target and utilising the *anterior segment single* mode.

The *anterior segment single* mode allows visualisation of the entire anterior segment, imaging at a resolution of 18 μm and penetrating a tissue depth of 6 mm with an image width of 16 mm. The *high resolution corneal* mode (10 mm x 3 mm) allows for detailed visualisation of the cornea when the subject is fixating straight ahead; transverse and optical axial resolutions are down to 60 μm and 18 μm , respectively (Zeiss, 2006).

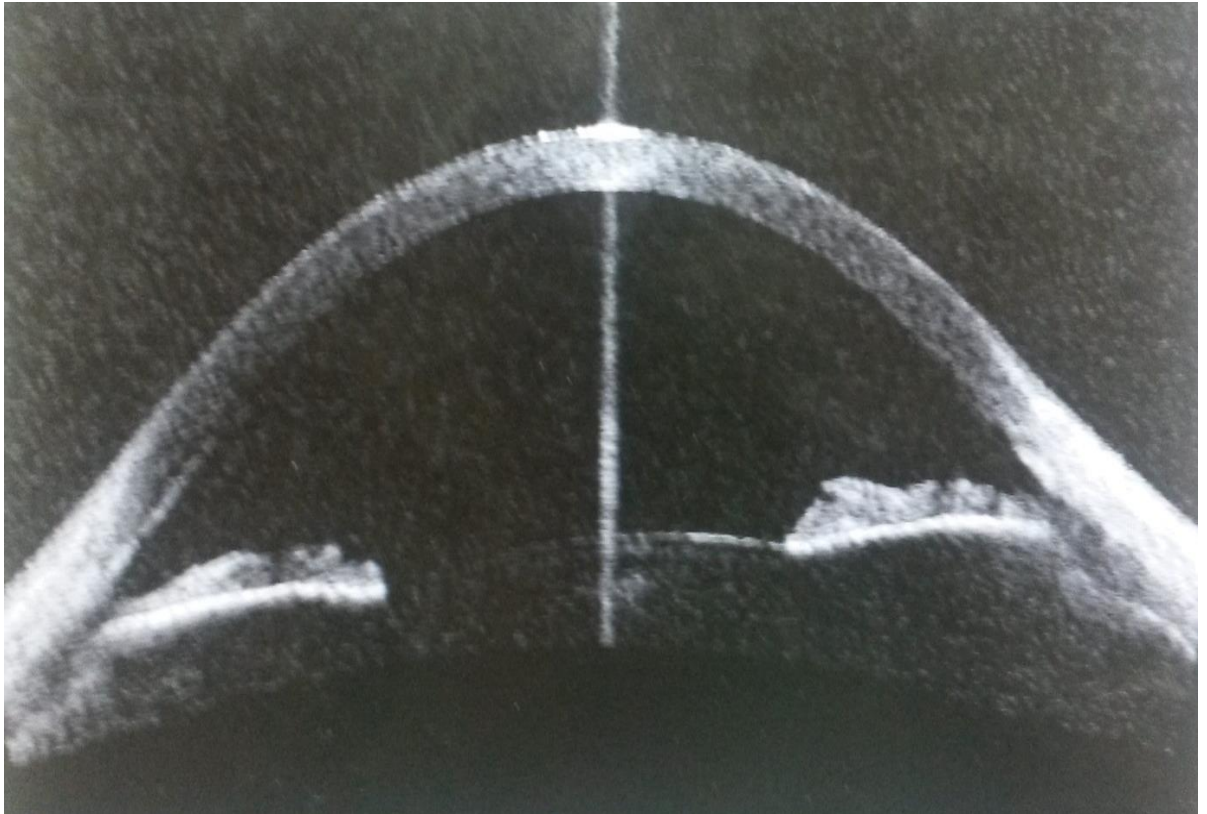


Figure 1.7. AS-OCT image of the anterior segment with distortion corrected for by the *Vistane*, utilising the *anterior segment single mode*.

1.5 Ciliary muscle morphology

Despite the potential role of the ciliary muscle in myopia (Mallen *et al.*, 2006; Bailey *et al.*, 2008; Buckhurst *et al.*, 2013; Pucker *et al.*, 2013), accommodation (Sheppard and Davies, 2010b; Lewis *et al.*, 2012; Lossing *et al.*, 2012) and presbyopia (Sheppard and Davies, 2011; Richdale *et al.*, 2013) there still remains a paucity of *in vivo* ciliary muscle research. *In vivo* imaging of the ciliary muscle is challenging due to the concealed position of the ciliary muscle behind the pigmented iris.

Various approaches to examine and measure the ciliary muscle have been employed. An investigation by Pardue and Sivak (2000) utilised 16 pairs of donor eyes, aged from 1 day to 107 years. One eye from each pair was treated with pilocarpine hydrochloride to pharmacologically stimulate ciliary muscle contraction, and the other treated in the same way with atropine sulphate to relax the ciliary muscle. Only a decline in anterior length of the ciliary muscle with age was significant ($R = -0.71$, $P < 0.001$), indicating that an increase in width and forward movement of the apical edge were the greatest age-related alterations in the

ciliary muscle. The chief accommodative alteration of the ciliary muscle was discovered to be a decline in length, presumed to be due to the longitudinal fibres.

More recent work (Sheppard and Davies, 2010b) utilised AS-OCT imaging to investigate ciliary muscle morphology in pre-presbyopes; The ciliary muscle in its relaxed state was found to have a significantly longer overall and anterior length in eyes of longer axial length (see figure 1.8).



Figure 1.8. Images demonstrating the noticeable difference in temporal ciliary muscle morphology between an axial myopic eye (top image; axial length 28.12 mm) and an emmetropic eye (bottom image; axial length 23.7 mm).

Anterior length was measured from the scleral spur to the point of ciliary muscle maximum width, using internal callipers of the *Visante* software to obtain the measurement. These measurements were taken at particular points along the ciliary muscle which were proportional to the ciliary muscle overall length, the most anterior measurement being represented as CM25, the muscle width at a point at which was 25 % of the overall length posterior to the scleral spur. Similarly CM50 and CM75 measures were taken at points 50 %

and 75 % (CM50 and CM75 respectively) of the total ciliary muscle length posterior to the scleral spur (see figure 1.9).



Figure 1.9. Measurements of ciliary muscle width were attained by Sheppard and Davies (2010b) with a calliper positioned perpendicular to the boundary between the ciliary muscle and sclera, with three chief width measurements obtained. These width measurements (CM25, CM50 and CM75) were taken at points along the ciliary muscle that were proportional to the overall length.

A different approach to measuring the ciliary muscle has been employed by other investigators, whereby thickness measurements were taken at fixed distances from the scleral spur (Oliveira *et al.*, 2005b; Bailey *et al.*, 2008; Lewis *et al.*, 2012; Pucker *et al.*, 2013); CMT1 represents a point 1 mm posterior to the scleral spur, with CMT2 and CMT3 taken at points 2 mm and 3 mm posterior to the scleral spur, respectively (see figure 1.10). CMTMAX represents the maximum ciliary muscle thickness. A potential limitation of this technique is that measurements do not take into consideration the fact that the total length of the ciliary muscle differs considerably with refractive error, such that a location 2 mm posterior to the scleral spur, for example, may signify a different ciliary body anatomical region in varying refractive errors (Sheppard and Davies, 2010b).

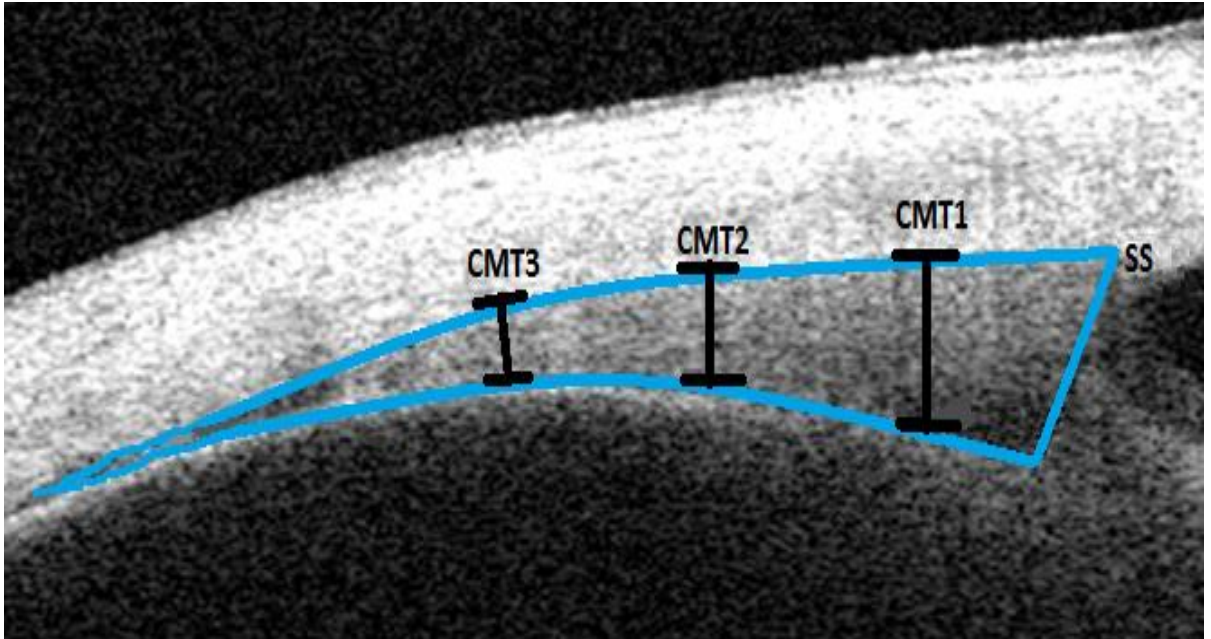


Figure 1.10. Representation of fixed width ciliary muscle thickness measurements. The blue outline represents the profile of the ciliary muscle. CMT1, CMT2 and CMT3 are taken 1, 2 and 3 mm posterior to the scleral spur (SS), respectively.

Nasal and temporal ciliary muscle discrepancies (within individuals) have been studied (Sheppard and Davies, 2010b) and interestingly, it was found that the accommodative shortening in the ciliary muscle anterior portion, is greater in the temporal ciliary muscle aspect than that of the nasal. Fittingly, in terms of nasal versus temporal disparity in ciliary muscle thickness, this was significantly increased temporally in CM50, CM75 and CM2. This nasal-temporal difference in thickness was least manifest for CM25, the most anteriorly measured location. Currently, the significance of this asymmetry is uncertain although it has been reasoned that the thicker side of the ciliary muscle would yield a more powerful contractile response, reinforced through the finding of increased accommodative shortening of the anterior portion of the temporal aspect of the ciliary muscle (Sheppard and Davies, 2010b). The nasal-temporal asymmetry in human ciliary body morphology has also been established through *in vitro* studies, identifying the temporal aspect being significantly longer throughout life (Aiello *et al.*, 1992). However, this discrepancy in length had not previously been observed *in vivo* (Sheppard and Davies, 2010b).

A limitation of previous studies is that inter-eye symmetry of the ciliary muscle has not been investigated as it has only been one eye, typically the right, which has been studied. A relatively recent investigation examined globe profile in emmetropia and myopia (Gilmartin *et al.*, 2013). Using a cohort of 55 adult participants, posterior vitreous chamber shapes were established using T2-weighted MRI. An emmetropic eye was mapped as coordinate

reference points to contrast with the myopic globe profile; these three-dimensional surface model coordinates were allotted to superior, inferior, nasal and temporal quadrants and plotted in a two-dimensional model to demonstrate the overall profile of respective quadrants (Gilmartin *et al.*, 2013). Asymmetry in the laterality of globe profile in myopia development was discovered, with nasal to temporal quadrants being asymmetric between right and left eyes- the temporal quadrant of the right eye corresponds with the nasal quadrant of the left eye (Gilmartin *et al.*, 2013). Since the division of nasal and temporal retinal nerve fibres into right and left visual fields occurs at the optic chiasm (Bron *et al.*, 1997), the coupling indicates that binocular growth may be synchronised by processes operating past the optic chiasm (Gilmartin *et al.*, 2013). Altered ciliary muscle morphology in myopia has been implicated in refractive error development (Bailey *et al.*, 2008) and such laterality in myopia development may translate to ciliary muscle laterality, though this matter has not been investigated in previous studies. More work is needed to fill this gap in the current knowledge, and one of the aims of this thesis is to provide answers relating to ciliary muscle morphology and laterality.

1.5.1 Ciliary muscle and refractive error

Myopia represents a significant health concern and is one of the foremost reasons for visual impairment worldwide (Lin *et al.*, 1996; Saw, 2003; Woodman *et al.*, 2011). The refractive condition affects approximately one sixth of the global population (Norton *et al.*, 2005; Logan *et al.*, 2011) and is continuing to increase in prevalence (Rose *et al.*, 2001; Vitale *et al.*, 2008), such that myopia has reached epidemic proportions in certain industrialised East Asian communities (e.g. Singapore) where at least 70 % of adolescents are myopic (Seet *et al.*, 2001; Logan *et al.*, 2011).

The effect of a high prevalence myopia on society is significant, and establishments in affected countries include refractive error in their health, educational and economic strategic plans (Logan *et al.*, 2011). Myopia can significantly hinder quality of life, ranging from being a simple visual inconvenience with financial cost to sufferers, to a predisposition to sight threatening pathological conditions (Mitchell *et al.*, 1999; Gilmartin, 2004; Logan *et al.*, 2011; O'Donoghue *et al.*, 2015). Pathologies linked to myopia include glaucoma (Mitchell *et al.*, 1999; Miki *et al.*, 2015), cataract (Lim *et al.*, 1999), chorioretinal degeneration and retinal detachment (Grossniklaus and Green, 1992). Whilst the specific cause of myopia is not fully understood, it is widely believed to have not only a genetic element but also environmental constituents (Mutti 2010; Woodman *et al.*, 2011; Ghosh *et al.*, 2014; Jin *et al.*, 2015; O'Donoghue *et al.*, 2015). In the current epidemic, axial length is regarded as the primary

ocular biometric component of refractive error, and is a well-known feature of myopia (Liao *et al.*, 2014; Jin *et al.*, 2015).

It would typically be expected that the ciliary muscle is longer in myopic eyes due to globe expansion, as van Alphen (1986) perceived a discernible thinning of the ciliary body with globe expansion *in vitro*. More recent work (Mutti *et al.*, 2000; Walker and Mutti, 2002; Harb *et al.*, 2006; Sheppard and Davies, 2010b; Buckhurst *et al.*, 2013) indicates that the ciliary region is not merely mechanically stretched with axial elongation, as the ciliary muscle in myopic subjects has not been found to be thinned as would be predicted by unaccompanied mechanical stretch.

Though it has previously been hypothesised that hyperopic subjects should exhibit a thicker ciliary muscle due to the increased accommodative effort expended compared to non-hyperopes (Oliveira *et al.*, 2005; Pucker *et al.*, 2013), no dependency between the proportional measurements of ciliary muscle thickness (CM25, CM50 & CM75) and axial length has been identified, (Sheppard and Davies, 2010). However, this contrasts to other work using AS-OCT, which determined a strong correlation between ciliary body thickness taken at fixed width measures, myopic refractive error and axial length (Bailey *et al.*, 2008). A common finding between both studies showed that the region 2 mm posterior to the scleral spur (CM2) did show an association of being thicker with greater axial length (Bailey *et al.*, 2008; Sheppard and Davies, 2010). Similarly, an investigation utilising UBM for the *in vivo* assessment of ciliary body thickness showed that the mean CBT2 (the ciliary body region 2 mm posterior to the scleral spur) was significantly greater in myopes than for hyperopes and emmetropes, whilst emmetropes also displayed a greater mean CBT2 than hyperopes. Likewise, mean CBT3 (the ciliary body region 3 mm posterior to the scleral spur) was shown to be significantly greater in myopes than emmetropes and hyperopes, and again, was significantly greater in emmetropes than that of hyperopes (Oliveira *et al.*, 2005). Interestingly, it was discovered that the inner apical angle of the ciliary muscle is wider in myopic subjects than emmetropes (see figure 1.11), though further research is needed to determine the relevance of this finding to refractive error development (Sheppard and Davies, 2010).



Figure 1.11. Top image shows the temporal ciliary muscle of an emmetropic eye (axial length 23.7 mm) and bottom image shows the temporal ciliary muscle of a myopic eye (axial length 28.12). The ciliary muscle inner apical angle appeared larger in the myopic eye (α , in myopia = 138° ; β , in emmetropia = 92°).

Eyes with longer axial lengths appeared to have greater ciliary muscle thickness values, both with accommodation, and in the cyclopleged state (Lewis *et al.*, 2012), linking mean axial length with ciliary muscle thickness and supporting previous findings that myopes have a thicker ciliary muscle than in emmetropic or hyperopic eyes (Bailey *et al.*, 2008). With accommodation, there was consistent ciliary muscle thickening in the anterior portion (CMTMAX and CMT1) with a thinning of the posterior portion of the ciliary muscle (CMT3) (Bailey *et al.*, 2008). Such results are consistent with the earlier findings of Sheppard and Davies (2010), that there is longitudinal and radial contraction of the ciliary muscle during accommodation. Interestingly, for CMT2, the measurements were relatively unchanged over a range of accommodative responses; where several subjects demonstrated thickening in this area with accommodation, other subjects showed thinning (Lewis *et al.*, 2012), highlighting that the accommodative response did not appear to be a significant contributor for shaping the behaviour of CMT2. There was also no suggestive trend to indicate which ciliary muscle are predisposed to thicken as opposed to thin at CMT2. Therefore, it was suggested that CMT2 is the approximate position of a fulcrum, providing the transition in the muscle from thickening action, to thinning during accommodation. The investigators indicate

that in some individuals the fulcrum position may be slightly ahead, or behind the CMT2 and that the position may also vary according to the level of accommodative effort expended (Lewis *et al.*, 2012).

Work by Sheppard and Davies (2010b) did not reveal any significant association between ciliary muscle thickness and refractive error and therefore, predicted that radial growth-thickening of the ciliary muscle occurs in conjunction with axial elongation during myopigenesis. Several other investigations have also contradicted the *in vitro* experimental findings of van Alphen, but by demonstrating the ciliary muscle to be thicker in the myopic eye compared with non-myopic eyes (Oliveira *et al.*, 2005a; Bailey *et al.*, 2008; Buckhurst *et al.*, 2013). Such thickening of the ciliary muscle indicates a potential physiological response of the myopic ciliary muscle, as opposed to a simple mechanical stretch (Bailey *et al.*, 2008), whilst the thinner hyperopic ciliary muscle has been hypothesised to result from a disruption of the basic stress-response relationship that occurs in all recognised muscles (Pucker *et al.*, 2013). Evidently, ciliary muscle morphology in terms of both length and thickness appears to be altered in myopic eyes. Nonetheless, there is ambiguity between findings of previous studies, and the relevance of these observations is not fully understood.

With respect to myopia development, it is well documented that principally there is an increase in axial length (Atchison *et al.*, 2004; Mutti *et al.*, 2007; Mutti 2010; Gilmartin *et al.*, 2013) of approximately 0.35 mm/ D, while dimensions of globe height and depth increase to a less significant degree (Atchison *et al.*, 2004). Figure 1.12 indicates the relationship between axial length and refractive error. Previously, it has been described that an acceleration of axial elongation occurs as spherical globe expansion becomes more prolate expansion (Mutti 2010), and other previous studies have describe the more prolate shape in myopia (Atchison *et al.*, 2004; Mutti *et al.*, 2007). It was predicted there is approximately a threefold increase in the rate of axial elongation when there is elliptical growth of the eye rather than spherical growth (Mutti *et al.*, 1998) and this has been shown to occur in the year prior to and subsequent to myopia onset (Mutti *et al.*, 2007; Mutti 2010). This lessened oblate shape in myopic eyes has been reported across several studies (Atchison *et al.*, 2004; Logan *et al.*, 2004; Mutti *et al.*, 2007; Bailey *et al.*, 2008), though the aetiology of this myopic prolate globe shape is uncertain.

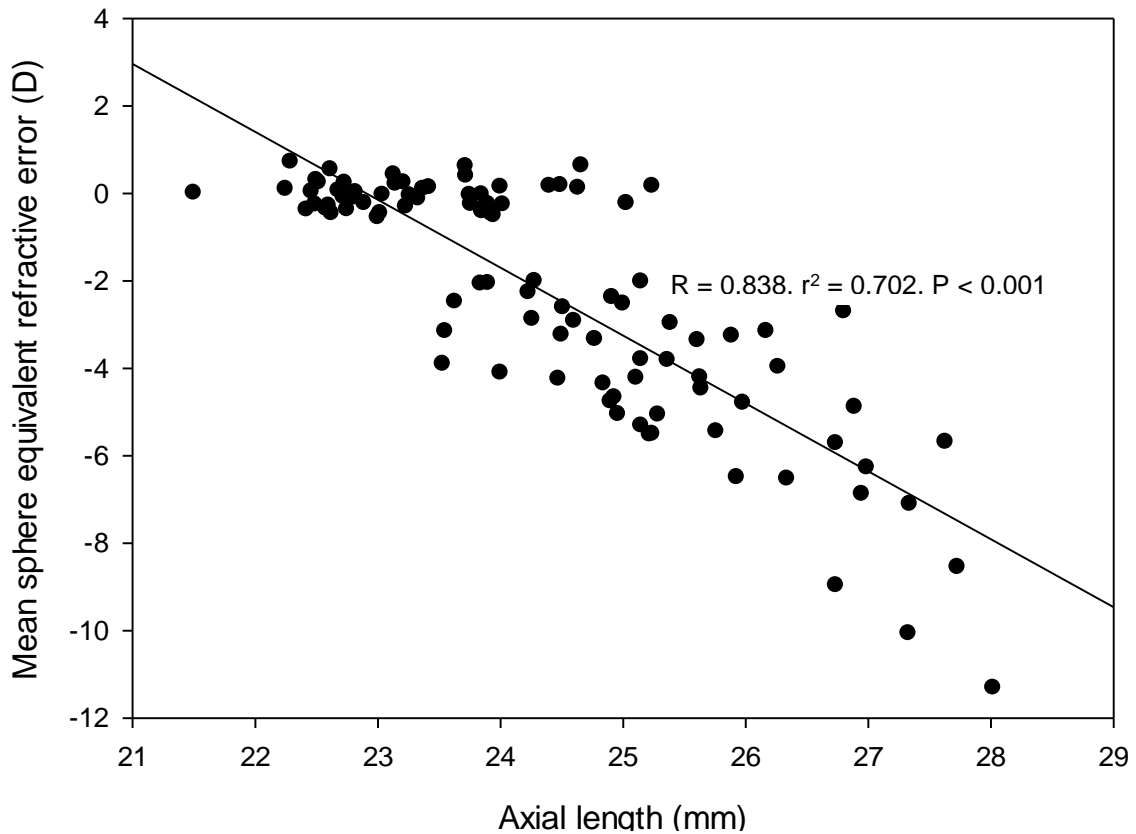


Figure 1.12. The relationship between mean sphere equivalent (MSE) refractive error and axial length, plotted using author's own data (n = 100). Axial length increases systematically with increasing negative MSE.

Lens thinning has been described as a significant process that maintains emmetropia, and an interruption of this precedes the development of myopia. During eye growth, there is expansion of the eye in all directions and the equatorial growth has reasonably been assumed to be responsible for this lens thinning (Mutti 2010). The mechanical stretching of the crystalline lens in the equatorial plane leads to a flatter and dioptrically weaker state; therefore an interruption to this process would provide no refractive compensation to the increasing axial length of the growing eye. So, Mutti hypothesises that myopia development is the optical consequence of limited crystalline lens compensation and more rapid axial elongation, due to interruption of the equatorial stretch and oblate globe shape which has been in place since infancy (Mutti 2010) (see Figure 1.13). This poses the question of what could cause this interruption to the equatorial expansion that allows for the lens thinning theory, or even the prolate expansion. Results from various studies including MRI work (Atchison *et al.*, 2004) and A-scan ultrasonography on the infant monkey (Smith *et al.*, 2005) indicate that equatorial expansion of the globe is a significant aspect in the development of myopia (Logan *et al.*, 2004; Mutti *et al.*, 2007; Bailey *et al.*, 2008). However, it is more difficult to measure the

equatorial diameter of the eye, compared with the axial length, hence there is not as much information relating to the former. Hypertrophy of the ciliary muscle could give rise to excessive collagen deposition running through the ciliary muscle in a circular orientation, such that the thickened ciliary muscle mechanically restricts equatorial expansion required for maintenance of emmetropia (see Figure 1.13) (Bailey *et al.*, 2008; Mutti 2010). Furthermore, this hypertrophic ciliary body would also cause enlargement of the ciliary muscle cells, yielding a reduced contractile response (Seidel and Weisbrodt, 1987; Bailey *et al.*, 2008).

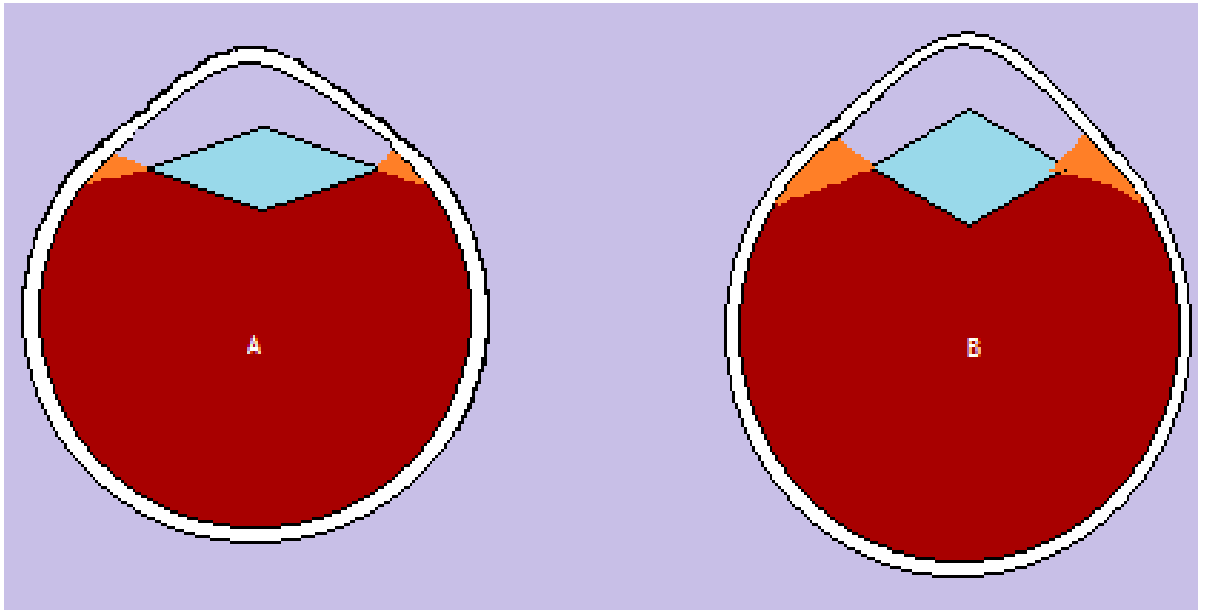


Figure 1.13. Illustration of theory of myopia development due to interruption to lens thinning adapted from Mutti *et al* (2010). 'A' represents an emmetropic eye, with moderate ciliary muscle size (orange) and axial length. 'B' represents myopic development with a thicker ciliary muscle mechanically restricting equatorial globe growth and thereby limiting lens (blue) thinning, such that axial elongation occurs.

In contrast to the previously documented globe profile in myopia, more recent findings have suggested that myopes rarely display prolate posterior chamber shapes (Gilmartin *et al.*, 2013). Regarding the vitreous chamber shape measured by MRI, the investigators describe emmetropic eye shape as being evidently oblate elliptical in shape, and in myopia, also an oblate ellipse but to a lesser extent such that the myopic vitreous chamber shape approximates to a spherical globe profile. It has been proposed that the myopic spherical globe shape may represent a biochemical limitation on advancing axial growth. Therefore, more oblate myopic eyes may be at increased risk of myopic progression than myopes with less oblate globe shapes (Gilmartin *et al.*, 2013). Prolate vitreous chamber shapes are likely to be just be distinctive to pathological myopia and high myopia (Moriyama *et al.*, 2011; Moriyama *et al.*, 2012; Ohno-Matsui *et al.*, 2012).

1.6 Theories of myopia development relating to the ciliary muscle

Theories of myopia development are extensive and a full review of all the theories is beyond the scope of this thesis. However, the theories linking myopia aetiology with accommodation and thereby the ciliary muscle, are documented in the following sections.

1.6.1 The hyperopic defocus model

A prevailing hypothesis concerning myopic development is the hyperopic defocus model (Harb *et al.*, 2006; Mutti *et al.*, 2006; Mutti 2010; Woodman *et al.*, 2011). In 1978, it was demonstrated that modest environmental changes to the chick during early visual experience could result in a high level of myopia in this species (Wallman *et al.*, 1978). Restriction to just the frontal visual field of the chicks produced extreme changes in ocular refraction (up to -24.00 D). Lateral field restriction was produced by translucent, hemispherical lenses that occluded each eye and a trapezoidal notch incised on the front of the occluder enabled the chicks to have frontal vision. The occluders were attached from hatching and were replaced by successively larger ones as the chicks grew. At 4-7 weeks the chicks were then refracted by streak retinoscopy, confirming highly myopic refractive errors. A decade later, work by Schaeffel and co-workers validated the research by showing that the axial length of the chick eye could be altered through the dioptric power and sign of the lenses provoking refractive error (Schaeffel *et al.*, 1988).

Subsequently, several studies utilising similar approaches have further developed the theory that eye growth is guided towards emmetropia by a visual feedback mechanism, detecting the sign and extent of blur (Irving *et al.*, 1992; Wildsoet and Wallman, 1995; McFadden *et al.*, 2004; Smith *et al.*, 2005; Berntsen *et al.*, 2011; Ho *et al.*, 2012). Specifically, according to the hyperopic retinal defocus model, the focal point of stimuli forms behind the retina, and this is believed to stimulate axial elongation so that the focal point is moved on the retina (Harb *et al.*, 2006; Mutti *et al.*, 2006; Berntsen *et al.*, 2010), as shown in Figure 1.14.

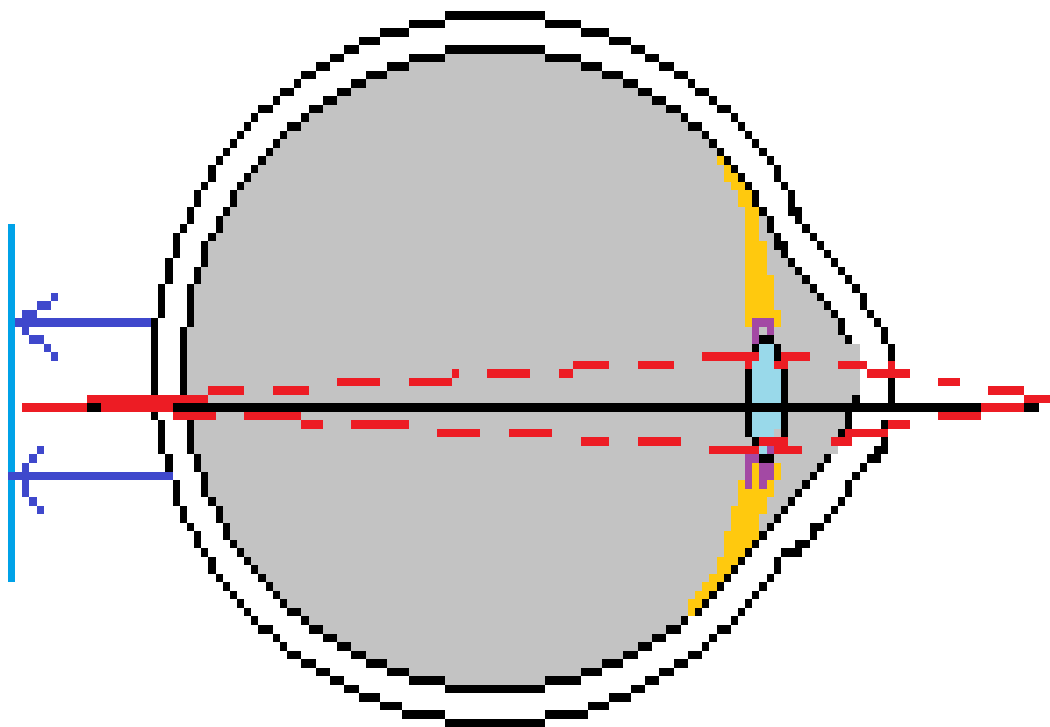


Figure 1.14. Illustration of the hyperopic defocus model. The light rays (red dotted lines) meet at a point posterior to the retina, on the blue vertical line. The eye is stimulated to grow towards this blue line (shown by blue arrows) so that the focal point falls on retina.

In contrast, myopic retinal defocus appears to inhibit axial growth, though this is vastly more robust in the chick eye than the mammalian eye, with the choroid of the chick actually pushing the retina forward towards the myopic conjugate point (Wallman *et al.*, 1995; Wildsoet and Wallman, 1995; Mutti *et al.*, 2006); several other animal species including the marmoset (Graham and Judge, 1999), monkey (Smith and Hung, 1999), and guinea pig (McFadden *et al.*, 2004) all demonstrated this response.

1.6.2 Hyperopic defocus and accommodative lag

Accommodative lag is the usual tendency to under accommodate to high demand stimuli and can be defined as the positive difference between the accommodative demand and accommodative response. This accommodative parameter can be accurately measured with an autorefractor to Badal stimuli (Berntsen *et al.*, 2010). The findings that myopic subjects between ages 5- 18 years accommodate with less accuracy than emmetropes, producing a lag of accommodative response, suggests there is a link with the resulting hyperopic retinal

defocus and accelerated axial growth in not just the animal based exemplar, but also in human myopia (Gwiazda *et al.*, 1993; Gwiazda *et al.*, 1995; Mutti *et al.*, 2006; Berntsen *et al.*, 2010; Berntsen *et al.*, 2011). Henceforth, what is of particular interest is whether increased accommodative lag is a precursor/ risk factor for myopia, or a consequence of the refractive condition.

Several studies on human participants (Goss, 1991; Drobe and Saint-Andre, 1995; Gwiazda *et al.*, 2005) have indicated that accommodative lag is increased prior to myopia onset. A longitudinal investigation by Gwiazda and co-workers (2005) identified an increase in accommodative lag in pre-myopic children two years before the onset of myopia. However, subsequent research by Mutti found that increased accommodative lag followed myopia onset by one year or greater (Mutti *et al.*, 2006), in agreement with studies documenting increased lag amongst myopic children (Gwiazda *et al.*, 1993; Gwiazda *et al.*, 1995). Results from this investigation indicated that 'became-myopic' children (those who had at least one non-myopic examination and developed myopia of at least -0.75 D in each principal meridian) that showed increased lag at myopia onset were those wearing spectacle correction, but this finding is unlikely to be a useful predictive factor of myopia as these children were already identified as being myopic by wearing the negative spectacle correction. The reason these children displayed a higher lag could simply be a result of additional accommodative demand with their correction in place. Similarly, accommodative lag was decreased along with accommodative demand for intermediate distance tasks in became-myopic children when their refraction was not fully corrected. This signifies the possibility that perhaps less hyperopic defocus is subjected to children with uncorrected myopia than with emmetropes during clinically substantial myopic development, providing they partake in intermediate-work visual tasks for a significant amount of time. It has been stated that accommodative lag might be a causative factor if lag escalated within a year before myopia onset, and the narrowness of this time scale reduces the basis of any preventative intervention as well as likelihood of it being a causative factor (Mutti *et al.*, 2006).

Interestingly, whilst accommodative lag is found to be greater in young progressing myopes than for emmetropes, it appears that the accommodation system may adapt and increase its response once myopia is stabilised, such that the differences in lags between stable myopic adults and adult emmetropes disappear (Abbott *et al.*, 1998; Nakatsuka *et al.*, 2003; Seidemann and Schaeffel, 2003; Harb *et al.*, 2006). Work investigating accommodative behaviour during sustained reading tasks in emmetropes and myopes (Harb *et al.*, 2006) showed no difference in lags between the two refractive categories during extended periods, consistent with various studies investigating brief accommodative periods (Gwiazda *et al.*,

1993; Nakatsuka *et al.*, 2003; Nakatsuka *et al.*, 2005). Similarly, more recent studies found an absence of a relationship between accommodative lag and myopia progression in children (Weizhong *et al.*, 2008; Berntsen *et al.*, 2011), disputing the hypothesis that foveal hyperopic defocus instigates myopia progression.

Blur adaptation is a neural mechanism which allows compensation of optical defocus by the visual system, to improve defocused visual acuity without changing ocular refraction (Pesudovs and Brennan, 1993; Mon-Williams *et al.*, 1998) and has been considered as a possible process linked to accommodation and myopia development (Harb *et al.*, 2006; Mutti *et al.*, 2006). Emmetropes and myopes both undergo blur adaptation, but this has been shown to be greater in myopic subjects, indicated from the improvements in grating acuity that they experience (George and Rosenfield, 2004). Controversially, another investigation showed an improvement in the accommodative response of myopes using blur adaptation from a diffusing film which was then removed, yet this had no effect on the response in emmetropic subjects (Vera-Diaz *et al.*, 2004). So if a greater amount of blur adaptation improves visual acuity and/ or accommodative response, it appears improbable that blur adaptation is responsible for the elevated accommodative lag following myopia onset (Mutti *et al.*, 2006).

The AC/A ratio is the amount of accommodative convergence (AC, prism dioptres) per unit of accommodative (A, Dioptres) response, and is a fundamental aspect of an individual's ocular motor system (Mutti *et al.*, 2000). Many cases of myopia show increased AC/A ratio (Gwiazda *et al.*, 1999; Mutti *et al.*, 2000), so it is this that may be responsible for the elevated lag, as sensory discrepancies between myopes and emmetropes may explain accommodative lag but do not account for the elevated convergence. The principle of this alternative viewpoint is that increased equatorial tension may result from excessive ciliary muscle and/ or lenticular stretch in the larger myopic eye (Mutti *et al.*, 2000) and it is this that may account for these accommodative characteristics linked with myopia (Mutti *et al.*, 2006). Physically, ciliary muscle tension could also warrant the more prolate ocular shape that has previously been observed in myopia (Mutti *et al.*, 2000; Atchison *et al.*, 2004; Logan *et al.*, 2004; Stone and Flitcroft, 2004; Mutti *et al.*, 2006; Verkharla *et al.*, 2012). It has been speculated that a mutual factor could link together a poorer accommodative response and myopia (Gwiazda *et al.*, 1995) and it is proposed that this mutual factor is a pseudocycloplegic state occurring in the eye at risk of myopia, and recently myopic eye. An increase in ciliary tension could heighten the accommodative effort required, giving rise to this term of pseudocycloplegia, as it reflects a trio of accommodative characteristics in cycloplegic eyes (Mutti *et al.*, 2000; Mutti *et al.*, 2006): a decline in tonic accommodation (Gilmartin and Hogan, 1985), a higher AC/A ratio (Gwiazda *et al.*, 1999; Mutti *et al.*, 2000) and an increased

accommodative lag (Gwiazda *et al.*, 1993; Mutti *et al.*, 2000; Harb *et al.*, 2006). Although increased magnitudes of tonic accommodation is linked with myopia onset in adults (Jiang, 1995), longitudinal investigations however, do not support this notion (Mutti *et al.*, 2000). Investigations have established that in spite of a relationship with prevalent refractive errors, tonic accommodation levels in non myopes are not a risk factor for myopia development (Zadnik *et al.*, 1999; Allen and O'Leary, 2006) and the concept is not discussed further in this thesis.

Researchers have hypothesised that the thicker ciliary muscle does not contract as accurately, resulting in an increased accommodative lag and resultant hyperopic defocus. However, whilst many researchers have described the morphology of the ciliary muscle, there is a paucity of information regarding how the morphology impacts accommodative function, if at all; one objective of this thesis is to fill this gap to enhance our understanding if, and how altered ciliary muscle morphology impacts on accommodative function.

1.6.3 Accommodative microfluctuations and refractive error

Microfluctuations are minute alterations in the ocular refractive power during steady- state accommodation (see Figure 1.15) and are comprised of both high and low frequency components (Campbell *et al.*, 1959; Kotulak and Schor, 1986; Winn *et al.*, 1990; Schultz *et al.*, 2009). An increase in the amplitude of the fluctuations occurs systematically with increasing stimulus demand, up to approximately -4.00 D (Kotulak and Schor, 1986; Harb *et al.*, 2006), predominantly as the power of the low frequency component increases (Day *et al.*, 2006; Schultz *et al.*, 2009).

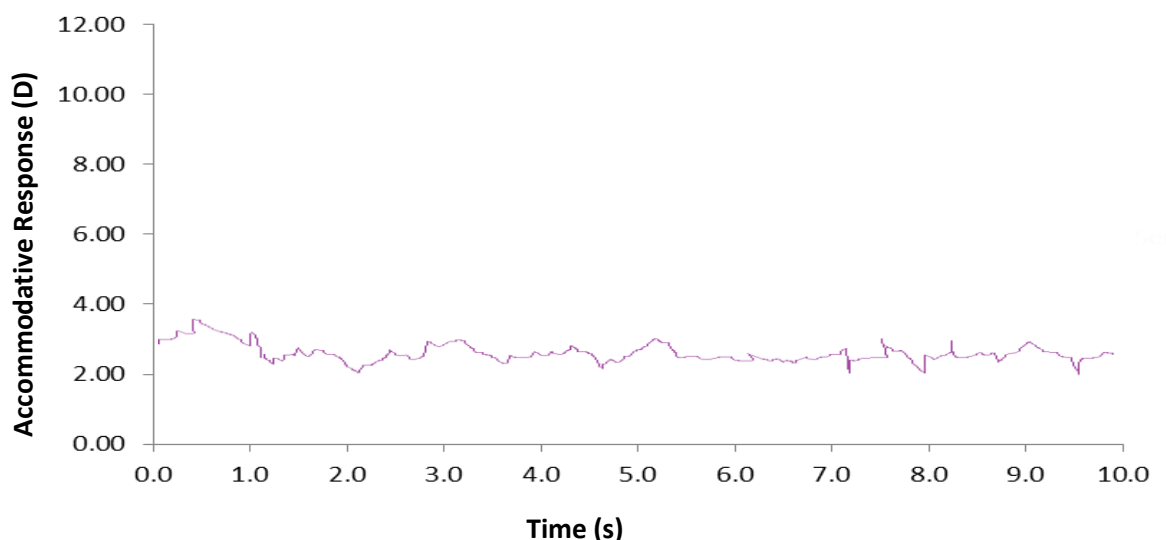


Figure 1.15. A typical accommodative response sample showing microfluctuations from a PowerRefractor measurement using -4.00 D stimulus demand.

Whilst the high frequency component appears to mirror noise from the arterial pulse in the accommodative apparatus (Collins *et al.*, 1995), not arising from anterior and posterior crystalline lens optical oscillations, the low frequency component appears to result from such lenticular oscillations, shown by ultrasound (Van der Heijde *et al.*, 1996; Schultz *et al.*, 2009). The power of this high frequency component attains a peak around the middle of the accommodative span or approximately -3.00 to -5.00 D, thereafter decreasing as the near point is approached (Miege and Denieul, 1988; Toshida *et al.*, 1998). Comparatively, accommodative fluctuations of the low frequency component are sustained drawing towards the near point (Schultz *et al.*, 2009). Importantly, the low frequency component may be involved in the mediation of the accommodative response (Charman and Heron, 1988; Winn *et al.*, 1989; Schultz *et al.*, 2009) owing to its link with conditions leading to a greater depth of focus (Schultz *et al.*, 2009) (e.g. amplified blur; Niwa and Tokoro, 1998) and smaller pupil size (Stark and Atchison, 1997). It is not influenced by the tension fluctuations of the zonules or lens capsule and has therefore been proposed to arise from a certain intrinsic characteristic of the lens, or feedback-control of noise in accommodative neural input (Miege and Denieul, 1988).

Refractive error groups have different microfluctuation characteristics. With a -4.00 D stimulus in a Badal system, investigators observed an increased power of the low frequency component with late-onset myopia, compared with that of early onset myopia and emmetropia (Seidel *et al.*, 2003). Yet, these variations were not observed in free-space viewing (Seidel *et al.*, 2005). Using multiple stimulus levels, late-onset myopes showed more power in the high frequency component unassociated with stimulus demand, and larger microfluctuations during long-distance viewing were evident. Such a rapid increase in power was not observed with the low frequency component when late-onset myopic subjects observed accommodative stimuli further than -3.00 D, as was the case with other refractive error groups (Day *et al.*, 2006). A more recent study found that the power of the accommodative microfluctuations was more variable amongst myopic individuals than in emmetropes (Harb *et al.*, 2006). Myopic subjects also demonstrated a significantly greater rise in accommodative microfluctuation power with closer sustained reading demands and with higher levels of myopia, at the closest reading demand (Harb *et al.*, 2006). It may be that the reason for this variation in results between these studies is that Harb and co-workers measured the accommodative microfluctuations during sustained reading when the subjects were likely to be fatigued, hence there is great importance in differentiating between fatigue-related accommodative microfluctuations and those anatomically based (Schultz *et al.*, 2009).

1.6.4 Ciliary muscle and accommodative microfluctuations

Fixation on a stationary near object results in rapid fluctuations about the mean level of accommodation (Charman and Heron, 1988). The power of the high frequency component peaks around the middle of the accommodative range for young individuals, or approximately -3.00 to -5.00 D, thereafter decreasing as the near point is approached (Miege and Denieul, 1988; Toshida *et al.*, 1998; Schultz *et al.*, 2009). Contrastingly, low frequency accommodative fluctuations are maintained towards the near point (Schultz *et al.*, 2009). The low frequency microfluctuations may be implicated in the mediation of the accommodative response (Charman and Heron, 1988; Winn *et al.*, 1989; Winn, 2000; Schultz *et al.*, 2009; Sreenivasan *et al.*, 2011) due to its relationship with conditions leading to a greater depth of focus (e.g. amplified blur (Niwa and Tokoro, 1998) and smaller pupil size (Stark and Atchison, 1997)); it has therefore been proposed to arise from a certain intrinsic characteristic of the lens, or feedback-control of noise in accommodative neural input, since they are not stimulated by zonular tension or lens capsule fluctuations (Miege and Denieul, 1988; Schultz *et al.*, 2009; Sreenivasan *et al.*, 2011).

A study in children (aged 8- 15 years) investigated the relationship between accommodative microfluctuations and size of the ciliary body (Schultz *et al.*, 2009). Results indicated that the high frequency component of accommodative microfluctuations had reduced power in association with thicker ciliary bodies measured at CM2, by 86 % for every 50 μm increase in ciliary body thickness. The authors suggest that perhaps a thicker ciliary body (associated with myopia) diminishes the effects of arterial pulse on accommodation and further hypothesised that with a thicker ciliary body, there is an improvement in the stability of the high frequency component of the accommodative response (Schultz *et al.*, 2009). In accordance with this finding, higher amounts of hyperopia were associated with greater powers of the high frequency accommodative fluctuations.

Such findings however, are at variance with other investigations reporting increased accommodative fluctuations with myopia (Seidel *et al.*, 2003; Day *et al.*, 2006; Harb *et al.*, 2006; Langaas *et al.*, 2008). For instance, studies have shown that subjects with late-onset myopia had increased accommodative microfluctuations during their myopia progression (Seidel *et al.*, 2003; Day *et al.*, 2006) and the power of the accommodative microfluctuations is more variable amongst myopic individuals than that of emmetropes (Harb *et al.*, 2006). In the latter study, myopic subjects also demonstrated a significantly greater rise in accommodative microfluctuation power with closer sustained reading demands and with higher levels of myopia, at the closest reading demand, contradicting the hypothesis that a

thicker ciliary muscle may stifle the effects of arterial pulse on accommodation. Schultz and co-workers (2009) predict the reason for this variation in results between these studies is that Harb *et al* (2006) measured the accommodative microfluctuations during sustained reading when the subjects were likely to be fatigued, and further stated the importance of differentiating between fatigue-related accommodative microfluctuations and those anatomically based. Whilst accommodative microfluctuations could be another characteristic of accommodation that is transitorily affected by the progression of myopia, more work is needed to establish whether a greater stability of accommodative microfluctuations is a precursor to myopigenesis.

1.6.5 Accommodative axial length changes

Several studies have demonstrated that intense close-work tasks, especially those involving high levels of cognitive demand, may result in transient periods of myopia (e.g. Wolffsohn *et al.*, 2003), leading to the development of permanent myopia (Adams and McBrien, 1992; Mallen *et al.*, 2006). Despite the uncertainty of the precise sequence of events causing myopia development, it is evident that vitreous chamber elongation is the chief structural correlate of myopia in both adults and children (McBrien and Adams, 1997; Mallen *et al.*, 2006; Gilmartin *et al.*, 2013). Many previous investigations have reported a temporary increase in axial length during (Drexler *et al.*, 1998; Mallen *et al.*, 2006; Read *et al.*, 2010) or directly following (Woodman *et al.*, 2010) an accommodative task, and have compared the differences in expandability between emmetropic and myopic subjects.

Partial coherence interferometry (PCI) was implemented by Drexler and co-workers (1998) to study the effect of accommodation on axial length (AXL) in myopic and emmetropic subjects. When observing a closed-loop accommodative target at a distance corresponding to their individual amplitude of accommodation (4.1 ± 2.0 D for the myopic group and 5.1 ± 1.2 D for the emmetropic group), the subjects displayed transient AXL increases; axial elongation was greatest in emmetropic eyes (mean $12.7 \mu\text{m}$), with myopic eyes lengthening by a significantly lesser magnitude (mean $5.2 \mu\text{m}$). It has been stated that, similar to previous reports of increased accommodative lags in myopes (Drexler *et al.*, 1998; Gwiazda *et al.*, 2005; Harb *et al.*, 2006; Mutti *et al.*, 2006), it could be assumed that the magnitude of accommodation, and hence AXL change during a near task would be slightly decreased in the myopic subjects (Woodman *et al.*, 2011). Despite this, results showed the opposite; larger increases in AXL following the near task were observed in myopic subjects compared to emmetropes: at 6 D, AXL change was $37 \pm 27 \mu\text{m}$ and $58 \pm 37 \mu\text{m}$ for emmetropes and

myopes, respectively (Mallen *et al.*, 2006) and at 5 D, AXL change was $10 \pm 15 \mu\text{m}$ and $20 \pm 20 \mu\text{m}$ for emmetropes and myopes, respectively (Woodman *et al.*, 2010).

The work of Mallen *et al.* (2006) also highlighted that the magnitude of transient axial elongation increased with the demand level of accommodative stimulation, as demonstrated by Drexler *et al.* (1998) in emmetropes. Moreover, it has been ascertained that this effect not only occurs in the emmetropic eye, but is more pronounced in myopic participants (see Figure 1.16) (Mallen *et al.*, 2006). The differences between both of these studies may be attributed to the fact that the latter investigation used a larger cohort of emmetropes and early-onset myopes with higher amplitudes of accommodation compared with the former study. The investigators of the latter study also controlled the accommodative demand between both emmetropic and myopic groups (2, 4, and 6 D above baseline), as opposed to the greatest extent of accommodative effort at the near point. In the study by Drexler *et al.* (1998), the accommodative response of the myopic participants was stimulated to a lesser degree than that of the emmetropic category (mean values of 5.1 D for the emmetropes and 4.1 D for myopes). As such, it is possible that the accommodative ocular expandability of the myopic subjects was somewhat underestimated (Mallen *et al.*, 2006). Transient increases in axial length were again observed during accommodation, but in contrast to Drexler *et al.*, the greatest magnitude of elongation was observed in myopic eyes.

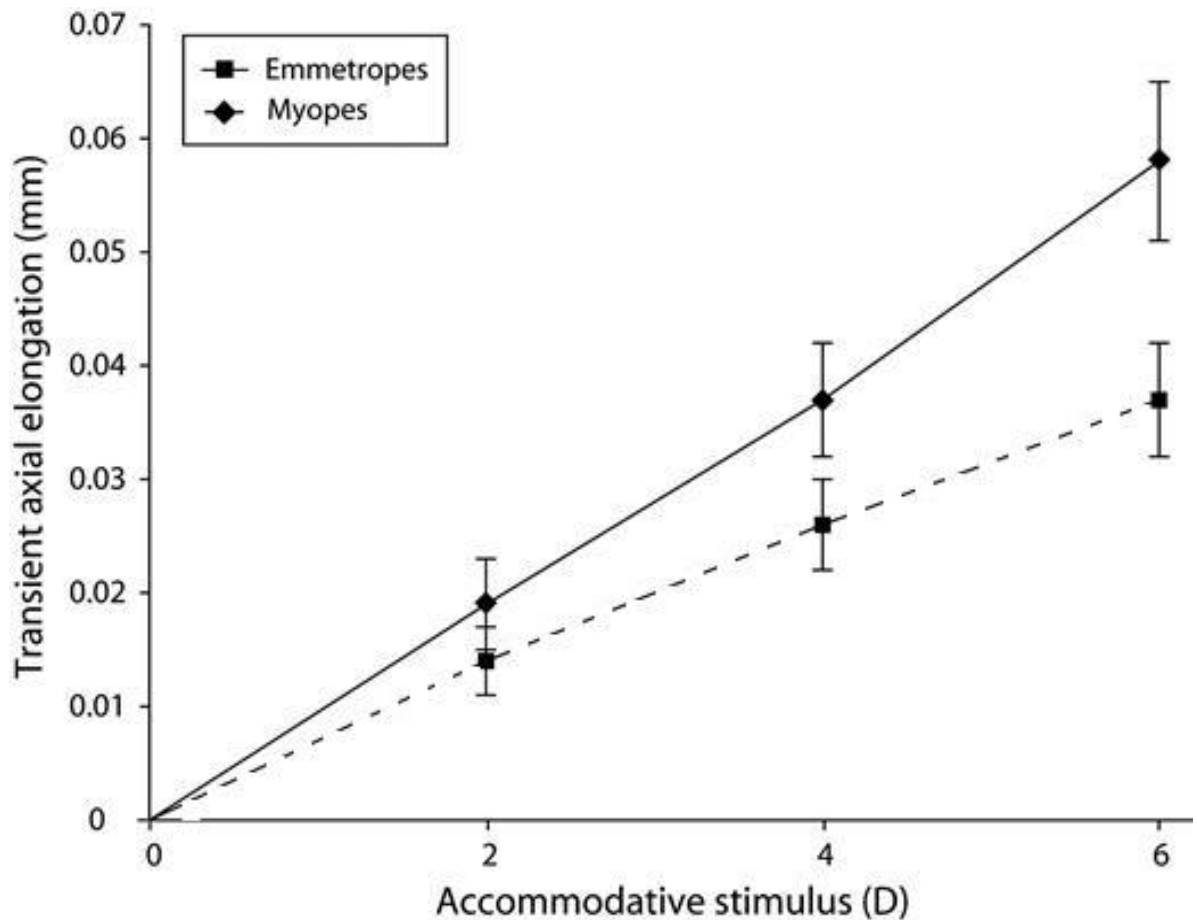


Figure 1.16. Magnitude of mean transient axial elongation in emmetropes (dashed line) and myopes (solid line) that occurred in the investigation by Mallen *et al* (2006) at 2 D, 4 D and 6 D. $n = 60$, error bars indicate the standard deviation.

The *IOLMaster* (Carl Zeiss Meditec, Inc., Dublin, CA) utilises an average ocular refractive index in order to calculate axial length from the optical path length, and hence may be liable to an overestimation of up to 0.02 mm (20 μ m) in axial length for an eye accommodating to a 10 D stimulus in comparison with PCI methods which assign individual refractive indices for the ocular components (Mallen *et al.*, 2006). Previous work has established that changes in the accommodative apparatus during accommodation may produce errors in axial length measurements obtained from the *IOLMaster* (Atchison and Smith, 2004). The basis of this potential error is the increase in optical path length (i.e., the outcome of the linear aspect of a specified optical medium and the refractive index of that medium; Mallen *et al.*, 2006) that results from the forward movement of the anterior vertex of the crystalline lens into the anterior chamber and the thickness increase of the crystalline lens during the accommodative response. During the response, the anterior portion of the crystalline lens which has a higher refractive index ($n' = 1.386$) than that of the aqueous humour ($n' = 1.336$) it displaces, results in an increase in optical path length (Atchison and Smith, 2004; Mallen *et al.*, 2006; Read *et*

al., 2010; Woodman *et al.*, 2010; Woodman *et al.*, 2012). Despite the possible *IOLMaster* exaggeration of the axial elongation accompanying the accommodative response that was not corrected for, myopic eyes still underwent a greater magnitude of transient axial expandability than that of emmetropes at higher accommodative demand levels (Mallen *et al.*, 2006).

Similarly, it was demonstrated in a more recent investigation that immediately after a period of sustained close work, significant axial elongation occurred in young adult subjects (Woodman *et al.*, 2010). Such work follows on from several previous investigations that determined the occurrence of significant axial elongation during accommodation (Drexler *et al.*, 1998; Mallen *et al.*, 2006; Read *et al.*, 2010), by determining that axial elongation also continues for a brief episode following the cessation of accommodation. Myopic subjects were segregated into either progressing or stable subcategories and it was found that the progressing myopes displayed the greatest magnitude of axial expansion of any group instantly succeeding the near task (Woodman *et al.*, 2010). Ten minutes after the accommodative task, axial lengths had reverted to their original levels (Woodman *et al.*, 2010; Woodman *et al.*, 2012).

The investigation by Mallen *et al.* (2006) also showed that there was no significant link observed between MSE and transient expandability during accommodation, or between baseline AXL and transient expandability. Such findings support a recent study which investigated the time course of expandability and recovery of axial length during a 30 minute 4 D accommodative task (Woodman *et al.*, 2012). Despite that the axial elongation during the accommodation task appeared to have a slightly higher magnitude in the myopic participants, corrected axial length data highlight that discrepancies in accommodative expandability during the task between the emmetropic and myopic groups were not statistically significant (Woodman *et al.*, 2012). Nevertheless, in the post- accommodative task measures, significant differences associated with refractive error were determined; Instantly following near task culmination AXL in the myopes was significantly greater than baseline levels ($13 \pm 28 \mu\text{m}$) and myopes demonstrated a significantly greater change in corrected AXL from baseline compared to emmetropes, both directly after the accommodative task and 5 minutes following task cessation. However, none of the AXL changes in the emmetropic group post-task were significantly different from baseline (Woodman *et al.*, 2012). Contrary to this, a further investigation using the *Lenstar LS 900* (Haag-Streit, Koeniz, Switzerland) noncontact optical biometer at three different accommodative demand levels (0 D, 3 D and 6 D) showed no significant difference in the magnitude of accommodative expandability between emmetropes

and myopes, with and without correction for axial length measurements (Read *et al.*, 2010). As a significant variation in elongation was identified for a 6 D accommodative stimulus (Mallen *et al.*, 2006), the investigators agreed with the concept that there is an intrinsic difference in the structural disposition of the myopic eye, such that eyes of myopic individuals are more prone to transient biometric alterations during high accommodation levels, than their emmetropic equivalents; changes in scleral biochemical, biomechanical and structural properties have been previously reported to show a link with myopia (Mallen *et al.*, 2006; McBrien *et al.*, 2009; Woodman *et al.*, 2010; Woodman *et al.*, 2012), which may therefore account for the disparities observed between myopes and emmetropes in accommodative expandability studies (Mallen *et al.*, 2006; Woodman *et al.*, 2010).

1.6.6 Ciliary muscle and accommodative axial length changes

As discussed in section 1.5.1, hyperopic defocus arising as a consequence of increased accommodative lag during near vision has been shown to be a plausible factor in myopigenesis. A very slight reduction of the amount of this hyperopic blur may occur from the transient axial elongation during sustained accommodative effort (Mallen *et al.*, 2006). Though this effect has been shown to be more pronounced in myopes than emmetropes, the authors stated that it is unlikely to be of any clinical significance. Transient elongation could be a result of the ciliary muscle contraction transmitting an inward pull force to an area of the sclera and choroid adjacent to the ciliary body. In order to maintain a constant ocular volume from this effect, a rearward displacement of the posterior portion of the globe is required, thereby resulting in a transient axial length increase (Mallen *et al.*, 2006).

Whilst to date, the cornea is not a recognised structure involved in the Helmholtz theory of ocular accommodation (Ni *et al.*, 2013), corneal alterations with accommodation have been debated across the literature (Buehren *et al.*, 2003; Yasuda *et al.*, 2003; Yasuda and Yamaguchi, 2005; Read *et al.*, 2007). Yasuda and Yamaguchi (2005) demonstrated a steepening of the central cornea instigated by ciliary muscle contraction, induced by pilocarpine. In contrast, Read *et al.* (2007) found no significant corneal changes with accommodation in young participants. However, it was later indicated that the results from the investigation by Read and co-workers (2007) did not wholly disprove corneal changes (Ni *et al.*, 2013) as one subject in the study ($n = 11$) was found to have significant accommodative corneal alterations, and suggested that the posterior cornea may be affected with ocular accommodation (Read *et al.*, 2007). A relatively recent study also reported that accommodation produced corneal changes, demonstrating alterations in central and peripheral corneal curvature (a steepening of both anterior and posterior cornea) in both

young and presbyopic subjects (Ni *et al.*, 2013). Such findings therefore signify the capability for transient biometric ocular alteration during the accommodative response (Yasuda and Yamaguchi, 2005; Mallen *et al.*, 2006); the cornea had been defined as elastic, soft and modifiable, and is implicated in the accommodation process (Ni *et al.*, 2013). It has been proposed that the reason for the greater elongation seen in myopic eyes, is decreased ocular rigidity and a greater efficiency of force transmission from the ciliary muscle to the sclera and choroid in myopic subjects (Mallen *et al.*, 2006; Woodman *et al.*, 2010). However, another investigation reported no variance in ocular rigidity between myopic and emmetropic children (Schmid *et al.*, 2003). Yet, it has been indicated that there may be discrepancies between myopes and emmetropes in the morphology of the ciliary body, causing ciliary muscle forces to be transmitted differently to the choroid and sclera amongst these different refractive groups (Mallen *et al.*, 2006; Woodman *et al.*, 2010; Ghosh *et al.*, 2014).

An alternative anatomical change has been proposed which could stimulate the apparent increase in axial length: a thinning of the choroid, as opposed to a stretching of the globe (Woodman *et al.*, 2012). In the investigation by Woodman and co-workers (2012), some evidence of decreased choroidal thickness during accommodation was found, and such choroidal changes displayed a significant negative correlation with the axial length alterations. Myopic participants demonstrated the most noticeable decreases in choroidal thickness during accommodation, with the greatest magnitude of change in choroidal thickness perceived 10 minutes following commencement of the accommodative task. The choroid of the myopic subjects became thinner on average by $9 \pm 18 \mu\text{m}$, and the emmetropes by $7 \pm 22 \mu\text{m}$; the emmetropic participants showed no significant reduction in choroidal thickness with accommodation (Woodman *et al.*, 2012). The magnitude of alteration in choroidal thickness during accommodation compared to axial length (38 %), along with the relatively weak relationship between the two measures led the authors to conclude that whilst choroidal thickness alterations appear to influence the alterations in axial elongation, multiple other factors such as scleral stretch are likely to also contribute to accommodative axial elongation (Woodman *et al.*, 2012).

It is feasible that ciliary muscle morphology impacts on transient accommodative elongation, though previous work has not examined this. Ciliary muscle parameters could be linked to ocular biometric differences between emmetropes and myopes. The present body of research is the first to explore the potential relationship between ciliary muscle characteristics with refractive error and accommodation, and is documented in subsequent chapters.

1.7 Ciliary muscle morphology in amblyopia and anisometropia

Amblyopia is a developmental disorder due to abnormal visual input in early life, during the critical period(s) of visual development, that causes reduced visual acuity in the affected eye(s) and subsequent binocular dysfunction (Wiesel and Hubel, 1963; Webber and Wood, 2005; Veneruso *et al.*, 2014). The prevalence of the condition in the population is approximately 3 % (Thompson *et al.*, 1991; Attebo *et al.*, 1998; Polling *et al.*, 2012). Clinically, amblyopia is characterised by a one or more line difference in visual acuity between both eyes (Thompson *et al.*, 1991), cannot be detected through physical ocular examination, and can be reversed by therapeutic treatment in some cases (Webber and Wood, 2005). When amblyopia, the most common cause of uncorrectable reduced vision in children and in adults up to 60 years of age, is not treated, a permanent deficit in vision ensues (Wang *et al.*, 2000; Simons, 2005; Bhola *et al.*, 2006; Xiao *et al.*, 2015). The most common risk factors for amblyopia include strabismus, presence of heterophoria or micro-squint (Attebo *et al.*, 1998; Webber and Wood, 2005), and anisometropia (Von Noorden, 1985; Attebo *et al.*, 1998; Webber and Wood, 2005), defined as a difference in the sphere or cylinder between the two eyes of at least one dioptre (Attebo *et al.*, 1998; Webber and Wood, 2005; Hashemi *et al.*, 2013). These conditions have therefore principally been targeted in childhood vision screenings (Webber and Wood, 2005).

Biometric data on the changes in ocular parameters and their involvement in emmetropisation have been widely studied (Ehrlich *et al.*, 1997; Mutti and Zadnik, 1998; Zadnik *et al.*, 2003; Mutti *et al.*, 2005; Mutti 2010; Flitcroft, 2014), as well as the ocular biometric correlates in myopia (McBrien and Adams, 1997; Atchison *et al.*, 2004; Mutti *et al.*, 2007; Buckhurst *et al.*, 2013; Gilmartin *et al.*, 2013). As such, a growing body of evidence supports the findings of increased length and thickness of the ciliary muscle (Oliveira *et al.*, 2005; Bailey *et al.*, 2008; Schultz *et al.*, 2009; Sheppard and Davies, 2010; Buckhurst *et al.*, 2013). However, whilst information relating to ocular biometric data in amblyopia has been investigated, there have been no reports of ciliary muscle morphology in amblyopia. Accommodation is considered to be a symmetrical response (Charman, 2004; Horwood and Riddell, 2010), whilst amblyopes demonstrate aniso-accommodation, with the accommodative response being driven by the least amblyopic eye (Horwood and Riddell, 2010). Similarly, reports indicate that the stimulus-response slope of the amblyopic eye is characteristically flatter than in the nonamblyopic eye (Ciuffreda *et al.*, 1984; Horwood and Riddell, 2010). Since amblyopic eyes have a reduced visual output and accommodation (Ciuffreda and Rumpf, 1985; Maheshwari *et al.*, 2011), it would intuitively be thought that ciliary muscle morphology should be altered in the amblyopic eye and asymmetry of the ciliary muscle across both eyes may be expected where amblyopia has been present for most of an adult's life.

Despite a paucity of information relating to ciliary muscle morphology and biometry in adult amblyopes, paediatric investigations indicate that reduced axial length is present in some amblyopias (Kugelberg *et al.*, 1996; Cass and Tromans, 2008). Ocular parameters and their relationship in both strabismic and anisometropic amblyopic eyes were studied (Cass and Tromans, 2008) and it was reported that the components of the amblyopic eye differ physically from their fellow non-amblyopic eye across both amblyopic groups. Whilst the anisometropic amblyopic eye seemed to be a proportionally smaller version of the fellow eye largely due to a greater magnitude of hyperopia, the strabismic amblyopic eye was found to have a disproportionately greater degree of anterior chamber reduction and crystalline lens thickness, a reduced vitreous chamber depth and therefore total axial length (Cass and Tromans, 2008); the authors suggested that the strabismic eye may be under-developed, with a delay of emmetropisation in the infantile phase though it has not been ascertained whether the reported biometric characteristics are a consequence of cause of amblyopia, hence, it is feasible that the ciliary muscle in amblyopia is also under-developed. More recently, a biometric investigation was carried out on an anisometropic adult cohort aged 40 – 64 years (Hashemi *et al.*, 2013) and reported that axial length asymmetry had the strongest relationship with anisometropia, in keeping with biometric findings in anisometropic children aged 6- 7 and 12 – 13 years (O'Donoghue *et al.*, 2013), though ocular biometry such as corneal power, lens power and anterior chamber depth were also linked to anisometropia in the investigation by Hashemi and co- workers (2013).

The literature on ciliary muscle morphology in anisometropia without amblyopia, albeit very limited, suggests that anisometropic subjects do not follow a different trend from the rest of the population (Kuchem *et al.*, 2013). Evidence from this investigation using AS-OCT to acquire ciliary muscle images, showed that in low levels of anisometropia (mean 1.85 ± 1.24 D) the ciliary muscle thickness of the more myopic eye does not differ significantly from that of the shorter, more hyperopic fellow- eye. Similarly the magnitude of the interocular difference in refractive error was not linked with an interocular difference of ciliary muscle thickness at any measured thickness parameter. As such, the authors stated that in anisometropic ocular development, it is possible for an eye to undergo a greater degree of myopic expansion than its fellow eye, without the concomitant thickening of the ciliary muscle (Kuchem *et al.*, 2013) that is generally observed in isometropic myopia (Oliveira *et al.*, 2005; Bailey *et al.*, 2008; Schultz *et al.*, 2009; Buckhurst *et al.*, 2013). However, the results from a previous investigation (Muftuoglu *et al.*, 2009), differ greatly from the work by Kuchem and co-workers (2013), as greater ciliary muscle thickness was observed in the more myopic eye of most subjects with unilateral high myopia.

As amblyopic eyes have reduced visual output and accommodation, it is of interest to understand how amblyopia which develops at a very young age, may impact on the growth and development of the ciliary muscle. Ciliary muscle morphology in anisometropic and strabismic amblyopia is documented for the first time, and detailed in chapter 6 of this thesis.

1.8 Instrumentation and measurement techniques

The subsequent experimental chapters describe the application of a range of advanced instrumentation to image the accommodative apparatus and measure structural and refractive changes. An account of the technical specification of the instruments used along with specific measurement techniques and bespoke instrument attachments developed for ophthalmic research, are discussed in this section.

1.8.1 Grand Seiko WAM-5500 auto ref/keratometer

Autorefractometry is widely used in clinical practice during the pre-screening examination as a starting point for subjective refraction, as well as in a research setting to objectively measure the refractive power of the eye (Bullimore, 2000; Sheppard and Davies, 2010a) through calculation of the vergence light reflected from the retina (Benjamin, 2006). The literature recognises that most modern open-view autorefractors are precise and highly consistent compared with subjective refraction (Kings *et al.*, 1996; Elliott *et al.*, 1997; Bullimore *et al.*, 1998; Mallen *et al.*, 2001; Cleary *et al.*, 2009; Sheppard and Davies, 2010a), making them effective tools in research investigations of refractive error (Bullimore *et al.*, 1998; Walline *et al.*, 1999).

The Grand Seiko WAM-5500 Auto Ref/Keratometer (Grand Seiko Co. Ltd., Hiroshima, Japan) is a binocular open-view instrument (see figure 1.16) that measures pupil size and keratometry in addition to refractive error, and has been previously described and validated (Sheppard and Davies, 2010a). Instrument-induced myopia generated by proximal accommodation is characteristic of closed-view devices, and is reduced by the open-view specification (Hennessy, 1975; Smith, 1983; Rosenfield and Ciuffreda, 1991; Sheppard and Davies, 2010a). An internal 5.6 inch colour monitor displays the pupil to allow subject fixation to be monitored and aid instrument alignment with the patient's visual axis. Pupil size data is obtained by automatic detection of the iris boundary and successive superimposition of a circle of best fit. Measurement data is also displayed, of which hard copies can be obtained from the in-built printer (Sheppard and Davies, 2010a).



Figure 1.17. The Grand Seiko WAM-5500 Auto Ref/Keratometer (Grand Seiko Co. Ltd., Hiroshima, Japan) within the Ophthalmic Research Group laboratories in Aston University.

Objective refraction is determined by multiple meridian digital analysis of an infra-red measurement ring, which is reflected off the retina and brought into approximate focus by an internal motorised rack. The WAM-5500 measures refraction with a range of ± 22.00 DS and ± 10.00 DC in increments of 0.01, 0.12 or 0.25 D for power and increments of 1° for cylindrical axis. The repeatability during measurement sessions, calculated from the standard deviation of 5 measurements obtained in one session is good, with reported values of ± 0.09 D for the spherical constituent; ± 0.14 D for the cylindrical component (Sheppard and Davies, 2010a). Similarly, between measurement sessions, bias for the spherical constituent were -0.04 ± 0.26 D; the cylindrical constituent: -0.07 ± 0.29 D, MSE -0.07 ± 0.26 D. The difference between subjective refraction and objective refraction with the WAM-5500 has been

determined: spherical constituent as 0.04 ± 0.41 D; cylindrical constituent - 0.10 ± 0.34 D; MSE - 0.01 ± 0.38 D; (Sheppard and Davies, 2010a).

The WAM-5500 like other autorefractors, may underestimate the level of hyperopia in a small number of young adults which is likely owing to the capability of young adults to expend their large amplitude of accommodation to achieve maximum clarity of the target (Mallen *et al.*, 2001; Davies *et al.*, 2003; Sheppard and Davies, 2010a). The minimum pupil size required for refraction is 2.3 mm, smaller than for several other autorefractors, such as the Shin-Nippon SRW-5000/Grand Seiko WV-500 (2.9 mm) (Mallen *et al.*, 2001) and Tracey VisualFunction Analyzer (2.5 mm) (Cleary *et al.*, 2009). Measurement of pupil size is obtained from the superimposition of a best-fit circle from the automatic detection of the iris boundary and is quantified in 0.1 mm increments concurrently with objective refraction. Keratometry is calculated with the instrument by analysis of the diameter of an additional infra-red ring reflected off the cornea, measured in 3 meridians which are each separated by 60° . Corneal power can be measured in the range of 33.75- 67.50 D. and corneal radii between 5.0 - 10.0 mm (0.01 mm increments). WAM-5500 keratometry measures are on average steeper compared with Javal-Schiotz values, by -0.06 ± 0.08 mm and -0.05 ± 0.07 mm in the vertical and horizontal meridians, respectively (Sheppard and Davies, 2010a). The WAM-5500 has been widely utilised across accommodative studies (e.g. Sheppard and Davies, 2010b; Alderson *et al.*, 2012).

1.8.2 Distance refractive error measurement technique

Binocular distance refractive error obtained with the Grand Seiko WAM-5500, utilises five measurements of refractive error taken for each eye, averaged and converted into MSE, for both eyes. The participant is instructed to look through the screen of the instrument at the centre of a Maltese cross fixation target through the mirror, stimulating a 6 metre distance.

1.8.3 Stimulus- response accommodative error measurement technique

To obtain stimulus- response accommodation data, static accommodation responses (0.0, 1.0, 2.0, 3.0, 5.0, 6.0, 8.0 D) are measured for the right eye of each participant (with the left eye occluded with a patch), using the Grand Seiko WAM 5500 with an attached Badal lens system and participant focussing on the centre of a Maltese cross target (see Figure 1.18), with five measurements being taken and converted into MSE in the same way as for distance refractive error. The sequence of stimulus demand level is randomised and the participant is asked to relax and stare into the distance for approximately 1 minute following measurements at each stimulus demand level. Myopic participants wear contact lenses appropriate for their habitual refractive error, for all accommodative measures.



Figure 1.18. Grand Seiko WAM 5500 with Badal lens system. The participant rests their chin on the chin rest (farthest left) and focusses through the window of the instrument and Badal lens respectively, to the centre of the Maltese cross. The Maltese cross target can be moved to varying distances to alter the accommodative demand.

1.8.4 Analysis of stimulus- response accommodation data

The stimulus- response curve has frequently been utilised to assess the overall steady- state accommodative response (Chauhan and Charman, 1995). Commonly, a single parameter, the linear regression slope of this function, has been employed to indicate the steady-state stimulus- response (see Figure 1.19). However, whilst the regression slope is known to be valuable, it is not a wholly accurate measure of the accommodative response and an alternative single-figure index to characterise the stimulus-response function has been proposed (Chauhan and Charman, 1995).

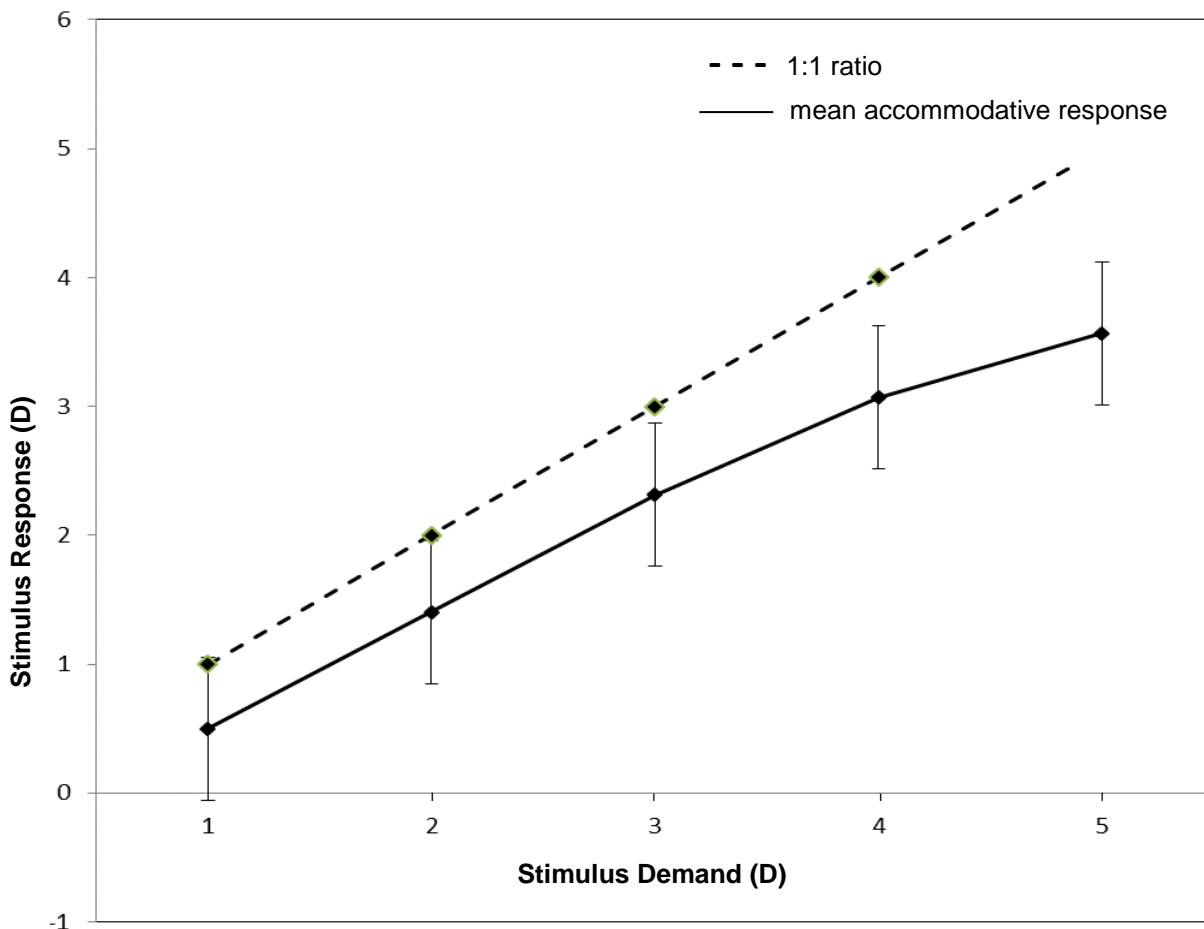


Figure 1.19. A mean accommodative stimulus- response curve for 100 pre-presbyopic subjects, taken from author's own data. The dotted line indicates a 1:1 relationship between the demand of the stimulus and the response to the stimulus at each demand level; the black complete line represents the mean accommodative response of the cohort. Error bars indicate the standard deviation. There is a greater lag of accommodation as stimulus demand is increased.

When analysing the accommodative stimulus- response curves, it is problematic determining which parameter, if any, of the linear regression analysis to use, as comparisons established on the curve alone may be misleading, as may be those utilising the correlation coefficient or intercept of the regression line (Chauhan and Charman, 1995). It would seem more valuable if there was an amalgamation of all the parameters into a single index which would review the precision of the response over a given stimulus interval. Chauhan and Charman (1995) suggested a method of defining such an index and thereby calculated the area between the best fit curve and the unit ratio; the accommodative stimulus response curves can now be compared by a method known as the accommodative error index (AEI) (Chauhan and Charman, 1995) and several subsequent investigations have since employed this method (e.g. Woodhouse *et al.*, 2000; Allen and O'Leary, 2006). Accurate accommodation at all stimulus demands is indicated by an AEI of 0 D. A value > 0 D indicates the level of

accommodative inaccuracy (Chauhan and Charman, 1995; Woodhouse *et al.*, 2000). The AEI for the monocular response to targets placed at the seven demand levels (1, 2, 3, 4, 5, 6 and 8 D) will be calculated using the following formula:

$$AEI = \frac{\left[(1 - m) \left[\frac{x_1 + x_2}{2} \right] - c \right]}{r^2}$$

Equation 1. Accommodative Error Index (Chauhan and Charman, 1995).

m = slope of response line

c = intercept of response line

x1 = farthest stimulus dioptic equivalent

x2 = nearest stimulus dioptic equivalent

r = correlation coefficient

1.8.5 Measure of accommodative axial length changes

The *Lenstar LS 900* biometer (Haag-Streit AG, Koeniz, Switzerland) is a relatively recently-developed device used for determination of ocular measurements and performance of calculations to facilitate in establishing the relevant type and power of intraocular lens for implantation following removal of the natural crystalline lens during cataract surgery (Cruysberg *et al.*, 2010). The instrument can measure corneal thickness (CT), anterior chamber depth (ACD; from corneal endothelium to lens surface), lens thickness (LT), axial length (AL), retinal thickness (RT) as well assessing keratometry and pupil diameter (Buckhurst *et al.*, 2009; Rohrer *et al.*, 2009; Cruysberg *et al.*, 2010; Alderson *et al.*, 2012; Zhao *et al.*, 2013) concurrently through image analysis within each measurement, without requiring realignment (Buckhurst *et al.*, 2009; Cruysberg *et al.*, 2010; Zhao *et al.*, 2013). The basis of the *Lenstar LS 900* is founded on optical low coherence reflectometry powered by a superluminescent diode of a broad band light source (20-30 nm) with a centre wavelength of 820 nm (Cruysberg *et al.*, 2010). Similar to the *IOLMaster*, the *Lenstar* utilises the effect of time domain interferometric or coherent superposition of light waves to measure ocular lengths, in a technique comparable to one-dimensional optical coherence tomography (Buckhurst *et al.*, 2009). Where the *IOLMaster* uses a diode laser, the superluminescent diode used by the *Lenstar* has a Gaussian shaped spectrum, permitting a higher axial resolution; thus the terminology optical low coherence reflectometry as opposed to partial coherence interferometry, has been coined (Buckhurst *et al.*, 2009).

The precise refractive index and method the *Lenstar* uses to calculate axial length is proprietary information, yet, it is established that the instrument does utilise an average ocular refractive index, in a similar way to the *IOLMaster*, to convert to geometric length from optical length in the axial length calculations (Read *et al.*, 2010). Therefore, it is likely as suggested by Atchison and Smith (2004) that during accommodation, the measurements collected with the *Lenstar* may overestimate axial length, due to the biometric changes that occur with accommodation effectively resulting in an increase of the average refractive index of the eye. However, because the *Lenstar* also offers the individual ocular component dimensions per measurement, the potential error associated with the accommodative measurements can be reasonably estimated for each individual subject, as achieved in several investigations (Read *et al.*, 2010; Woodman *et al.*, 2012; Ghosh *et al.*, 2014).

From a single measurement, which is acquired in approximately 20 seconds, all the mentioned parameters above can be evaluated and multiple measurements can be taken successively to improve the accuracy (Cruysberg *et al.*, 2010). The ocular measurements obtained from the *Lenstar* biometer have been demonstrated to be highly precise, reliable and comparable to previously validated ocular biometry instruments, including the *IOLMaster* (Buckhurst *et al.*, 2009; Rohrer *et al.*, 2009; Cruysberg *et al.*, 2010; Read *et al.*, 2010).

1.8.6 Badal modification of the *Lenstar LS 900*

Following the preliminary ocular and refractive measurements, each participant will undergo axial length measures under 2 different accommodative demands (0 D and 5 D). Badal modifications are utilised for examination of axial length changes with accommodation, allowing for axial length determination at 0 D and 5 D demands.

All measurements are to be performed on the right eye only while the left eye is occluded. To allow performance of biometry while participants are accommodating, a similar experimental setup will be used to that of Read *et al* (2010) and Alderson *et al* (2012), comprising of a back-illuminated text target viewed through a pellicle beam splitter (thickness approximately 2 μm) and + 10 D Badal lens (25.4 mm diameter, 100 mm focal length achromatic doublet; Edmund Optics) mounted in front of the *Lenstar* instrument (see Figure 1.20). The eye under investigation is 100 mm from the Badal lens and the 0 D and 5 D stimulus levels are situated 100 mm and 50 mm, respectively, from the Badal lens.

A

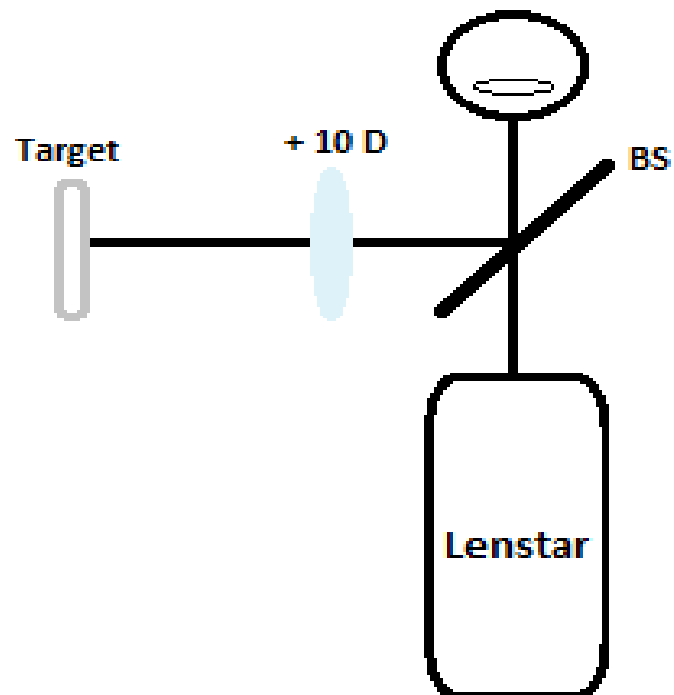


Figure 1.20 A) Diagram of experimental setup for accommodative axial length changes using the *Lenstar LS 900*. A back-illuminated text target is viewed through a beamsplitter (BS) and a +10 D Badal lens to enable ocular biometry measurements to be performed at different accommodative demand levels. The back-illuminated text target was positioned to stimulate 0 D from the Badal lens for relaxed accommodation biometry, and moved 50 mm forward towards the Badal lens for a 5 D stimulus demand.



Figure 1.20 B) Photograph of the *Lenstar LS 900* and bespoke attachment including: pellicle beamsplitter (A), +10 D achromatic doublet Badal lens (B) and retro-illuminated text target (C).

Pellicle beamsplitters are particularly advantageous owing to their considerable thinness of approximately $2 \mu\text{m}$ which minimises undesirable secondary reflections (Alderson *et al.*, 2012), such that the beamsplitter used exhibited a transmittance of 92 % for the 820 nm wavelength used by the *Lenstar*. Measurements with the inclusion of the pellicle beamsplitter to the optical path with the *Lenstar* have been tested and shown to be robust; it has been reported that no statistical significance was present with the beamsplitter inclusion for any biometric parameters for any subject. However, using the *Lenstar* calibration eye to again test for any difference in the biometric parameters with the beamsplitter in place, the only statistically significant difference was for axial length (at 0.007 mm); this difference cannot be deemed clinically significant (Alderson *et al.*, 2012).

The accommodative target consists a 5 x 5 grid of high-contrast letters, with each letter equivalent to 0.8 logMAR. The participants are asked to maintain maximum clarity of the

letters at all times. Myopic participants wear daily disposable soft contact lenses in a power appropriate to their refractive error.

1.8.7 IOLMaster

A commercially available optical biometer, *IOLMaster* (Carl Zeiss Jena, Germany), based on the principle of dual beam PCI, is a widely used non-contact instrument (Vogel *et al.*, 2001; Santodomingo-Rubido *et al.*, 2002; Eleftheriadis, 2003). The *IOLMaster* is a high-resolution instrument principally developed to establish ocular biometry prior to intraocular lens (IOL) implantation with cataract extraction (Santodomingo-Rubido *et al.*, 2002). A resolution of 0.01 mm for AXL measurements is utilised (Drexler *et al.*, 1998; Mallen *et al.*, 2006) and such measures are acquired along the visual axis, whilst the participant fixates an internal light. The device employs infrared light (wavelength of 780 nm) of short coherence to measure the optical AXL, which is converted to geometric AXL by utilising a group refractive index (Hitzenberger *et al.*, 1993; Vogel *et al.*, 2001; Read *et al.*, 2010). Additionally, the *IOLMaster* measures the ACD, corneal curvature, and the corneal diameter and calculates the optimum IOL power from the biometric data obtained, operating several IOL power calculation formulae built within its internal software (Eleftheriadis, 2003). The high resolution, precision, accuracy, and reproducibility of the AXL biometry obtained with the *IOLMaster* instrument have been demonstrated, (Lam *et al.*, 2001; Vogel *et al.*, 2001; Santodomingo-Rubido *et al.*, 2002; Eleftheriadis, 2003) and has henceforth been widely implemented across ocular biometric research (Atchison and Smith, 2004; Mallen *et al.*, 2006; Bailey *et al.*, 2008; Sheppard and Davies, 2010b; Kuchem *et al.*, 2013).

The *IOLMaster* utilises infrared light ($\lambda = 780$ nm) of short coherence for the AXL measures, which is converted to geometric AXL by using a group refractive index (Vogel *et al.*, 2001; Read *et al.*, 2010). After being introduced in Germany in September 1999 and accepted in 2000, there have since been several versions of the instrument over the years (Vogel *et al.*, 2001); whilst dense cataracts may limit the ability to measure AXL, the software and hardware upgrades (e.g. version 5 and 500) have increased successful acquisition in dense cataract cases (Hill *et al.*, 2008; Epitropoulos, 2014). A noise reduction filter is applied by the *IOLMaster 500* to each individual scan, diminishing the variable noise in each measurement whilst calculating the composite signal; this relatively recent version offers an AXL calculation algorithm that uses a composite of 20 scans (Epitropoulos, 2014). The most recent version is the *IOLMaster 700* and incorporates swept source OCT into biometry, acquiring 2000 scans per second. Furthermore, the OCT image shows anatomical details on a longitudinal plane through the entire eye (from cornea to retina); any unusual biometric geometries, such as decentration or tilt of the crystalline lens, can therefore be detected. Repeatability and

reproducibility of the *IOLMaster 700* was recently investigated, and was found to be excellent, and agreement with the *IOLMaster 500* (see figure 1.21) was very high. The swept-source optical biometer had better lens penetration ability compared with the *IOLMaster 500* (Srivannaboon *et al.*, 2015).



Figure 1.21. *IOLMaster 500* (Carl Zeiss Jena, Germany) in the Ophthalmic Research Group laboratories of Aston University.

1.8.8 Ciliary muscle image acquisition

AS-OCT (Visante; Carl Zeiss Meditec. Inc., Dublin, CA) images of nasal and temporal ciliary muscle were obtained from right and left eyes of participants, using the *high-resolution corneal* (8 μm axial resolution and scanning area of 10 mm width and 3 mm depth) mode for all imaging. The scanning plane was set horizontally, at 0° throughout image acquisition. The fixation stimulus was a Maltese cross target, viewed through a 0 D Badal lens and suspended in free space from an adjustable apparatus positioned at a 45° angle (see Figure 1.22), which allowed the head of the participant to remain in primary position on the forehead and chin rest while the participant occupied a horizontal gaze. Positioning of the fixation stimulus 45° external to the centre of the AS-OCT headrest enables the optical axis of the instrument to pass through the eye imaged (nasal and temporal). For each eye, the target was positioned along the same axis and the participant asked if the centre of the Maltese cross was in view with horizontal gaze in order to reduce any potential variance in acquisition planes. At least three images of good visibility of the nasal and temporal ciliary muscle was acquired for each eye in the non-accommodated state. Each participant was instructed to carefully focus on the centre of the Maltese cross during the process of image capture. Acquisition lasted approximately 5 seconds per scan.



Figure 1.22. AS-OCT with external fixation target. The participant fixates on the centre of the suspended Maltese cross by gazing laterally through the Badal lens. The Maltese cross fixation target and Badal lens can be adjusted to maintain the 45° fixation angle by movement of the rotatable metal rod.

1.8.9 Ciliary muscle image analysis

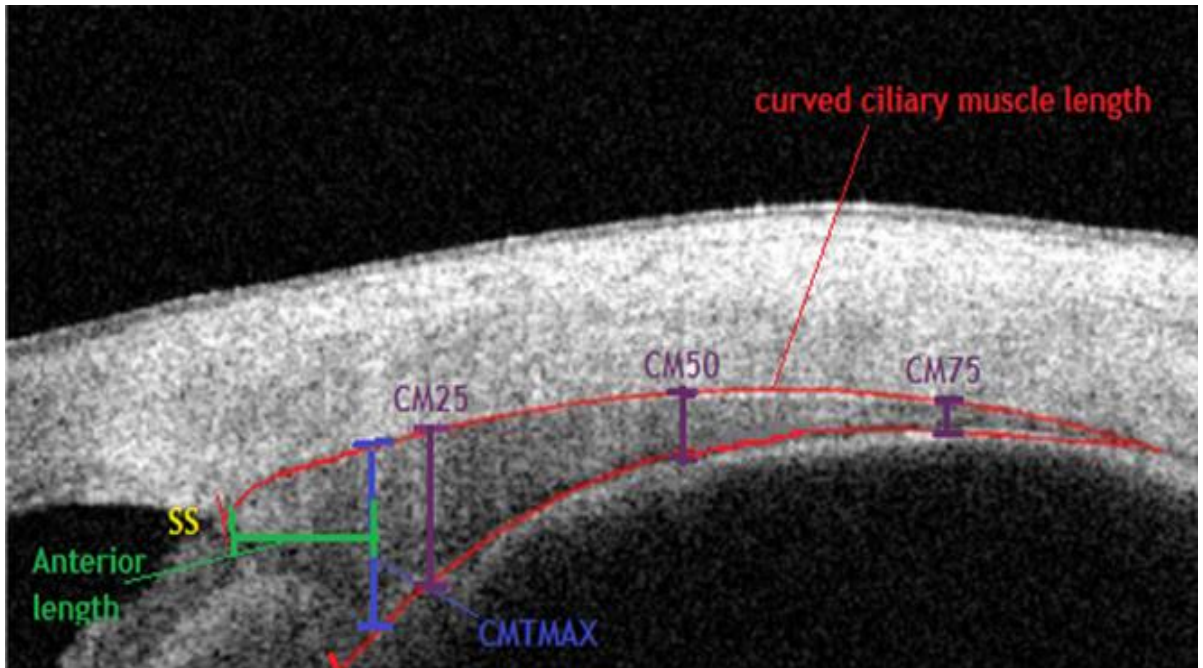


Figure 1.23. AS-OCT image of a temporal ciliary muscle with associated parameters. The anterior length is taken from the scleral spur (SS) to the point of maximum ciliary muscle thickness (CMTMAX). CM25, CM50 and CM75 are taken at 25, 50 and 75 % of the curved CM length, respectively.

Inbuilt *Visante* AS-OCT callipers have been previously utilised to measure the range of ciliary muscle parameters, in the same way described by Sheppard and Davies (2010). The internal software enables a maximum of seven callipers at a time to be positioned over each acquired image, with the ability to remove callipers from view when not required, for instance, if the calliper is obstructing the view for another measurement. During image analysis, the boundaries of the ocular media are outlined and corrective refractive indices (n) are applied to correct distortion (anterior to the cornea: $n = 1.000$, cornea: $n = 1.338$, posterior to the cornea: $n = 1.343$). However, the same refractive index adjustments are applied to ciliary muscle images by the system, without an option to vary the scale of the tiered refractive index corrections (Laughton *et al.*, 2015). As such, previous investigators have employed a refractive index of 1.000 to the entire ciliary muscle image (Bailey *et al.*, 2008; Sheppard and Davies, 2010b; Sheppard and Davies, 2011). Calliper measurements of ciliary muscle have then been adjusted to account for a refractive index of 1.382 (Sheppard and Davies, 2010b; Sheppard and Davies, 2011), which is the best current approximation of the ciliary muscle refractive index, based on *in vitro* methods of human ventricular muscle studies using OCT (Tearney *et al.*, 1995) and bovine muscle tissue studies using confocal microscopy (Dirckx *et al.*, 2005). Yet, the refractive indices of the overlying sclera and the ciliary muscle itself must be compensated for to maximise accuracy of the measured ciliary muscle parameter. Moreover, the straight lines of the *Visante* callipers do not accurately depict the ciliary muscle

tissue as both scleral and ciliary muscle tissue are curved, and with varying magnitudes in different subjects (Kao *et al.*, 2011; Laughton *et al.*, 2015). To overcome these limitations and address the subjective nature of the calliper technique (particularly identifying the posterior point of the ciliary muscle), a bespoke semi-automated analysis programme was developed at Aston University, and has since been described and validated (Laughton *et al.*, 2015).

The semi-automated ciliary muscle analysis programme was utilised for full analysis of images acquired with the AS-OCT and included in the dataset for the subsequent experimental chapters. Overall ciliary muscle length is expressed as anteroposterior distance from the scleral spur, to the posterior point of the ciliary muscle where no more thinning occurs (see Figure 1.23). Anterior length is the measurement from the scleral spur to the point of maximum width, CMTMAX (see Figure 1.23). The width measures are calculated from the dimension between the ciliary muscle- sclera boundary to the pigmented ciliary epithelium. Ciliary muscle thickness measures at set points along the ciliary muscle from the scleral spur were obtained as achieved originally by Bailey *et al.* (2008) and described previously in section 1.4 (see Figure 1.11). Similarly, measurements proportional to the overall length of the ciliary muscle were obtained (see Figure 1.9), as achieved by Sheppard and Davies (2010) and described previously in section 1.4.

1.8.10 Validation of bespoke ciliary muscle analysis software

A bespoke semi- automated software programme has been developed by the Ophthalmic Engineering Department at Aston University to assist in the more objective measurement ciliary muscle parameters acquired from the AS-OCT ciliary muscle images. The purpose of the software was to remove the subjectivity from manually measuring parameters as was done in previous work. The software had not previously been validated for any ciliary muscle parameters, and was carried out to test the robustness of the semi-automated measurements.

Simulated ciliary regions were constructed using bespoke rigid gas permeable lenses of constant centre thickness, and consisted of two lenses combined; a greater diameter base lens, L1 (10 mm total diameter), representing the sclera, and five smaller diameter, L2 lenses (6 mm total diameter) that represented the ciliary muscle (see figure 1.24), with each of these lenses varying in thickness (0.30, 0.45, 0.60, 0.75, 0.90 mm). The refractive index of the L1 and L2 lens were chosen in accordance with that of the sclera and ciliary muscle, at 1.479 and 1.440 respectively.

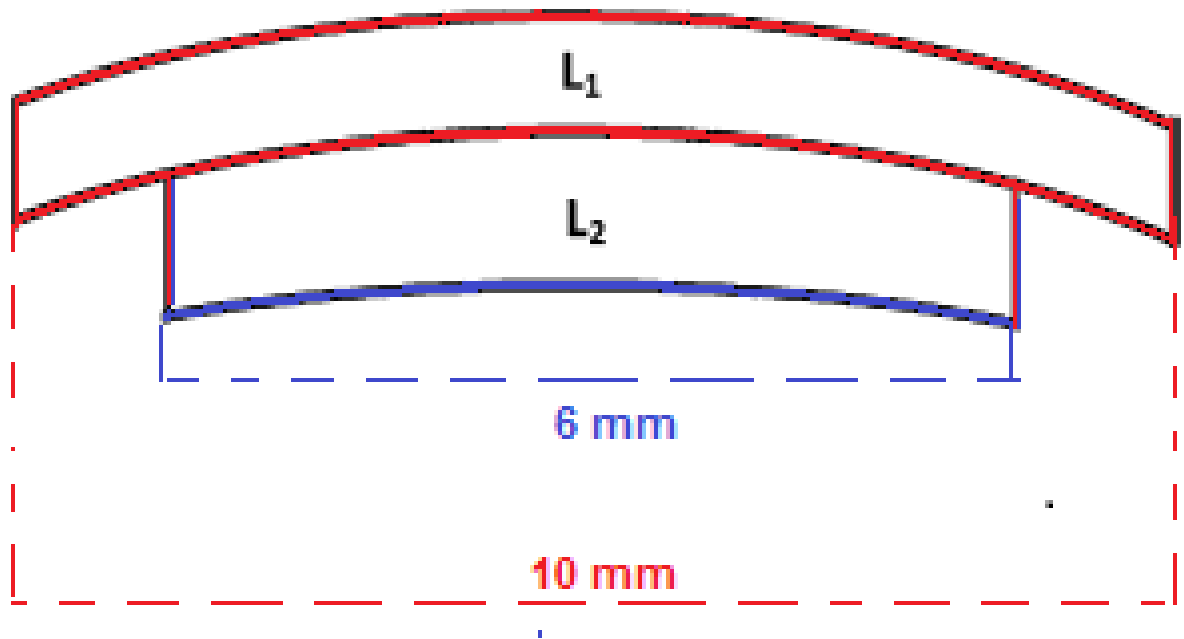


Figure 1.24. Schematic diagram of two rigid gas-permeable lenses designed to simulate the sclera (L1) and ciliary muscle (L2), and associated diameters of lenses.

The L1 lens fitted behind the L2 lens and was manually centred, with the front curvature of the L1 lens in contact with the back curvature of L2 lens (see Figure 1.24). This resultant simulated ciliary region was held in place by a bespoke mount (see Figure 1.25) which attached to the chin rest of the AS-OCT. The slot that held the lenses was 10 mm in diameter and allowed the protrusion of the front surface of the L2 lens. A metal prong was twisted in to place to hold the L2 lens in its central position on the L1 lens and to thereafter push the L2 lens forward in to the back surface curvature of the L1 lens with minimal or no visible air gap when imaging the simulated eye. 10 images were acquired for each L2 lens in this way, using the *high resolution corneal* mode, as is normally utilised for ciliary muscle imaging.

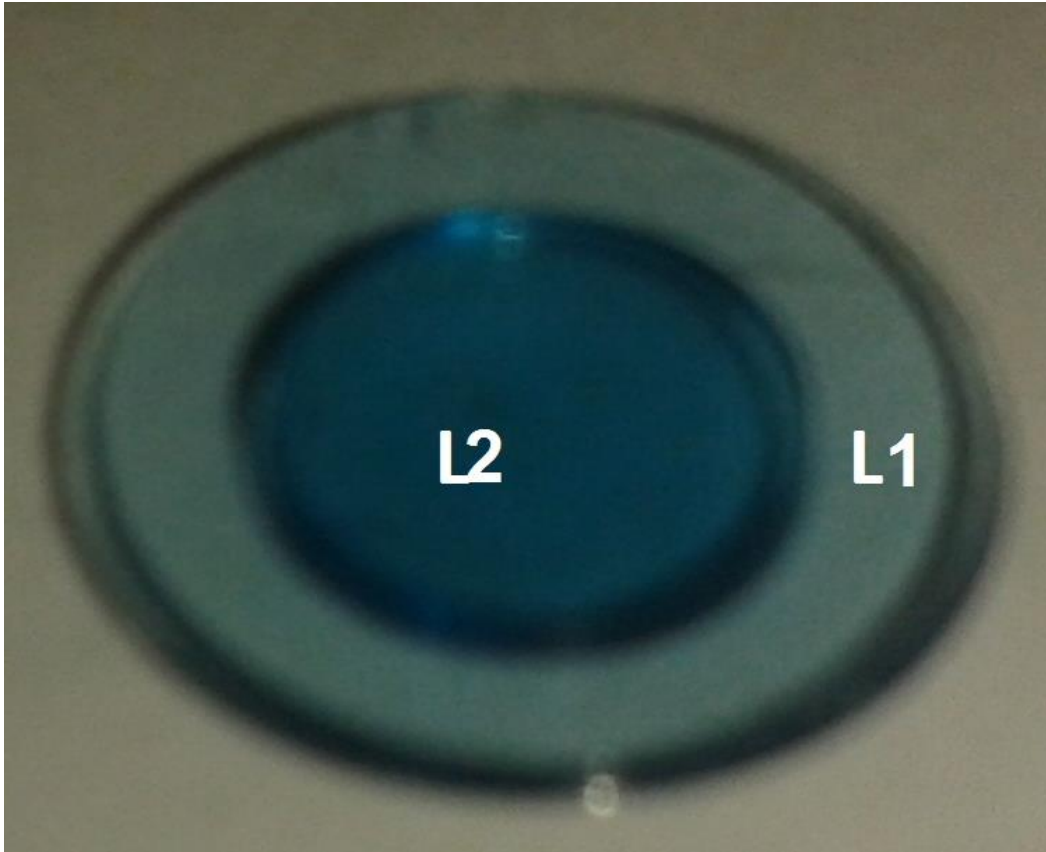


Figure 1.25. Arrangement of ciliary muscle lens, L2, in direct contact with, and centred on sclera lens, L1.

Following image acquisition, the semi-automated software was utilised on the simulated ciliary muscle thicknesses to compare the actual measurements with those attained by the software; the images were saved on the *Visante* software of the AS-OCT and exported in raw DICOM (Digital Imaging and Communications in Medicine) form. The analysis was then performed on a spare computer, using Matlab R2012b (The MathWorks Inc., Massachusetts, USA). The thicknesses of the ciliary muscle lenses were measured at CM25, CM50 and CM75 of the lens diameter and each thickness measurement was calculated perpendicular to the scleral/ ciliary muscle boundary curve. The scleral and ciliary muscle lens refractive indices (1.48 and 1.44, respectively) were inputted to compensate the calculations by the software. Furthermore, ciliary muscle lens diameter and thickness was also measured 10 times by Vernier callipers and compared to the data produced by the programme. For each artificial ciliary muscle thickness parameter measured, there was no significant difference between the results found with the analysis software and the Vernier callipers (CM25: $P = 0.671$; CM50; $P = 0.151$; CM75: $P = 0.857$). The robustness of the analysis technique has been established as the programme extracts valid and repeatable ciliary muscle parameters and increases the objectivity of ciliary muscle analysis (Laughton *et al.*, 2015).



Figure 1.26 Setup of simulated ciliary muscle image acquisition. 'A' illustrates the plastic material that encapsulates the lenses. 'B' shows the metal prong which can be twisted to maintain centration of L2 and ensure no air gap between the two lenses. 'C' demonstrates the position of the simulated eye within the lens mount.

1.9 Summary

The literature is in agreement in relation to alteration of ciliary muscle morphology with refractive error (Bailey *et al.*, 2008; Sheppard and Davies, 2010; Pucker *et al.*, 2013). However, there is a paucity of information pertaining to how this altered morphology relates to myopia development. It has been suggested that the thicker ciliary muscle in myopia is hypertrophic and leads to a reduced contractile response (Bailey *et al.*, 2008), which accounts

for the accommodative lag that is well documented in myopia (Goss, 1991; Gwiazda *et al.*, 2005; Mutti *et al.*, 2006), and results in the hyperopic model of myopigenesis. A slight reduction of the amount of hyperopic blur may occur from transient axial elongation during sustained accommodative effort (Mallen *et al.*, 2006). Myopic eyes may demonstrate the largest expandability during (Drexler *et al.*, 1998; Mallen *et al.*, 2006; Read *et al.*, 2010), and immediately following an accommodative task. There may be discrepancies between myopes and emmetropes in the morphology of the ciliary body, causing a difference in ciliary muscle force transmission to the choroid and sclera amid these different refractive groups and thereby resulting in differences in the magnitude of transient axial elongation (Mallen *et al.*, 2006). Nevertheless, the potential relationship between ciliary muscle morphology and accommodative function has not been investigated.

Previous human ciliary muscle studies *in vivo* have typically investigated only one eye, and/or just one aspect (e.g. just the temporal side) (Bailey *et al.*, 2008); as such, laterality and symmetry of the ciliary muscle which may be relevant to refractive error development, is not well understood. Bilateral globe profile in emmetropia and myopia was recently investigated (Gilmartin *et al.*, 2013) using high-resolution MRI. Globe shape was linked to retinotopic projection in both myopes and emmetropes, and showed that emmetropic and myopic eyes could not be differentiated with regards to equatorial dimensions. It is not known whether ciliary muscle morphology displays similar properties between the refractive error groups. Asymmetry in the laterality of globe profile between myopic eyes was also evident, with nasal to temporal quadrants being asymmetric between right and left eyes (Gilmartin *et al.*, 2013). Since the division of nasal and temporal retinal nerve fibres into right and left visual fields occurs at the optic chiasm (Bron *et al.*, 1997), such coupling indicates that binocular growth may be coordinated by processes operating past the optic chiasm (Gilmartin *et al.*, 2013). Such laterality in myopia development may be linked to ciliary muscle morphology and this matter has not been previously examined. Review of current research has highlighted the gap in the literature regarding altered ciliary muscle morphology with refractive error and its link with accommodation, and particularly the need for a large scale investigation on an emmetropic cohort, where the ciliary muscle is influenced only by normal ocular development; where normal variations in biometric characteristics of the emmetropic ciliary muscle are not yet known.

1.10 Aims of this thesis

The literature review presented in this chapter has highlighted numerous uncertainties relating to differences in accommodative function between emmetropes and myopes, and the role of altered ciliary muscle morphology which may be implicated in refractive error

development. Consequently, this thesis will address five pertinent topics related to ciliary muscle, accommodation and refractive error. The specific aims of the thesis were as follows:

1. To determine if there is any diurnal variation in axial length change with accommodation and/ or accommodative error
2. To describe the ciliary muscle and ocular biometric correlates in emmetropia, as the ciliary muscle parameters that relate to particular ocular biometric correlates will help determine what defines ciliary muscle growth with normal ocular development
3. To compare ciliary muscle morphology in emmetropia and myopia, and determine the level of inter-eye symmetry
4. To elucidate any potential link between ciliary muscle morphology and accommodative function
5. To describe the ciliary muscle morphology in amblyopia and anisometropia
6. To investigate new parameters for measuring the ciliary muscle from *in vivo* AS-OCT imaging

The research involved the operation of relatively new biometric and complementary high-resolution imaging that allow visualisation of the ciliary muscle *in vivo* as described in this chapter; the application of such methodologies permit a high level of precision in examining the morphology of the ciliary muscle. Previous work has shown insight into a potential link between ciliary muscle morphology, accommodative function and refractive error. However, much still remains unanswered and the research presented in this thesis aimed to fill this gap in our current understanding.

Chapter 2

Diurnal stability of accommodative accuracy and axial length change with accommodation

2.1 Introduction

Despite the wide acceptance that axial length (AXL) undergoes significant diurnal variation in both animal (Nikla *et al.*, 1998; Nikla, 2006; Tian and Wildsoet, 2006; Read *et al.*, 2008); and human models (Stone *et al.*, 2004; Wilson *et al.*, 2006; Read *et al.*, 2008) and it is well known that AXL is increased temporarily with accommodation (Drexler *et al.*, 1998; Mallen *et al.*, 2006; Read *et al.*, 2010; Ghosh *et al.*, 2014; Zhonga *et al.*, 2014) which may be relevant to refractive error development (Mallen *et al.*, 2006; Woodman *et al.*, 2012), there is a paucity of information relating to diurnal changes in AXL with accommodation and alterations in accommodative function throughout the day.

AXL is longest in the day and shortest during the night (Stone *et al.*, 2004; Read *et al.*, 2008; Chakraborty *et al.*, 2011), varying in the range of 15 – 46 μm (Stone *et al.*, 2004; Chakraborty *et al.*, 2011). In a study consisting of two consecutive days of diurnal testing on human participants, the AXL underwent significant diurnal changes; the link between vitreous chamber depth fluctuations and axial length suggested that diurnal axial length variations occur largely due to alterations in the posterior portion of the globe (Chakraborty *et al.*, 2011). A significant diurnal rhythm has also been observed in choroidal thickness, with the choroid being thickest at night and thinnest during the day, in close correspondence with previous animal research (Nikla *et al.*, 1998; Nikla, 2006), and demonstrating an antiphase to diurnal AXL fluctuations (Brown *et al.*, 2009; Chakraborty *et al.*, 2011).

Considerable alteration of intraocular pressure (IOP) could be responsible for the diurnal variation in AXL. Significant changes in IOP mechanically or surgically, can result in large predictable AXL fluctuations, coherent with the globe expansion and contraction in accordance with the IOP (Cashwell and Martin, 1999; Phillips and McBrien, 2004; Read *et al.*, 2008). Another investigation in emmetropic and myopic cohorts found a weak association between the diurnal AXL changes and IOP, yet the larger amplitudes in IOP variation were not in accordance with amplitudes of AXL change (Nikla *et al.*, 1998; Chakraborty *et al.*, 2011). Diurnal variations in AXL were not different between refractive groups. Whilst diurnal changes in AXL have been studied with regard to the various factors which may be causally related and the magnitude of AXL variation throughout the day, potential diurnal AXL changes associated with accommodation have not previously been reported. It is important for investigations in this field, and studies detailed in the thesis, to know if accommodative axial

expandability varies diurnally, as this would impact on both results and subsequent experimental designs, which may need account for time of day. In comparing the differences in transient AXL change with accommodation between emmetropes and myopes (Drexler *et al.*, 1998; Mallen *et al.*, 2006; Read *et al.*, 2010; Woodman *et al.*, 2010; Woodman *et al.*, 2012; Ghosh *et al.*, 2014; Zhonga *et al.*, 2014) (see table 2.1), it therefore must be determined if, and to what extent any diurnal variation occurs in a myopic and emmetropic cohort.

Whilst various ocular diurnal variations are known, very little is known about changes in accommodative function throughout the day. Results from a previous investigation (Murphy *et al.*, 1977) showed that there was no diurnal change in the values of volitional control of accommodation, near-point of accommodation and accommodative tracking. Similarly, a further investigation demonstrated that there is short-term stability during the day in tonic accommodation and does not undergo diurnal fluctuations (Krumholz *et al.*, 1986). Conversely, a study by Kurtev *et al.* (1990) showed that tonic accommodation varied throughout the day (by approximately 1 D) and the discrepancies between this study and that of Krumholz and co-workers (1986) was attributed to differences in measurement techniques (Kurtev *et al.*, 1990). Whilst these few studies have provided the literature with some evidence for diurnal change with particular aspects of accommodation, no reports have described the possibility of diurnal changes on accommodative accuracy despite the large body of literature relating to accommodative lag, due to its widely accepted association with myopia (Gwiazda *et al.*, 1993; Gwiazda *et al.*, 1995; Harb *et al.*, 2006; Mutti *et al.*, 2006; Berntsen *et al.*, 2010; Berntsen *et al.*, 2011). Mallen *et al.* (2006) observed the greatest AXL changes in myopic participants, with a mean increase of 58 μm , compared to 37 μm in emmetropes, when viewing a 6 D stimulus and subsequent work found that myopes also had the largest accommodative AXL elongation directly following a prolonged near task (Woodman *et al.*, 2010). Such accommodative axial changes are considered to be a mechanism to maintain a constant ocular volume whilst the ciliary muscle contraction pulls the choroid and sclera adjacent to the ciliary body inwards (Drexler *et al.*, 1998; Mallen *et al.*, 2006). Given the current hypothesis that the eyes of myopic individuals are more malleable and susceptible to AXL changes with accommodation (Mallen *et al.*, 2006; Woodman *et al.*, 2010), the accommodative accuracy should also be lesser at the point in time when the retina has undergone greater amounts of this elongation. Hence, the accommodative lag would intuitively be thought to be greater during periods of the day where AXL change with accommodation is greatest.

The purpose of this study was to determine if diurnal variation occurs with AXL change with accommodation, accommodative accuracy, and to what extent the diurnal variation in these accommodative functions occurs across myopic and emmetropic refractive groups.

Author & study details	Results	Implications
<p>Drexler et al., 1997. 11 emmetropes (MSE ranging from +0.38 D to -0.75 D), and 12 myopes (MSE ranging from -1.0 D to -9.5 D) Accommodative demand: the greatest extent of accommodative effort at the near point (mean for emmetropes: 5.1 D, for myopes: 4.1 D)</p>	<p>Accommodative AXL in emmetropes and myopes: 12.7 μm (range, 8.6-19.2 μm) and 5.2 μm, respectively (range, 2.1-9-5 μm). (UC)</p>	<p>AXL change with accommodation is greater in emmetropes, compared with myopes.</p>
<p>Mallen et al., 2006. 30 emmetropes (mean MSE = -0.07 \pm 0.23); 30 myopes (mean MSE = -3.59 \pm 0.75), Accommodative demand: 0, 2, 4 & 6 D</p>	<p>Mean AXL change at 2 D, 4D, 6D: 14 \pm 19 μm & 19 \pm 20 μm for emmetropes and myopes, respectively; 26 \pm 21 μm & 37 \pm 26 μm for emmetropes and myopes, respectively; 37 \pm 27 μm and 58 \pm 37 μm for emmetropes & myopes, respectively. (UC)</p>	<p>The magnitude of accommodative AXL change systematically increases with increasing stimulus demand, this effect was more marked in myopes; myopic eyes are more susceptible to transient biometric changes than with emmetropes.</p>
<p>Read et al., 2010. 19 emmetropes (mean MSE: +0.05 \pm 0.27 D); 21 myopes (mean MSE: -1.82 \pm 0.84 D). Accommodative demand: 0, 3, & 6 D</p>	<p>No significant differences in AXL change with accommodation between refractive groups. Mean AXL increased by 5.2 \pm 11.2 μm and 7.4 \pm 18.9 μm for 3 D and 6 D demands, respectively. (C)</p>	<p>Significant AXL increase is linked with brief periods of accommodation; the magnitude of AXL change increases for larger demands. There is no significant difference in the magnitude of AXL elongation in myopes and emmetropes, though structural ocular changes linked with greater magnitudes of myopia may be associated with the eye being more susceptible to accommodative AXL changes</p>
<p>Woodman et al., 2010. 20 emmetropes (mean MSE: -0.10 \pm 0.23 D); 20 myopes (mean MSE: 3.11 \pm 2.24 D). Accommodative demand: sustained near work at 5 D for 30 minutes</p>	<p>Mean accommodative AXL change: 10 \pm 15 μm and 20 \pm 20 μm for emmetropes and myopes, respectively. (UC)</p>	<p>Myopes showed the greatest AXL change instantly following the near task. AXL returns to baseline levels 10 minutes following near task cessation.</p>
<p>Woodman et al., 2012. 22 emmetropes (mean MSE: +0.16 \pm 0.28 D);</p>	<p>Accommodative AXL change between refractive groups was not significant ($P = 0.136$): mean AXL change</p>	<p>In post-accommodative task measures (10 minutes following end of near task), myopes still showed a small</p>

37 myopes (mean MSE: -2.90 ± 1.57 D) Accommodative demand: 4D for 30 minutes continuously	with accommodation was 14 ± 28 μ m (C)	degree of AXL elongation, whilst AXL of emmetropes returned to baseline measures.
Zhong et al., 2014. 10 myopes (mean MSE: -1.95 ± 0.88 D), 11 emmetropes (mean MSE not stated) Accommodative demand: 6 D	Baseline AXL was 24.519 ± 0.917 mm And significantly increased to 24.545 ± 0.915 mm with accommodation. There was no significant differences in accommodative AXL changes between refractive groups. (UC)	With accommodation, whole eye axial biometry altered, including a decreased ACD, and increased lens thickness and AXL. UL-OCT may provide an alternative method appropriate for ocular biometry measures during accommodation.
Ghosh et al., 2014 Accommodative demand: 2.5 D for 10 minutes	AXL was significantly greater for downward gaze with accommodation (mean change, 23 ± 13 μ m at 10 minutes) compared with primary gaze accommodation (8 ± 15 μ m at 10 minutes). There was no significant difference between refractive groups for AXL change in primary position or downward gaze (C).	AXL, choroidal thickness, LT & ACD alter significantly during accommodation in downward gaze, perhaps influenced by biomechanical factors (i.e., extraocular muscle forces, ciliary muscle contraction) associated with near tasks in downward gaze.

Table 2.1. Key findings from accommodative axial length change studies in emmetropes and myopes. C = correction factors for AXL change with accommodation was applied. UC = uncorrected values for AXL change.

2.2 Methods

2.2.1 Subjects

Twenty eight subjects (20 females, 8 males) aged 19-26 years were recruited from the student body of Aston University, and were classified according to their mean sphere equivalent refractive error (MSE; sphere + $\frac{1}{2}$ cylinder (D)) as emmetropes ((MSE) ≥ -0.55 ; $< +0.75$ D; $n = 14$) and myopes (MSE ≥ -1.50 D; $n = 14$). A cohort size of twenty four was based on a sample size calculation (GPower based on effect size of 0.25, for a repeated measures, within – between interaction ANOVA for 4 repeated measurements amongst 2 groups, an error probability (α) of 0.05 and required power ($1-\beta$) of 0.80). More subjects than the required sample size were recruited to allow for some attrition from missed appointments or drop-outs. Exclusion criteria were amblyopia, cylindrical refractive errors greater than 2.00 D, systemic conditions known to affect ocular health, and previous history of ocular trauma, surgery or pathology. All participants had corrected visual acuities of 0.00 logMAR or better in each eye and exhibited a monocular amplitude of accommodation ≥ 9 D (as measured with

the push-up method using the RAF rule). Myopic participants wore 31% Nelfilcon A (Focus Dailies) contact lenses appropriate for their habitual refractive error for all measures. Ethical approval was obtained from the Aston University Life and Health Sciences Research Ethics Committee and the study adhered to the tenets of the Declaration of Helsinki. Written, informed consent was obtained from all volunteers prior to participation after explanation of the nature and possible consequences of the study.

2.2.2 Measurements

Ocular biometric parameters and accommodative responses in the right eye only were measured within each of the four time periods (08:00 – 09:00, 12:00 – 13:00, 16:00 – 17:00, 20:00 – 21:00). For each participant, the measurements were separated by four hours in a single study day (Monday – Friday) and subjects resumed their regular academic activities between individual measurement sessions. The first measurement slot was within one hour of waking and prior to commencement of any studying or prolonged near work.

Binocular distance refractive error was measured with an infra-red binocular open-view autorefractor (Grand Seiko WAM 5500; (Sheppard and Davies, 2010a)) at the first session whilst subjects viewed a distance (6 m) Maltese cross target. A minimum of five measurements of refractive error were taken for each eye, averaged and converted into MSE.

To indicate the level of accommodative inaccuracy at various times during the day, the accommodative error index (AEI) was used, which amalgamates all the parameters of the accommodative stimulus- response curve into a single index ((Chauhan and Charman, 1995; Woodhouse *et al.*, 2000; Allen and O’Leary, 2006).

Accurate accommodation at all stimulus demands is indicated by an AEI of 0 D. A value > 0 D indicates the level of accommodative inaccuracy (Chauhan and Charman, 1995; Woodhouse *et al.*, 2000). At each session the accommodative response was measured in the right eye to targets placed at 8 randomised-order stimulus demands (0.0, 1.0, 2.0, 3.0, 4.0, 5.0, 6.0, 8.0 D) to produce the AEI, calculated using equation 1, detailed in section 1.7.3.

AXL, anterior chamber depth (ACD), lens thickness (LT), and corneal thickness (CT) of the right eye in the unaccommodated and accommodated states were obtained using the *Lenstar LS 900* biometer (Haag-Streit AG, Koeniz, Switzerland). Participants viewed a back-illuminated text target through a pellicle beam splitter (thickness approximately 2 μm) and + 10 D Badal lens (25.4 mm diameter, 100 mm focal length achromatic doublet; Edmund Optics) mounted in front of the *Lenstar* instrument (Alderson *et al.*, 2012) and fixated on a letter (a 5 x 5 grid of high-contrast letters, with each letter equivalent to 0.8 logMAR) closest

to the central red dot. The eye under investigation was 100 mm from the Badal lens and the retro-illuminated text target was situated 100 mm from the Badal lens to stimulate a 0 D demand level (see figure 1.18). Participants were asked to maintain maximum clarity of the letter throughout data acquisition whilst four separate biometric measurements were taken and averaged at 0 D, before repeating these measurements while the participant accommodated to 5 D stimulus demand, by shifting the back- illuminated text target 50 mm forward towards the Badal lens (Alderson *et al.*, 2012), as described in section 1.7.5.

2.2.3 Analysis

The *Lenstar* instrument, like the *IOLMaster*, utilises an average ocular refractive index in order to calculate axial length from the optical path length. Previous work has established that changes in the accommodative apparatus, principally lens thickness, during accommodation may produce errors in these AXL measurements (Atchison and Smith, 2004). The basis of this potential error is from the anterior portion of the crystalline lens which has a higher refractive index than that of the aqueous humour it displaces, resulting in an increase in optical path length (Atchison and Smith, 2004; Mallen *et al.*, 2006; Read *et al.*, 2010; Woodman *et al.*, 2010; Woodman *et al.*, 2012) and thereby overestimating AXL during accommodation. The formulae and methods outlined by Atchison and Smith were applied by utilising each participant's individual ocular biometric parameters; the error associated with the change in AXL from baseline to the 5 D accommodative demand was calculated for each participant and these values were used to determine the corrected accommodative AXL changes (from equations 2.1- 2.7).

$$ACT = LT * \frac{0.51 + 0.012 * age}{(0.51 + 0.012 * age) + (2.11 + 0.003 * age) + (0.33 + 0.0082 * age)}$$

Equation 2.1: Anterior cortex thickness (ACT)

$$NT = LT * \frac{2.11 + 0.003 * age}{(0.51 + 0.012 * age) + (2.11 + 0.003 * age) + (0.33 + 0.0082 * age)}$$

Equation 2.2: Nucleus thickness (NT)

$$PCT = LT * \frac{0.33 + 0.0082 * age}{(0.51 + 0.012 * age) + (2.11 + 0.003 * age) + (0.33 + 0.0082 * age)}$$

Equation 2.3: Posterior corneal thickness (PTC)

$$OPL = (CT * 1.376) + (ACD * 1.336) + (ACT * 1.386) + (NT * 1.406) + (PCT * 1.386) + (VCD * 1.336)$$

Equation 2.4: Optical path length (OPL)

$$nave = [(CTAXL) * 1.376] + [(ACDAXL) * 1.336] + [(ACTAXL) * 1.386] + [(NTAXL) * 1.406] + [(PCTAXL) * 1.386] + [(VCDAXL) * 1.336]$$

Equation 2.5: Average refractive index (n_{ave})

$$E = OPL / nave - AXL_{dissaccommodated}$$

Equation 2.6: Error (E)

$$AXL_{corrected} = AXL_{accommodated} - E$$

Equation 2.7

To assess the differences in AXL change with accommodation and AEI across the four different time periods and between the refractive groups, a repeated-measures analysis of variance (ANOVA) was performed with one within-subject factor (time) and one between-subjects factor (refractive group) (SPSS Statistics 21; IBM, Illinois, USA). An independent samples t-test was performed to check for differences in age between the refractive groups. A P value of less than 0.05 was considered significant. All data were stored in an Excel spreadsheet (Microsoft 2010, Redmond, Washington, USA).

2.3 Results

Summary characteristics of emmetropic and myopic participants are provided in table 2.2. There was no significant difference in age between the refractive groups ($P = 0.826$). The corrected AXL values listed are a summary from all four measurement sessions. Mean AXL change and AEI for each time period is summarised in table 2.3.

	Emmetropes	Myopes
	Mean	Mean
Age (years)	21.6 ± 2.16	22.2 ± 1.22
Right eye MSE (D)	+0.05 ± 0.34*	-3.39 ± 1.52*
AXL 0D (mm)	22.93 ± 0.78*	25.25 ± 1.23*
AXL 5D (mm)	22.97 ± 0.77*	25.36 ± 1.23*
Accommodative change in AXL (µm)	16.48 ± 25.52	16.57 ± 25.07
ACD 0D (mm)	2.99 ± 0.27*	3.24 ± 1.21*
ACD 5D (mm)	2.72 ± 0.28*	3.00 ± 0.24*
Accommodative change in ACD	0.25 ± 0.04	0.24 ± 0.11

Table 2.2. Summary characteristics of emmetropic and myopic participants, including the grouped means of biometric data across the 4 measurement session. *represents significant difference between refractive groups.

Time	Rx group	Mean AEI (D)	Mean AXL at 0 D (mm)	Mean AXL at 5 D (mm)	Mean AXL change (µm)
0800-0900	Emmetrope	0.91 ± 0.35	22.93 ± 0.78	22.95 ± 0.78	17.67 ± 19.69
	Myope	0.66 ± 0.30	25.23 ± 1.22	25.24 ± 1.23	6.60 ± 15.44
	Total	0.77 ± 0.35	24.08 ± 1.54	24.09 ± 1.54	12.14 ± 18.26
1200-1300	Emmetrope	0.85 ± 0.32	22.95 ± 0.77	22.96 ± 0.77	9.08 ± 18.67
	Myope	0.70 ± 0.32	25.24 ± 1.22	25.25 ± 1.23	12.43 ± 17.17
	Total	0.78 ± 0.32	24.09 ± 1.53	24.11 ± 1.54	13.05 ± 17.69
1600-1700	Emmetrope	0.90 ± 0.28	22.94 ± 0.78	22.96 ± 0.77	26.53 ± 39.02
	Myope	0.69 ± 0.37	25.23 ± 1.22	25.24 ± 1.23	10.58 ± 14.78
	Total	0.79 ± 0.34	24.08 ± 1.54	24.11 ± 1.54	18.56 ± 30.07
2000-2100	Emmetrope	0.80 ± 0.33	22.93 ± 0.77	22.95 ± 0.77	20.60 ± 42.83
	Myope	0.71 ± 0.33	25.21 ± 1.24	25.24 ± 1.23	29.13 ± 48.28
	Total	0.76 ± 0.33	24.07 ± 1.54	24.03 ± 1.54	24.86 ± 45.00

Table 2.3. Mean AXL change with accommodation (corrected values) and AEI values at each measurement session for emmetropic (n = 14) and myopic (n = 14) refractive groups and for the whole cohort (n = 28).

Significant diurnal variation in unaccommodated AXL were observed at the different time points across the whole cohort ($P = 0.040$). There was no significant relationship between mean AXL change and AEI at any time period (e.g. 1200-1300 emmetropes: $R = 0.420$, $r^2 = 0.177$, $P = 0.097$; 1200-1300 myopes: $R = 0.032$, $r^2 = 0.001$, $P = 0.917$). Between refractive groups, there was no significant difference in accommodative AXL change for any

measurement session (see figure 2.1) (0800-0900: $P = 0.110$; 1200-1300: $P = 0.678$; 1600-1700: $P = 0.206$; 2000-2100: $P = 0.808$) or AEI (see figure 2.2) (0800-0900: $P = 0.060$; 1200-1300: $P = 0.102$; 1600-1700: $P = 0.241$; 2000-2100: $P = 0.885$).

For emmetropes, mean AEI was maximal at 0.91 D (0800-0900 session) and minimal at 0.80 D (2000-2100 session), while AXL change was maximum at 26.53 μm (1600-1700) and minimal at 9.08 μm (1200-1300), though there was no significant difference between the different time points in either accommodative aspects (AXL change: $F = 1.650$, $P = 0.235$; AEI: $F = 0.915$, $P = 0.465$). For myopes, mean AEI was minimal at 0.66 D (0800-0900) and maximal at 0.71 D (2000-2100), while mean accommodative AXL change was minimal at 6.60 μm (0800-0900) and maximal 29.13 μm (2000-2100) (see table 2), though the difference for both was not significant (AXL change: $F = 0.684$, $P = 0.580$; AEI: $F = 0.259$, $P = 0.854$) between any measurement session.

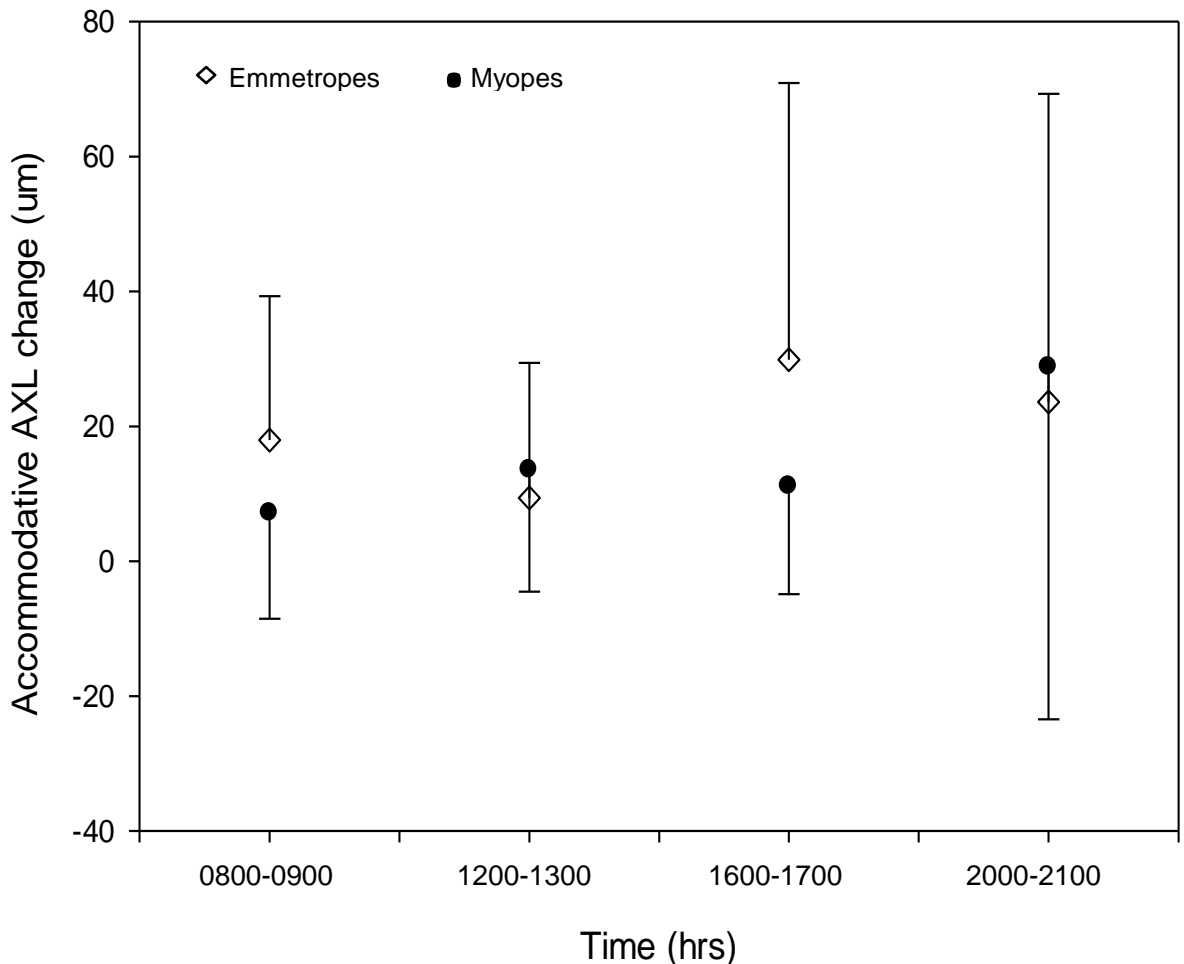


Figure 2.1. AXL change with accommodation throughout the day in emmetropes and myopes, with associated unidirectional error bars, representing standard deviation. Neither refractive group demonstrated any significant diurnal changes (emmetropes: $P = 0.401$; myopes: $P = 0.329$).

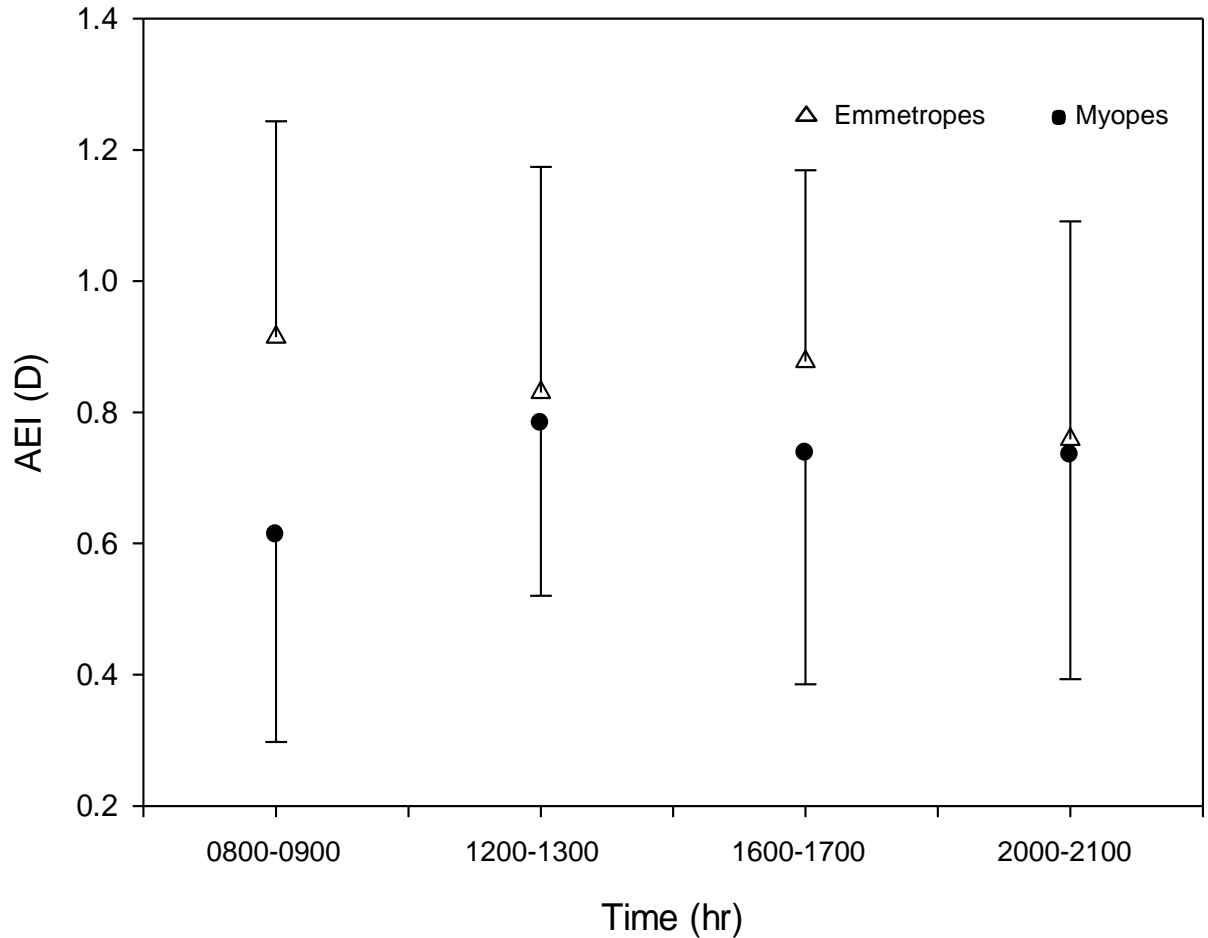


Figure 2.2. Accommodative error throughout the day in emmetropes and myopes, with associated unidirectional error bars representing standard deviation. Neither refractive group demonstrated any significant diurnal changes (emmetropes: $P = 0.482$; myopes: $P = 0.499$).

2.4 Discussion

Whilst differences in transient AXL change with accommodation between emmetropes and myopes have been compared (Mallen *et al.*, 2006; Read *et al.*, 2010; Woodman *et al.*, 2010; Woodman *et al.*, 2012; Ghosh *et al.*, 2014), it has not previously been determined if any diurnal variation occurs in a myopic and emmetropic cohort. Furthermore, this is the first study to investigate diurnal changes in accommodative error despite the large body of literature relating to accommodative lag, due to its widely accepted association with myopia (Gwiazda *et al.*, 1993; Gwiazda *et al.*, 1995; Harb *et al.*, 2006; Mutti *et al.*, 2006; Berntsen *et al.*, 2010; Berntsen *et al.*, 2011).

Diurnal variation of AXL has been reported in both animal (Nikla *et al.*, 1998; Nikla, 2006; Tian and Wildsoet, 2006; Read *et al.*, 2008) and human models (Stone *et al.*, 2004; Wilson

et al., 2006; Read *et al.*, 2008), and the results from this study also indicate significant diurnal variation in AXL across the whole cohort. In accordance with previous studies (Nikla *et al.*, 1998; Chakraborty *et al.*, 2011), there was no significant difference in diurnal variation between refractive groups. Previous studies over a two day period have reported AXL to be longest around midday and shortest in the night (Stone *et al.*, 2004; Chakraborty *et al.*, 2011), consistent with the findings of this study, as mean AXL of both refractive groups was greatest at 1200-1300 and shortest at 2000-2100. The magnitude of diurnal AXL variation across the whole cohort in this investigation was 20 μm , in keeping with previous findings, reporting AXL changes in the region of 15- 46 μm (Stone *et al.*, 2004; Read *et al.*, 2008; Chakraborty *et al.*, 2011). It has been suggested based on repeated measurements that the diurnal variations may be regulated by a range of physiologic factors (such as sleep amount, daily lighting exposure, and diet) (Stone *et al.*, 2004). Reports from marmoset (Nikla *et al.*, 2002) and chick (Papastergiou *et al.*, 1998) data suggest that diurnal axial length variations alter with age. However, a further study in humans utilised a similar age cohort of 20 – 27 years and also reported significant AXL variation over a 24 hour time period (Read *et al.*, 2008).

Various studies have demonstrated that intense close-work tasks, may result in transient periods of myopia (Wolffsohn *et al.*, 2003), potentially leading to the development of permanent myopia (Adams and McBrien, 1992; Mallen *et al.*, 2006). Transient axial length increase during sustained accommodative effort may lead to a slight reduction in the amount of hyperopic blur (Mallen *et al.*, 2006). Eyes of myopic individuals have demonstrated the largest expandability during (Drexler *et al.*, 1998; Mallen *et al.*, 2006; Read *et al.*, 2010), and immediately succeeding an accommodative task (Woodman *et al.*, 2010; Woodman *et al.*, 2012). Whilst many studies have reported increased AXL with accommodation as this may be relevant to refractive error development, it was not previously recognised whether accommodative AXL change shows diurnal variation. Unlike the significant effect of AXL diurnal variation that was observed, there was no change in accommodative AXL change in either refractive group. In accordance with this, in both emmetropic and myopic cohorts, there was no significant difference in accommodative axial elongation across measurement sessions. As such, accommodative AXL change data from previous studies are not significantly affected by diurnal variation and future investigations using this accommodative parameter do not need to account for the time of day the measurement was taken.

Accommodative accuracy has been reported widely with regards to myopia development; increased accommodative error may produce hyperopic retinal defocus considered to instigate axial elongation (Harb *et al.*, 2006; Mutti *et al.*, 2006; Berntsen *et al.*, 2010), as the theory that ocular growth is guided towards emmetropia by a visual feedback mechanism, detecting the sign and extent of retinal blur, is broadly acknowledged (Irving *et al.*, 1992;

Wildsoet and Wallman, 1995; McFadden *et al.*, 2004; Smith *et al.*, 2005; Berntsen *et al.*, 2011; Ho *et al.*, 2012). This is the first study, however, to explore the possibility of diurnal variations in accommodative error across emmetropic and myopic refractive groups; the results indicate that in both refractive groups, no significant difference in accommodative error occurred between any measured time points. Similarly, between the refractive groups, there was no significant difference in accommodative error for any time period, indicating that accommodative error is another element of accommodative function that is unaffected by ocular daily fluctuations.

As it has been hypothesised that myopic eyes are more malleable and susceptible to accommodative AXL elongation (Mallen *et al.*, 2006; Woodman *et al.*, 2010), the accommodative error should also be greater at the point in time when the retina has undergone greater magnitudes of this elongation. Whilst the accommodative error would therefore intuitively be thought to be greater during periods of the day where accommodative AXL change is greatest, the results do not support this hypothesis as accommodative axial elongation was constant. The lack of a significant relationship between accommodative AXL elongation and accommodative error at any measured time period indicates that these two elements of accommodative function are not related to one another.

2.5 Conclusion

In conclusion, this is the first study to investigate diurnal variation in accommodative AXL change and accommodative error. Both of these accommodative functions are not shown to fluctuate diurnally in either refractive group, and there was no relationship between AEI and accommodative AXL change at any measured time point. Hence, future work utilising these accommodative measures does not need to account for any diurnal variation during the investigation.

Chapter 3

Ciliary muscle morphology and ocular biometric correlates in emmetropia

3.1 Introduction

Evidence for altered ciliary muscle morphology with axial myopia is increasing (Oliveira *et al.*, 2005; Bailey *et al.*, 2008; Sheppard and Davies 2010; Buckhurst *et al.*, 2013) and indicates that the ciliary region is not stretched with axial elongation; the ciliary muscle in myopic eyes has not been found to be thinned, and moreover, a body of research has shown the myopic ciliary muscle to be thicker than that of emmetropes (Oliveira *et al.*, 2005; Bailey *et al.*, 2008; Buckhurst *et al.*, 2013).

Despite the reports of altered ciliary muscle morphology in myopia (which are documented in depth in the following chapter), normal variations in biometric characteristics of the emmetropic ciliary muscle are not yet known. The emmetropic ciliary muscle is influenced only by normal globe development. The morphology of the ciliary muscle in emmetropia is therefore of significant interest as the parameters which relate with particular ocular biometric correlates will indicate what defines ciliary muscle growth with normal ocular development, in the developed eye. Furthermore, other ocular biometric parameters have been investigated in emmetropes and gender contrasts were identified, with males having significantly longer vitreous chambers and axial length (AXL), flatter anterior corneal radii of curvature and lower lens powers than that of females. There were trends for other gender discrepancies including greater anterior chamber depth (ACD), and crystalline lens thickness (LT) in males that did not reach statistical significance (Atchison *et al.*, 2008; Atchison, 2009) though were of the order of significant differences identified in larger scale investigations (Klein *et al.*, 1998; Nomura *et al.*, 2002; Cosar and Sener, 2003; Wickremasinghe *et al.*, 2004; Shufelt *et al.*, 2005; Suzuki *et al.*, 2005; Li *et al.*, 2006a). Though there have been numerous reports comparing ciliary muscle morphology across refractive error groups (Oliveira *et al.*, 2005a; Bailey *et al.*, 2008; Schultz *et al.*, 2009; Sheppard and Davies, 2010b; Buckhurst *et al.*, 2013), it is not known whether such gender differences translate to ciliary muscle morphology and thus have a potential effect on any morphological alterations found.

Previous work investigating ocular biometry and ciliary muscle morphology in emmetropia was based on *in vitro* methods (Lutjen, 1966; van Alphen, 1986; Aiello *et al.*, 1992; Pardue and Sivak, 2000; Augusteyn *et al.*, 2012). Whilst such *in vitro* investigations have advanced our understanding in this area, findings may be modified by post mortem chemical tissue

changes, (Weale, 1999; Kasthurirangan *et al.*, 2008) along with handling and storage processes; the extent of these changes cannot be known (Strenk *et al.*, 2004; Werner *et al.*, 2008; Sheppard and Davies, 2010). *In vitro* methods also involve dissection of the accommodative apparatus (Lutjen-Drecoll *et al.*, 2010), and results in ambiguity as to whether the accommodative structures under investigation are behaving as they would in their habitual and intact accommodative system; therefore the ability to visualise the active human ciliary muscle and ocular biometric parameters *in vivo* is highly beneficial. The use of *in vivo* imaging techniques as research devices allows an enhanced comprehension of the anatomical and physiological ocular structures.

The work presented in this chapter is the first to investigate emmetropic eyes specifically, on a large scale and the biometric correlates of ciliary muscle parameters *in vivo*. Furthermore any gender differences in the morphology of the ciliary muscle is explored, when the eye has not undergone any pathological expansion.

3.2 Methods

3.2.1 Subjects

Sixty-nine subjects including thirty-nine females and thirty males, aged 19-26 years were recruited from the student and staff body of Aston University, with a mean sphere equivalent (MSE) ≥ -0.55 ; $< +0.75$ D. The narrow age band was selected to reduce variation in ciliary muscle data due to ageing, most notably thickening of the ciliary muscle (Sheppard and Davies, 2010). Exclusion criteria were cylindrical refractive errors greater than 2.00 D, amblyopia, previous history of ocular trauma, surgery or pathology, and systemic conditions known to affect ocular health. All participants had corrected visual acuities of 0.0 logMAR or better in each eye. Ethical approval was obtained from the Aston University Life and Health Sciences Research Ethics Committee and the study adhered to the tenets of the Declaration of Helsinki. Written, informed consent was obtained from all participants prior to commencement after explanation of the nature and possible consequences of the study.

3.2.2 Measurements

Binocular distance refractive error was measured with a validated infra-red binocular open-view autorefractor (Grand Seiko WAM 5500; Sheppard and Davies, 2010) whilst subjects viewed a distance (6 m) Maltese cross target. A minimum of five measurements of refractive error were taken for each eye, averaged and converted into MSE.

ACD, AXL, and LT in the unaccommodated state were obtained in the right eyes only of participants using the *Lenstar LS 900* biometer (Haag-Streit AG, Koeniz, Switzerland). Each

participant fixated on the letter closest to the central red fixation light whilst four separate biometric measurements were taken and averaged at 0 D.

3.2.3 Ciliary muscle image acquisition and analysis

AS-OCT (*Visante*; Carl Zeiss Meditec. Inc., Dublin, CA) images of nasal and temporal ciliary muscle regions were obtained from right eyes only of participants, using high-resolution corneal mode, as described in detail in section 1.7.7.

Several length and width measurements were acquired; curved ciliary muscle total length (CML) was determined as the anteroposterior distance from the scleral spur, signifying the anterior insertion along the ciliary muscle-scleral border, to the visible posterior tip of the ciliary muscle. The anterior length (AL) is measured from the scleral spur to the point of ciliary muscle maximum width (CMTMAX). CM25 is the muscle width at a point which was 25 % of the CML posterior to the scleral spur; similarly CM50 and CM75 values were measured at points 50 % and 75 % (CM50 and CM75 respectively) of the CML posterior to the scleral spur. Ciliary muscle thickness values were additionally measured at fixed distances from the scleral spur; CMT1 represents a point 1 mm posterior to the scleral spur, with CMT2 and CMT3 taken at points 2 mm and 3 mm posterior to the scleral spur, respectively.

Ciliary muscle images were exported from the AS-OCT in raw DICOM (Digital Imaging and Communications in Medicine) form for analysis purposes. A validated bespoke analysis programme (Laughton *et al.*, 2015; described in section 1.7.9), produced by the Aston University Ophthalmic Engineering Department, was used to measure ciliary muscle parameters; all image analysis was carried out by a single examiner (RNS). The programme calculates the distance between the scleral spur and a point beyond the posterior visible limit and the change in pixel intensity along each line is determined to help define the curved superior and inferior ciliary muscle border, as described in section 1.7.8.. A tiered refractive index correction was assigned by the programme to the scleral and ciliary muscle tissue (1.41 and 1.38, respectively) in each section of the image to adjust its dimensions accordingly (Laughton *et al.*, 2015).

3.3 Statistical Analysis

The relationship between axial length and emmetropic ciliary muscle parameters was determined by linear regression analysis, as was the relationship between anterior chamber depth and axial length, and anterior chamber depth and each ciliary muscle measure. To assess the differences in ciliary muscle parameters between male and female cohorts,

independent sample t-tests were utilised. A *P* value of less than 0.05 was considered significant in all analyses.

3.4 Results

Summary characteristics of emmetropic participants are provided in table 3.1. Ciliary muscle morphological parameters are displayed in table 3.2.

	Mean	Minimum	Maximum
Overall Age (years)	21.1 ± 8.63	19.1	26.8
Males:	21.5 ± 2.01	19.1	25.9
Females:	21.8 ± 2.08	19.3	26.8
Overall Axial length (mm)	23.56 ± 0.88*	21.50	25.56
Males:	24.14 ± 0.78	22.62	25.56
Females:	23.12 ± 0.66	21.50	24.40
Overall MSE (D)	-0.02 ± 0.32	-0.51	0.75
Males:	0.00 ± 0.33	-0.51	0.75
Females:	-0.03 ± 0.32	-0.47	0.72
Overall ACD (mm)	3.03 ± 0.29	2.43	3.68
Males:	3.15 ± 0.25	2.77	3.62
Females:	2.97 ± 0.30	2.43	3.68
Overall LT (mm)	3.41 ± 0.22	3.11	3.94
Males:	3.48 ± 0.16	3.29	3.72
Females:	3.57 ± 0.24	3.11	3.94

Table 3.1. Summary characteristics of the RE of emmetropic participants, n = 69 consisting of 39 females and 30 males. There was no significant difference in age between the gender groups (*P* = 0.495). *Indicates a significant difference between females and males.

Parameter (mm)	Nasal	Temporal
Overall CML	3.82 ± 0.61*	4.10 ± 0.63*
Males	4.28 ± 0.60	4.60 ± 0.60
Females	3.53 ± 0.40	3.80 ± 0.41
Overall AL	0.64 ± 0.15*	0.66 ± 0.15*
Males	0.68 ± 0.16	0.74 ± 0.22
Females	0.60 ± 0.15	0.59 ± 0.13
Overall CMT1	0.50 ± 0.06	0.50 ± 0.07
Males	0.51 ± 0.07	0.51 ± 0.07
Female	0.49 ± 0.06	0.49 ± 0.06
CMT2	0.30 ± 0.05*	0.33 ± 0.05*
Males	0.32 ± 0.05	0.34 ± 0.05
Females	0.29 ± 0.05	0.32 ± 0.04
CMT3	0.15 ± 0.04*	0.17 ± 0.04*
Males	0.16 ± 0.05	0.19 ± 0.05
Females	0.13 ± 0.04	0.16 ± 0.04
CM25	0.50 ± 0.06	0.49 ± 0.06
Males	0.49 ± 0.05	0.48 ± 0.05
Females	0.51 ± 0.05	0.50 ± 0.05
CM50	0.32 ± 0.03*	0.32 ± 0.04*
Males	0.29 ± 0.03	0.30 ± 0.04
Females	0.34 ± 0.03	0.33 ± 0.03
CM75	0.16 ± 0.02*	0.18 ± 0.03*
Males	0.14 ± 0.03	0.15 ± 0.03
Females	0.18 ± 0.03	0.18 ± 0.02
CMTMAX	0.56 ± 0.07	0.55 ± 0.07
Males	0.56 ± 0.07	0.54 ± 0.07
Females	0.57 ± 0.06	0.55 ± 0.06

Table 3.2. Mean ciliary muscle parameters across the emmetropic cohort. *Indicates significant difference between females and males.

3.4.1 Ciliary muscle length parameters and ocular biometric correlates

Temporal CML was greater than nasal CML (3.58 ± 0.40 mm and 3.85 ± 0.39 mm for nasal and temporal aspects, respectively, $P < 0.001$) though temporal AL was not significantly greater than nasal AL (0.64 ± 0.15 and 0.66 ± 0.16 mm for nasal and temporal aspects, respectively, $P = 0.598$). Across the whole cohort, AXL was linked with CML ($R = 0.519$, $r^2 = 0.268$, $P = 0.001$ for nasal aspect; $R = 0.475$, $r^2 = 0.226$, $P = 0.001$ for temporal aspect), AL (nasal: $R = 0.436$, $r^2 = 0.190$, $P = 0.001$; temporal: $R = 0.469$, $r^2 = 0.324$, $P = 0.001$) and ACD ($R = 0.335$, $r^2 = 0.112$, $P = 0.028$) There was no relationship between ACD and both CML aspects (nasal: $P = 0.362$; temporal: $P = 0.331$) or AL aspects (nasal: $P = 0.594$; temporal: $P = 0.401$) though ACD was significantly linked with nasal AL ($R = 0.369$, $r^2 = 0.136$, $P = 0.010$).

3.4.2 Gender differences in ciliary muscle length and ocular biometric correlates

In males, temporal CML was greater than nasal CML (4.28 ± 0.60 mm and 4.60 ± 0.62 mm for nasal and temporal aspects, respectively, $P = 0.031$) though temporal AL was not significantly greater than nasal AL ($P = 0.187$). In females, temporal CML was also greater than nasal CML (3.53 ± 0.40 and 3.80 ± 0.41 mm for nasal and temporal aspects, respectively) whilst there was no significant thickness difference between nasal and temporal AL ($P = 0.802$).

A significant gender difference occurred for AXL (24.14 ± 0.78 mm and 23.12 ± 0.66 for males and females, respectively, $P = 0.001$) (see figure 3.1), though not for ACD (3.15 ± 0.25 mm and 2.97 ± 0.30 mm for males and females, respectively, $P = 0.075$) or LT (3.48 ± 0.16 mm and 3.56 ± 0.24 mm for males and females, respectively, $P = 0.304$). Males were found to have significantly longer ciliary muscle, for both CML (nasal: 4.28 ± 0.60 mm and 3.53 ± 0.40 mm for males and females, respectively, $P = 0.002$; temporal: 4.60 ± 0.60 mm and 3.80 ± 0.41 mm for males and females respectively, $P = 0.001$) (see figure 3.1 and 3.2) and AL (nasal: 0.68 ± 0.16 mm and 0.63 ± 0.16 mm for males and females, respectively, $P = 0.028$; temporal: 0.74 ± 0.21 mm and 0.59 ± 0.13 mm for males and females, respectively, $P = 0.001$). In females, there was a significant link between AXL and nasal CML ($R = 0.949$, $r^2 = 0.900$, $P = 0.035$) though not with temporal CML ($P = 0.334$) or AL (nasal: $P = 0.438$; temporal: $P = 0.552$). Across males, there was a significant link between AXL and nasal CML ($R = 0.414$, $r^2 = 0.171$, $P = 0.023$) and AL (nasal: $R = 0.457$, $r^2 = 0.209$, $P = 0.006$; temporal: $R = 0.487$, $r^2 = 0.237$, $P = 0.004$) though not with temporal CML ($P = 0.093$).

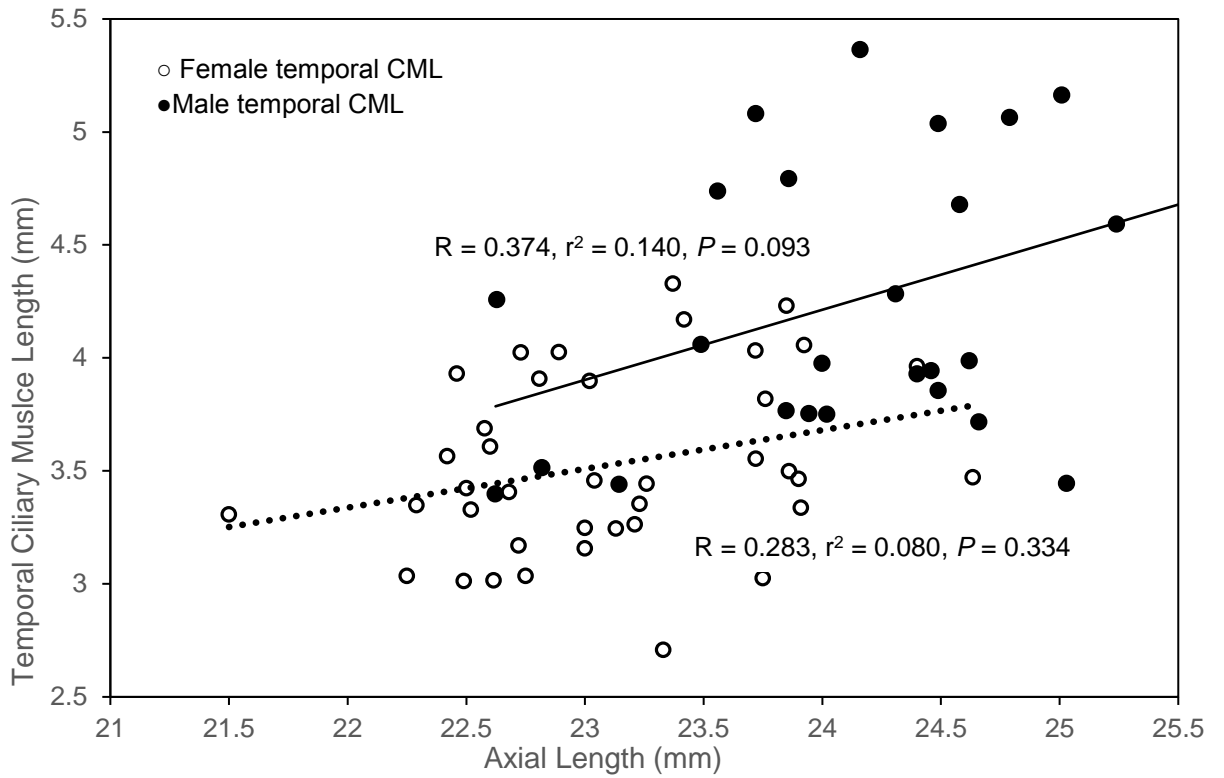


Figure 3.1 Relationship between AXL and temporal CML in male (solid line) emmetropes ($n = 30$) and female (dashed line) emmetropes ($n = 39$). Temporal CML was significantly longer than temporal CML in females ($P = 0.001$)

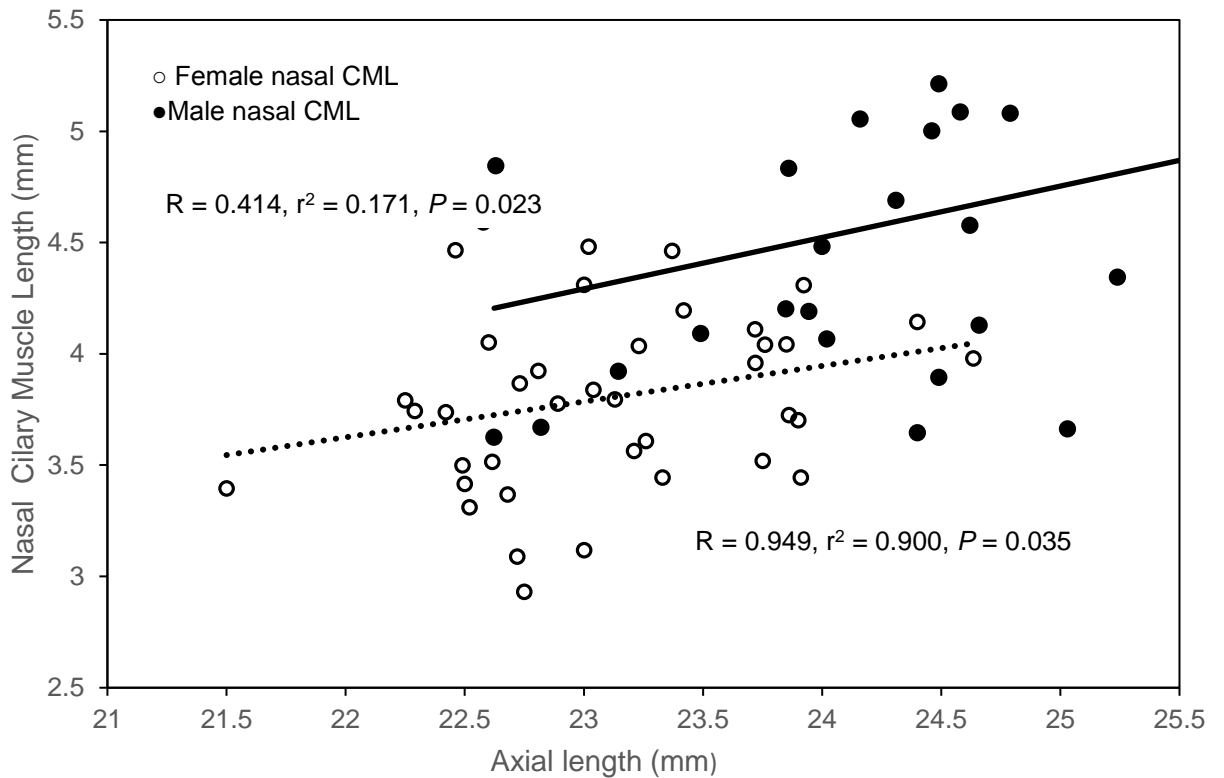


Figure 3.2. Relationship between AXL and nasal CML in male (solid line) emmetropes ($n = 30$) and female (dashed line) emmetropes ($n = 39$). The AXL in males was significantly longer in females ($P = 0.001$), as was nasal CML ($P = 0.002$).

3.4.3 Ciliary muscle thickness parameters and ocular biometry

Across the whole cohort, there was no significant thickness difference at CMT1 and CM25 between nasal and temporal aspects ($P = 0.649$ for CMT1 and $P = 0.121$ for CM25). Temporal CMT2 and CMT3 were greater than nasal CMT2 and CMT3, respectively (CMT2: $P < 0.002$; CMT3: $P < 0.001$). Thickness difference between nasal and temporal aspects at CM50 and CM75 was not significant ($P = 0.618$ for CM50 and $P = 0.501$ for CM75). There was no significant thickness difference between nasal and temporal aspects for CMTMAX ($P = 0.134$).

AXL across the whole cohort was linked significantly with CMT at nasal CM75 ($R = 0.354$, $r^2 = 0.125$, $P = 0.002$), temporal CMT75 ($R = 0.381$, $r^2 = 0.145$, $P = 0.001$), nasal CM2 ($R = 0.235$, $r^2 = 0.055$, $P = 0.030$) nasal CM3 ($R = 0.224$, $r^2 = 0.050$, $P = 0.036$) and temporal CM50 ($R = 0.285$, $r^2 = 0.081$, $P = 0.010$). AXL was not significantly related with nasal CM50 ($P = 0.063$), CM25 for either aspect (nasal: $P = 0.538$; temporal: $P = 0.823$), CM1 for either aspect (nasal: $P = 0.145$; temporal: $P = 0.450$), temporal CM2 ($P = 0.166$) or temporal CM3 ($P = 0.181$). ACD was significantly linked with nasal CM1 ($R = 0.261$, $r^2 = 0.068$, $P = 0.041$).

3.4.4 Gender differences in ciliary muscle thickness

In males, temporal CM2 and CM3 was significantly greater than nasal CM2 (0.32 ± 0.05 and 0.34 ± 0.05 mm for nasal and temporal aspects, respectively; $P = 0.023$) and CM3 (0.16 ± 0.05 and 0.19 ± 0.05 mm for nasal and temporal aspects, respectively, $P = 0.003$), respectively. There was no significant difference between nasal and temporal aspects for CM1 ($P = 0.939$) and CM25 ($P = 0.383$), or CM50 ($P = 0.358$), CM75 ($P = 0.290$) or CMTMAX ($P = 0.132$). In females, there was also a significant thickness difference between nasal and temporal CM2 (0.29 ± 0.05 and 0.32 ± 0.04 mm, for nasal and temporal and temporal aspects, respectively, $P = 0.025$) and CM3 (0.13 ± 0.04 and 0.16 ± 0.04 mm for nasal and temporal aspects, respectively, $P = 0.006$) and no significant difference between nasal and temporal aspects for CM1 ($P = 0.959$), CM25 ($P = 0.436$), or CM50 ($P = 0.911$), CM75 ($P = 0.932$) or CMTMAX ($P = 0.835$).

There were no significant gender differences for CM1 (0.51 ± 0.07 and 0.49 ± 0.06 mm for males and females, respectively, for both aspects, $P = 0.610$), CM25 (nasal: 0.49 ± 0.05 mm and 0.50 ± 0.05 mm for males and females, respectively, $P = 0.770$; temporal: 0.48 ± 0.05 mm and 0.50 ± 0.05 mm for males and females, respectively, $P = 0.527$) or CMTMAX (nasal: 0.56 ± 0.07 mm and 0.57 ± 0.06 mm for males and females, respectively, $P = 0.496$; temporal: 0.54 ± 0.07 mm and 0.55 ± 0.06 mm for males and females, respectively, $P = 0.130$). Males showed significantly greater thickness at CM2 (nasal: 0.32 ± 0.05 mm and 0.29 ± 0.05 mm

for males and females, respectively, $P = 0.035$; temporal: 0.34 ± 0.05 mm and 0.32 ± 0.04 mm for males and females, respectively) and CM3 (nasal: 0.16 ± 0.05 mm and 0.13 ± 0.04 mm for males and females, respectively, $P = 0.017$; temporal: 0.19 ± 0.05 mm and 0.16 ± 0.04 mm for males and females, respectively, $P = 0.002$). Thickness measures proportional to CML showed females to have significantly greater thickness values than males at CM50 (nasal: 0.29 ± 0.03 mm and 0.34 ± 0.03 mm for males and females, respectively, $P = 0.001$; temporal: 0.30 ± 0.04 mm and 0.34 ± 0.03 mm for males and females, respectively, $P = 0.001$) and CM75 (nasal: 0.14 ± 0.03 mm and 0.18 ± 0.03 mm for males and females, respectively, $P = 0.001$; temporal: 0.15 ± 0.03 mm and 0.18 ± 0.03 mm for males and females, respectively, $P = 0.001$).

3.5 Discussion

Whilst comparisons have been made regarding ciliary muscle morphology across emmetropic and myopic cohorts (Bailey *et al.*, 2008; Sheppard and Davies, 2010; Buckhurst *et al.*, 2013; Pucker *et al.*, 2013), the ciliary muscle has not been evaluated in emmetropes specifically. Since the emmetropic ciliary muscle is only influenced by normal globe development and with absence of any pathological globe expansion, the morphology of the ciliary muscle in emmetropia is therefore of significant interest; the ciliary muscle parameters which are linked with particular ocular biometric correlates implicates what defines ciliary muscle growth with normal ocular development. This study is the first to investigate ciliary muscle morphology and ocular biometric correlates in an emmetropic cohort, on a large scale.

Across the emmetropic cohort, AXL was linked with ACD, ciliary muscle length (both AL and CML) and CMT, whilst ACD was linked with AL and CMT, indicating ciliary muscle growth with normal ocular development. The temporal ciliary muscle aspect was longer (for both AL and CML) and thicker at CM2 and CM3; such nasal-temporal asymmetry has been identified in *in vitro* investigations of human ciliary body morphology, with a longer temporal aspect established (Aiello *et al.*, 1992), and this discrepancy corresponds with the thicker temporal side and increased contractile response from this aspect found *in vivo* (Sheppard and Davies, 2010b). Though the significance of this intraocular asymmetry is not well understood, ciliary apparatus asymmetry has been observed in the rhesus monkey *in vitro* (Glasser *et al.*, 2001), where it was suggested that this morphological variation may be required to permit lenticular axis alignment and maintain binocular single vision during accommodative convergent eye movements (Glasser *et al.*, 2001; Sheppard and Davies, 2010b).

In keeping with previous biometric findings across varying refractive errors (Wickremasinghe *et al.*, 2004; Hashemi *et al.*, 2012; Wang *et al.*, 2015), and specifically in an emmetropic cohort (Atchison *et al.*, 2008; Atchison *et al.*, 2009), AXL was found to be significantly longer in males

compared with females (see figure 3.1), with a mean difference of 1.02 mm. This difference is somewhat larger than that found by Atchison and co-workers (2009), who found a greater AXL in males by a mean difference of 0.72 mm, though mean overall non-gender specific AXL found here in this study was 23.56 mm, similar to that found by Atchison *et al* (2009), at 23.39 mm. There was also a trend for males to have a greater ACD compared to females, but similar to previous work in emmetropes (Atchison *et al.*, 2008; Atchison *et al.*, 2009), this difference, and the difference in LT between males and females, did not reach statistical significance, indicating that the increased AXL in males is attributable to vitreous elongation.

Since males were found to have a significantly longer AXL compared with females, it is fitting therefore that ciliary muscle morphology is altered between gender, given the current evidence of increased ciliary muscle length and thickness in axially longer eyes (Oliveira *et al.*, 2005; Bailey *et al.*, 2008; Buckhurst *et al.*, 2013; Pucker *et al.*, 2013). Both CML and AL were significantly longer in males, relative to females. There was no thickness difference between the gender groups for CM25 and CM1, however, the data indicates that females have significantly greater CMT at CM50 and CM75, for both nasal and temporal aspects. Conversely, males had significantly greater CMT at CM2 and CM3, compared with females.

Whilst these findings appear contradictory at first, since it is assumed that CM50 and CM75 are in a similar ciliary muscle region to CM2 and CM3, respectively, the differences in these two methods (thicknesses taken proportional to the CML, and at fixed width measures) to measure ciliary muscle thickness explain the findings (see figure 3.3); because males have a longer AXL and therefore a longer CML compared with females, a measure of CM2 in a longer, male ciliary muscle is not in the same anatomical region in a shorter, female ciliary muscle. The same concept applies for CM3 as demonstrated in figure 3.3, and highlights that CM2 and CM50 are not at all the same anatomical regions, as CM75 and CM3 are evidently not either. Moreover, in a shorter ciliary muscle representative of that in the female cohort, CM50 and CM75 are regions which fall anterior to CM2 and CM3, respectively, whereas in a longer ciliary muscle which is characteristic of those in males, CM50 and CM75 are regions which fall posterior to CM2 and CM3, respectively. Therefore, the reason the data suggests that males have increased CMT compared with females, at CM2 and CM3, is due to the fact that in a longer ciliary muscle, these fixed width measures fall on a relatively more anterior, and consequently thicker region of the ciliary muscle than in a shorter ciliary muscle. It can be deduced from the thickness measures proportional to the CML, that females demonstrate greater ciliary muscle thickness compared with males, despite males possessing a significantly longer ciliary muscle. It would be expected for males to have increased CMT considering the data indicates AXL is linked with CMT, and previous work has shown that

CMT increases with increasing negative refractive error (Oliveira *et al.*, 2005; Bailey *et al.*, 2008). Such findings cannot be explained and warrant further investigation.

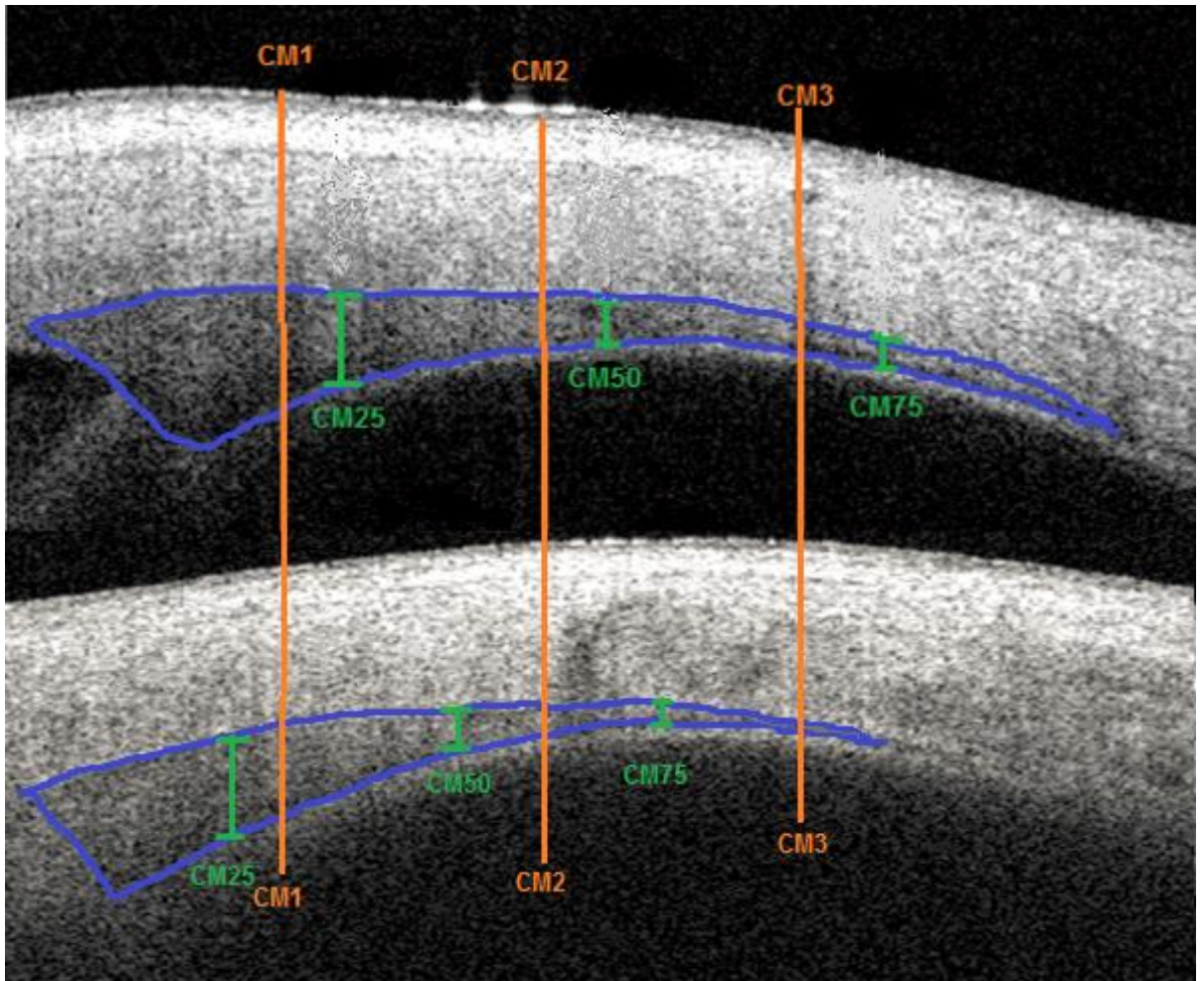


Figure 3.3. Top image is the ciliary muscle of a male emmetropic subject with an axial length of 25.56 mm. Bottom image is the ciliary muscle of a female emmetropic subject with an axial length of 22.60 mm and correspondingly shorter ciliary muscle. The orange lines depict where the fixed width measures (CM1, CM2 and CM3) are taken along the ciliary muscle, relative to thickness measures proportional to the overall length (CM25, CM50, CM75). The proportional measures all lie posterior to the fixed width measures in the longer, male ciliary muscle and anterior in the shorter, female ciliary muscle.

Since the proportional ciliary muscle measures fall posteriorly to the fixed width parameters in the longer, male ciliary muscle, it is therefore demonstrated that the arbitrary, fixed width measures evidently do not take into consideration that ciliary muscle lengths vary with varying AXL and may therefore present data with somewhat misleading outcomes. The findings here are in agreement with previous work which suggested that fixed width measures may signify a different ciliary body anatomical region in varying refractive errors (Sheppard and Davies, 2010b). Thickness measures proportional to the CML do not have the same shortcomings

and aim to measure thickness of the ciliary muscle at the same regions of the ciliary muscle, across varying ciliary muscle morphology.

3.6 Conclusion

To conclude, this is the first study to investigate specifically the emmetropic ciliary muscle, on a large scale. Length and thickness were greater than that of the nasal aspect. Gender differences in the overall length were found, corresponding with the significantly longer axial lengths and therefore CML, in males. However, thickness measures proportional to the CML (CM50 and CM75) were found to be greater in females. Arbitrary, fixed width measures, relative to the scleral spur do not take into account that the ciliary muscle length varies amongst individuals, and may produce misleading results.

Chapter 4

Inter- eye ciliary muscle symmetry and morphological variation with refractive error

4.1 Introduction

Myopia represents a considerable health concern and is one of the foremost global causes of visual impairment (Lin *et al.*, 1996; Saw, 2003; Woodman *et al.*, 2011; Ghosh *et al.*, 2014). The refractive condition affects approximately one sixth of the worldwide population (Norton *et al.*, 2005; Logan *et al.*, 2011) and its prevalence is continuing to increase (Rose *et al.*, 2001; Vitale *et al.*, 2008; Williams *et al.*, 2015), such that myopia has expanded to epidemic proportions in certain industrialised East Asian communities (e.g. Singapore) where at least 70 % of adolescents are myopic (Seet *et al.*, 2001; Logan *et al.*, 2011). There is a significant effect of myopia on all spheres of society, and East Asian countries include refractive error in their educational, health, and economic strategic plans (Logan *et al.*, 2011). Myopia can impact considerably on quality of life, ranging from having cost implications and being a simple visual inconvenience to sufferers, to a predisposition to certain sight threatening pathological conditions (Mitchell *et al.*, 1999; Gilmartin *et al.*, 2004; Logan *et al.*, 2011). Associated ocular pathologies include glaucoma (Mitchell *et al.*, 1999), cataract (Lim *et al.*, 1999), retinal detachment and chorioretinal degeneration (Grossniklaus and Green, 1992). Whilst the precise aetiology of myopia is not fully understood, it is believed to be multifactorial in origin, consisting of both genetic and environmental constituents (Mutti 2010; Woodman *et al.*, 2011; Williams *et al.*, 2015).

There is increasing evidence of altered ciliary muscle morphology in myopia (van Alphen, 1986; Mutti *et al.*, 2000; Walker and Mutti, 2002; Harb *et al.*, 2006; Sheppard and Davies, 2010b; Buckhurst *et al.*, 2013). *In vitro* findings have indicated that the ciliary muscle in myopic eyes is longer due to simple globe expansion (van Alphen, 1986). However, several more recent *in vivo* studies investigating ciliary muscle morphology (Mutti *et al.*, 2000; Walker and Mutti, 2002; Harb *et al.*, 2006; Sheppard and Davies, 2010b; Buckhurst *et al.*, 2013) dispute such evidence, as the ciliary region in myopic eyes is not thinned as would be expected from simple mechanical stretching with axial growth (Bailey *et al.*, 2008; Sheppard and Davies, 2010b; Lewis *et al.*, 2012; Buckhurst *et al.*, 2013). Several other investigations have also contradicted the *in vitro* experimental findings of van Alphen, but by demonstrating that the ciliary muscle is thicker in the myopic eye compared with non-myopic eyes (Oliveira *et al.*, 2005a; Bailey *et al.*, 2008; Buckhurst *et al.*, 2013). Though it may have been assumed that hyperopic eyes should exhibit greater ciliary muscle thickness owing to the increased accommodative effort expended compared to the non-hyperope (Oliveira *et al.*, 2005; Pucker

et al., 2013), there was no dependency between axial length and the proportional measurements of ciliary muscle thickness (CM25, CM50 & CM75; Sheppard and Davies, 2010). However, such findings differ from previous work using AS-OCT, which acknowledged a strong relationship between ciliary body thickness at areas 2 mm and 3 mm posterior to the scleral spur (CM2 and CM3, respectively) and axial myopia (Bailey *et al.*, 2008). A mutual finding between both investigations revealed that CM2 did show an association of being thicker with increased axial length (Bailey *et al.*, 2008; Sheppard and Davies, 2010). Similarly, a study utilising UBM for the *in vivo* assessment of ciliary body thickness demonstrated that the mean CBT2 was significantly greater in myopes than emmetropes and hyperopes, whilst emmetropes also displayed an increased mean CBT2 compared with hyperopes. Also, mean CBT3 was shown to be significantly greater in myopes than emmetropes and hyperopes, and again, was significantly increased in emmetropes compared with hyperopes (Oliveira *et al.*, 2005).

Further anterior segment optical coherence tomography (AS-OCT) - based research of the ciliary region by Lewis *et al* (2012) revealed that eyes of longer axial lengths show greater ciliary muscle thickness values at CMT2 and CMT3, in both the relaxed state, and with accommodation, supporting previous findings that myopes have a regionally thicker ciliary muscle than hyperopic or emmetropic subjects (Bailey *et al.*, 2008). Such thickening of the ciliary muscle has been implicated as a potential physiological response in myopic eyes, (Bailey *et al.*, 2008), whilst the thinner hyperopic ciliary muscle has been hypothesised to result from a disruption of the basic stress-response relationship that occurs in all recognised muscles (Pucker *et al.*, 2013). The pre-presbyopic ciliary muscle was also studied with AS-OCT by Sheppard and Davies (2010) and results indicated that the relaxed ciliary muscle has a significantly longer overall and anterior length in eyes of greater axial length. It was predicted that radial growth-thickening of the ciliary muscle occurs in conjunction with axial elongation during myopigenesis (Sheppard and Davies, 2010). Key findings of *in vivo* studies of human ciliary muscle morphology with refractive error are summarised in table 4.1. Evidently, ciliary muscle morphology in terms of both length and particular thickness sections appear to be altered in myopic eyes. Nonetheless, ambiguity between findings of previous studies remain, and the significance of these observations is not fully understood.

Results from various studies including human MRI work (Atchison *et al.*, 2004) and study of the infant monkey (Smith *et al.*, 2005) indicate that equatorial expansion of the globe is a significant aspect in the development of myopia (Logan *et al.*, 2004; Mutti *et al.*, 2007). Thickening of the ciliary muscle may develop from hypertrophy, resulting in excessive collagen deposition running through the ciliary muscle in a circular orientation. As such, the

thickened ciliary muscle mechanically blocks equatorial expansion necessary for maintenance of emmetropia (Bailey *et al.*, 2008; Mutti 2010). Moreover, this hypertrophic ciliary body would also cause enlargement of the ciliary muscle cells, reducing the contractile response (Seidel and Weisbrodt, 1987; Bailey *et al.*, 2008).

Authors & study title	Imaging method	Cohort	Key findings	Implications
Oliveira <i>et al.</i> 2005 Ciliary body thickness increases with increasing axial myopia	UBM	n = 75 (mean age 51.8 ± 16.5 years)	Mean CB2 values vary with refractive group: Myopes = 490 µm Emmetropes = 362 µm Hyperopes = 317 µm	Strong association between CB2 and refractive error. CB2 increases with myopia and axial length.
Bailey <i>et al.</i> 2008 Ciliary body thickness and refractive error in children	AS-OCT	n = 53 children (mean age 11.8 years ± 2.31; range: 8 – 15 years)	Mean ciliary body thickness in myopes = 630 µm and emmetropes = 574 µm. CB2 strongly correlated with axial length and myopia	Hypertrophy of ciliary muscle could be implicated in myopigenesis, due to increased accommodative lag, key to the retinal defocus model of myopia development.
Sheppard and Davies, 2010 <i>In vivo</i> analysis of ciliary muscle morphologic changes with accommodation and axial ametropia	AS-OCT	n = 50 presbyopes (mean age 28.5 ± 4.5 years; range: 19- 34 years)	The ciliary muscle was longer in eyes with greater axial length. The ciliary muscle was thicker and showed a greater contractile response on the temporal aspect.	Axial elongation is accompanied by some radial growth—thickening of the ciliary muscle during myopigenesis
Pucker <i>et al.</i>, 2013 Region-specific relationships between refractive error and ciliary muscle thickness in children	AS-OCT	n = 269 children (mean age 8.7 ± 1.51 years; range: 6 – 14 years)	Refractive error was significantly associated only with CMT2 and CMT3. Apical fibers at CMT1 and CMTMAX had a significant relationship with refractive error.	Posterior ciliary muscle fibers (CMT2 & CMT3) are thicker in myopia, but the apical ciliary muscle fibers (CMTMAX & CMT1) are thicker in hyperopia
Buckhurst <i>et al.</i>, 2013 Ocular biometric correlates of ciliary muscle thickness in human myopia	AS-OCT	n = 62 (mean age 27.7 years ± 5.29; range: 18 – 40 years)	Refractive error was significantly associated with CMT, with thicker CMT2 and CMT3 found in the myopic eyes.	Increased CMT is associated with myopia.

Table 4.1. Key findings from *in vivo* studies of human ciliary muscle morphology and refractive error. CB2 is ciliary body thickness, measured 2 mm posterior to the scleral spur. CMT1, CMT2 and CMT3 are ciliary muscle thickness measurements at 1mm, 2 mm and 3 mm posterior to the scleral spur, respectively. CMTMAX is the ciliary muscle maximum thickness.

Previous *in vivo* human ciliary muscle investigations have investigated only one eye, and many have been limited to just one aspect (e.g. the temporal side); as such, the inter-eye symmetry of the ciliary muscle, which may be relevant to refractive error development, is not understood. Similarly, many studies of refractive error have reported data from one eye (Shufelt *et al.*, 2005; Mutti *et al.*, 2007; Liao *et al.*, 2014). However, a relatively recent MRI investigation examined bilateral globe profile in myopia and emmetropia (Gilmartin *et al.*, 2013). Posterior vitreous chamber shapes were established from T2-weighted MRI, using a cohort of 55 adult participants. Coordinate reference points to contrast with the myopic globe profile were mapped to an emmetropic eye; these three-dimensional surface model coordinates were allotted to inferior, superior, temporal and nasal quadrants and plotted in a two-dimensional model to reveal the compound profile of respective quadrants (Gilmartin *et al.*, 2013). Globe shape was linked to retinotopic projection in both myopes and emmetropes; emmetropic and myopic eyes could not be differentiated with regards to equatorial dimensions. While symmetry was observed between the two eyes of each subject for the superior to inferior vitreous chamber shape, asymmetry in the horizontal laterality of globe profile in myopia development was found; there was asymmetry between nasal and temporal quadrants in right and left eyes, but a symmetrical relationship between the temporal quadrant of one eye and the contralateral nasal quadrant, and vice versa (Gilmartin *et al.*, 2013). Since the decussation of nasal and temporal retinal nerve fibres into right and left visual fields occurs at the optic chiasm (Bron *et al.*, 1997), the coupling indicates that binocular growth may be coordinated by signals produced beyond the optic chiasm (Gilmartin *et al.*, 2013). It is not known whether ciliary muscle morphology displays similar properties between the refractive error groups. Such laterality in myopia development may reflect ciliary muscle laterality, and previous investigations have not studied this matter. More work was needed to fill this gap in the current knowledge in this area, and this investigation aimed to provide answers relating to ciliary muscle morphology and laterality.

The purpose of this investigation was to link the morphological characteristics of the ciliary muscle with axial length across emmetropes and myopes, and to study the inter-eye ciliary muscle symmetry of both aspects (nasal and temporal), for the first time on a large scale.

4.2 Methods

4.2.1 Subjects

One hundred subjects aged 19-26 years were recruited from the student body of Aston University, consisting of fifty emmetropic volunteers with a mean sphere equivalent ($MSE \geq -0.55$; $< +0.75$ D) and fifty myopes ($MSE \leq -2.00$ D). The narrow age range was chosen to reduce discrepancies in ciliary muscle data due to ageing, most notably ciliary muscle

thickening (Sheppard and Davies, 2010). Exclusion criteria were cylindrical refractive errors greater than 2.00 D, anisometropia ≥ 1.00 D, amblyopia, previous history of ocular trauma, surgery or pathology, and systemic conditions known to affect ocular health. All participants had corrected visual acuities of 0.0 logMAR or better in each eye. Myopic participants wore 31% Nelfilcon A (Focus Dailies) contact lenses appropriate for their habitual refractive error for all ciliary muscle imaging. Ethical approval was obtained from the Aston University Life and Health Sciences Research Ethics Committee and the study adhered to the tenets of the Declaration of Helsinki. Written, informed consent was obtained from all participants prior to commencement after explanation of the nature and possible consequences of the study.

4.2.2 Measurements

Binocular distance refractive error was measured with a validated infra-red binocular open-view autorefractor (*Grand Seiko WAM 5500*; Sheppard and Davies, 2010) whilst subjects viewed a distance (6 m) Maltese cross target. A minimum of five measurements of refractive error were taken for each eye, averaged and converted into MSE.

AXL in the unaccommodated state was obtained in each eye, and ACD and LT was obtained in the unaccommodated state in right eyes only, using the *Lenstar LS 900* biometer (*Haag-Streit AG*, Koeniz, Switzerland). Each participant fixated on the letter closest to the central red fixation light whilst four separate biometric measurements were taken and averaged at 0 D.

4.2.3 Ciliary muscle image acquisition and analysis

AS-OCT (*Visante*; Carl Zeiss Meditec. Inc., Dublin, CA) images of nasal and temporal ciliary muscle regions were obtained from right and left eyes of participants, using high-resolution corneal mode, as detailed in section 1.7.7. Ciliary muscle images were exported from the AS-OCT in raw DICOM (Digital Imaging and Communications in Medicine) form for analysis purposes. A validated bespoke analysis programme (Laughton *et al.*, 2015) was used to measure ciliary muscle parameters, as detailed in section 1.7.8. All image analysis was carried out by a single examiner (RNS).

Several length and width measurements were acquired (see figure 1.23); ciliary muscle total length (CML) was determined as the anteroposterior distance from the scleral spur, signifying the anterior insertion along the ciliary muscle-scleral border, to the visible posterior tip of the ciliary muscle. The anterior length (AL) is from the scleral spur to the point of ciliary muscle maximum width (CMTMAX). CM25 is the muscle width at a point which was 25 % of the CML posterior to the scleral spur; similarly CM50 and CM75 measures were taken at points 50 %

and 75 % (CM50 and CM75 respectively) of the CML posterior to the scleral spur. Additionally, ciliary muscle thickness measurements were taken at fixed distances from the scleral spur; CMT1 represents a point 1 mm posterior to the scleral spur, with CMT2 and CMT3 taken at points 2 mm and 3 mm posterior to the scleral spur, respectively.

4.2.4 Statistical analysis

The data for each variable were normally distributed, as examined by tests of normality (Shapiro-Wilk) (SPSS Statistics 21; IBM, Illinois, USA). The relationship between axial length and ciliary muscle parameters was determined by linear regression analysis for each refractive group, as was the relationship between anterior chamber depth and axial length, and anterior chamber depth and each ciliary muscle measure. A *P* value of < 0.05 was considered significant. To assess the differences in ciliary muscle parameters between aspects (nasal and temporal) and refractive groups and to determine whether any differences occurred between eyes, two-way, mixed-factor ANOVAs were performed (SPSS Statistics 21; IBM, Illinois, USA.)

4.3 Results

Summary characteristics of emmetropic and myopic participants are provided in table 4.2. Mean axial length in both eyes (*P* < 0.001) and anterior chamber depth (*P* = 0.001) were significantly greater in the myopic group, though no significant difference between the refractive groups found for LT (*P* = 1.000). Ciliary muscle morphological parameters are displayed in table 4.3. There was no significant difference in age between the refractive groups (*P* = 0.884) or in axial length between right and left eyes across the whole cohort (*P* = 0.431).

	Emmetropes (n = 50)			Myopes (n = 50)		
	Mean	Minimum	Maximum	Mean	Minimum	Maximum
Age (years)	21.1 ± 8.63	19.2	26.8	21.7 ± 8.84	19.3	26.1
Right eye axial length (mm)	23.29 ± 0.80*	21.50	25.24	25.46 ± 1.16*	23.53	28.02
Left eye axial length (mm)	23.23 ± 0.80*	21.55	25.00	25.47 ± 1.28*	23.48	27.98
ACD (mm)	3.03 ± 0.29*	2.43	3.68	3.23 ± 0.25*	2.67	3.71
LT (mm)	3.53 ± 0.22	3.11	3.94	3.51 ± 0.23	3.14	3.78

Table 4.2. Summary characteristics of emmetropic (n= 50) and myopic (n= 50) participants. Both eyes were grouped for MSE; there was no significant difference in MSE between the two eyes of emmetropic (*P* = 0.062) and myopic (*P* = 0.793) participants. Similarly, there was no significant difference in AXL between the two eyes of emmetropic (*P* = 0.232) and myopic (*P* = 0.527). *Indicates significant difference between the refractive groups.

Parameter (mm)	Emmetropes		Myopes	
	RE	LE	RE	LE
Nasal CML	3.58 ± 0.40	3.65 ± 0.35	5.01 ± 0.54	4.99 ± 0.55
<i>Range</i>	2.71 – 4.59	2.94 – 4.40	3.85 – 5.98	4.00 – 6.57
Temporal CML	3.85 ± 0.39	3.88 ± 0.41	5.53 ± 0.54	5.47 ± 0.52
<i>Range</i>	2.93 – 4.59	2.97 – 4.78	4.57 – 6.54	4.47 – 6.62
Nasal AL	0.60 ± 0.15	0.61 ± 0.15	0.73 ± 0.12	0.73 ± 0.11
<i>Range</i>	0.25 – 0.89	0.39 – 0.97	0.50 – 1.06	0.46 – 0.99
Temporal AL	0.60 ± 0.13	0.60 ± 0.14	0.82 ± 0.14	0.80 ± 0.11
<i>Range</i>	0.33 – 0.82	0.35 – 0.94	0.57 – 1.20	0.55 – 1.08
Nasal CMT1	0.49 ± 0.06	0.48 ± 0.06	0.59 ± 0.04	0.59 ± 0.04
<i>Range</i>	0.36 – 0.66	0.38 – 0.61	0.47 – 0.66	0.50 – 0.66
Temporal CMT1	0.49 ± 0.07	0.50 ± 0.07	0.61 ± 0.05	0.60 ± 0.06
<i>Range</i>	0.30 – 0.62	0.34 – 0.65	0.51 – 0.70	0.46 – 0.69
Nasal CMT2	0.29 ± 0.05	0.30 ± 0.05	0.39 ± 0.05	0.38 ± 0.05
<i>Range</i>	0.19 – 0.44	0.18 – 0.44	0.26 – 0.49	0.28 – 0.48
Temporal CMT2	0.32 ± 0.05	0.32 ± 0.05	0.42 ± 0.04	0.42 ± 0.05
<i>Range</i>	0.22 – 0.46	0.23 – 0.46	0.32 – 0.53	0.33 – 0.50
Nasal CMT3	0.13 ± 0.04	0.14 ± 0.04	0.23 ± 0.05	0.22 ± 0.05
<i>Range</i>	0.06 – 0.26	0.05 – 0.25	0.12 – 0.33	0.15 – 0.35
Temporal CMT3	0.16 ± 0.04	0.16 ± 0.05	0.27 ± 0.05	0.27 ± 0.04
<i>Range</i>	0.10 – 0.29	0.07 – 0.27	0.16 – 0.38	0.18 – 0.35
Nasal CM25	0.51 ± 0.06	0.51 ± 0.06	0.54 ± 0.04	0.54 ± 0.03
<i>Range</i>	0.39 – 0.62	0.39 – 0.70	0.44 – 0.60	0.47 – 0.60
Temporal CM25	0.50 ± 0.06	0.50 ± 0.06	0.54 ± 0.04	0.53 ± 0.05
<i>Range</i>	0.38 – 0.62	0.36 – 0.66	0.46 – 0.67	0.41 – 0.63
Nasal CM50	0.33 ± 0.03	0.33 ± 0.03	0.31 ± 0.03	0.31 ± 0.03
<i>Range</i>	0.27 – 0.42	0.26 – 0.41	0.23 – 0.37	0.24 – 0.40
Temporal CM50	0.33 ± 0.04	0.34 ± 0.04	0.31 ± 0.04	0.31 ± 0.04
<i>Range</i>	0.27 – 0.44	0.26 – 0.45	0.23 – 0.46	0.24 – 0.43
Nasal CM75	0.18 ± 0.02	0.18 ± 0.03	0.14 ± 0.02	0.14 ± 0.02
<i>Range</i>	0.13 – 0.24	0.12 – 0.26	0.09 – 0.22	0.10 – 0.19
Temporal CM75	0.18 ± 0.03	0.18 ± 0.03	0.15 ± 0.03	0.15 ± 0.02
<i>Range</i>	0.13 – 0.24	0.12 – 0.24	0.11 – 0.25	0.11 – 0.21
Nasal CMTMAX	0.56 ± 0.07	0.75 ± 0.05	0.64 ± 0.06	0.65 ± 0.05
<i>Range</i>	0.41 – 0.70	0.41 – 0.69	0.52 – 0.78	0.54 – 0.72
Temporal CMTMAX	0.55 ± 0.07	0.55 ± 0.07	0.64 ± 0.06	0.63 ± 0.07
<i>Range</i>	0.40 – 0.66	0.37 – 0.68	0.51 – 0.79	0.48 – 0.82

Table 4.3. Mean ciliary muscle parameters in emmetropic and myopic participants. There was no significant differences between RE and LE for any ciliary muscle parameter in emmetropes or myopes.

4.3.1 Ciliary muscle length and symmetry

In both refractive groups, temporal CML was greater than nasal CML, in right and left eyes (right mean CML = 3.58 ± 0.40 mm and 3.85 ± 0.39 mm for nasal and temporal aspects, respectively, $P < 0.001$; left: 3.65 ± 0.35 mm and 3.88 ± 0.41 mm for nasal and temporal aspects, respectively, $P < 0.001$), though the difference between eyes for both aspects was not significant (temporal: $P = 0.393$ and nasal: $P = 0.095$) (see figure 4.1). Temporal AL was greater than nasal AL, in both eyes, though there was no significant difference between ciliary muscle aspects in each eye (temporal: $P = 0.745$; nasal: $P = 0.589$) or between eyes (right: $P = 0.598$ and left: $P = 0.590$). No significant difference was found for any CM length parameter between the eyes (CML: $F = 0.003$, $P = 0.960$; AL: $F = 0.002$, $P = 0.800$). The CM of myopes was longer than in emmetropes (CML: $F = 224.82$, $P < 0.001$; AL: $F = 69.128$, $P < 0.001$).

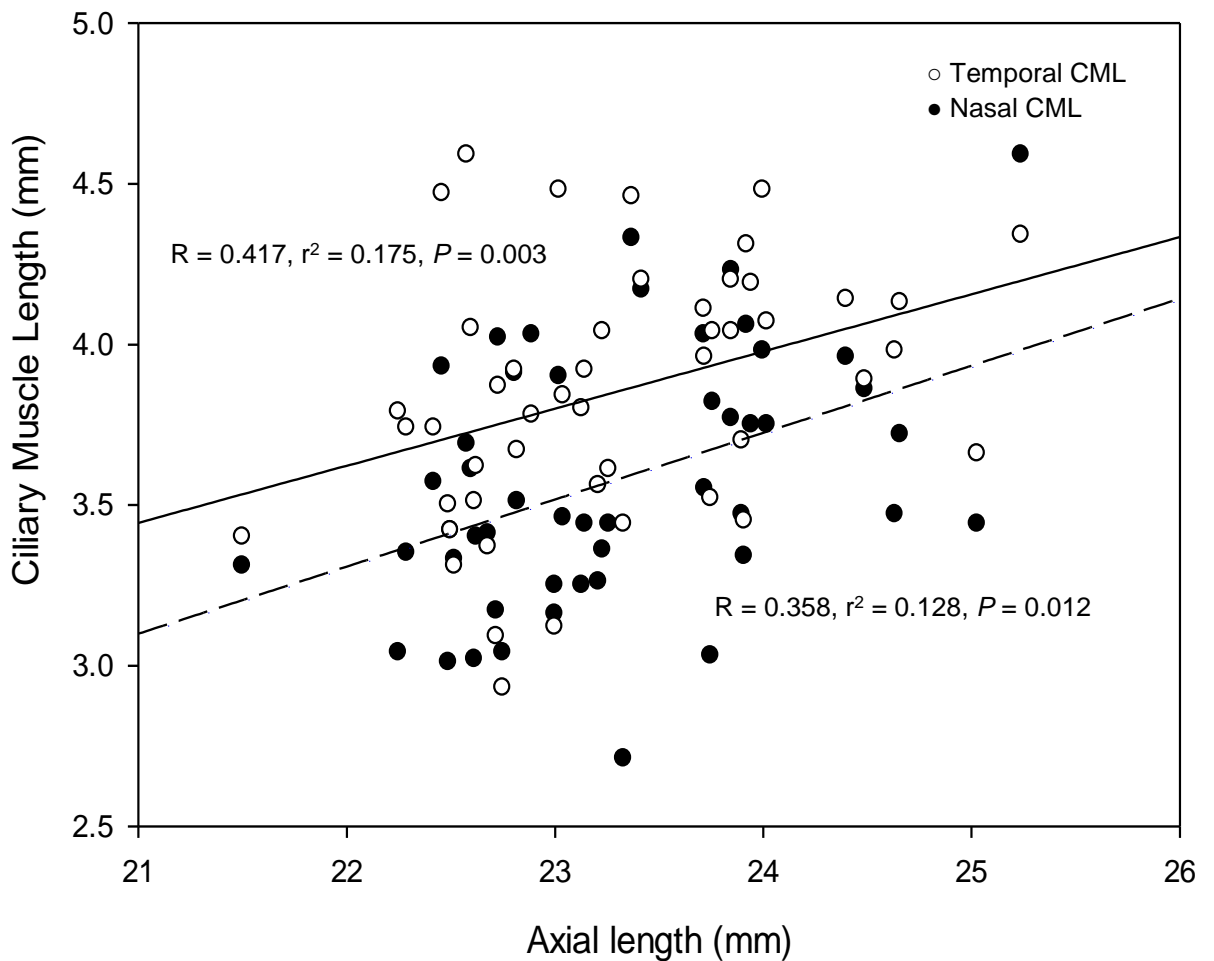


Figure 4.1a: Relationship of RE nasal (solid line) and temporal (dashed line) CML with AXL in emmetropes, with greater temporal CML length than nasal ($n = 50$).

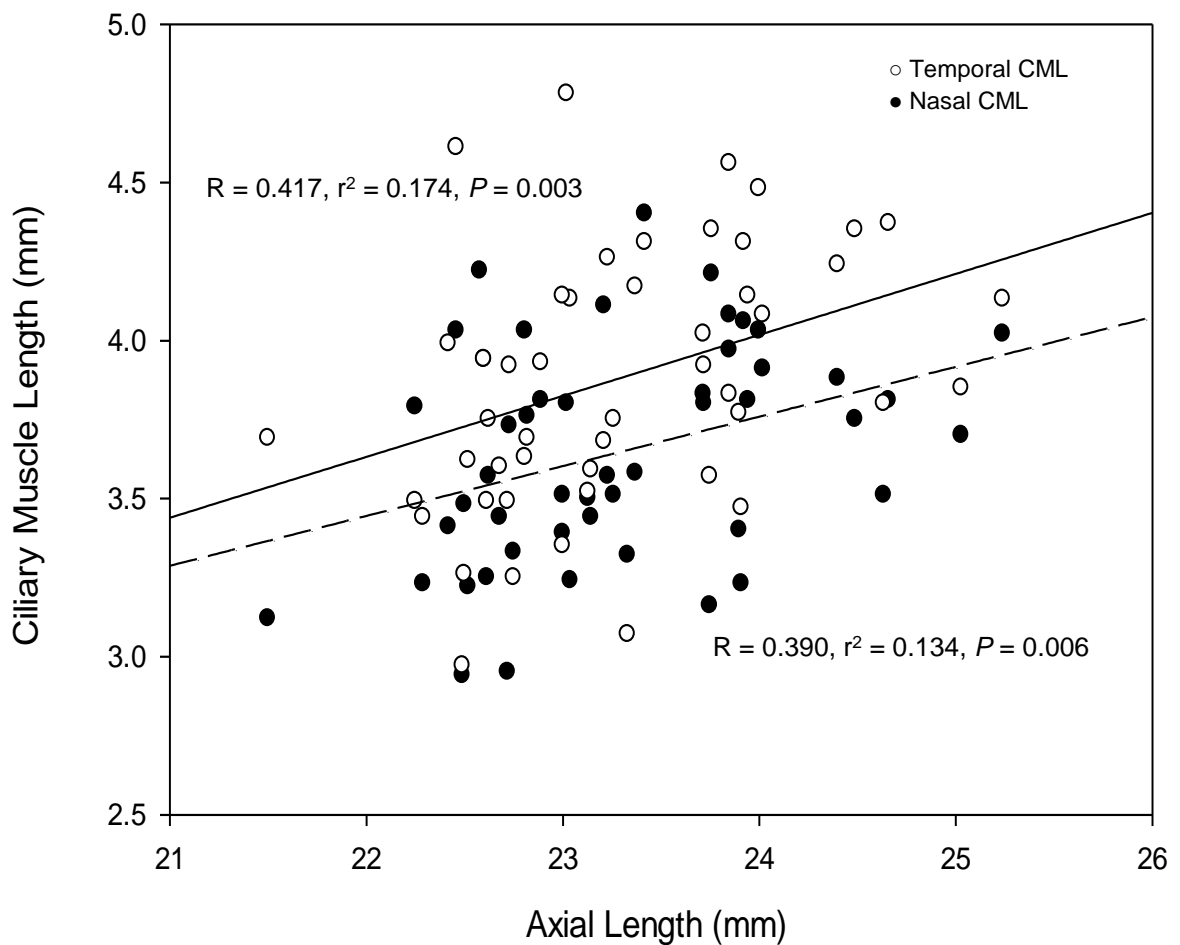


Figure 4.1b: Relationship of RE nasal (dashed line) and temporal (solid line) CML with AXL in myopes ($n = 50$), with greater temporal CML length than nasal, mirroring the relationship between AXL and CML in emmetropes.

AXL was related to CML in emmetropes ($r = 0.417$, $r^2 = 0.175$, $P = 0.003$ for right temporal aspect; $r = 0.358$, $r^2 = 0.128$, $P = 0.010$, for right nasal aspect; $r = 0.355$, $r^2 = 0.126$, $P = 0.011$ for left nasal aspect; $r = 0.370$, $r^2 = 0.137$, $P = 0.008$ for left temporal aspect), myopes ($r = 0.511$, $r^2 = 0.261$, $P < 0.001$ for left nasal aspect; $r = 0.422$, $r^2 = 0.178$, $P = 0.001$ for right temporal aspect) and ACD in emmetropes ($r = 0.425$, $r^2 = 0.181$, $P = 0.010$). There was a positive association between ACD and both CML aspects in emmetropic right (nasal: $r = 0.382$, $r^2 = 0.146$, $P = 0.008$; temporal: $r = 0.524$, $r^2 = 0.274$, $P = 0.001$) and left (nasal: $r = 0.432$, $r^2 = 0.187$, $P = 0.012$; temporal: $r = 0.491$, $r^2 = 0.241$, $P = 0.009$) eyes. In myopic eyes, ACD was related to both CML aspects in the right eye (nasal: $r = 0.403$, $r^2 = 0.162$, $P = 0.004$; temporal: $r = 0.326$, $r^2 = 0.106$, $P = 0.018$), left eye temporal CML ($r = 0.385$, $r^2 = 0.148$, $P = 0.006$), right eye nasal CMT1 ($r = 0.311$, $r^2 = 0.097$, $P = 0.002$), right eye temporal AL ($r = 0.342$, $r^2 = 0.117$, $P = 0.023$) and left eye nasal AL ($r = 0.311$, $r^2 = 0.097$, $P = 0.041$); there was no significant link between ACD and AXL ($r = 0.195$, $r^2 = 0.038$, $P = 0.108$).

4.3.2 Ciliary muscle thickness and symmetry

In both refractive groups, temporal CMT was thicker than nasal CMT at CMTMAX ($F = 8.21$, $P = 0.005$) and at each fixed measure from the scleral spur (CMT1: $F = 6.310$, $P = 0.014$; CMT2: $F = 113.47$, $P < 0.001$; CMT3: $F = 141.90$, $P < 0.001$), though there was no significant difference between aspects in any CMT measures proportional to the CML (CM25: $F = 3.81$, $P = 0.054$; CM50: $F = 3.110$, $P = 0.81$; CM75: $F = 4.101$, $P = 0.460$). There was no significant difference for any CM thickness parameter between the eyes (e.g. CMT1: $F = 0.160$, $P = 0.690$; CMT3: $F = 0.201$, $P = 0.650$). All CM thickness parameters were greater in myopes compared with emmetropes (CMT1: $F = 127.041$, $P < 0.001$; CM25: $F = 15.456$, $P < 0.001$; CMT2: $F = 113.851$, $P < 0.001$; CM50: $F = 17.492$, $P < 0.001$; CMT3: $F = 136.664$, $P < 0.001$; CM75: $F = 79.722$, $P < 0.001$; CMTMAX: $F = 69.321$, $P < 0.001$).

In emmetropes, AXL was linked to CMT at fixed width measures and those proportional to CML in both eyes, for nasal (e.g. right eye CMT1: $r = 0.351$, $r^2 = 0.123$, $P = 0.014$; left eye CMT3: $r = 0.263$, $r^2 = 0.069$, $P = 0.036$) and temporal (e.g. right eye CMT2: $r = 0.400$, $r^2 = 0.152$, $P = 0.001$; left eye CM25: $r = 0.379$, $r^2 = 0.144$, $P = 0.004$) aspects. ACD was linked to CMT at CMT2 and CMT3 for both nasal and temporal aspects and eyes (e.g. right eye nasal CMT2: $r = 0.394$, $r^2 = 0.155$, $P = 0.007$; left eye nasal CMT3: $r = 0.406$, $r^2 = 0.165$, $P = 0.006$; right eye temporal CMT3: $r = 0.344$, $r^2 = 0.118$, $P = 0.017$). For myopes, the positive association between AXL and CMT was present in both eyes at CMT2 and CMT3 (see figure 4.2) fixed width measures only, for nasal (e.g. right eye CMT3: $r = 0.437$, $r^2 = 0.191$, $P = 0.001$; left eye CMT3: $r = 0.472$, $r^2 = 0.223$, $P < 0.001$) and temporal (e.g. right eye CMT3: $r = 0.332$, $r^2 = 0.110$, $P = 0.019$; left eye CMT3: $r = 0.313$, $r^2 = 0.098$, $P = 0.015$). A relationship was found between ACD and CMT at CMT2 (e.g. temporal: $r = 0.278$, $r^2 = 0.077$, $P = 0.042$).

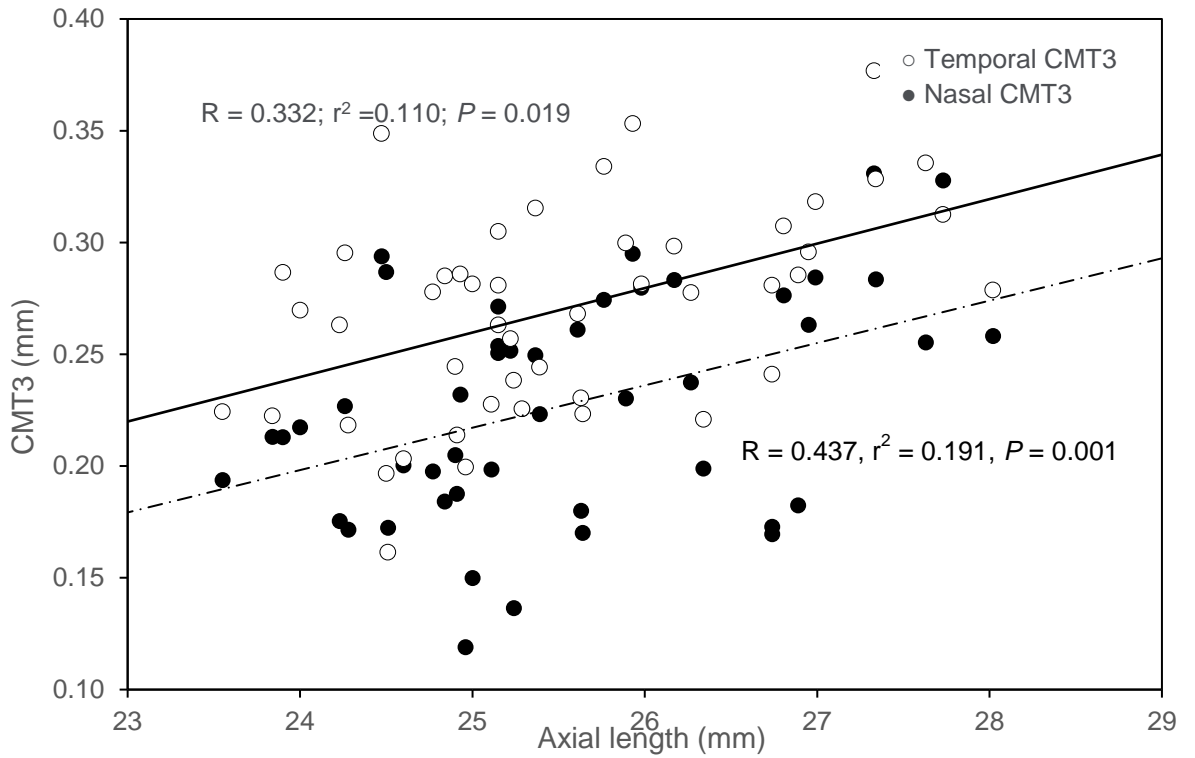


Figure 4.2a Relationship of RE nasal (dotted line) and temporal (solid line) CMT3 with AXL in myopes (n = 50), with greater temporal CMT3 than nasal CMT3.

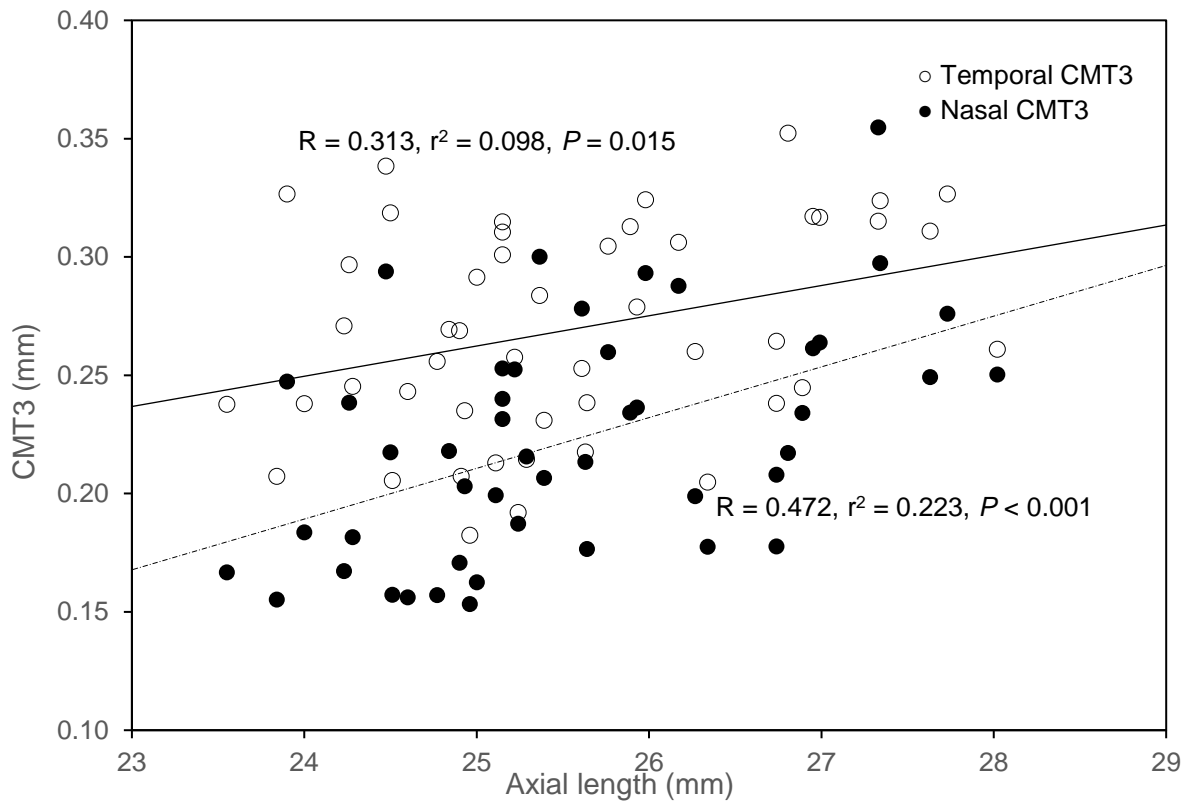


Figure 4.2b Relationship between LE nasal (dotted line) and temporal (solid line) CMT3 with AXL in myopes (n = 50), with greater temporal CMT3 than nasal CMT3, mirroring the relationship between AXL and CMT3 in emmetropes.

4.4 Discussion

Despite a growing body of research relating to ciliary muscle morphology and refractive error, there is a paucity of information regarding inter- eye symmetry of the ciliary muscle. Previous investigations have typically investigated one eye only, usually the right (Oliveira *et al.*, 2005; Bailey *et al.*, 2008; Sheppard and Davies, 2010; Buckhurst *et al.*, 2013) or one aspect (Bailey *et al.*, 2008; Pucker *et al.*, 2013); hence, there has been limited information relating to the normal variations in the inter- eye ciliary muscle symmetry, and those observed in myopia. This study is the first to examine ciliary muscle morphology across both eyes, and both aspects, across a fairly large emmetropic and myopic cohort.

Baseline AXL and ACD were significantly greater in the myopic group, as found in previous studies (Park *et al.*, 2010; Buckhurst *et al.*, 2013) and in keeping with the evidence that increased axial elongation and globe expansion occurs with myopia (Atchison *et al.*, 2004; Mutti *et al.*, 2007; Mutti 2010; Gilmartin *et al.*, 2013). The present study has established high levels of inter- eye symmetry in ciliary muscle morphology in both refractive groups; there was no significant difference between the eyes for any length or thickness ciliary muscle parameter in either refractive group. Gilmartin *et al.* (2013) discovered asymmetry in the laterality of globe profile in myopia development; with nasal to temporal quadrants being asymmetric between right and left eyes, with the temporal quadrant of the right eye corresponding with the nasal quadrant of the left eye. However, the similarity between nasal aspects between the eyes and temporal aspects between both eyes of myopes observed in this study, demonstrates that the variance in globe profile is not translated to ciliary muscle morphology.

In both emmetropic and myopic refractive groups, ACD and AXL was linked to nasal and temporal CML, and CMT in both aspects was linked with AXL. Furthermore, the r^2 values for the relationship between AXL and CML are highly similar between emmetropes and myopes, as for the relationship between AXL and CMT, and CML with ACD; the relationship is unchanged as the eye undergoes myopic elongation and indicates ciliary muscle growth that is consistent with normal ocular development. However, AXL and ACD each only accounted for around 17 – 18 % of the variance in CML. The data (see figure 4.2) indicate that the ciliary muscle plays a passive role in myopigenesis, and altered ciliary muscle morphology is unlikely to be the aetiology, though appears to be an anatomical consequence, of myopia development. However, ACD in emmetropes was linked with AXL whilst there was no relationship between these two biometric correlates in myopic eyes, suggesting that while the ACD in myopes is significantly greater than in emmetropes, this deeper anterior chamber is

not the chief structural correlate in myopia, supporting findings that show vitreous chamber elongation is evidently this (McBrien and Adams, 1997; Mallen *et al.*, 2006; Gilmartin *et al.*, 2013). There was a relationship between ACD and CMT in emmetropes, and ACD was linked with CMT in myopes. Previous work has found ACD in myopia to be significantly associated with both temporal and nasal CMT2 and CMT3 (Buckhurst *et al.*, 2013), though AXL and myopic refractive error have previously been shown to be linked with ACD (Hosny *et al.*, 2000; Antodomingo-Rubido *et al.*, 2002). Van Alphen attributed a thinner crystalline lens and deeper ACD to larger, myopic eyes. During normal eye growth, there is expansion of the eye in all directions and the equatorial growth has been considered to be responsible for this lens thinning (Mutti 2010; Buckhurst *et al.*, 2013). However, the results of this study do not indicate lens thickness difference between refractive groups. It has been suggested the ciliary muscle may limit the equatorial expansion (Bailey *et al.*, 2008; Mutti, 2010) required for emmetropisation; as such, it may be possible to expect that CMT would be related differently with ACD in myopes (Buckhurst *et al.*, 2013).

The ciliary muscle temporal aspect was longer (for CML) and thicker at CMT2 and CMT3 across both eyes and refractive groups. This nasal-temporal asymmetry has been identified in *in vitro* studies of human ciliary body morphology, with a significantly longer temporal aspect recognised (Aiello *et al.*, 1992), and this disparity agrees with the thicker temporal side and increased contractile response from this aspect found *in vivo* (Sheppard and Davies, 2010b). Whilst the significance of this intraocular asymmetry is not well understood, ciliary apparatus asymmetry has been observed in the rhesus monkey *in vitro* (Glasser *et al.*, 2001), where it was proposed that this morphological variation may be essential to permit lenticular axis alignment and maintain binocular single vision during accommodative convergent eye movements (Glasser *et al.*, 2001; Sheppard and Davies, 2010b).

The results from the present study are in accordance with the literature, that myopic eyes had longer (Sheppard and Davies, 2010) and thicker ciliary muscle (Bailey *et al.*, 2008; Buckhurst *et al.*, 2013) compared with emmetropes, for every fixed width measure and those proportional to the CML. Similarly, Bailey *et al.* (2008) utilised fixed width measurements for analysis of nasal ciliary muscle imaging of the right eye, and found that CMT2 and CMT3 were both negatively correlated with refractive error in children, as did CMT1, CMT2 and CMT3 in adult subjects (Kuchem *et al.*, 2013). The reason for this thicker ciliary muscle in myopes remains unclear, yet several investigators have suggested that hypertrophy of the ciliary muscle could give rise to excessive collagen deposition running through the ciliary muscle in a circular orientation, such that the thickened ciliary muscle mechanically restricts equatorial expansion (Bailey *et al.*, 2008; Mutti 2010). Furthermore, this enlargement of the ciliary muscle cells would occur with a hypertrophic ciliary body, reducing the contractile

response (Seidel and Weisbrodt, 1987; Bailey *et al.*, 2008) responsible for the increased accommodative lag associated with myopia (Gwiazda *et al.*, 1993; Gwiazda *et al.*, 1995; Mutti *et al.*, 2006; Berntsen *et al.*, 2010; Berntsen *et al.*, 2011).

4.5 Conclusion

In summary, this study is the first to establish high levels of inter-eye ciliary muscle symmetry, across emmetropic and myopic refractive groups. In both groups, nasal and temporal CML and CMT was linked with AXL in both eyes, with the same relationship, indicating normal ocular development. Across both eyes, the ciliary muscle was both longer and thicker in myopes, though this altered ciliary muscle morphology does not appear to play a physiological role in the development of myopia, but a passive result of myopigenesis.

Chapter 5

Ciliary muscle morphology and associated accommodative function

5.1 Introduction

The previous experimental chapter, and other *in vivo* investigations indicate that the ciliary muscle is both longer (Sheppard and Davies, 2010) and thicker in myopic eyes compared with that of emmetropes (Oliveira *et al.*, 2005a; Bailey *et al.*, 2008; Lewis *et al.*, 2012; Buckhurst *et al.*, 2013). How this altered ciliary muscle morphology is linked with myopigenesis and accommodation remains unclear. It has been suggested that the enlarged ciliary muscle cells result in a hypertrophic ciliary body, reducing ciliary muscle contraction (Seidel and Weisbrodt, 1987; Bailey *et al.*, 2008), and produces the greater accommodative lag that is documented widely in myopia (Goss, 1991; Gwiazda *et al.*, 2005; Mutti *et al.*, 2006). A slight reduction in the amount of hyperopic blur, of approximately 0.1 D, may occur from transient axial length increase during sustained accommodative effort (Mallen *et al.*, 2006). Transient elongation could be a result of the ciliary muscle contraction transmitting an inward pull force to an area of the sclera and choroid adjacent to the ciliary body. Myopic eyes may demonstrate the largest axial expandability during (Drexler *et al.*, 1998; Mallen *et al.*, 2006; Read *et al.*, 2010), and immediately following an accommodative task (Woodman *et al.*, 2012).

The greater accommodative error is largely involved in the hyperopic defocus model of myopia; in 1978, it was demonstrated that simple environmental changes during early visual experience could result in high levels of myopia in chicks (Wallman *et al.*, 1978). Extreme changes in ocular refraction (up to -24.00 D) were generated by restriction of vision to just the frontal visual field. Restriction of the lateral field was produced by translucent, hemispherical lenses; attached from hatching and occluding each eye, a trapezoidal notch incised on the front of the occluder enabled the chicks to have frontal vision. The occluders were replaced by increasingly larger ones as the chicks grew; by 4- 7 weeks the chicks were refracted by streak retinoscopy and shown to have developed extreme levels of myopia. The work was validated a decade later, as work by Schaeffel and co-workers demonstrated that in the chick eye, refractive error could be instigated, as axial length could be altered through manipulations to the dioptric power and sign of inducing lenses (Schaeffel *et al.*, 1988). Subsequently, many investigations utilising similar approaches have further progressed the theory that axial growth of the eye is guided towards emmetropia by a visual feedback mechanism, detecting the optical sign and extent of blur (Irving *et al.*, 1992; Wildsoet and

Wallman, 1995; McFadden *et al.*, 2004; Smith *et al.*, 2005; Berntsen *et al.*, 2011; Ho *et al.*, 2012), generating the theory of foveal hyperopic defocus in the development of myopia.

Myopic subjects 5- 18 years have been found to have reduced accommodative accuracy compared with emmetropes, suggesting a link with the resulting hyperopic retinal defocus and accelerated axial growth in not just the animal based exemplar, but also in human myopia (Gwiazda *et al.*, 1993; Gwiazda *et al.*, 1995; Mutti *et al.*, 2006; Berntsen *et al.*, 2010; Berntsen *et al.*, 2011). Hence, what has been of particular interest is whether increased accommodative lag is a precursor/ risk factor to myopia, or a consequence of myopigenesis, and is widely debated; several previous human studies investigated this matter (Goss, 1991; Drobe and Saint-Andre, 1995; Gwiazda *et al.*, 2005) and indicated that prior to myopia onset, accommodative lag is increased. For example, a longitudinal study by Gwiazda *et al.* (2005) described an elevation in accommodative lag in pre-myopic children two years before myopia onset. Yet subsequently, Mutti *et al.* (2006) measured accommodative lag annually (for 5 years prior to, and 5 years following myopia onset) demonstrated that increased accommodative lag followed myopia onset by a minimum of one year, in agreement with investigations reporting increased lag amongst myopic children (Gwiazda *et al.*, 1993; Gwiazda *et al.*, 1995). Accommodative lag was decreased along with accommodative demand for intermediate distance tasks in became-myopic children (those who had at least one non-myopic examination and developed myopic refractive error of at least -0.75 D in each principal meridian), when their refraction was only partially corrected; the possibility that less hyperopic defocus is subjected to children with uncorrected myopia than with emmetropes during clinically substantial myopic development, providing they partake in intermediate-work visual tasks for a significant amount of time, was indicated. Mutti and co-workers (2006) reported that accommodative lag might be only considered a causative factor of myopia if this error was escalated within a year before myopia onset, though the narrowness of this time period reduces the potential for any preventative intervention as well as likelihood of it being a causative factor. More recent investigations in children however, found no relationship between myopia progression and accommodative lag (Weizhong *et al.*, 2008; Berntsen *et al.*, 2011), opposing the hypothesis that foveal hyperopic defocus instigates axial elongation and myopia progression.

Drexler and co-workers (1998) first utilised partial coherence interferometry (PCI) to study accommodative AXL changes in myopic and emmetropic participants. When observing a closed-loop accommodative target at a distance corresponding to their individual amplitude of accommodation (4.1 ± 2.0 D for the myopic group and 5.1 ± 1.2 D for the emmetropic group), the participants demonstrated transient axial elongation; AXL increase was greatest in emmetropic eyes (mean $12.7 \mu\text{m}$), with axial elongation in myopic eyes of a significantly

lesser magnitude (mean 5.2 μm). Mallen *et al* (2006) also studied the transient ocular expandability across emmetropic and myopic subjects during an accommodative task. It has been hypothesised that, based on previous reports of increased accommodative error in myopes (Drexler *et al.*, 1998; Gwiazda *et al.*, 2005; Harb *et al.*, 2006; Mutti *et al.*, 2006), the magnitude of accommodation during a near task would be decreased somewhat in myopic participants (Woodman *et al.*, 2011). Results however, demonstrated the opposite; larger AXL increases following the near task were observed in myopic subjects compared to emmetropes (Mallen *et al.*, 2006; Woodman *et al.*, 2012). Mallen *et al* (2006) also highlighted that the level of transient axial elongation relates to the magnitude of accommodative stimulation. This was also demonstrated by Drexler *et al* (1998) in emmetropes, who showed that transient axial elongation systematically increased with increasing accommodative stimulus. Moreover, it has been ascertained that this effect not only occurs in the emmetropic eye, but is more marked in myopic subjects (Mallen *et al.*, 2006). Differences between these studies may be attributed to the fact that different accommodative demands were utilised across both studies (see table 2.1). Drexler *et al* (1998) stimulated accommodation in myopes to a lesser degree than Mallen and co-workers (2006), it is possible the AXL increase in myopes was underestimated by Drexler (1998). However further investigations (see table 2.1) in addition to chapter 2 of this thesis showed no difference in the accommodative transient axial expandability between emmetropes and myopes during the accommodative task (Read *et al.*, 2010; Woodman *et al.*, 2012; Ghosh *et al.*, 2014; Zhonga *et al.*, 2014). An investigation that studied the time course of expandability and recovery of transient AXL increase during a sustained (30 minute) 4 D accommodative task (Woodman *et al.*, 2012) found that discrepancies in accommodative expandability during the task between the emmetropic and myopic groups were not statistically significant (Woodman *et al.*, 2012). Nevertheless, in the post- accommodative task measures, significant differences linked with refractive error were determined. During this period, myopic subjects still showed a small amount of axial elongation, whilst the axial length of the emmetropic subjects did not display a significant difference to the baseline measures (Woodman *et al.*, 2012).

It has been suggested that variations between myopes and emmetropes in the morphology of the ciliary body may cause ciliary muscle forces to be transmitted differentially to the choroid and sclera amid these different refractive groups and thereby resulting in discrepancies in the magnitude of transient axial elongation (Mallen *et al.*, 2006). However, such findings do not seem to be coherent; if the thickened ciliary muscle in myopia results in a greater force transmission that delivers increased transient axial elongation compared with emmetropes, then the thickened ciliary muscle cannot have a reduced contractile ability from cellular hypertrophy. The link between ciliary muscle morphology, accommodative accuracy

and accommodative axial length change has not been investigated and there is a paucity of information relating to how ciliary muscle morphology impacts on accommodative function.

Despite the theory that increased ciliary muscle thickness in myopia results in a reduced contractile response (Bailey *et al.*, 2008), the potential link between accommodative function and ciliary muscle morphology is unclear. An investigation in children (aged 8- 15 years) studied the relationship between ciliary body morphology and accommodative microfluctuations (Schultz *et al.*, 2009). Such fluctuations are minute alterations in the ocular refractive power (around 0.1 D - 0.5 D) (Sreenivasan *et al.*, 2011) during steady- state accommodation (see Figure 1.13) and are comprised of both high frequency and low frequency components (Campbell *et al.*, 1959; Kotulak and Schor, 1986; Winn *et al.*, 1990; Schultz *et al.*, 2009). The high frequency component is believed to mirror noise from the arterial pulse in the accommodative apparatus (Collins *et al.*, 1995), whereas the low frequency component appears to result from anterior and posterior lenticular oscillations, shown by ultrasound (Van der Heijde *et al.*, 1996; Schultz *et al.*, 2009).

Differences in the characteristics of the microfluctuations across refractive error groups have been described, with myopes demonstrating greater power and variability of the fluctuations compared with emmetropes (Seidel *et al.*, 2003; Day *et al.*, 2006; Harb *et al.*, 2006; Langaas *et al.*, 2008; Sreenivasan *et al.*, 2011). However, another investigation indicated that the high frequency component of accommodative microfluctuations had reduced power in association with thicker ciliary bodies measured at CM2, by 86 % for every 50 μm increase in ciliary body thickness. The authors suggest that the thicker ciliary body in myopia diminishes the effects of arterial pulse on accommodation and further hypothesised that the thicker ciliary body improves the stability of the high frequency component of the accommodative response. In accordance with this finding, higher amounts of hyperopia were associated with greater powers of the high frequency accommodative fluctuations (Schultz *et al.*, 2009).

Investigations have shown that subjects with late-onset myopia had increased accommodative microfluctuations during their myopia progression (Seidel *et al.*, 2003; Day *et al.*, 2006) and the power of the accommodative microfluctuations is more variable amongst myopic individuals compared with emmetropes (Harb *et al.*, 2006). Schultz and co-workers (2009) predict however, that the reason for such discrepancy is that Harb *et al.* (2006) measured the accommodative microfluctuations during sustained reading when the subjects were likely to be fatigued, as opposed to anatomical micro-fluctuations in the absence of prolonged fatigue. Similarly, the authors (Schultz *et al.*, 2009) added that because errors in accommodative function may be more likely present during active myopia progression, investigating accommodative function and comparing to previous work is somewhat

problematic in a cross-sectional study, where children may be at varying, unknown stages of myopia development.

Previous work that studied *in vivo* morphological changes in the ciliary muscle with accommodation (Sheppard and Davies, 2010b) identified a contractile shortening and thickening of the anterior portion of the ciliary muscle, using vergence levels of -4.0 and -8.0 D. The ciliary muscle was also shown to be significantly thicker on the temporal side, in keeping with nasal versus temporal asymmetry found from UBM analysis of the ciliary region in cyclopleged monkeys (Glasser *et al.*, 2001), and corresponding with a greater contractile response of the temporal aspect. For the ciliary muscle temporal aspect, overall length reduced on average by 80 ± 100 and 50 ± 120 μm per diopter of accommodative response between the 0.19- to 4.0 D and 4.0 to 8.0 D demand levels, respectively. Similarly, anterior length decreased by 60 ± 40 and 30 ± 30 μm per diopter of response between the lower and higher demand levels, respectively. For the nasal side, the mean reductions in anterior length were significantly less: 30 ± 14 μm from 0.19 to 4.0 D and -20 ± 20 μm from 4.0 to 8.0 D. However, it is not yet known if this increased contractile response of the temporal ciliary muscle would result in a greater magnitude of axial elongation with accommodation, or a reduced accommodative error, compared with the nasal aspect (Sheppard and Davies, 2010b).

Evidently, there is debate in the literature regarding the link between accommodative dysfunction and myopia. Considering this link and the hypothesis that a thicker ciliary body suppresses the high frequency accommodative microfluctuations, and that a thicker ciliary muscle results in greater accommodative inaccuracy, no study has yet investigated the relationship between ciliary muscle morphology and accommodative function. The study presented in this chapter explores, for the first time, the link between ciliary muscle morphology, accommodative error and axial length changes with accommodation, in emmetropes and myopes.

5.2 Methods

5.2.1 Subjects

One hundred subjects aged 19 - 26 years were recruited from the student body of Aston University, consisting of fifty emmetropic volunteers with a mean sphere equivalent ($\text{MSE} \geq -0.55$; $< +0.75$ D) and fifty myopes ($\text{MSE} \leq -2.00$ D). The narrow age band was selected to reduce variation in ciliary muscle data due to ageing, most notably thickening of the ciliary

muscle (Sheppard and Davies, 2010). Exclusion criteria were cylindrical refractive errors greater than 2.00 D, amblyopia, previous history of ocular trauma, surgery or pathology, and systemic conditions known to affect ocular health. All participants had corrected visual acuities of 0.0 logMAR or better in each eye and exhibited a monocular amplitude of accommodation ≥ 9 D (as measured with the push-up method). Myopic participants wore 31% Nelfilcon A (Focus Dailies) contact lenses appropriate for their habitual refractive error for all accommodative measures and ciliary muscle imaging, as functional emmetropia was required to ensure near-identical accommodative demand for each participant. Ethical approval was obtained from the Aston University Life and Health Sciences Research Ethics Committee and the study adhered to the tenets of the Declaration of Helsinki. Written, informed consent was obtained from all participants prior to commencement after explanation of the nature and possible consequences of the study.

5.2.2 Measurements

Binocular distance refractive error was measured with a validated infra-red binocular open-view autorefractor (Grand Seiko WAM 5500; Sheppard and Davies, 2010) whilst subjects viewed a distance (6 m) Maltese cross target. A minimum of five measurements of refractive error were taken for each eye, averaged and converted into MSE.

To indicate the level of accommodative inaccuracy for each participant, the accommodative error index (AEI) was used, which combines all the parameters of the accommodative stimulus- response curve into a single index (Chauhan and Charman, 1995; Woodhouse *et al.*, 2000; Allen and O'Leary, 2006).

Accurate accommodation at all stimulus demands is indicated by an AEI of 0 D. A value > 0 D indicates the level of accommodative inaccuracy (Chauhan and Charman, 1995; Woodhouse *et al.*, 2000). For each subject, the accommodative response was measured in the right eye to targets placed at 8 randomised-order stimulus demands (0.0, 1.0, 2.0, 3.0, 4.0, 5.0, 6.0, 8.0 D) to produce the AEI, calculated using equation 1, detailed in section 1.7.3 and 2.3. Pupil size measures were obtained for all accommodative demand levels, using the *Grand Seiko WAM 5500* (see figure 5.1).

ACD, AXL, and LT in the unaccommodated state were obtained from the right eye of each participant using the *Lenstar LS 900* biometer (Haag-Streit AG, Koeniz, Switzerland). Each participant fixated on the letter closest to the central red fixation light (a 5 x 5 grid of high-contrast letters, with each letter equivalent to 0.8 logMAR) whilst four separate biometric measurements were taken and averaged at 0 D. The eye under investigation was 100 mm from the Badal lens and the 0 D stimulus demand was situated 100 mm from the Badal lens

(Alderson *et al.*, 2012). These measures were then repeated whilst the participant accommodated to 5 D stimulus demand, by shifting the back-illuminated text target 50 mm forward towards the Badal lens (Alderson *et al.*, 2012), as described as described in detail in section 1.7.5 and 2.3.



Figure 5.1. Image of display screen of Grand Seiko WAM 5500, showing a pupil diameter measurement of 5.2 mm, in conjunction with the refractive error of the participant.

5.2.3 Ciliary muscle image acquisition and analysis

AS-OCT (*Visante*; Carl Zeiss Meditec. Inc., Dublin, CA) images of nasal and temporal ciliary muscle regions were obtained from the right eye of participants only, using high-resolution corneal mode, as detailed in section 1.7.7. Ciliary muscle images were exported from the AS-OCT in raw DICOM form for analysis purposes. A validated bespoke analysis programme

(Laughton *et al.*, 2015) was used to measure ciliary muscle parameters, as detailed in section 1.7.8; all image analysis was carried out by a single examiner (RNS).

Various length and width measurements were obtained; ciliary muscle total length (CML) was determined as the curved anteroposterior distance from the scleral spur, signifying the anterior insertion along the ciliary muscle-scleral border, to the visible posterior tip of the ciliary muscle. The anterior length (AL) is from the scleral spur to the point of ciliary muscle maximum width (CMTMAX). CM25 is the muscle width at a point which was 25 % of the CML posterior to the scleral spur. Similarly CM50 and CM75 measures were taken at points 50 % and 75 % (CM50 and CM75 respectively) of the CML posterior to the scleral spur. Additionally, ciliary muscle thickness measurements were taken at fixed distances from the scleral spur; CMT1 represents a point 1 mm posterior to the scleral spur, with CMT2 and CMT3 taken at points 2 mm and 3 mm posterior to the scleral spur, respectively.

5.2.4 Statistical analysis

Comparable to the *IOLMaster*, the *Lenstar* instrument utilises an average ocular refractive index in order to calculate axial length from the optical path length. Previous work has established that changes in the accommodative apparatus, principally lens thickness, during accommodation may produce errors in these AXL measurements (Atchison and Smith, 2004), as described in section 2.3. The formulae and methods outlined by Atchison and Smith were applied by utilising each subject's individual ocular biometric parameters; the error associated with the change in AXL from baseline to the 5 D accommodative demand was calculated for each subject and these values were used to determine the corrected accommodative AXL changes (from equations 2.1- 2.7).

The data for each variable were normally distributed, according to tests of normality (Shapiro-Wilk, SPSS Statistics 21; IBM, Illinois, USA). Independent samples t-tests were performed to indicate any significant difference between the change in pupil sizes with accommodation from baseline between refractive groups, AEI of emmetropes and myopes, and the accommodative axial length change between the refractive groups. The relationships between these accommodative functions and ciliary muscle morphological parameters were determined by linear regression analysis. An independent samples t-test was performed to check for differences in age between the refractive groups, and difference between refractive groups in pupil diameter change from baseline at each demand level. A *P* value of less than 0.05 was considered significant. All data were stored in an Excel spreadsheet (Microsoft 2010, Redmond, Washington, USA).

5.3 Results

Pupil size across the refractive groups at different accommodative demand levels is shown in table 5.1. The expected pupil constriction with increased accommodative effort was observed. For each accommodative demand (above 0.0 D), the emmetropic pupil size was significantly greater than that of myopes (1.0 D: $P = 0.043$; 2.0 D: $P = 0.030$; 3 D: $P = 0.018$; 4 D: $P = 0.003$; 5 D: $P = 0.010$; 6 D: $P < 0.001$; 8 D: $P = 0.018$).

Accommodative Demand (D)	Mean Pupil size (mm)		
	Emmetropes	Myopes	Whole Cohort
0.0	6.56 ± 0.90	6.31 ± 0.83	6.41 ± 1.03
1.0	6.34 ± 0.91	5.99 ± 0.79	6.14 ± 1.01
2.0	6.29 ± 0.90	5.93 ± 0.72	5.98 ± 1.27
3.0	5.95 ± 0.87	5.53 ± 0.87	5.74 ± 1.04
4.0	5.87 ± 0.98	5.31 ± 0.86	5.39 ± 1.40
5.0	5.73 ± 1.05	5.19 ± 0.99	5.26 ± 1.42
6.0	5.61 ± 0.91	4.84 ± 0.98	5.20 ± 1.01
8.0	4.74 ± 1.04	4.27 ± 0.90	4.51 ± 1.12

Table 5.1. Mean pupil size and associated accommodative demand levels. There was a significant difference between refractive groups in pupil diameter change from baseline at each demand level.

5.3.1 Accommodative error index

Mean AEI values of emmetropes, myopes and the whole cohort are shown in table 4.2.

	Emmetropes	Myopes	Whole Cohort
AEI (D)	0.97 ± 0.60	0.80 ± 0.51	0.90 ± 0.49

Table 5.2. AEI values for emmetropes, myopes and the whole cohort. There was no significant difference between the AEI of emmetropes and myopes ($P = 0.098$).

Stimulus response curves in emmetropes and myopes are shown in figure 5.2 and are compared with a theoretical 1:1 ratio between stimulus demand and response. There is a mirrored response between the two refractive groups, whereby with increasing stimulus demand, there is a greater accommodative error.

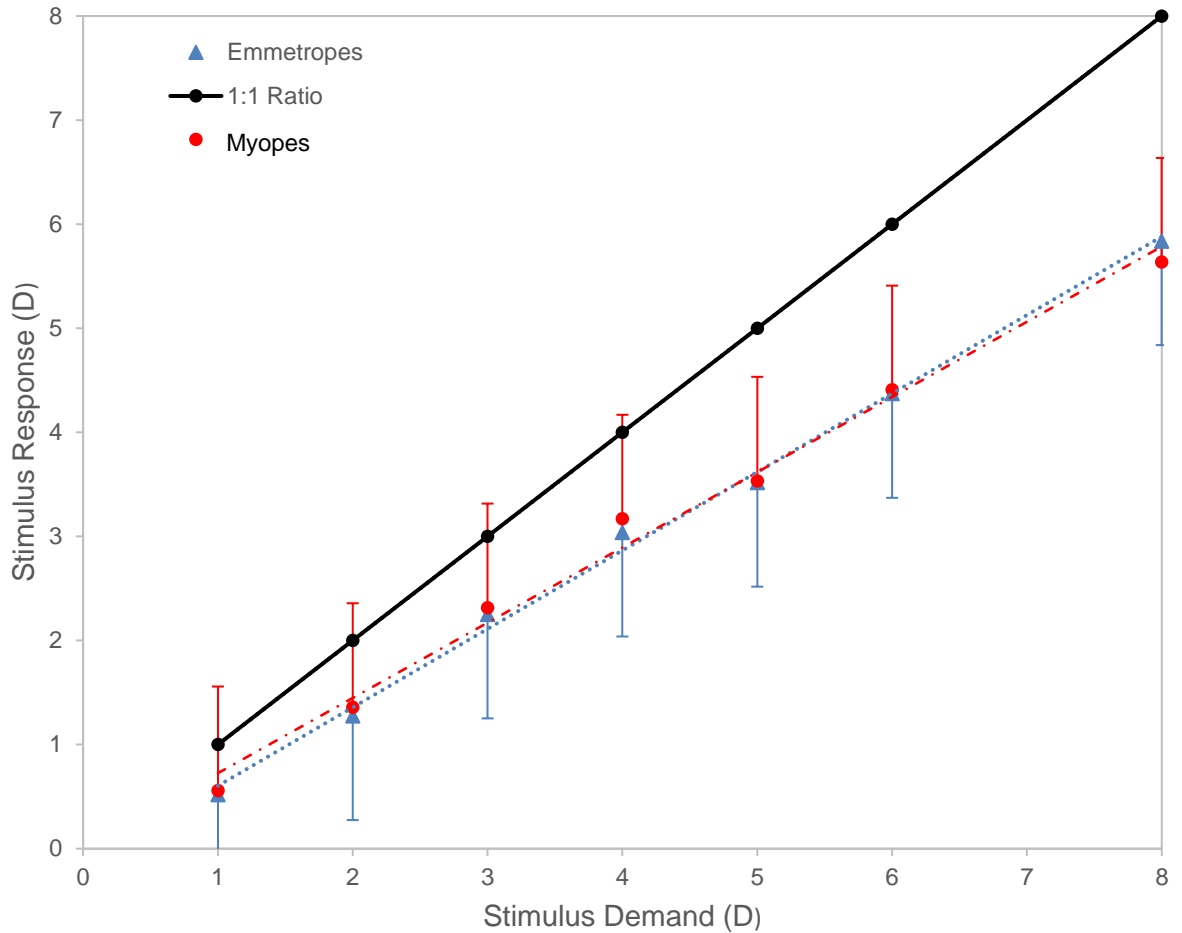


Figure 5.2. A mean accommodative stimulus- response curve for emmetropic subjects ($n = 50$) and myopic subjects ($n = 50$). The black solid line indicates a 1:1 relationship between the demand of the stimulus and the response to the stimulus at each demand level; the blue dotted line represents the mean accommodative response of the emmetropic cohort and the red dotted line indicates the mean accommodative response of the myopic cohort. Unidirectional error bars indicate the standard deviation of the mean.

Across the whole cohort, there was no significant relationship between AEI and any ciliary muscle thickness parameter (e.g. nasal CM1: $P = 0.190$, $r^2 = 0.002$; nasal CM3: $P = 0.617$, $r^2 = 0.003$, nasal CM50; $P = 0.998$, $r^2 = 0.026$; temporal CM2: $P = 0.252$, $r^2 = 0.003$; temporal CM25; $P = 0.323$, $r^2 = 0.010$; temporal CMTMAX: $P = 0.525$, $r^2 = 0.040$) or length parameter (nasal CML: $P = 0.061$, $r^2 = 0.026$; temporal CML; $P = 0.249$; $r^2 = 0.004$; nasal AL: $P = 0.052$, $r^2 = 0.029$; temporal AL: $P = 0.076$; $r^2 = 0.022$). Figure 5.3 shows the relationship between AEI and temporal CM50. The relationship between temporal CM2 and AEI is shown in figure 5.4. No significant relationship was found in either refractive group between AEI and accommodative AXL change (emmetropes: $P = 0.415$, $r^2 = 0.078$; myopes: $P = 0.476$, $r^2 = 0.011$).

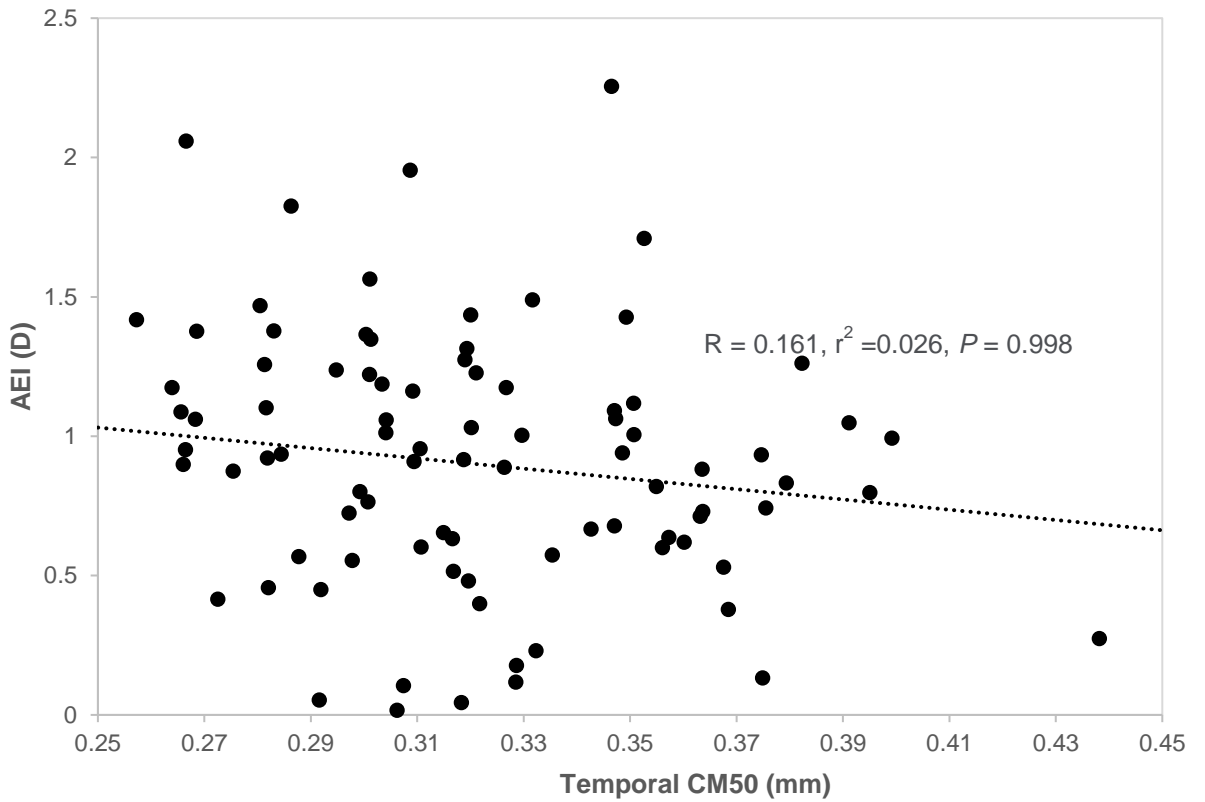


Figure 5.3. Relationship between temporal CM50 and AEI. No significant relationship occurred ($P = 0.998$) between AEI and temporal CM50 across the whole cohort ($n = 100$).

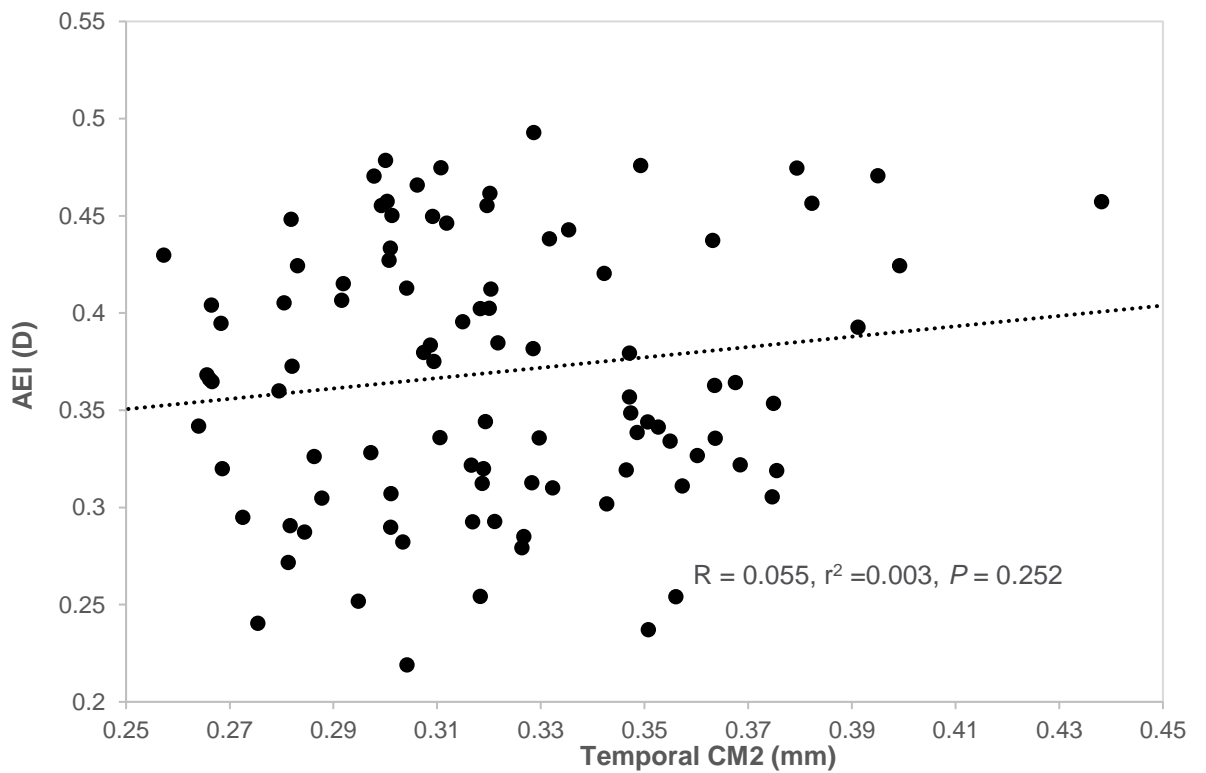


Figure 5.4. Relationship between temporal CM2 and AEI. No significant relationship occurred ($P = 0.252$) between AEI and temporal CM2 across the whole cohort ($n = 100$).

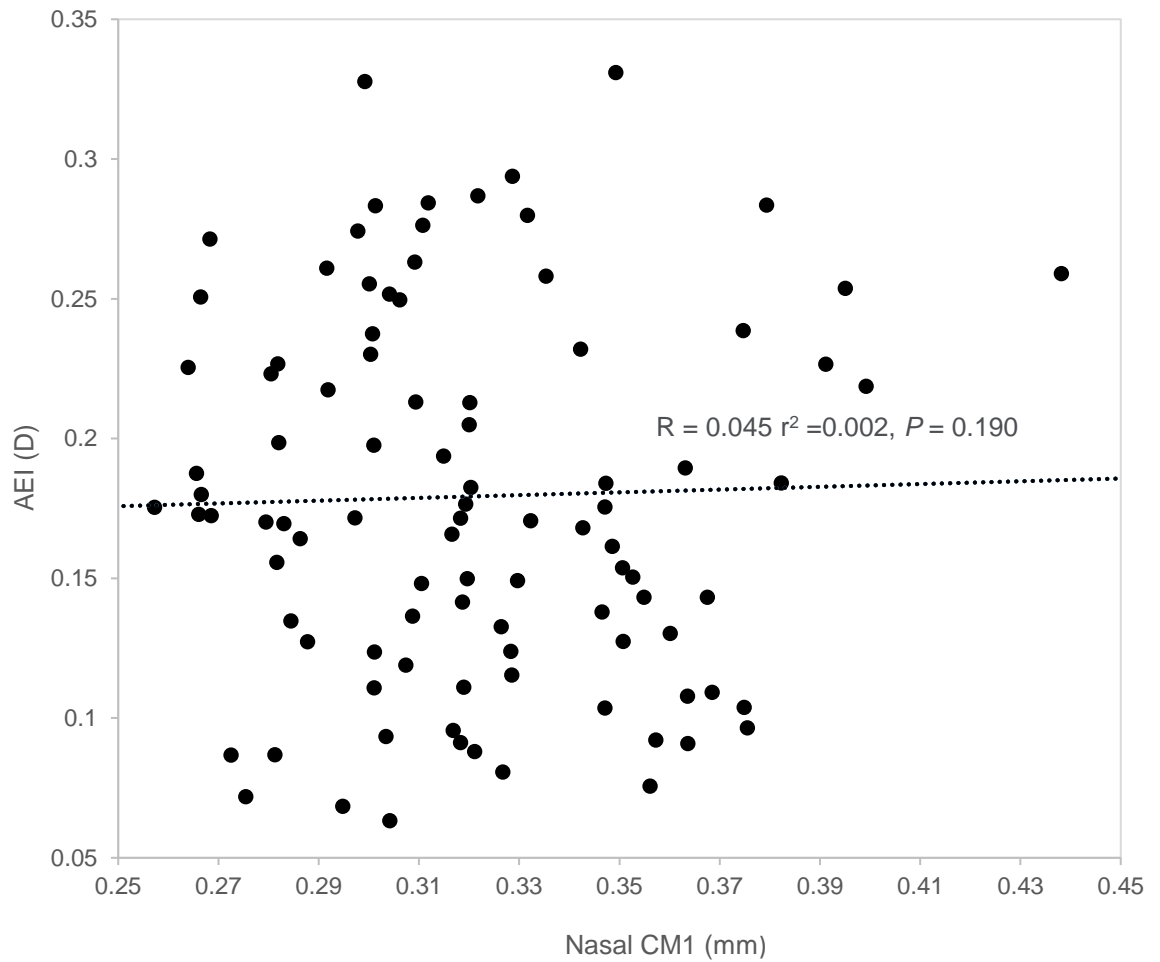


Figure 5.5 Relationship between nasal CM1 and AEI. No significant relationship occurred $P = 0.190$ between AEI and temporal CM2 across the whole cohort ($n = 100$).

5.3.2 Transient accommodative axial length change

Transient accommodative AXL changes, and the summary characteristics of emmetropic and myopic cohorts, are shown in table 5.3.

	Emmetropes (n = 50)	Myopes (n = 50)
	Mean	
Age (years)	21.1 ± 8.63	21.7 ± 8.84
0 D Axial length (mm)	23.29 ± 0.79*	25.46 ± 1.16*
0 D ACD (mm)	3.03 ± 0.29*	3.23 ± 0.25*
0 D LT (mm)	3.53 ± 0.22	3.51 ± 0.23
5 D Axial length (mm)	23.24 ± 0.79*	25.49 ± 1.16*
5 D ACD (mm)	2.78 ± 0.27	2.99 ± 0.25
5 D LT (mm)	3.86 ± 0.24	3.81 ± 0.55
Corrected 5 D Axial length (mm)	23.32 ± 0.79*	25.51 ± 1.16*
Axial length change with accommodation (µm)	16.48 ± 25.52	16.57 ± 25.07

Table 5.3. Summary biometric characteristics and AXL changes with accommodation in emmetropic and myopic participants. There was no significant difference in age between the refractive groups ($P = 0.884$). *Indicates significant difference between the refractive groups. Axial length measures were obtained in every participant. In the emmetropic cohort, LT data was gathered from the *Lenstar LS 900* in 31 subjects; in the myopic cohort, LT data were obtained in this way for 28 subjects. For ACD, the *Lenstar LS 900* obtained measures for 42 subjects in the emmetropic cohort and in 48 subjects in the myopic refractive group. The missing data for ACD and LT was replaced with predicted ACD and LT, respectively, based on participant age and published work by Atchison *et al* (2008).

The mean transient accommodative AXL change in emmetropes was $16.48 \mu\text{m} \pm 25.52$ and in myopes was $16.57 \mu\text{m} \pm 25.07$; the difference in accommodative AXL change between the refractive groups was not significant ($P = 0.768$). No relationship was found between AXL change and any CM thickness or length parameter (e.g. nasal CM1: $P = 0.974$, $r^2 = 0.001$; nasal CM2: $P = 0.484$, $r^2 = 0.05$; nasal CM3: $P = 0.925$, $r^2 = 0.010$; nasal CM25: $P = 0.181$, $r^2 = 0.03$; nasal CM75: $P = 0.460$, $r^2 = 0.003$; temporal CM3: $P = 0.712$; $r^2 = 0.003$; temporal CML: $P = 0.868$, $r^2 = 0.000$; temporal CM50: $P = 0.996$, $r^2 = 0.001$; temporal CM75: $P = 0.750$, $r^2 = 0.001$; temporal CMTMAX: $P = 0.659$, $r^2 = 0.002$; temporal AL: $P = 0.506$; $r^2 = 0.005$; nasal CML: $P = 0.145$; $r^2 = 0.024$).

5.4 Discussion

Whilst it has been widely hypothesised that an increased accommodative error would induce the hyperopic retinal defocus considered to stimulate axial elongation (Harb *et al.*, 2006; Mutti *et al.*, 2006; Berntsen *et al.*, 2010), accommodative error has been studied with regard to ciliary muscle morphology for the first time. Previous work has compared the accommodative axial elongation between emmetropes and myopes (Drexler *et al.*, 1998; Mallen *et al.*, 2006; Read *et al.*, 2010; Woodman *et al.*, 2010), where it has been shown that the myopic eye may

demonstrate the largest transient axial changes (Mallen *et al.*, 2006). It has been proposed the ciliary muscle in myopes may transmit a greater force to the choroid and sclera, resulting in the larger magnitude of transient accommodative axial elongation, compared with emmetropes (Mallen *et al.*, 2006). However, these transient axial length changes have never before been studied with regards to ciliary muscle morphology.

There is increasing evidence of a thicker ciliary muscle in the myopic eye, as discussed in the previous chapter. Previous investigators have speculated this altered morphology is due to hypertrophy of the ciliary muscle, which could give rise to excessive collagen deposition running through the ciliary muscle in a circular orientation, and such hypertrophy would also cause enlargement of the ciliary muscle cells, yielding a reduced contractile response (Seidel and Weisbrodt, 1987; Bailey *et al.*, 2008) responsible for the increased accommodative lag associated with myopia (Gwiazda *et al.*, 1993; Gwiazda *et al.*, 1995; Mutti *et al.*, 2006; Berntsen *et al.*, 2010; Berntsen *et al.*, 2011). However, the link between accommodative error and ciliary muscle morphology has never previously been examined; the results demonstrate no significant difference in accommodative inaccuracy between the refractive groups, and that in both ciliary muscle aspects (nasal and temporal), no significant relationship was present between any ciliary muscle thickness parameter and the level of accommodative inaccuracy. As such, the results suggest no intrinsic difference between emmetropes and myopes in the physiology of the ciliary muscle pertaining to accurate accommodation; the hypothesis that a thicker ciliary muscle is hypertrophic and leads to the development of myopia by producing a greater accommodative error, is not supported by this study.

Many previous investigations have exposed a temporary increase in axial length during (Drexler *et al.*, 1998; Mallen *et al.*, 2006; Read *et al.*, 2010) or directly following (Woodman *et al.*, 2010) an accommodative task, and results showed larger increases in axial length following the near task in myopic subjects compared to emmetropes (Mallen *et al.*, 2006; Woodman *et al.*, 2012). Transient elongation is likely to result from the ciliary muscle contraction transmitting an inward pull force to an area of the sclera and choroid adjacent to the ciliary apparatus. In order to maintain a constant ocular volume from this effect, a rearward displacement of the posterior portion of the globe is needed, thereby resulting in a transient axial length increase (Mallen *et al.*, 2006) and it has been proposed that a partial reason for the greater elongation seen in myopic eyes is greater efficiency of force transmission from the ciliary muscle to the sclera and choroid in myopic subjects (Mallen *et al.*, 2006; Woodman *et al.*, 2010). However, corrected AXL data in this investigation show no significant difference in AXL changes with accommodation between refractive groups, coherent with more recent investigations (Read *et al.*, 2010; Woodman *et al.*, 2012). The mean corrected AXL change ($16.52 \pm 25.16 \mu\text{m}$) is of larger magnitude than that of Read *et al.* (2010) ($\sim 7 \mu\text{m}$ for 6 D

accommodative demand) and similar to that of Woodman *et al* (2012) during the accommodative task at 4 D ($20 \pm 31 \mu\text{m}$).

No study has previously documented the relationship between ciliary muscle morphology and accommodative AXL change; just as no link appears to be present between ciliary muscle morphology and AEI, the findings indicate no clear relationship between ciliary muscle morphology and transient accommodative AXL change, or between AEI and accommodative AXL change. This suggests that transient AXL change with accommodation is another element of accommodative function in which ciliary muscle morphology is not responsible. In the investigation by Woodman *et al* (2012) some evidence of decreased choroidal thickness during accommodation was found, and such choroidal changes displayed a significant negative correlation with the axial length alterations. It was suggested that choroidal thickness alterations and multiple other factors such as scleral stretch are highly likely to contribute in the accommodative axial elongation (Woodman *et al.*, 2012), opposed to ciliary muscle forces. The similar levels of AEI and AXL change with accommodation between the refractive groups, together with the lack of relationship with ciliary muscle morphology indicate that the thicker ciliary muscle in myopia does not impact overall on accommodative function, or myopic development.

Interestingly, the pupil size was found to be significantly larger in emmetropes, compared with myopes, for each accommodative demand above baseline. In both refractive groups, pupil size decreased with increasing accommodative demand, consistent with widely acknowledged findings that the primary stimuli for the pupil near response is accommodation and convergence, as part of the near triad accommodative response (Marg and Morgan, 1949; Marg and Morgan, 1950; Kasthurirangan and A., 2005). Whilst baseline pupil size did not significantly vary between the refractive groups, in keeping with previous work (Winn *et al.*, 1994; Orr *et al.*, 2015), findings of different pupil sizes between the refractive groups for various accommodative demands differ from previous investigations, which report that pupil size does not vary with refractive error, irrespective of accommodative demand (Orr *et al.*, 2015). In the study by Winn and co-workers, a wide age range of participants were used (17 to 83 years), such that differences in pupil diameter between refractive groups may have been confounded by age effects (Watson and Yellott, 2012; Orr *et al.*, 2015) which are known to affect pupil diameter (Kadlecova *et al.*, 1958; Schaeffel *et al.*, 1993). In the study by Orr *et al* (2015), the cohort ranged from ages 20 – 35 years, whereas in the present study the cohort age was between 19 – 26 years, a much narrower age band which reduces the likelihood for confounding age effects on pupil size. Similarly, target vergences of just 0.0 D and -3.0 D were used in the investigation by Orr and co-workers (2015), whereas 7 accommodative demands were utilised in the present study. Whilst both investigations showed no significant

difference in pupil size at the 0.0 D demand level, more accommodative demands were presented in the current study, perhaps allowing for more opportunity for pupil differences across varying vergence levels, to arise between refractive groups. However, a full investigation of pupil size to follow up these findings is required, though such investigations are beyond the aims of this thesis.

During the present investigation, the *Lenstar LS 900* biometer (Haag-Streit AG, Koeniz, Switzerland) was unable to obtain crystalline lens thickness values in all subjects (measures were obtained in 59 out of 100 study participants). In the emmetropic cohort, it failed to gather lens thickness information, at both 0 D and 5 D accommodation demands in 19 subjects, and in 22 subjects of the myopic cohort. For ACD, the biometer did not obtain measures for both 0 D and 5 D accommodative demands in 8 emmetropes and 2 myopes. It is widely accepted that there is greater central thickness of the unaccommodated lens with age due to increases in cortical thickness, while concurrently a decrease in anterior chamber depth occurs (Brown, 1973b; Niesel, 1982; Koretz *et al.*, 1989; Dubbelman *et al.*, 2001; Atchison *et al.*, 2008; Shamma and Shamma, 2015). Such missing biometric data from the *Lenstar* was replaced with predicted values based on age by Atchison and co-workers (2008), shown by equations 5.1 for LT, and 5.2, 5.3 and 5.4 for ACD with corneal thickness (CT), CT, and the resultant ACD, respectively. Previous work has also shown that whilst anterior corneal radius, vitreous length and retinal shape alters with refraction, there is no significant effect of refraction on lens thickness or anterior chamber depth (Atchison, 2006). As such, biometric data for the myopic cohort was extracted in the same way as for emmetropes, using the equations outlined below.

Equation 5.1: $LT = 3.1267 + (0.02351 * age)$

Equation 5.2: $CT + ACD = 3.857 + (0.0106 * age)$

Equation 5.3: $CT = 0.5667 + (0.00077 * age)$

Equation 5.4: $resultant\ ACD = (CT + ACD) - CT$

The reason for the limited ability of the *Lenstar LS 900* biometer to obtain all crystalline lens thickness measures from every participant is unclear. It is established that the instrument can measure CT, ACD (from corneal endothelium to lens surface), LT, AXL, RT, as well as assessing keratometry and pupil diameter (Buckhurst *et al.*, 2009; Rohrer *et al.*, 2009; Cruysberg *et al.*, 2010; Alderson *et al.*, 2012; Zhao *et al.*, 2013) concurrently through image analysis within each measurement, without needing realignment (Buckhurst *et al.*, 2009; Cruysberg *et al.*,

2010; Zhao *et al.*, 2013). The instrument is therefore marketed as a highly efficient research tool by obtaining LT measures simultaneously with AXL and biometric data. A recent study that investigated accommodative changes during incipient presbyopia also could not obtain crystalline lens thickness values in all subjects, and it was suggested that this may be due to high light transmittance of the posterior lenticular surface (Laughton *et al.*, 2016). However, this issue may not be linked to all *Lenstar* biometers, although a software update did not resolve the problem on the Aston device.

5.5 Conclusion

In summary, this is the first study to relate ciliary muscle thickness with accommodative error and transient accommodative axial elongation. It has been shown, for the first time, that there was no relationship between ciliary muscle morphology and axial length change with accommodation or accommodative inaccuracy, or any difference between the refractive groups in these accommodative measures. It is therefore indicated that the altered ciliary muscle morphology in myopia has no impact on accommodative function, and hence, is unlikely to play a role in the hyperopic defocus model of myopia.

Chapter 6

Ciliary muscle morphology in amblyopia and anisometropia

6.1 Introduction

Amblyopia is a neurodevelopmental disorder that causes reduced visual acuity, usually in one eye (Wiesel and Hubel, 1963; Webber and Wood, 2005; Veneruso *et al.*, 2014; Solebo *et al.*, 2015), despite refractive correction and in the absence of ocular disease (Ciuffreda *et al.*, 1991; Astle *et al.*, 2011). The condition is due to abnormal visual input in early life, during the critical period(s) of visual development (believed to span from infancy to around 9 years of age), and is characterised by binocular dysfunction (Thompson *et al.*, 1991; Astle *et al.*, 2011; Solebo *et al.*, 2015). Recent investigations however, indicate that the plasticity period may exert its influence much longer, into adolescent and early adult life (Mora *et al.*, 2007; Domínguez, 2014). The prevalence of the disorder in the Western population is approximately 3% (Thompson *et al.*, 1991; Attebo *et al.*, 1998; Polling *et al.*, 2012) and is the most common cause of uncorrectable reduced vision in children and in adults up to 60 years of age (Thompson *et al.*, 1991). Clinically, amblyopia is characterised by at least one line difference in visual acuity between both eyes (Thompson *et al.*, 1991), cannot be detected through physical ocular examination, and in certain cases can be reversed by therapeutic treatment (Webber and Wood, 2005). Such treatment is conventionally undertaken by optical correction of any refractive error, surgical correction of any associated strabismus, and/ or occlusion therapy of the non-amblyopic eye with a patch or through atropine penalisation (Astle *et al.*, 2011). The most common amblyogenic factors include strabismus, presence of micro-squint or heterotropia (Attebo *et al.*, 1998; Webber and Wood, 2005), and anisometropia (Von Noorden, 1985; Attebo *et al.*, 1998; Webber and Wood, 2005). Anisometropia is defined as asymmetry in refraction between fellow eyes (O'Donoghue *et al.*, 2013; Sonia *et al.*, 2013), or a difference in the sphere or cylinder between the two eyes of at least one dioptre (Attebo *et al.*, 1998; Webber and Wood, 2005; Hashemi *et al.*, 2013; Kuchem *et al.*, 2013). These conditions have been targeted in vision screenings programmes for children aged 4-5 years (Webber and Wood, 2005; Solebo *et al.*, 2015) to allow timely intervention, usually within the critical period (Solebo *et al.*, 2015).

A wide range of studies have reported biometric data on the normal changes in ocular parameters that occur during visual development (Ehrlich *et al.*, 1997; Mutti and Zadnik, 1998; Zadnik *et al.*, 2003; Mutti *et al.*, 2005; Mutti 2010; Flitcroft, 2014), in addition to the ocular biometric correlates in myopia (McBrien and Adams, 1997; Atchison *et al.*, 2004; Mutti *et al.*,

2007; Buckhurst *et al.*, 2013; Gilmartin *et al.*, 2013). For example, axial length and anterior chamber depth are greater in myopes compared with emmetropes, (Park *et al.*, 2010; Buckhurst *et al.*, 2013) which is consistent with the evidence that increased axial elongation and globe expansion occurs with myopic development (Atchison *et al.*, 2004; Mutti *et al.*, 2007; Mutti 2010; Gilmartin *et al.*, 2013). As such, an increasing body of evidence supports the findings of increased ciliary muscle length and thickness (Oliveira *et al.*, 2005; Bailey *et al.*, 2008; Schultz *et al.*, 2009; Sheppard and Davies, 2010; Buckhurst *et al.*, 2013), as detailed in chapter 4. However, whilst ocular biometric data in amblyopia have been documented, there have been no reports to date of ciliary muscle morphology in amblyopia.

Accommodation is considered to be a symmetrical response between both eyes (Charman, 2004; Horwood and Riddell, 2010). However, amblyopes demonstrate aniso-accommodation, with the least amblyopic eye driving the accommodative response (Horwood and Riddell, 2010). Fittingly, reports also indicate that the stimulus- response slope of the amblyopic eye is characteristically flatter than in the fellow eye (Ciuffreda *et al.*, 1984; Horwood and Riddell, 2010). Chapter 4 showed high levels of ciliary muscle symmetry between the eyes of non-amblyopes. Since amblyopic eyes have a reduced visual output and accommodation (Ciuffreda and Rumpf, 1985; Maheshwari *et al.*, 2011), it might intuitively be expected that the amblyopic ciliary muscle morphology should be altered, and inter- ocular asymmetry of ciliary muscle parameters may be anticipated where amblyopia has been present for most of an individual's life.

Despite a paucity of information regarding amblyopic ciliary muscle morphology and biometry in adults, paediatric studies reveal that a reduction in axial length is evident in some amblyopias (Kugelberg *et al.*, 1996; Cass and Tromans, 2008; Mori *et al.*, 2015). Ocular biometric components and their relationship in both anisometropic and strabismic amblyopic eyes were investigated using A-scan ultrasound biometry (Cass and Tromans, 2008) and it was reported that the parameters of the amblyopic eye differ physically from their non-amblyopic counterparts, across both amblyopic cohorts. The anisometropic amblyopic eye appeared to be a proportionally smaller version of the fellow eye largely due to the presence of higher magnitudes of hyperopia found in the anisometropic eyes. However, the strabismic amblyopic eye was found to have a significantly greater, and disproportionate degree of anterior chamber reduction (10 % shorter than that of the non-amblyopic eye, which cannot be accounted for by difference in refractive error) and crystalline lens thickness, a reduced vitreous chamber depth and therefore total axial length (Cass and Tromans, 2008). The authors therefore indicated that the strabismic eye may be under-developed, with a delay of emmetropisation in the infantile phase, though it has not been determined whether the reported biometric characteristics are a consequence or cause of amblyopia; hence, it is

feasible that the ciliary muscle in amblyopia is also under-developed, though how the morphology would be altered is not known. A more recent biometric investigation utilising PCI on an anisometric adult cohort aged 40 – 64 years (Hashemi *et al.*, 2013) reported that axial length asymmetry had the strongest relationship with anisometropia, though ocular biometry such as lens power, corneal power, and anterior chamber depth were also altered.

Anisometropia, refractive asymmetry between fellow eyes, may be an underdiagnosed cause of amblyopia as it is not instantly apparent to the child or parents, and may go undetected until the later in the child's life (Attebo *et al.*, 1998; Sonia *et al.*, 2013). The prevalence of the condition varies between approximately 2 – 10 % under 50 years of age (Weale, 2002; Haegerstrom-Portnoy *et al.*, 2014). The literature on ciliary muscle morphology in anisometropia, albeit very limited, indicates that anisometric participants follow a similar trend to the isometric population (Kuchem *et al.*, 2013). Utilising AS-OCT for ciliary muscle image acquisition, it was shown that in low- moderate levels of anisometropia (mean 1.85 ± 1.24 D), the ciliary muscle thickness of the more hyperopic eye does not differ significantly from that of the longer, more myopic fellow- eye. The thickness measures were obtained at CM1, CM2, CM3 and CMTMAX as well as apical fibres at CMTMAX (the thickness difference between CMTMAX and CM2) and apical fibres at CM1 (the thickness difference between CM1 and CM2). Similar to the previous finding, the magnitude of the interocular refractive error difference was not linked with an interocular difference in ciliary muscle thickness, at any measured thickness parameter. It may therefore be that in ocular development in anisometropia, it is possible for an eye to undergo greater magnitudes of myopic expansion than its fellow eye, without the concomitant ciliary muscle thickening (Kuchem *et al.*, 2013) that is demonstrated in isometric myopia (Oliveira *et al.*, 2005; Bailey *et al.*, 2008; Schultz *et al.*, 2009; Buckhurst *et al.*, 2013). However, the results from a previous investigation (Muftuoglu *et al.*, 2009), are inconsistent with the investigation by Kuchem and co-workers (2013), as greater ciliary muscle thickness was observed in the more myopic eye of most participants with unilateral high myopia and other parameters such as ciliary muscle lengths or proportional thickness measures have not previously been reported.

As amblyopic eyes have reduced visual output and accommodation, it is of interest to understand how amblyopia which is known to develop at a very young age, may impact on the growth and development of the ciliary muscle. Ciliary muscle morphology in anisometric and strabismic amblyopia is documented for the first time, and compared to ciliary muscle morphology in anisometric subjects without the presence of amblyopia. Measurements of morphological parameters are compared between the two eyes of each subject, which reduce the potential influence of environmental and genetic factors that vary between individuals and govern ocular growth (Kutchem *et al.*, 2013).

6.2 Methods

6.2.1 Subjects

The study recruited both amblyopic subjects and anisometric participants without amblyopia. All participants were aged 18- 29 years and were recruited from the staff and student body of Aston University. The fairly narrow age band was selected to reduce variation in ciliary muscle data due to ageing, most notably increased ciliary muscle thickness (Sheppard and Davies, 2010). Exclusion criteria were cylindrical refractive errors greater than 2.75 D, previous history of ocular trauma, refractive surgery, pathology and systemic conditions known to affect ocular health. Ethical approval was obtained from the Aston University Life and Health Sciences Research Ethics Committee and the study adhered to the tenets of the Declaration of Helsinki. Written, informed consent was obtained from all participants prior to commencement after explanation of the nature and possible consequences of the study.

Ten unilateral amblyopic subjects were recruited, in which amblyopia was defined as an interocular difference in visual acuity of two logMAR lines or greater (Pascual *et al.*, 2014). All participants had corrected visual acuities of 0.0 logMAR or better in the non amblyopic eye. Eight anisometric subjects without the presence of amblyopia were recruited, defined as an interocular difference of at least 1.50 D mean sphere equivalent (MSE; sphere + ½ cylinder (D)). Anisometric participants had corrected visual acuities of 0.0 logMAR or better in each eye.

6.2.2 Measurements

Binocular distance refractive error was measured with a validated infra-red binocular open-view autorefractor (Grand Seiko WAM 5500; Sheppard and Davies, 2010) whilst subjects viewed a distance (6 m) Maltese cross target. A minimum of five measurements of refractive error were taken for each eye, averaged and converted into MSE. In line with previous reports of refractive error in young and older populations (Cregg *et al.*, 2003; Owsley *et al.*, 2007), mean absolute refractive error (MAE) was also calculated for amblyopic participants to reflect the fact that the cohort consisted of some moderate-high myopes as well as hyperopes.

Axial length in the relaxed state were obtained in both eyes using the *Lenstar LS 900* biometer (Haag-Streit AG, Koeniz, Switzerland). Each participant fixated on the central red fixation light whilst four separate biometric measurements were taken and averaged at 0 D.

6.2.3 Ciliary muscle image acquisition and analysis

AS-OCT (Visante; Carl Zeiss Meditec. Inc., Dublin, CA) images of nasal ciliary muscle regions were obtained from right and left eyes of participants to compare with previous work (Kuchem *et al.*, 2013), using high-resolution corneal mode, as described in detail in section 1.7.7. Ciliary muscle images were exported from the AS-OCT in raw DICOM form for analysis purposes. A validated bespoke analysis programme (Laughton *et al.*, 2015) was used to measure ciliary muscle parameters, as detailed in section 1.7.8; all image analysis was carried out by a single examiner (RNS).

Various length and width measurements were obtained; curved ciliary muscle total length (CML) was defined as the anteroposterior distance from the scleral spur, representing the anterior insertion along the ciliary muscle-scleral border, to the visible posterior tip of the ciliary muscle. The anterior length (AL) is from the scleral spur to the point of maximum ciliary muscle width (CMTMAX). CM25 is the ciliary muscle width at an area which was 25 % of the CML posterior to the scleral spur; similarly CM50 and CM75 measures were taken at areas 50 % and 75 % (CM50 and CM75 respectively) of the CML posterior to the scleral spur. Additionally, ciliary muscle thickness measurements at fixed distances from the scleral spur were taken to compare with previous work (Kuchem *et al.*, 2013); CMT1 represents a point 1 mm posterior to the scleral spur, with CMT2 and CMT3 taken at locations 2 mm and 3 mm posterior to the scleral spur, respectively.

6.2.4 Statistical Analysis

The relationship between axial length and ciliary muscle parameters was determined by linear regression analysis for each cohort. To assess the differences in ciliary muscle parameters between eyes of each cohort, independent samples t- tests were performed (SPSS Statistics 21; IBM, Illinois, USA.) A *P* value of less than 0.05 was considered significant for all analyses.

6.3 Results

6.3.1 Amblyopes

Table 6.1 shows the characteristics of amblyopic participants. Table 6.2 shows the ciliary muscle characteristics in amblyopic subjects. There was no significant difference in MSE between the eyes of amblyopes (*P* = 0.931). However, the MAE between the amblyopic eyes and the non- amblyopic eyes showed a significant difference (*P* = 0.013).

	Mean	Minimum	Maximum
Age (years)	22.61 ± 3.38	18.5	29.1
Axial length of amblyopic eye (mm)	23.30 ± 1.35	21.57	24.45
Axial length of non- amblyopic eye (mm)	23.61 ± 1.05	22.20	25.40
MSE of amblyopic eye (D)	-1.05 ± 3.09	-5.38	6.97
MSE of non- amblyopic eye (D)	-1.16 ± 2.60	-4.13	5.54
MAE of amblyopic eye (D)	2.59 ± 1.45	0.00	6.97
MAE of non- amblyopic eye (D)	1.29 ± 1.87	0.25	5.54

Table 6.1. Characteristics of amblyopic participants (n = 10). There was a significant difference in axial length between amblyopic and non-amblyopic eyes ($P = 0.040$).

Parameter (mm)	Amblyopic eye	Non- amblyopic eye
CML	4.26 ± 0.51	4.25 ± 0.51
AL	0.63 ± 0.14	0.65 ± 0.12
CMT1	0.70 ± 0.22	0.69 ± 0.18
CMT2	0.45 ± 0.17	0.42 ± 0.15
CMT3	0.24 ± 0.12	0.21 ± 0.11
CM25	0.68 ± 0.20	0.68 ± 0.16
CM50	0.41 ± 0.13	0.41 ± 0.13
CM75	0.20 ± 0.07	0.18 ± 0.05
CMTMAX	0.67 ± 0.16	0.78 ± 0.20

Table 6.2. Nasal ciliary muscle morphological characteristics of amblyopic participants (n = 10).

Between the eyes of amblyopes, there was no significant difference for any length measure (AL: $P = 0.754$; CML: $P = 0.954$) or thickness parameter (CM1: $P = 0.938$; CM2: $P = 0.713$; CM3: $P = 0.420$; CM25: $P = 0.723$; CM50: $P = 0.681$; CM75: $P = 0.855$; CMTMAX: $P = 0.751$). In the non- amblyopic eye, there was a significant association between CML and AXL ($P = 0.010$, $r^2 = 0.534$) as shown by figure 6.1, though there was no link between AXL and AL ($P = 0.532$). For ciliary muscle thickness measures in the non- amblyopic eye, there was a relationship between AXL and CM3 only ($P = 0.039$, $r^2 = 0.359$). CML was linked to CMT at CM2 ($P = 0.010$, $r^2 = 0.535$) and CM3 ($P = 0.001$, $r^2 = 0.746$). In the amblyopic eye, there was no link between AXL and CML ($P = 0.065$) as shown in figure 6.2, or between AXL and AL ($P = 0.154$). AXL was not linked to CMT (e.g. CM1: $P = 0.239$, CM50: $P = 0.152$, CM3: $P = 0.057$, CM75: $P = 0.087$) though CML was related with CMT at CM3 only ($P = 0.048$; $r^2 = 0.330$). CML in the amblyopic eye was related to AXL of the non- amblyopic eye ($P = 0.022$, $r^2 = 0.438$), as was CM3 in the amblyopic eye ($P = 0.033$, $r^2 = 0.384$).

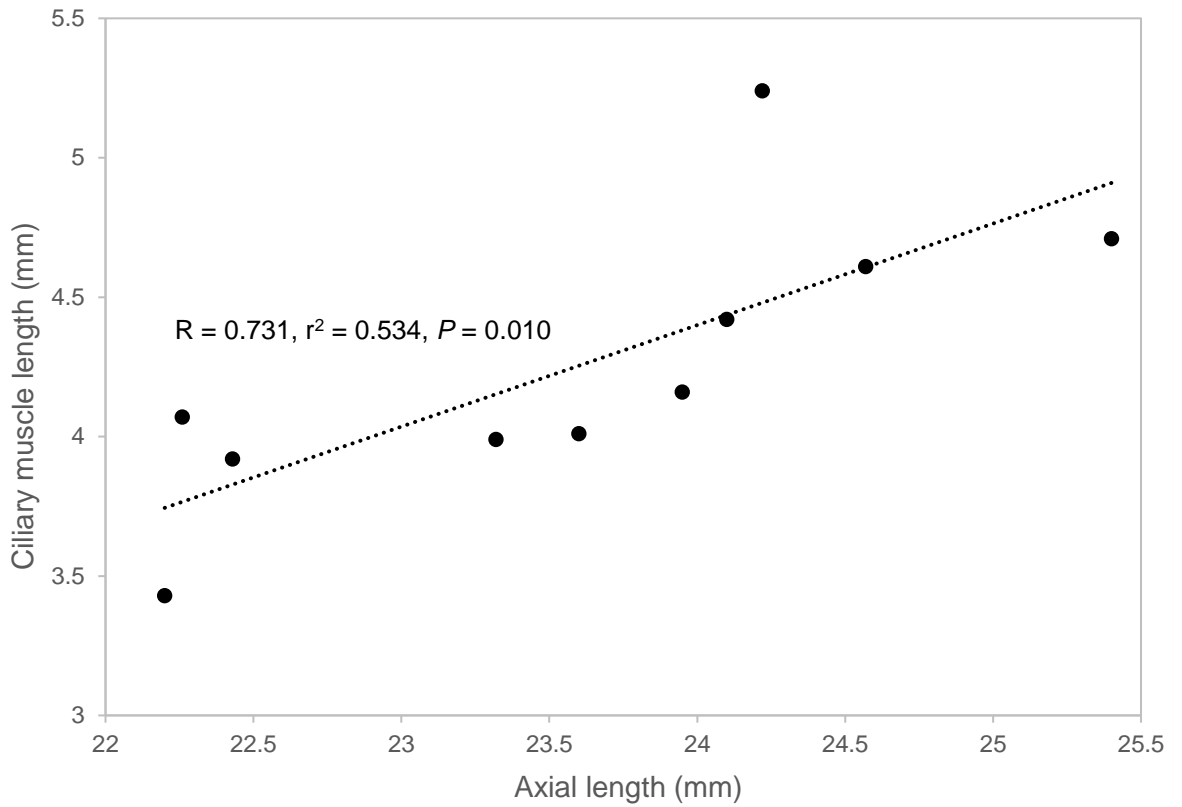


Figure 6.1. Relationship between axial length and nasal ciliary muscle length in the non- amblyopic eye of the amblyopic cohort (n = 10).

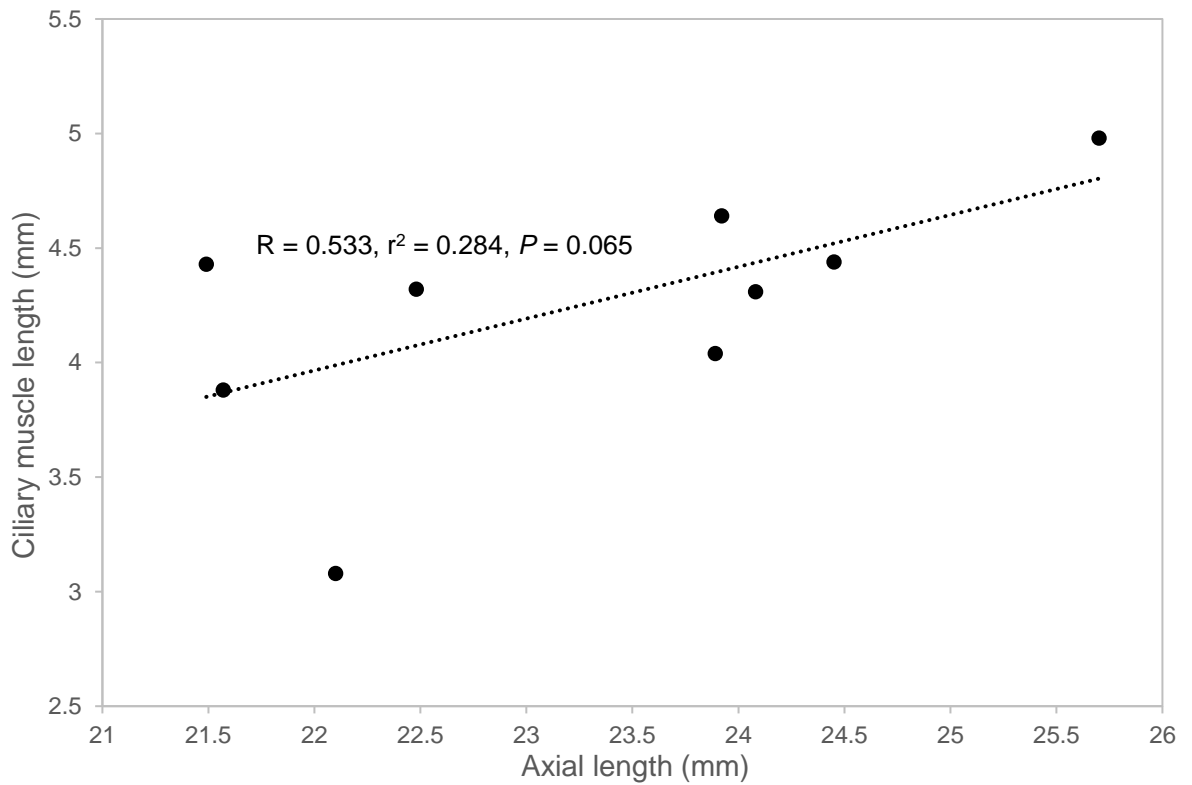


Figure 6.2. Relationship between axial length and nasal ciliary muscle length in the amblyopic eye (n = 10).

6.3.2 Anisometropes

Table 6.3 shows the characteristics of anisometropic participants. Mean values for ciliary muscle morphological parameters are shown in table 6.4. There was a significant difference in MSE between eyes ($P < 0.001$).

	Mean	Minimum	Maximum
Age (years)	20.29 ± 1.60	19.0	23.5
Axial length of most myopic eye (mm)	24.29 ± 1.35	21.55	26.34
Axial length of least myopic eye (mm)	23.12 ± 1.23	21.19	24.97
MSE of most myopic eye (D)	-2.46 ± 2.01	-6.54	0.75
MSE of least myopic eye (D)	-0.57 ± 2.06	-4.98	2.25
Difference in MSE between eyes (D)	1.89 ± 0.52	1.50	3.00

Table 6.3. Characteristics of anisometropic participants (n = 8). There was a significant difference in axial length between both eyes ($P = 0.029$).

Parameter (mm)	Most myopic eye	Least myopic eye
CML	4.73 ± 0.74	4.71 ± 0.81
AL	0.63 ± 0.21	0.65 ± 0.17
CMT1	0.72 ± 0.15	0.72 ± 0.15
CMT2	0.49 ± 0.13	0.47 ± 0.10
CMT3	0.28 ± 0.10	0.26 ± 0.08
CM25	0.69 ± 0.15	0.67 ± 0.14
CM50	0.42 ± 0.11	0.42 ± 0.10
CM75	0.20 ± 0.06	0.19 ± 0.04
CMTMAX	0.85 ± 0.21	0.84 ± 0.18

Table 6.4. Nasal ciliary muscle characteristics across both eyes of anisometropes (n = 8).

There was no significant difference between eyes of anisometropes in any ciliary muscle length (CML: $P = 0.959$; AL: $P = 0.842$) or thickness (CM1: $P = 0.978$; CM2: $P = 0.962$; CM3: $P = 0.695$; CM25: $P = 0.835$; CM50: $P = 0.971$; CM75: $P = 0.531$; CMTMAX: $P = 0.872$) parameter. In the most myopic eye, there was no relationship between AXL and CML ($P = 0.178$) or between AXL and AL ($P = 0.316$). AXL was not linked with ciliary muscle thickness at any measures parameter (e.g. CM1: $P = 0.929$, CM3: $P = 0.607$; CM75: $P = 0.881$) and there was no relationship between CML and any thickness measurement (e.g. CM1: $P = 0.953$, CM3: $P = 0.154$; CM50: $P = 0.732$). In the least myopic eye, there was no link between AXL and CML ($P = 0.703$) or between AXL and AL ($P = 0.309$). AXL was not related with any ciliary muscle parameter measured (e.g. CM25: $P = 0.081$, CM3: $P = 0.215$, CM75: $P = 0.214$).

and there was no relationship between CML and any thickness parameter (e.g. CM50: $P = 0.707$; CM3: $P = 0.132$).

6.4 Discussion

Though several investigations have studied ciliary muscle morphology with refractive error (Oliveira *et al.*, 2005; Bailey *et al.*, 2008; Schultz *et al.*, 2009; Sheppard and Davies, 2010; Buckhurst *et al.*, 2013), the ciliary muscle in amblyopia has not previously been described. Since amblyopic eyes are known to have reduced visual output and an altered accommodative response (Ciuffreda *et al.*, 1984; Horwood and Riddell, 2010) compared with their fellow eyes, it may be expected that ciliary muscle morphology between the eyes does not display the symmetry demonstrated in myopic and emmetropic eyes (detailed in chapter 4). Similarly, there is a paucity of information relating to the ciliary muscle morphology between eyes of anisometropes (Kuchem *et al.*, 2013), as such, the ciliary muscle was investigated between the eyes of amblyopes and anisometropes, to determine if, and what impact these neurological and refractive conditions have on the symmetry of ciliary muscle morphology.

The axial length of the amblyopic eye was found to be significantly shorter than the fellow eye, consistent with previous findings in paediatric amblyopias (Cass and Tromans, 2008; Debert *et al.*, 2011; Mori *et al.*, 2015) and in amblyopia present in adults (Lempert and Porter, 1998). It has been suggested that the strabismic amblyopic eye is under-developed, impeding emmetropisation in the infantile phase (Cass and Tromans, 2008). Similarly, in another investigation studying optic disc dysversion and axial length measurements in a population of adult amblyopes, it was indicated that reduced vision in smaller eyes may result from a decrease in nerve fibres and photoreceptors (Lempert and Porter, 1998). Whether the altered ocular biometry observed is a result of or a cause of amblyopia, cannot be answered in this investigation.

Ciliary muscle morphology is known to vary with axial length, and has found to be longer (Sheppard and Davies, 2010) and thicker (Oliveira *et al.*, 2005; Bailey *et al.*, 2008; Schultz *et al.*, 2009; Buckhurst *et al.*, 2013) with increasing axial length, in the non- amblyopic population. Since the amblyopic eye has a significantly smaller axial length than its fellow non- amblyopic eye, and suffers visual loss (Wiesel and Hubel, 1963; Webber and Wood, 2005; Veneruso *et al.*, 2014; Solebo *et al.*, 2015) and reduced accommodative response (Ciuffreda *et al.*, 1984; Horwood and Riddell, 2010), asymmetry of ciliary muscle morphology would be expected between the eyes of amblyopes. However, between the amblyopic eyes and the fellow eyes, there was unexpectedly no significant difference in ciliary muscle morphology for any length or thickness parameter measured. In the non- amblyopic eye, axial

length was linked to ciliary muscle length (for CML) and thickness at CM3, and CML was also linked with ciliary muscle thickness. Yet, in the amblyopic eye, there was no relationship between axial length and ciliary muscle length or thickness, though CML was linked with ciliary muscle thickness. It is shown therefore, that amblyopic participants display high levels of ciliary muscle symmetry between the eyes, as the ciliary muscle length and thickness in the amblyopic eye is not governed by the axial length of the amblyopic eye, but appears to grow in accordance with the fellow non- amblyopic eye.

The sample of adult anisometropes in this study behaved in accordance with the literature (Hashemi *et al.*, 2013, Jiang *et al.*, 2013), in showing a significant difference between the axial lengths of both eyes. In anisometric participants, between the most myopic and least myopic eye, though myopic eyes tended to have a thicker ciliary muscle, there was no significant difference in any ciliary muscle thickness parameter measured, consistent with previous AS-OCT work investigating ciliary muscle morphology in anisometropes (Kuchem *et al.*, 2013). Similarly, no significant difference for ciliary muscle length parameters were found between the eyes of anisometropes, a finding that has not previously been reported. In each eye, there was no link between axial length or any ciliary muscle length or thickness parameter, and length of the ciliary muscle was not linked with thickness. Such findings vary with outcomes in the isometric population, whereby ciliary muscle morphology is known to be associated with axial length (Oliveira *et al.*, 2005; Bailey *et al.*, 2008; Schultz *et al.*, 2009; Sheppard and Davies, 2010) and with findings by Kuchem *et al.* (2013). However, whilst the present study only included anisometric subjects with a minimum of 1.50 D difference in MSE, the previous investigation included subjects with a spherical equivalent refractive error of less than 1 D difference between eyes, with a difference as little as 0.75 D included (Kuchem *et al.*, 2013). Hence, the inclusion of subjects regarded as isometric (since anisometropia can be defined as a difference in MSE of at least 1 D) and of a much wider age range (18 – 40 years) when the ciliary muscle thickness is known to increase with advancing age (Pardue and Sivak, 2000; Sheppard and Davies, 2010), may have caused the discrepancy between the two investigations. However, in agreement with the investigation by Kuchem and co- workers (2013), it seems plausible in anisometric ocular development, that an eye can expand and become more myopic than its fellow eye, without a concurrent increase in ciliary muscle length or thickness. This contrasts with previous research in high unilateral myopia (Muftuoglu *et al.*, 2009) which found increased ciliary muscle thickness in the longer eye, more myopic eye of most, though not all, subjects with unilateral high myopia. The participants had a much greater level of anisometropia (≥ 5.00 D) compared with the present study and the investigation by Kuchem *et al.* (2013) (≥ 0.75 D). It has been suggested

that the mechanisms governing ocular growth in a high degree of anisometropia differ from those regulating ocular growth in lower magnitudes of anisometropia (Kuchem *et al.*, 2013).

The relatively small sample size used in this investigation was due to the low prevalence of the conditions, particularly with the narrow age range selected. Where the present investigation utilised a sample of eight anisometropes, other biometric studies of anisometropia (≥ 1 D) have included cohorts of between 19 – 354 participants (Muftuoglu *et al.*, 2009; Hashemi *et al.*, 2013; Jiang *et al.*, 2013; Kuchem *et al.*, 2013). Similarly, studies of ocular biometry in amblyopia have included samples of between 12 – 45 amblyopic participants (Kugelberg *et al.*, 1996; Cass and Tromans, 2008; Debert *et al.*, 2011; Mori *et al.*, 2015), whereas the present investigation utilised a sample size of ten amblyopes. Therefore, the smaller sample size in this investigation may have reduced the statistical power of the analytical tests. Further work is required in this area amongst a larger cohort of anisometropes and amblyopes, and to determine whether the relationships shown in amblyopic eyes apply across both anisometropic and strabismic sub- groups.

6.5 Conclusion

To conclude, this is the first investigation to study ciliary muscle morphology between eyes of amblyopes. High levels of ciliary muscle symmetry were found between the amblyopic eye and the fellow eye. In the non- amblyopic eye, ciliary muscle length and thickness were linked to axial length, whereas growth of the ciliary muscle in the amblyopic eye appears to passively mirror ciliary muscle morphology in the non- amblyopic eye. Similarly, there were high levels of ciliary muscle symmetry between the eyes of anisometropes, indicating that when an eye increases in axial length, becoming more myopic than the fellow eye, there is not accompanying ciliary muscle growth.

Chapter 7

New parameters for analysis of ciliary muscle morphology

7.1 Introduction

Before the utilisation of *in vivo* imaging techniques to view the human ciliary muscle, information regarding the ciliary muscle was extracted from *in vitro* studies. Such investigations have fuelled our understanding of human and primate accommodative physiology (Aiello *et al.*, 1992; Tamm *et al.*, 1992; Poyer *et al.*, 1993). However *in vitro* methods are subject to limitations (Weale, 1999; Kasthurirangan *et al.*, 2008) as discussed in section 1.4. Over several years the *Vistante* AS-OCT has been widely used to image the active ciliary muscle (Bailey *et al.*, 2008; Sheppard and Davies 2010b; Lewis *et al.*, 2012; Buckhurst *et al.*, 2013; Pucker *et al.*, 2013; Laughton *et al.*, 2016). However, standardised criteria for ciliary muscle measurement do not currently exist. There is debate in the literature regarding the appropriate refractive index that should be used when analysing ciliary muscle images, which metrics should be used, and the best reference point for these metrics (Bailey *et al.*, 2008; Sheppard and Davies, 2010b; Bailey, 2011). Whilst different examiners have used slightly different techniques, there may be further parameters other than length and thickness which have not been measured previously (Bailey *et al.*, 2008; Sheppard and Davies 2010b; Lewis *et al.*, 2012; Buckhurst *et al.*, 2013; Pucker *et al.*, 2013), which are valuable to assess with regard to ciliary muscle morphology and refractive error.

Similar to UBM devices, incorporated AS-OCT software (*Zeiss, Vistante*) permits superimposed callipers on acquired images to extract measurement data (Sheppard and Davies, 2010b; Kao *et al.*, 2011; Laughton *et al.*, 2015) (see figure 7.1). The limitations of the calliper method, detailed in section 1.8.9, were overcome through the development of a bespoke semi-objective analysis programme at Aston University, and is described in section 1.7.9. The programme has since been described, validated (Laughton *et al.*, 2015) and utilised throughout this body of research and in other ciliary muscle investigations (Laughton *et al.*, 2016).

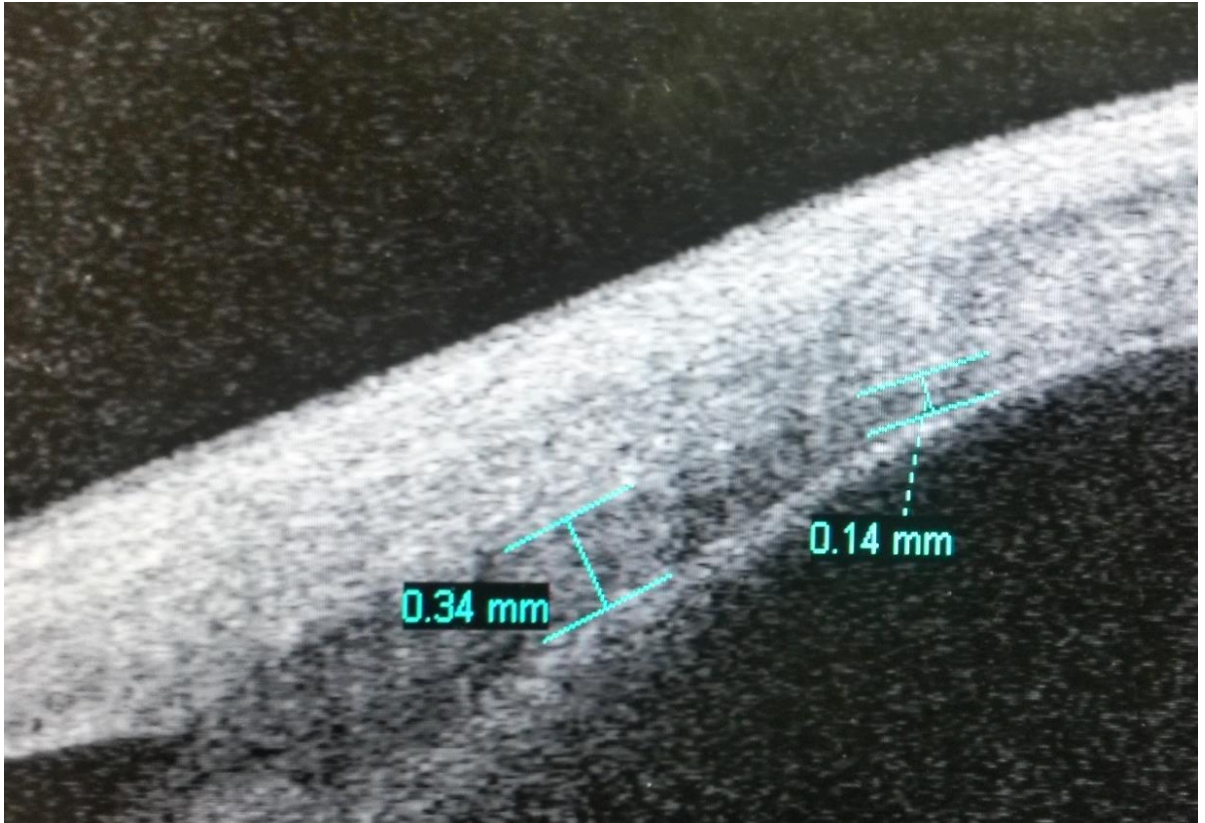


Figure 7.1. User controlled in-built callipers of the *Visante* AS-OCT, superimposed on the acquired ciliary muscle image to provide morphological ciliary muscle data for the designated parameters.

Similar to the software developed at Aston University, the analysis programme by Kao *et al.* (2011) required localisation of the scleral spur manually, prior to automated image analysis because of varying ciliary muscle contour in *Visante* AS-OCT images. Subsequent to the outline of the sclera and ciliary muscle, refractive indices of 1.41 and 1.38 were employed across the y-axis of the sclera and ciliary muscle image portions, respectively, and previous work has reported the refractive index for rabbit sclera and ciliary body to be 1.41 and 1.38, respectively (Nemati *et al.*, 1997; Nemati *et al.*, 1998). However, in the software by Kao and co-workers (2011) the edge detection algorithms appeared to combine both the pigmented ciliary epithelium and the ciliary muscle, which may overestimate ciliary muscle thickness measurements. Whilst the same refractive indices applied to the AS-OCT ciliary muscle images have been used amongst authors (Kao *et al.*, 2011; Laughton *et al.*, 2015), there is not yet a universally accepted method agreed to measure ciliary muscle parameters (Bailey 2011). In the programme developed by Kao *et al.* (2011), ciliary muscle length parameters were not acquired, and thickness measures have since been taken at fixed points posterior to the scleral spur (CM1, CM2 and CM3) (Lewis *et al.*, 2012; Buckhurst *et al.*, 2013; Pucker *et al.*, 2013); measurements in this way do not account for the fact that the ciliary muscle length varies with different axial lengths (Bailey *et al.*, 2008; Sheppard and Davies 2010b), so width measures are not attained at the same anatomical region of the muscle. The location

of the width measures established by Sheppard and Davies (2010b) are proportional to the overall length of the ciliary muscle (CM25, CM50 and CM75), addressing the shortcomings of the arbitrary measures. Both fixed arbitrary width measures and those proportional to the curved overall ciliary muscle length have been utilised throughout the body of research in this thesis, and are compared in detail across an emmetropic cohort in chapter 3, and illustrated how the fixed width measures may present data with not entirely accurate outcomes.

Despite the validity and robust nature of the ciliary muscle programme developed at Aston University (Laughton *et al.*, 2015), there have been previous concerns regarding the visibility of the posterior limit of the ciliary muscle (Bailey, 2011) that are not completely groundless (see figure 7.2); extensive ciliary muscle image analysis during semi-objective programme development showed there can be inter-subject inconsistency in the visibility of the posterior limit of the ciliary muscle. To simplify localisation for the programme, the definition of the posterior visible limit (PVL) was given as the point where the scleral/ ciliary muscle and ciliary muscle/ pigmented ciliary epithelium boundaries reached minimum separation posteriorly, which generated highly repeatable results (Laughton *et al.*, 2015). Previous findings have demonstrated that the greater anterior ciliary muscle length occurs with increased axial length, suggesting that the structure grows in the anteroposterior direction with globe elongation, with the scleral spur as the set anchor point (Sheppard and Davies, 2010). Similarly, it was speculated that the inner apical angle of the ciliary muscle is wider in myopic participants than in emmetropes (see figure 1.11), though further research is required to determine the relevance of this finding to refractive error development (Sheppard and Davies, 2010).

To date, the investigations regarding ciliary muscle morphology have measured the ciliary muscle with regard to length and width (Oliveira *et al.*, 2005; Bailey *et al.*, 2008; Sheppard and Davies 2010b; Sheppard and Davies, 2011, Lewis *et al.*, 2012; Buckhurst *et al.*, 2013; Pucker *et al.*, 2013; Laughton *et al.*, 2016) which are known to be linked with axial length (Oliveria *et al.*, 2005; Bailey *et al.*, 2008; Buckhurst *et al.*, 2013). Such measures are therefore linked to the overall cross- sectional area, the size of the surface of the ciliary muscle, an important parameter which has not before been reported in previous studies investigating the ciliary muscle (Oliveira *et al.*, 2005; Bailey *et al.*, 2008; Sheppard and Davies 2010b; Sheppard and Davies, 2011, Lewis *et al.*, 2012; Buckhurst *et al.*, 2013; Pucker *et al.*, 2013; Laughton *et al.*, 2016) and would be expected to be greater in eyes with longer axial lengths. The cross- sectional area of the ciliary muscle requires judgement of the posterior visible limit, and the investigation presented in this chapter addressed the effect on area that varying posterior visible limit localisation would incur. This study was the first to examine the most

effective parameters to measure the ciliary muscle, including the inner apical angle and cross-sectional area of the ciliary muscle, and their relationship with axial length in both emmetropes and myopes. The repeatability of these parameters are assessed for the first time.

7.2 Methods

7.2.1 Subjects

One hundred participants aged 19-26 years were recruited from the student body of Aston University, comprising of fifty emmetropic volunteers with a mean sphere equivalent (MSE) ≥ -0.55 ; $< +0.75$ D and fifty myopes (MSE ≤ -2.00 D). The narrow age range was implemented to decrease variation in ciliary muscle data due to ageing, particularly thickening of the ciliary muscle (Sheppard and Davies, 2010). Exclusion criteria were cylindrical refractive errors greater than 2.00 D, previous history of ocular trauma, amblyopia, surgery or pathology, and systemic conditions known to affect ocular health. All subjects had corrected visual acuities of 0.0 logMAR or better in each eye. Ethical approval was obtained from the Aston University Life and Health Sciences Research Ethics Committee and the study adhered to the tenets of the Declaration of Helsinki. Written, informed consent was attained from all subjects prior to commencement, after explanation of the nature and possible consequences of the investigation.

7.2.2 Measurements

A validated infra-red binocular open-view autorefractor (Grand Seiko WAM 5500; Sheppard and Davies, 2010) was used to measure binocular distance refractive error, whilst subjects viewed a distance (6 m) Maltese cross target. AS-OCT (Visante; Carl Zeiss Meditec. Inc., Dublin, CA) images of temporal ciliary muscle regions were obtained from the right eye only of participants, using high-resolution corneal mode, as detailed in section 1.7.7. Ciliary muscle images were exported from the AS-OCT in raw DICOM form for analysis purposes with the validated bespoke analysis programme (Laughton *et al.*, 2015).

The analysis programme was used to measure the straight line length of the ciliary muscle, from the scleral spur to the PVL, and three images of the temporal ciliary muscle of the right eye were analysed. Data was stored in an Excel spreadsheet (Microsoft 2010, Redmond, Washington, USA). Currently, the analysis programme does not facilitate area measures of the ciliary muscle, or the inner apical angle. Snipping Tool (Microsoft 2010, Redmond, Washington, USA) was used to capture and save the ciliary muscle image to be imported subsequently to ImageJ, a biomedical image processing software (Schindelin *et al.*, 2015) that has been validated with high repeatability and sensitivity in detection of acetylcholine

esterase inhibitory activity at very low concentration levels (Abou-Donia *et al.*, 2014) and used to measure ciliary muscle parameters.

Due to the somewhat contentious issue of the posterior visible limit location that has been implied (Bailey, 2011; Laughton *et al.*, 2015), the influence of posterior visible location on cross-sectional area was assessed by considering cross-sectional area measures when the posterior visible limit location was varied. Using ImageJ software, the following parameters were measured: cross-sectional area of the ciliary muscle extending from the scleral spur to the posterior visible limit (the point at which the scleral/ ciliary muscle and ciliary muscle/ pigmented ciliary epithelium outlines reached minimum separation posteriorly) shown by figure 7.2, the area of the ciliary muscle when the posterior visible limit is located 0.25 mm anterior to the originally selected PVL (area-0.25), the area of the ciliary muscle when the posterior visible limit is located 0.25 mm posterior to the originally selected PVL (area+0.25), The inner apical angle was also measured (see figure 7.3). The area measures were taken using the ImageJ area tool, whilst the inner apical angle was measured with the angle tool. In order to convert the pixel measurement to millimetres, each image was initially scaled to a known length; a straight line was drawn from the scleral spur to the posterior visible limit using ImageJ, and the value of the straight line length of the ciliary muscle obtained from the semi-objective bespoke analysis programme, was inputted (see figure 7.4). Visual inspection was used to ensure that the outline was smooth and followed the ciliary muscle boundary. Figure 7.2 demonstrates an accepted area outline for analysis and the regions of area+0.25 and area-0.25. The straight line tool was again utilised for location of the posterior visible limit in all area+0.25 and area-0.25 analysis. All analyses were carried out by a single examiner (RNS).

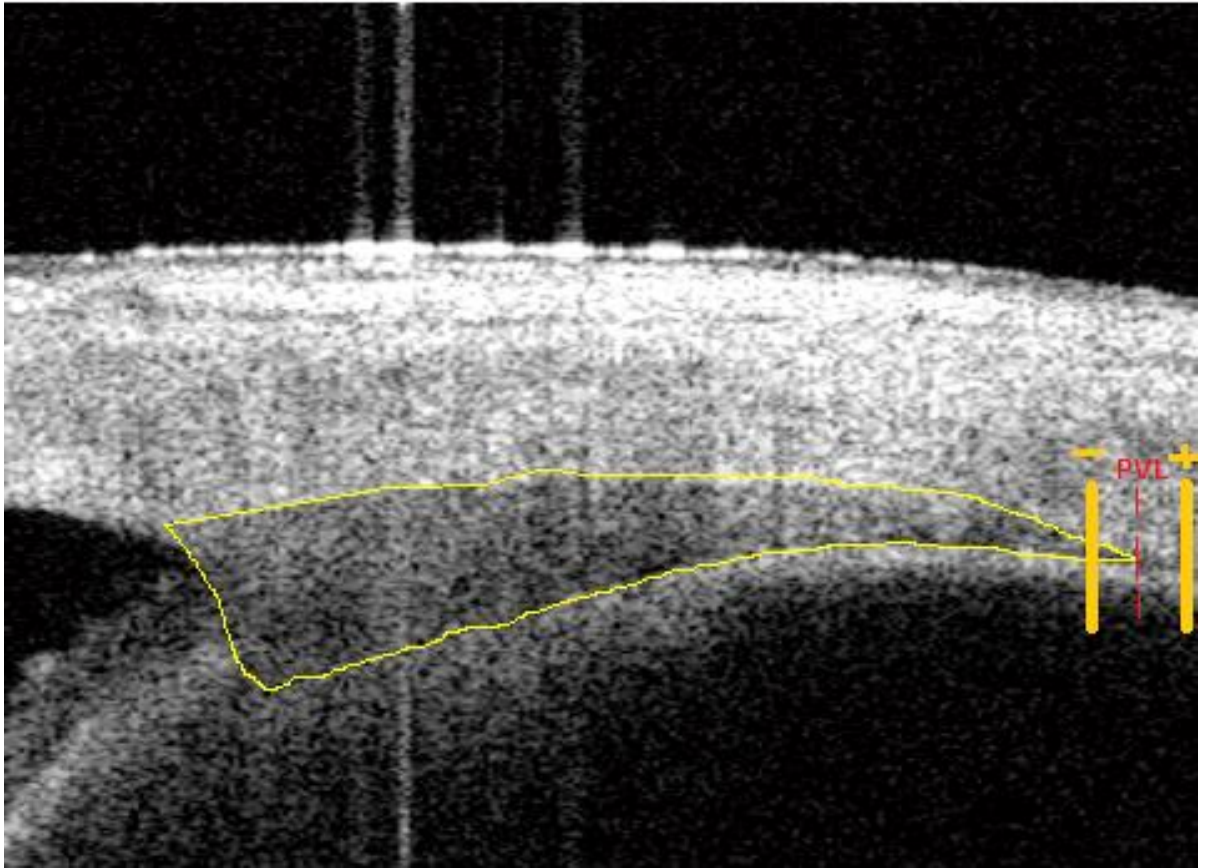


Figure 7.2. ImageJ analysis of the ciliary muscle area, extending from the scleral spur to the posterior visible limit (PVL) indicated by the red dashed line, and showing an accepted area outline image for analysis. Area+0.25 is the cross-sectional area of the ciliary muscle where the PVL is situated 0.25 mm posterior to the original PVL and area-0.25 is the ciliary muscle cross-sectional area when the PVL falls 0.25 mm anterior to the original PVL.

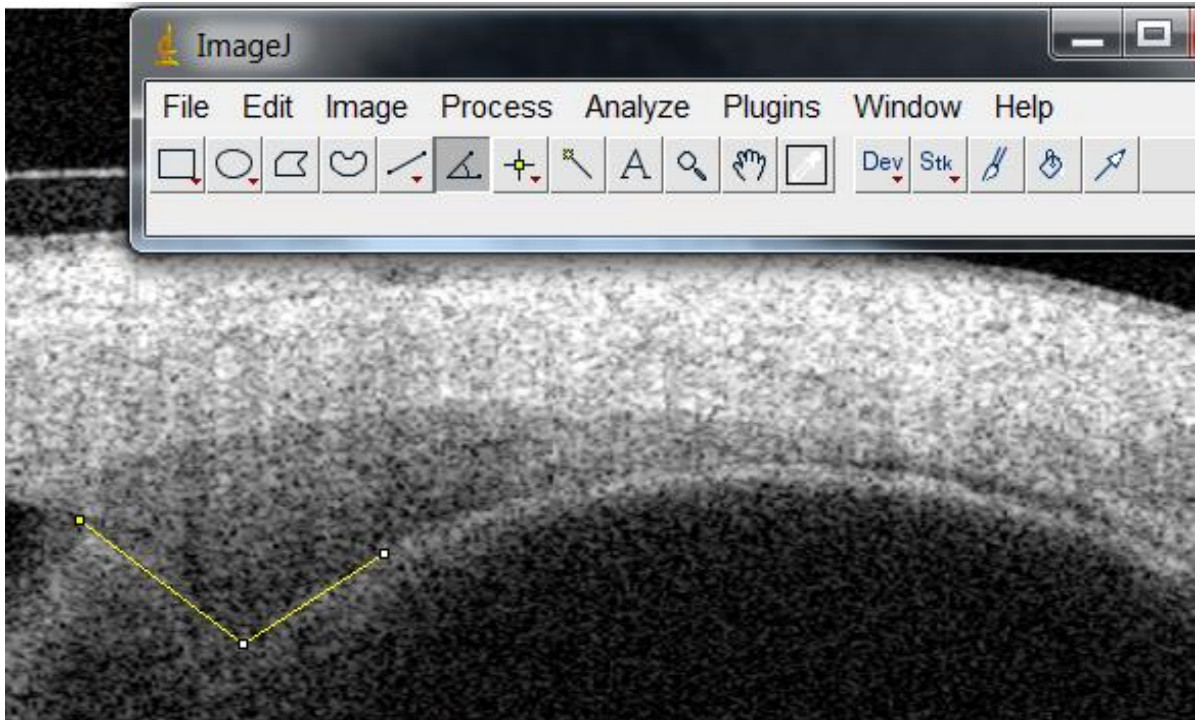


Figure 7.3. Inner apical angle of the temporal ciliary muscle in the right eye, outlined by the angle tool of ImageJ (indicated on the ImageJ toolbar). The user manually selects the starting point of the measurement and drags the line towards the point at which the ciliary muscle boundaries meet, and towards the following intersecting boundary in order to create the angle. On selecting the 'Analyse' tab, the measurement function can be selected in order to display the value of the measured parameter.

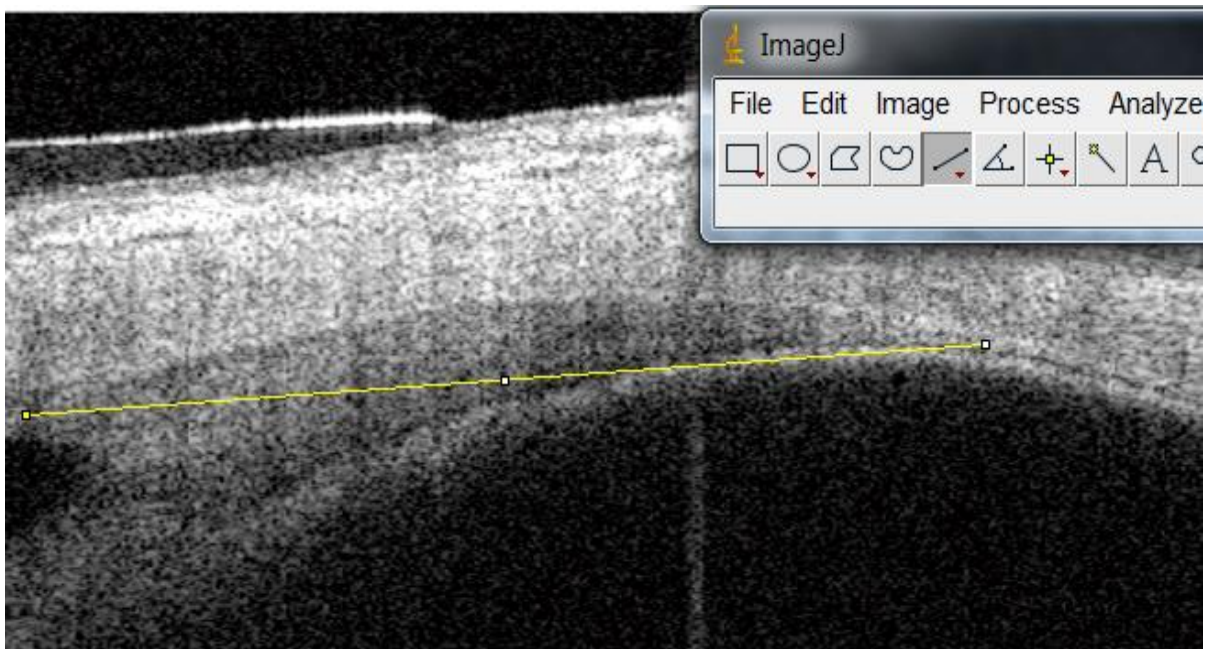


Figure 7.4. The straight line tool extending from the scleral spur to the posterior visible limit. Following superimposition of this line, the user can select 'Analyse' in the ImageJ tab to set the scale of this known length parameter.

7.2.3 Repeatability

The repeatability of the image analysis method with ImageJ was studied, as this is the first investigation to examine the ciliary muscle by the technique described. To determine the repeatability of the measurements, a randomly selected temporal aspect image from the cohort was analysed ten times by a single examiner (RNS). The mean value and standard deviation of the measured ciliary muscle parameters (inner apical angle and cross-sectional area) were calculated. The inter-examiner repeatability was determined by randomly selecting 5 emmetropic and 5 myopic participant ciliary muscle images (3 images analysed per subject), measured by a different examiner (ALS), and calculating the mean difference between the two examiners for cross-sectional ciliary muscle area and inner apical angle.

7.2.4 Statistical analysis

The data for each variable were normally distributed, as examined by tests of normality (Shapiro-Wilk, SPSS Statistics 21; IBM, Illinois, USA). Independent samples t-tests were performed to indicate any significant difference between the ciliary muscle cross-sectional area between refractive groups and the inner apical angle between emmetropes and myopes, and the difference in cross-sectional area and inner apical angle measures obtained between the two different examiners. A one-way ANOVA was performed to assess the difference between area+0.25, area-0.25 and ciliary muscle cross-sectional area amongst the refractive groups. The relationships between ciliary muscle cross-sectional area, inner apical angle and axial length were determined by linear regression analysis. An independent samples t-test was performed to check for differences in age between the refractive groups. A *P* value < 0.05 was considered significant. All data were stored in an Excel spreadsheet (Microsoft 2010, Redmond, Washington, USA).

7.3 Results

7.3.1 Repeatability

The results from analysing a single image ten times by a single examiner (RNS) are shown in table 7.1. The image analysis using ImageJ software appear robust, with a standard deviation for cross-sectional ciliary muscle area of 0.04 mm², indicating that most values (68 % for a normal distribution) are within 0.04 mm² of the mean and the vast majority (95%) are within 0.08 mm²; this standard deviation of 0.04 mm² represents a 2.15 % variation of the mean area. Similarly, the standard deviation of the apical angle was 2.97°, indicating that most values are within 2.97° of the mean whilst the overall majority (95%) are within 5.94°; this 2.97° standard deviation corresponds to a 2.78 % change. Table 7.2 shows the variation

between ciliary muscle cross-sectional areas utilising different PVL locations. There was no significant variation between area+0.25 and ciliary muscle area ($F = 0.795$; $P = 0.198$), though there was a significant difference between PVL-0.25 and ciliary muscle area ($F = 0.565$; $P = 0.020$), however the magnitude of difference between the latter means are so small (2.15 %) that it cannot be deemed relevant.

Repeat	Area (mm ²)	Angle (°)
1	1.85	107.6
2	1.94	108.2
3	1.86	102.5
4	1.87	101.2
5	1.85	108.1
6	1.80	106.1
7	1.88	106.8
8	1.89	111.6
9	1.86	108.1
10	1.86	106.5
Mean	1.86	106.7
SD	0.04	2.97

Table 7.1. Repeatability of ImageJ analysis technique on cross sectional area and inner apical angle, from a single ciliary muscle image analysed ten times, by examiner RNS.

	Area (mm ²)	Area+0.25 (mm ²)	Difference Between Area and Area+0.25 (mm ²)	Area-0.25 (mm ²)	Difference Between Area and Area-0.25 (mm ²)
Mean	1.86	1.89	0.03	1.82	0.04
SD	0.04	0.03	0.02	0.05	0.03

Table 7.2. The effect of varying PVL locations on the cross-sectional area of the ciliary muscle. A single ciliary muscle image was analysed ten times by examiner RNS. There was no significant difference between area and area+0.25, with a magnitude of difference of 1.61 %. Whilst there was a statistically significant difference between area and area-0.25 ($P = 0.020$), the magnitude of difference is 2.15%.

Table 7.3 shows the inter-examiner repeatability results for ciliary muscle cross-sectional area and inner apical angle measures. Between the two examiners, there was no significant difference between cross-sectional area measures ($P = 0.897$) or for inner apical angle ($P = 0.937$).

	Examiner 1 (RNS)		Examiner 2 (ALS)	
	Cross- sectional area (mm ²)	Inner apical angle (°)	Cross- sectional area (mm ²)	Inner apical angle (°)
Mean	1.67	117.0	1.64	117.3
SD	0.58	5.84	0.59	8.19

Table 7.3. Mean results for ciliary muscle cross- sectional area and inner apical angle measures for 2 different examiners (RNS and ALS), through ImageJ ciliary muscle image analysis of 10 participants. There was no statistically significant difference between examiners for cross- sectional area ($P = 0.897$) or inner apical angle ($P = 0.937$).

7.3.2 Ciliary muscle parameters

Summary characteristics of emmetropic and myopic participants are shown in table 7.4. Mean axial length ($P < 0.001$) was significantly greater in the myopic group. There was no significant difference in age between the refractive groups ($P = 0.884$).

	Emmetropes (n = 50)	Myopes (n = 50)
	Mean	Mean
Age (years)	21.1 ± 8.63	21.7 ± 8.84
Refractive error (D)	-0.03 ± 0.32*	-4.54 ± 2.08*
Axial length (mm)	23.29 ± 0.79*	25.46 ± 1.16*
Ciliary muscle area (mm ²)	1.35 ± 0.22*	2.47 ± 0.57*
Apical angle (°)	101.45 ± 10.61*	120.99 ± 12.58*

Table 7.4. Summary characteristics of emmetropic and myopic participants. *Indicates statistically significant difference between the refractive groups.

7.3.3 Ciliary muscle area

Mean ciliary muscle area was significantly larger in myopes compared to emmetropes (emmetropes: 1.35 ± 0.22 mm², myopes: 2.47 ± 0.57 mm², $P < 0.001$). In both emmetropes and myopes, there was no significant difference between ciliary muscle cross- sectional area and area+0.25 ($F = 0.263$; $P = 0.610$). There was a significant difference between ciliary muscle area and area-0.25 ($F = 0.692$; $P = 0.042$) and between area-0.25 and area+0.25 ($F = 196.771$; $P < 0.001$). Across the whole cohort, ciliary muscle area was linked with axial length ($R = 0.732$, $r^2 = 0.536$, $P < 0.001$), shown by figure 7.5. The ciliary muscle area across the whole cohort was linked with the inner apical angle ($R = 0.425$, $r^2 = 0.181$, $P = 0.001$).

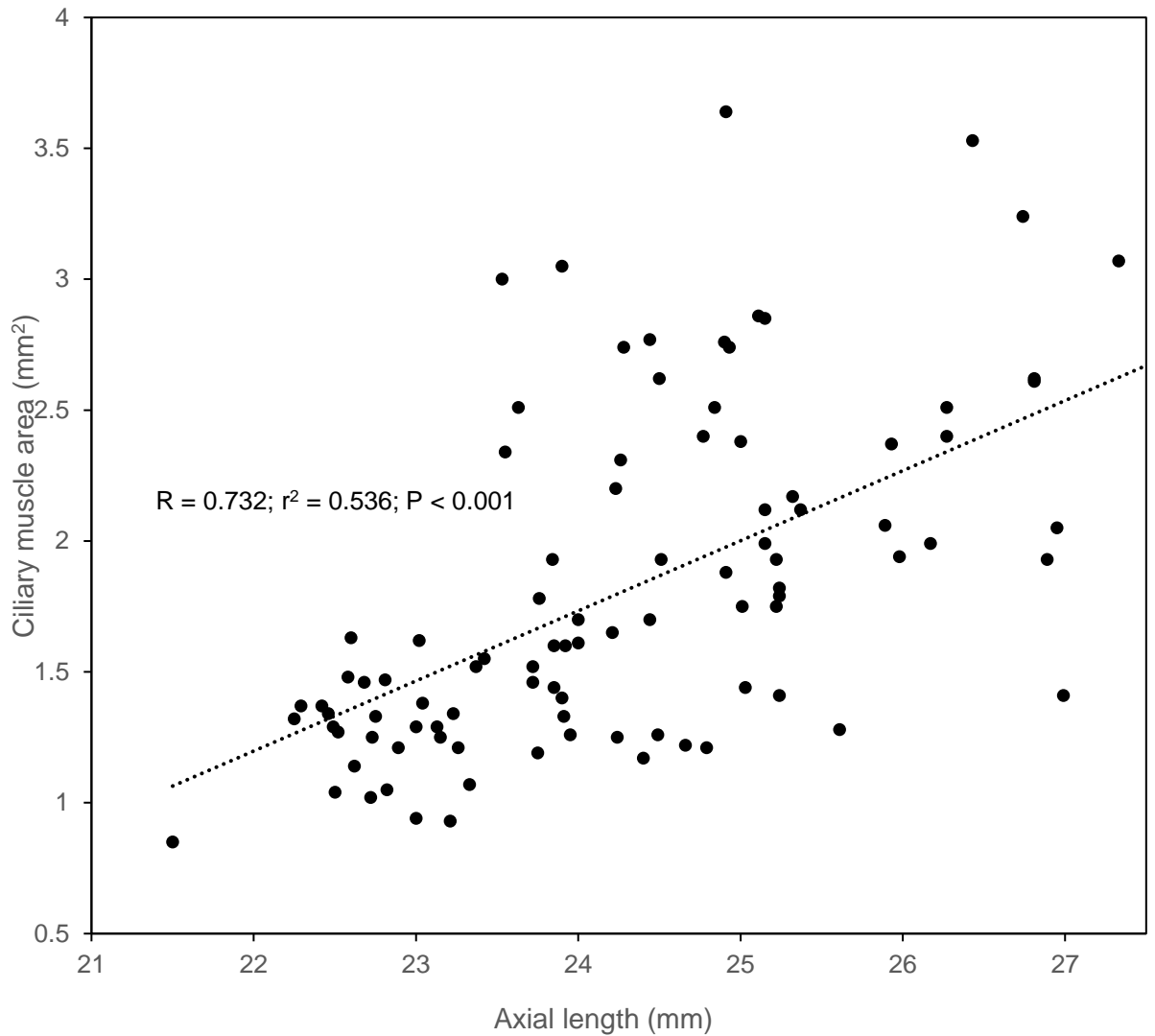


Figure 7.5. Relationship between ciliary muscle area and axial length ($n = 100$). A significant relationship occurred between the two parameters across the whole cohort ($R = 0.732$, $r^2 = 0.536$, $P < 0.001$).

7.3.4 Ciliary muscle inner apical angle

Between refractive error groups, myopes had a significantly wider inner apical angle compared with emmetropes (emmetropes: $101.45 \pm 10.61^\circ$, myopes: $120.99 \pm 12.58^\circ$; $P < 0.001$). Across the whole cohort, inner apical angle was linked with axial length ($R = 0.465$, $r^2 = 0.216$, $P < 0.001$); figure 7.6 shows the relationship between axial length and ciliary muscle inner apical angle.

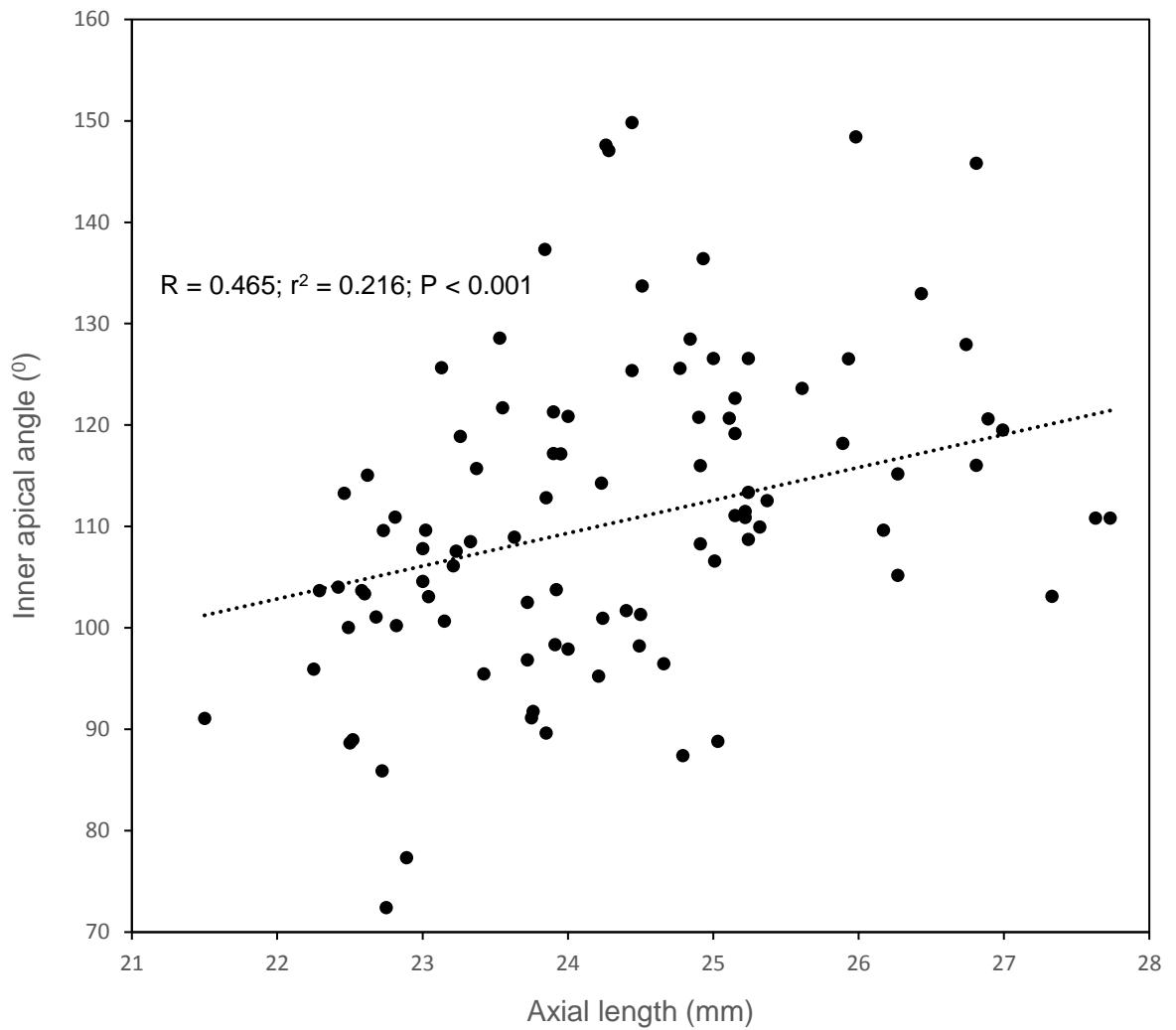


Figure 7.6. Relationship between axial length and ciliary muscle inner apical angle across the whole cohort (n = 100). There is a significant link between the two parameters ($R = 0.465$; $r^2 = 0.216$; $P < 0.001$).

7.4 Discussion

In recent years, the ciliary muscle has been studied widely due to its association with refractive error (Bailey *et al.*, 2008; Oliveira *et al.*, 2008; Sheppard and Davies, 2010; Buckhurst *et al.*, 2013; Pucker *et al.*, 2013). Whilst there has been MRI investigations of ciliary muscle ring diameter (apex to apex) in the role of accommodation and presbyopia (Strenk *et al.*, 1999; Strenk *et al.*, 2006), much of the current methods of analysis of *in vivo* imaging involve width and length measurements only, either dependent on fixed arbitrary measures posterior to the scleral spur (Bailey *et al.*, 2008; Oliveria *et al.*, 2008; Buckhurst *et al.*, 2013; Kuchem *et al.*, 2013; Pucker *et al.*, 2013) or utilising measures that are proportional to the overall length of the ciliary muscle (Sheppard and Davies, 2010; Sheppard and Davies, 2011).

Recent methods employ the latter technique (due to the greater accuracy of targeting the same anatomical regions across varying ciliary muscle) by using validated semi-objective ciliary muscle analysis software (Laughton *et al.*, 2015; Laughton *et al.*, 2016). However, a point has been raised regarding the subjective nature of determining the end point of the ciliary muscle (Bailey, 2011), which the proportional length and width measures depend upon. The magnitude of inaccuracy of posterior limit determination has been previously reported (Sheppard and Davies, 2010) by determining the repeatability of ciliary muscle biometric measures through analysis of a single temporal ciliary muscle image, ten times; out of the various parameters measured (anterior length, overall length, CM25, CM5, CM75 and CM2), the overall length had the highest standard deviation of 32.2 μm , compared with 26.4 μm for anterior length, suggesting this parameter that depends predominantly on posterior visible limit location, is the most difficult to define. Since both length and width measures are related (Bailey *et al.*, 2008; Oliveria *et al.*, 2008; Buckhurst *et al.*, 2013), it can be expected that the ciliary muscle area is also linked; this was the first AS-OCT study to utilise the cross-sectional area parameter, which may be more a more effective method to measuring the ciliary muscle, and to establish the effect on area of varying the posterior visible limit by 0.25 mm posteriorly, and anteriorly. Furthermore, apical angle was analysed across emmetropes and myopes, and this angle parameter and ciliary muscle area are linked with axial length for the first time, to help establish the most appropriate method to measure the ciliary muscle.

The ciliary muscle area was significantly greater in myopes compared to emmetropes, consistent with findings of longer (Sheppard and Davies, 2010) and thicker ciliary muscle morphology across myopes (Bailey *et al.*, 2008; Oliveria *et al.*, 2008; Buckhurst *et al.*, 2013; Pucker *et al.*, 2013). Similarly, across the whole cohort, ciliary muscle cross-sectional area was strongly linked with axial length, in keeping with the previous finding. Moreover the R and r^2 values for the relationship between axial length and this ciliary muscle parameter were greater than for the axial length relationship with any other ciliary muscle parameter previously detailed in this thesis, highlighting the effectiveness of this parameter when relating ciliary muscle morphology with refractive error. Across the whole cohort, there was no significant difference between ciliary muscle cross-sectional area and the area where the posterior visible limit was selected 0.25 mm posteriorly to the originally selected, true posterior visible limit. Whilst there was a significant difference between cross-sectional area and the area where the posterior visible limit was selected 0.25 mm anterior to the original posterior visible limit, the magnitude of difference was just 2.15 %, hence, has limited impact on the overall results. It can therefore be confirmed that width measures proportional to the overall curved length of the muscle maintain their accuracy, when using an experienced examiner for analysis, due to the unlikelihood of an experienced examiner selecting the posterior visible

limit beyond 0.25 mm of this area. Similarly, inter-examiner repeatability was determined for ciliary muscle cross-sectional area, with no significant difference between analysis results by both examiners. As such, it is demonstrated that the ciliary muscle cross-sectional area parameter is a highly repeatable method for analysing the ciliary muscle and it combines both length, and width measurements proportional to the ciliary muscle overall length, as a singular overall measure.

The ciliary muscle apical angle was significantly wider in myopic eyes, compared with that of emmetropes. Similarly, across the whole cohort, the inner apical angle was significantly linked with axial length. These findings link with previous work indicating that the inner apical angle appears wider, and a longer anterior length of the myopic ciliary muscle suggests that the muscle grows in an anteroposterior direction with ocular elongation, whilst the scleral spur acts as a fixed anchor point (Sheppard and Davies, 2010). Furthermore, across the whole cohort, inner apical angle was related with ciliary muscle area, demonstrating a triad link between axial length, inner apical angle and area of the ciliary muscle. This finding has not been previously reported and signifies the importance of implementing these new parameters when analysing the ciliary muscle. Despite the robust nature of the ImageJ analysis utilising these parameters, which demonstrate high repeatability, future work is needed to implement these measures within a semi-objective analysis programme to reduce the subjectivity of the technique.

7.5 Conclusion

To conclude, this is the first investigation to utilise the cross-sectional area parameter to measure the ciliary muscle from AS-OCT imaging. Both ciliary muscle cross-sectional area and inner apical angle were linked to axial length, as were the area and apical angle; similarly, inner apical angle was significantly wider in myopic eye compared with emmetropes, as was ciliary muscle area significantly greater in myopes compared to emmetropes. There was no difference in ciliary muscle cross-sectional area when the PVL was selected 0.25 mm anterior or posterior to the original PVL, signifying the accuracy of measurements that are proportional to the overall length of the ciliary muscle when using an experienced examiner, compared with fixed arbitrary measures. Both inner apical angle and cross-sectional area measures are highly effective ciliary muscle analysis parameters, demonstrating high repeatability, and morphological assessment of the ciliary muscle should utilise such measures for future work in this area.

Chapter 8

Conclusions and potential future research

8.1 General conclusions

Despite previous *in vivo* research findings of longer and thicker ciliary muscle in myopes, the relevance of such findings was uncertain. There have been indications that altered ciliary muscle morphology in myopia is related to refractive error aetiology, with the thickened ciliary muscle resulting in a reduced contractile response and generating the hyperopic defocus that stimulates axial elongation (Bailey *et al.*, 2008). However, no previous investigation has linked ciliary muscle morphology with accommodative function and many questions regarding the ciliary muscle in refractive error remained. Therefore, the key experimental theme of this thesis has been analysis of ciliary muscle morphology in refractive error and accommodative function in young adult participants, both with and without refractive error, and with particular reference to symmetry of the ciliary muscle across both eyes.

Ciliary muscle morphology and ocular biometric correlates were studied in emmetropia (n = 69) where the eye had not undergone myopic expansion, and between sexes, for the first time on a large scale (chapter 3). Images of the ciliary muscle were acquired *in vivo* with the *Visante* AS-OCT (chapters 3 – 6), which is a non- contact technique and permits rapid, high-resolution image acquisition. Ocular biometry was measured by the *Lenstar* LS-900, which allows simultaneous measurement of axial length, anterior chamber depth, crystalline lens thickness and corneal thickness. Across the cohort, the temporal ciliary muscle was significantly longer and thicker than the nasal aspect, consistent with previous *in vivo* research and findings of an increased contractile response of the temporal aspect (Sheppard and Davies, 2010). Axial length and anterior chamber depth was linked with ciliary muscle length and thickness, in keeping with previous findings of a longer (Sheppard and Davies, 2010) and thicker (Oliveria *et al.*, 2005; Bailey *et al.*, 2008; Buckhurst *et al.*, 2013) ciliary muscle with increasing axial length. Axial length and ciliary muscle length was found to be significantly longer in males, compared to females. However, it was found that the ciliary muscle was thicker in females, in thickness measures proportional to the overall curved ciliary muscle length. Such an outcome is unexpected and warrants further investigation to understand the implications.

In chapter 4, it was shown that similar to emmetropes, the relationship between axial length, ciliary muscle length and thickness also occurred in myopes, indicating ciliary muscle growth

in line with normal ocular development. The myopic ciliary muscle was significantly longer and thicker for every ciliary muscle parameter measured, in agreement with findings of altered ciliary muscle morphology in axial myopia (Oliveira *et al.*, 2005; Bailey *et al.*, 2008; Schultz *et al.*, 2009; Sheppard and Davies, 2010; Buckhurst *et al.*, 2013). Symmetry of the ciliary muscle between both eyes of isometric participants was studied for the first time ($n = 100$), and both emmetropes and myopes were shown to present high levels of symmetry for every measured ciliary muscle parameter. It therefore seems likely that the altered ciliary muscle morphology is a passive result of myopia, not linked to the aetiology of refractive error.

Prior to investigating the link between ciliary muscle morphology, accommodative axial elongation and accommodative error in emmetropes and myopes (chapter 5), the possibility of diurnal changes of these accommodative functions were explored in chapter 2. Despite the large body of literature relating to accommodative lag owing to its association with myopia (Goss, 1991; Gwiazda *et al.*, 2005; Mutti *et al.*, 2006), and of transient accommodative axial elongation due to findings that myopic eyes may be more malleable to accommodative ciliary muscle forces (Mallen *et al.*, 2006), diurnal changes of this accommodative error and the transient accommodative expandability were investigated in emmetropic and myopic participants for the first time ($n = 28$). Axial length was shown to fluctuate significantly throughout the day, being longest around midday, and shortest at night, consistent with previous diurnal findings (Stone *et al.*, 2004; Read *et al.*, 2008; Chakraborty *et al.*, 2011). However, transient axial length changes with accommodation did not vary significantly throughout the day, and neither did accommodative error, for either refractive group. Investigations of and utilising these accommodative measures therefore, do not need to account for any diurnal variation during the investigation. It was also found that there was no significant difference between the refractive groups in either of these accommodative functions at any measured time point, and the same was found in chapter 5 ($n = 100$); there was no significant difference in the measured accommodative functions between emmetropes and myopes, and neither accommodative error or transient accommodative axial elongation was linked to ciliary muscle morphology. Hence, it is demonstrated for the first time, that accommodative error is not linked to the altered ciliary muscle morphology in myopia, and this altered morphology is unlikely to relate to the hyperopic defocus model of myopia development, but is a passive result of myopic ocular growth (Chapters 4 and 5).

High levels of symmetry were found between eyes of anisometropes and amblyopes ($n = 18$) (chapter 6), despite the axial length between both eyes being significantly different in both cohorts. Previous investigations have not studied the ciliary muscle in amblyopia, and in the non- amblyopic eye a relationship was found between axial length, ciliary muscle length and thickness, consistent with ciliary muscle growth in the isometric population (Chapters 3 and

4). However, there was no relationship between axial length, ciliary muscle length and ciliary muscle thickness in the amblyopic eye. As both length and thickness measures of the amblyopic ciliary muscle are linked with the axial length of the non- amblyopic eye, it therefore appears that the ciliary muscle in amblyopic eyes grow in accordance with ciliary muscle development in the non- amblyopic eye. Similarly, high levels of ciliary muscle symmetry were found between the eyes of anisometropes, suggesting that when an eye increases in axial length compared to its fellow eye, there is not accompanying ciliary muscle growth.

Novel parameters to analyse the ciliary muscle were investigated (n = 100; chapter 7), and was the first investigation to utilise the cross- sectional area parameter to measure the ciliary muscle from AS-OCT imaging. Both inner apical angle and ciliary muscle cross- sectional area were linked to axial length, as were the area and apical angle; similarly, inner apical angle was significantly wider in myopic eyes compared with emmetropes, as was ciliary muscle area significantly greater in myopes compared to emmetropes. The cross sectional area parameter showed the strongest relationship with axial length, compared with all other ciliary muscle parameters described in this thesis. Both novel measures are highly effective ciliary muscle analysis parameters which demonstrate high repeatability. Therefore, morphological assessment of the ciliary muscle should utilise such measures for future work in this area.

8.2. Evaluation of experimental work: suggestions for improvement and plans for future research

The ciliary muscle analysis and ocular biometric data detailed in chapter 5 allowed ciliary muscle morphology to be linked with accommodative function. The data confirmed that eyes of myopes have longer axial lengths and anterior chamber depths (Park *et al.*, 2010; Buckhurst *et al.*, 2013), consistent with the evidence that increased axial elongation and globe expansion occurs with myopia development (Atchison *et al.*, 2004; Mutti *et al.*, 2007; Mutti 2010; Gilmartin *et al.*, 2013). However, the *Lenstar LS 900* biometer (Haag-Streit AG, Koeniz, Switzerland) was unable to obtain crystalline lens thickness and anterior chamber depth values in all subjects. Such missing biometric data from the *Lenstar* was therefore replaced with predicted values based on age by Atchison and co-workers (2008), leading to a small difference in ocular biometric data acquisition amongst participants. The reason for the limited ability of the *Lenstar LS 900* biometer to obtain all crystalline lens thickness and anterior chamber depth measures from every participant is unclear and this issue may not be linked to all *Lenstar* biometers. An adaptation to ocular biometric data acquisition could be to acquire all ocular biometric data (axial length, lens thickness, anterior chamber depth and corneal

thickness) with the recent *IOLMaster 700*. Unlike the previous *IOLMaster (500)*, the newer model is now able to measure crystalline lens thickness (Akman *et al.*, 2015; Kurian *et al.*, 2016) and is shown to be highly repeatable and in agreement with the *Lenstar LS 900*. Obtaining all biometric measurements with the *IOLMaster 700* would allow the same technique to be utilised across the whole cohort, to strengthen the validity of the results.

The investigation of ciliary muscle morphology in amblyopia and anisometropia in chapter 6 was limited to a relatively small cohort of 10 amblyopic participants and 8 anisometropes (aged 18 – 29 years), due to the relatively low prevalence of the conditions. While the data provided novel information regarding symmetry between the eyes of these groups, further data collection amongst a larger cohort of these groups is planned by the author to determine if the trend shown in amblyopic eyes is replicated across both strabismic and anisometropic amblyopic sub- groups. Furthermore, within- eye comparisons could be made on a larger scale, to determine if the nasal versus temporal ciliary muscle asymmetry that occurs within the isometric population, is also present amongst amblyopes and anisometropes.

The validity of utilising the cross- sectional area and inner- apical angle parameters to analyse the ciliary muscle presented in chapter 7, was achieved through employment of ImageJ, free biomedical image analysis software. The data presented was shown to be repeatable, despite the high level of subjectivity of the measurement technique. The validated bespoke semi-objected ciliary muscle analysis programme developed at Aston University does not currently incorporate cross- sectional area and inner- apical angle measurements into its ciliary muscle analysis. The author therefore plans to integrate the parameters into the bespoke analysis programme, to develop a more objective method to measure the inner- apical angle and cross- sectional area of the ciliary muscle, and to determine the accuracy and repeatability of these parameters measured by the ciliary muscle analysis programme.

It was shown in chapters 2 and 5 that the transient accommodative axial elongation and accommodative error index did not significantly differ between the developed eyes of emmetropes and myopes aged 19 – 26 years. Previous research has shown that whilst accommodative lag is greater in young progressing myopic subjects than for emmetropes, the accommodation system appears to adapt and increase its response once myopia is stable, such that the differences in lags between myopic and emmetropic adults disappear (Abbott *et al.*, 1998; Nakatsuka *et al.*, 2003; Seidemann and Schaeffel, 2003; Harb *et al.*, 2006). It is plausible that this phenomenon also exists for the transient axial length increase with accommodation. However, it is currently not known whether accommodative axial elongation differences occur across refractive groups in children, where the eye is not fully developed and the transient axial elongation with accommodation has not been studied in the

developing eye. Hence, there is clear scope for further research into ocular elongation with accommodation in children, and to link the findings with the associated ciliary muscle morphology, which may be relevant to development of myopia.

8.3 Concluding statement

The investigations presented in this thesis are the first to study ciliary muscle morphology in both eyes of participants, across different refractive error groups and demonstrated high levels of symmetry between eyes of myopes, emmetropes, anisometropes and amblyopes. The findings provide further evidence of altered ciliary muscle morphology in myopia (Oliveira *et al.*, 2005; Bailey *et al.*, 2008; Sheppard and Davies, 2010, Buckhurst *et al.*, 2013), though dispute the role of the ciliary muscle in the hyperopic defocus model of myopia development as accommodative error was not related with ciliary muscle morphology in adults. Amid great interest in refractive error and ciliary muscle morphology (Oliveira *et al.*, 2005; Bailey *et al.*, 2008; Buckhurst *et al.*, 2013, Kuchem *et al.*, 2013), this thesis provides insight in to ciliary muscle morphology and accommodative function in refractive error, which will aid the development and direction of future research in ciliary muscle morphology and myopia development, with new beneficial parameters to analyse the ciliary muscle.

References

- Abbott, M. L., Schmid, K. L. & Strang, N. C. (1998). Differences in the accommodation stimulus-response curves of adult myopes and emmetropes. *Ophthalmic and Physiological Optics*, **18**, 13-20.
- Abou-Donia, A. H., Darwish, F. A., Toaima, S. M., Shawky, E. & Takla, S. S. (2014). A new approach to develop a standardized method for assessment of acetylcholinesterase inhibitory activity of different extracts using HPTLC and image analysis. *Journal of Chromatography B*, **955**, 50-57.
- Adams, D. W. & McBrien, N. A. (1992). Prevalence of myopia and myopic progression in a population of clinical microscopists. *Optometry and Vision Science*, **69**, 467-473.
- Aiello, A. L., Tran, V. T. & Rao, N. A. (1992). Postnatal development of the ciliary body and pars plana. *Archives of Ophthalmology*, **110**, 802-805.
- Akman, A., Asena, L. & Güngör, S. G. (2015). Evaluation and comparison of the new swept source OCT-based IOLMaster 700 with the IOLMaster 500. *British Journal of Ophthalmology*, **0**, 1-5.
- Alderson, A., Davies, L. N., Mallen, E. A. H. & Sheppard, A. L. (2012). A method for profiling biometric changes during disaccommodation. *American Academy of Optometry*, **89**, 738–748.
- Allen, M. P. & O’Leary, D. J. (2006). Accommodation functions: Co-dependency and relationship to refractive error. *Vision Research*, **46**, 491-505.
- Antodomingo-Rubido, J., Mallen, E. A., Gilmartin, B., Wolffsohn, J. S. & Ophthalmol, B. J. (2002). A new non-contact optical device for ocular biometry. *British Journal of Ophthalmology*, **86**, 458-462.
- Ardiomand, N., Hau, S., McAlister, J. C., Bunce, C., Galaretta, D. & Tuft, S. J. (2007). Quality of vision and graft thickness in deep anterior lamellar and penetrating corneal allografts. *American Journal of Ophthalmology*, **143**, 228-235.
- Asrani, S., Sarunic, M., Santiago, C. & Izatt, J. (2008). Detailed visualization of the anterior segment using Fourier-domain optical coherence tomography. *Archives of Ophthalmology*, **126**, 765-771.
- Astle, A. T., Webb, B. S. & McGraw, P. V. (2011). Can perceptual learning be used to treat amblyopia beyond the critical period of visual development? *Ophthalmic and Physiological Optics*, **31**, 564-573.
- Atchison, D. A. (1995). Accommodation and presbyopia. *Ophthalmic and Physiological Optics*, **15**, 255-272.
- Atchison, D. A. (2006). Optical models for human myopic eyes. *Vision Research*, **46**, 2236–2250.

- Atchison, D. A. (2009). Age-related paraxial schematic emmetropic eyes. *Ophthalmic and Physiological Optics*, **29**, 58-64.
- Atchison, D. A., Jones, C. E., Schmid, K. L., Pritchard, N., Pope, J. M., Strugnell, W. E. & Riley, R. A. (2004). Eye shape in emmetropia and myopia. *Investigative Ophthalmology and Visual Science*, **45**, 2152-2162.
- Atchison, D. A., Markwell, E. L., Kasthurirangan, S., Pope, J. M., Smith, G. & Swann, P. G. (2008). Age-related changes in optical and biometric characteristics of emmetropic eyes. *Journal of Vision*, **8**, 1-20.
- Atchison, D. A. & Smith, G. (2004). Possible errors in determining axial length changes during accommodation with the IOLMaster. *Optometry and Visual Science*, **81**, 282-285.
- Attebo, K., Mitchell, P., Cumming, R., Smith, W., Jolly, N. & Sparkes, R. (1998). Prevalence and causes of amblyopia in an adult population. *Ophthalmology*, **105**, 154-159.
- Augusteyn, R. C., Nankivil, D., Mohamed, A., Maceo, B., Pierre, F. & Parel, J. M. (2012). Human ocular biometry. *Experimental Eye Research*, **102**, 70-75.
- Baikoff, G. (2006). Anterior segment OCT and phakic intraocular lenses: a perspective. *Journal of Cataract and Refractive Surgery*, **32**, 1827-1835.
- Baikoff, G., Lutun, E., Ferraz, C. & Wei, J. (2004). Static and dynamic analysis of the anterior segment with optical coherence tomography. *Journal of Cataract and Refractive Surgery*, **30**, 1843-1850.
- Bailey, M. D. (2011). How should we measure the ciliary muscle? *Investigative Ophthalmology & Visual Science*, **52**, 1817-1818.
- Bailey, M. D., Sinnott, L. T. & Mutti, D. O. (2008). Ciliary body thickness and refractive error in children. *Investigative Ophthalmology and Visual Science*, **49**, 4353-4360.
- Bakri, S. J., Sears, J. E. & Lewis, H. (2007). Management of macular hole and submacular hemorrhage in the same eye. *Graefes Archives of Clinical and Experimental Ophthalmology*, **245**, 609-611.
- Ben Simon, G. J., Annunziata, C. C., Fink, J., Villablanca, P., McCann, J. D. & Goldberg, R. A. (2005). Establishing guidelines for interpreting orbital imaging studies and evaluating their predictive value in patients with orbital tumors. *Ophthalmology*, **112**, 2196-2207.
- Benjamin, W. J. (2006). Borish's Clinical Refraction, St. Louis, Butterworth Heinemann. Elsevier 99-105.

- Berntsen, D. A., Mutti, D. O. & Zadnik, K. (2010). The effect of bifocal add on accommodative lag in myopic children with high accommodative lag. *Investigative Ophthalmology and Visual Science*, **51**, 6104-6110.
- Berntsen, D. A., Sinnott, L. T., Mutti, D. O. & Zadnik, K. (2011). Accommodative lag and juvenile-onset myopia progression in children wearing refractive correction. *Vision Research*, **51**, 1039–1046.
- Bhola, R., Keech, R. V. & Kutschke, P. (2006). Recurrence of amblyopia after occlusion therapy. *Ophthalmology*, **113**, 2097–2100.
- Bozler, E. (1948). Conduction, automaticity and tonus of visceral muscle. *Experimentia*, **4**, 213-218.
- Bron, A. J., Tripathy, R. C. & Tripathy, B. J. (1997). Wolffe's anatomy of the eye and orbit 8th ed. London: Chapman & Hall Medical 535-587.
- Brown, J., Flitcroft, D. I. & Ying, G. (2009). In vivo human choroidal thickness measurements: evidence for diurnal fluctuations. *Investigative Ophthalmology and Visual Science*, **50**, 5-12.
- Brown, N. (1973b). Quantitative slit-image photography of the anterior chamber. *Transcripts of the American Ophthalmology Society UK*, **93**, 277-286.
- Brown, N. (1974). The change in lens curvature with age. *Experimental Eye Research*, **19**, 175-183.
- Brown, N. P. (1973). The change in shape and internal form of the lens of the eye on accommodation. *Experimental Eye Research*, **15**, 441-459.
- Brown, N. P. (1973a). The change in shape and internal form of the lens of the eye on accommodation. *Experimental Eye Research*, **15**, 441-459.
- Buckhurst, H., Gilmartin, B., Cubbidge, R. P., Nagra, M. & Logan, N. S. (2013). Ocular biometric correlates of ciliary muscle thickness in human myopia. *Ophthalmic and Physiological Optics*, **33**, 294-304.
- Buckhurst, P. J., Wolffsohn, J. S., Shah, S., Naroo, S. A., Davies, L. N. & Berrow, E. J. (2009). A new optical low coherence reflectometry device for ocular biometry in cataract patients. *British Journal of Ophthalmology*, **93**, 949–953.
- Buehren, T., Collins, M. J. & Loughridge, J. (2003). Corneal topography and accommodation. *Cornea*, **22**, 311-316.

- Bullimore, M. A. (2000). Will the auto-refractor ever replace the optometrist? *Ophthalmic and Physiological Optics*, **20**, S4-S5.
- Bullimore, M. A., Fusaro, R. E. & Adams, C. W. (1998). The repeatability of automated and clinician refraction. *Optometry and Vision Science*, **75**, 617-622.
- Campbell, F. W., Robson, J. G. & Westheimer, G. (1959). Fluctuations of accommodation under steady viewing condition. *Journal of Physiology* **145**, 579-594.
- Cashwell, L. F. & Martin, C. A. (1999). Axial length decrease accompanying successful glaucoma filtration surgery. *Ophthalmology* **106**, 2307-2311.
- Cass, K. & Tromans, C. (2008). A biometric investigation of ocular components in amblyopia. *Ophthalmic and Physiological Optics*, **28**, 429-440.
- Chakraborty, R., Read, S. A. & Collins, M. J. (2011). Diurnal variations in axial length, choroidal thickness, intraocular pressure, and ocular biometrics. *Investigative Ophthalmology and Visual Science*, **52**, 5121-5129.
- Charman, W. (2004). Aniso-accommodation as a possible factor in myopia development. *Ophthalmic and Physiological Optics*, **24**, 471-479.
- Charman, W. N. (2008). The eye in focus: accommodation and presbyopia. *Clinical and Experimental Optometry*, **91**, 207-225.
- Charman, W. N. & Heron, G. (1988). Fluctuations in accommodation: a review. *Ophthalmic and Physiological Optics*, **8**, 153-164.
- Chaudhry, I. A., Shamsi, F. A., Elzaridi, E., Arat, Y. O. & Riley, F. C. (2007). Congenital cystic eye with intracranial anomalies: a clinicopathologic study. *International Ophthalmology Clinics*, **27**, 223-233.
- Chauhan, K. & Charman, W. N. (1995). Single figure indices for the steady-state accommodative response. *Ophthalmic and Physiological Optics*, **15**, 217-221.
- Choma, M. A., Sarunic, C., Yang, C. & Izatt, J. (2003). Sensitivity advantage of swept source and Fourier domain optical coherence tomography. *Optics Express*, **11**, 2183-2189.
- Christopoulos, V., Kagemann, L. & Wollstein, G. (2007). In vivo corneal high-speed, ultra high-resolution optical coherence tomography. *Archives of Ophthalmology*, **125**, 1027-1035.
- Ciuffreda, K. J., Hokoda, S. C., Hung, G. K. & Semmlow, J. L. (1984). Accommodative stimulus/response function in human amblyopia. *Documenta Ophthalmologica*, **29**, 303-326.

- Ciuffreda, K. J., Levi, D. M. & Selenow, A. (1991). Amblyopia: basic and clinical aspects. *Butterworth-Heinemann: Stoneham*.
- Ciuffreda, K. J. & Rumpf, D. (1985). Contrast and accommodation in amblyopia. *Vision Research*, **25**, 1445-1457.
- Cleary, G., Spalton, D. J., Patel, P. M., Lin, P.-F. & Marshall, J. (2009). Diagnostic accuracy and variability of autorefractometry by the Tracey Visual Function Analyzer and the Shin-Nippon NVision-K 5001 in relation to subjective refraction. *Ophthalmic and Physiological Optics*, **29**, 173-181.
- Coleman, D. J. (1986). On the hydraulic suspension theory of accommodation. *Transcripts of the American Ophthalmology Society*, **84**, 846-868.
- Collins, M., Davis, B. & Wood, J. (1995). Microfluctuations of steady-state accommodation in the cardiopulmonary system. *Vision Research*, **35**, 2491-2502.
- Cosar, C. B. & Sener, A. B. (2003). Orbscan corneal topography system in evaluating the anterior structures of the human eye. *Cornea*, **22**, 118–121.
- Crawford, K. S., Kaufman, P. L. & Bito, L. Z. (1990). The role of the iris in accommodation of rhesus monkeys. *Investigative Ophthalmology and Visual Science*, **31**, 2185-2190.
- Cregg, M., Woodhouse, M., Stewart, R. E., Pakeman, V. H., Bromham, N. R., Gunter, H. L., Trojanowska, L., Parker, M. & Fraser, W. I. (2003). Development of refractive error and strabismus in children with Down syndrome. *Investigative Ophthalmology & Visual Science*, **44**, 1023–1030.
- Croft, M. A., Glasser, A. & Kaufman, P. L. (2001). Accommodation and presbyopia. *International Ophthalmology Clinics*, **41**, 33-46.
- Croft, M. A., Nork, T. M., McDonald, J. P., Katz, A., Lutjen-Drecoll, E. & Kaufman, P. L. (2013). Accommodative movements of the vitreous membrane, choroid, and sclera in young and presbyopic human and nonhuman primate eyes. *Investigative Ophthalmology and Visual Science*, **54**, 5049–5058.
- Cruysberg, L. P., Doors, M., Verbakel, F., Berendschot, T. T., De Brabander, J. & Nuijts, R. M. (2010). Evaluation of the *Lenstar LS 900* non-contact biometer. *British Journal of Ophthalmology*, **94**, 106–110.
- Davies, L. N., Dunne, M. C. M., Gibson, G. A. & Wolffsohn, J. S. (2010). Vergence analysis reveals the influence of axial distances on accommodation with age and axial ametropia. *Ophthalmic and Physiological Optics*, **30**, 371-378.

- Davies, L. N., Mallen, E. A., Wolffsohn, J. S. & Gilmartin, B. (2003). Clinical evaluation of the Shin-Nippon NVision-K 5001/Grand Seiko WR-5100 K autorefractor. *Optometry and Vision Science*, **80**, 320–324.
- Day, M., Strang, N. C., Seidel, D., Gray, L. S. & Mallen, E. A. (2006). Refractive group differences in accommodation microfluctuations with changing accommodation stimulus. *Ophthalmic and Physiological Optics*, **26**, 88-96.
- Debert, I., Malta de Alencar, L., Polati, M., Souza, M. B. & Alves, M. R. (2011). Oculometric parameters of hyperopia in children with esotropic amblyopia. *Ophthalmic and Physiological Optics*, **31**, 389-397.
- Dirckx, J. J., Kuypers, L. C. & Decraemer, W. F. (2005). Refractive index of tissue measured with confocal microscopy. *Journal of Biomedical Optics*, **10**, 440141–440148.
- Domínguez, P. R. (2014). Promoting our understanding of neural plasticity by exploring developmental plasticity in early and adult life. *Brain Research Bulletin*, **107**, 31-36.
- Drexler, W., Baumgartner, A., Findl, O., Hitzenberger, C. K. & Fercher, A. F. (1997). Biometric investigation of changes in the anterior eye segment during accommodation. *Vision Research*, **37**, 2789-2800.
- Drexler, W., Findl, O. & Schmetterer, L. (1998). Eye elongation during accommodation in humans: differences between emmetropes and myopes. *Investigative Ophthalmology and Vision Science*, **1998**, 2140-2147.
- Drexler, W. & Fujimoto, J. G. (2007). Optical coherence tomography in ophthalmology. *Journal of Biomedical Optics*, **12**, 041201.
- Drobe, B. & Saint-Andre, R. (1995). The pre-myopic syndrome. *Ophthalmic and Physiological Optics*, **15**, 375-378.
- Dubbelman, M., van der Heijde, G. L. & Weeber, H. A. (2001). The thickness of the aging human lens obtained from corrected Scheimpflug images. *Optometry and Vision Science*, **78**, 411–416.
- Dubbelman, M., van der Heijde, G. L. & Weeber, H. A. (2005). Change in shape of the aging human crystalline lens with accommodation. *Vision Research*, **45**, 117-132.
- Dubbleman, M., Van der Heijde, G. L., Weeber, H. A. & Vrensen, G. F. J. M. (2003). Changes in the internal structure of the human crystalline lens with age and accommodation. *Vision Research*, **43**.
- Duke-Elder, S. (1961). *The Anatomy Of The Visual System. System of Ophthalmology, Vol. 2.* London, Henry Kimpton 146-167.

Dunne, M. C. M., Davies, L. N. & Wolffsohn, J. S. (2007). Accuracy of cornea and lens biometry using anterior segment optical coherence tomography. *Journal of Biomedical Optics*, **12**, 1-5.

Eleftheriadis, H. (2003). IOLMaster biometry: refractive results of 100 consecutive cases. *British Journal of Ophthalmology*, **87**, 960-963.

Elliott, M., Simpson, T., Richter, D. & Fonn, D. (1997). Repeatability and accuracy of automated refraction: a comparison of the Nikon NRK-8000, the Nidek AR-1000, and subjective refraction. *Optometry and Vision Science*, **74**, 434-438.

Epitropoulos, A. (2014). Axial length measurement acquisition rates of two optical biometers in cataractous eyes. *Clinical Ophthalmology*, **8**, 1369–1376.

Farnsworth, P. N. & Burke, P. (1977). Three-dimensional architecture of the suspensory apparatus of the lens of the rhesus monkey. *Experimental Eye Research*, **25**, 563-577.

Farnsworth, P. N. & Shyne, S. E. (1979). Anterior zonular shifts with age. *Experimental Eye Research*, **28**, 291-297.

Federici, J. F., Guzelsu, N., Lim, H. C., Jannuzzi, G., Findley, T., Chaudhry, H. R. & Ritter, A. B. (1999). Noninvasive light-reflection technique for measuring soft-tissue stretch. *Applied Optics*, **38**, 6653–6660.

Fincham, E. F. (1937). The mechanism of accommodation. *British Journal of Ophthalmology Supplement*, **8**, 5-80.

Fisher, R. F. (1982). The vitreous and lens in accommodation. *Transcripts of the Ophthalmology Society of the United Kingdom*, **102**, 318-322.

Fisher, R. F. (1983). Is the vitreous necessary for accommodation in man? *British Journal of Ophthalmology*, **67**, 206.

Fisher, R. F. & Pettet, B. E. (1973). Presbyopia and the water content of the human crystalline lens. *Journal of Physiology (London)*, **234**, 443-447.

George, S. & Rosenfield, M. (2004). Blur adaptation and myopia. *Optometry and Vision Science*, **81**, 543-547.

Ghosh, A., Collins, M. J., Read, S. A., Davis, B. A. & Chatterjee, P. (2014). Axial elongation associated with biomechanical factors during near work. *Optometry and Vision Science*, **91**, 322–329.

- Gilmartin, B. (1995). The aetiology of presbyopia: a summary of the role of lenticular and extralenticular structures. *Ophthalmic and Physiological Optics.*, **15**, 431-437.
- Gilmartin, B. (2004). Myopia: precedents for research in the twenty-first century. *Clinical and Experimental Optometry*, **32**, 305-324.
- Gilmartin, B. & Hogan, R. E. (1985). The relationship between tonic accommodation and ciliary muscle intervention. *Investigative Ophthalmology and Visual Science*, **26**, 1024-1028.
- Gilmartin, B., Hogan, R. E. & Thompson, S. M. (1984). The effect of timolol maleate on tonic accommodation, tonic vergence, and pupil diameter. *Investigative Ophthalmology and Visual Science*, **25**, 763-770.
- Gilmartin, B., Nagra, M. & Logan, N. S. (2013). Shape of the posterior vitreous chamber in human emmetropia and myopia. *Investigative Ophthalmology and Visual Science*, **54**, 7240-7251.
- Glasser, A. (2008). Restoration of accommodation: surgical options for correction of presbyopia. *Clinical and Experimental Optometry.* , **91**, 279-295.
- Glasser, A., Croft, M. A., Brumback, L. & Kaufman, P. L. (2001). Ultrasound biomicroscopy of the aging rhesus monkey ciliary region
Optometry and Vision Science, **78**, 417-424.
- Goldsmith, J. A., Li, Y., Chalita, M. R., Westphal, V., Patil, C., Rollins, A., Izatt, J. & Huang, D. (2005). Anterior chamber width measurement by high speed optical coherence tomography. *Ophthalmology*, **113**, 238-244.
- Gora, M., Karnowski, K., Szkulmowski, M., Kaluzny, B. J., Huber, R., Kowalczyk, A. & Wojtkowski, M. (2009). Ultra high-speed swept source OCT imaging of the anterior segment of human eye at 200 kHz with adjustable imaging range *Optics Express*, **17**, 14880-14894.
- Goss, D. A. (1991). Clinical accommodation and heterophoria findings preceding juvenile onset of myopia. *Optometry and Vision Science*, **68**, 110-116.
- Graham, B. & Judge, S. J. (1999). The effects of spectacle wear in infancy on eye growth and refractive error in the marmoset (*Callithrix jacchus*). *Vision Research*, **39**, 189–206.
- Grossniklaus, H. E. & Green, W. R. (1992). Pathological findings in pathological myopia. *Retina*, **12**, 127-133.
- Gwiazda, J., Bauer, J., Thorn, F. & Held, R. (1995). A dynamic relationship between myopia and blur-driven accommodation in school-aged children. *Vision Research*, **35**, 1299–1304.

- Gwiazda, J., Grice, K. & Thorn, F. (1999). AC/A ratios are elevated in myopic children. *Ophthalmic and Physiological Optics*, **19**, 173-179.
- Gwiazda, J., Thorn, F., Bauer, J. & Held, R. (1993). Myopic children show insufficient accommodative response to blur. *Investigative Ophthalmology and Visual Science*, **34**, 690-694.
- Gwiazda, J., Thorn, F. & Held, R. (2005). Accommodation, accommodative convergence, and response AC/A ratios before and at the onset of myopia in children. *Optometry and Vision Science*, **82**, 273-278.
- Haegerstrom-Portnoy, G., Schneck, M. E., Hewlett, S. E. & Brabyn, J. A. (2014). Longitudinal increase in anisometropia in older adults. *Optometry and Vision Science*, **91**, 60-67.
- Harb, E., Thorn, F. & Troilo, D. (2006). Characteristics of accommodative behavior during sustained reading in emmetropes and myopes. *Vision Research*, **46**, 2581-2592.
- Hashemi, H., Khabazkhoob, M., Emamian, M. H., Mohammad, S., Abdolahi-nia, T. & Fotouhi, A. (2013). All biometric components are important in anisometropia, not just axial length. *British Journal of Ophthalmology*, **97**, 1586-1591.
- Hashemi, H., Khabazkhoob, M., Mirafteb, M., Emamian, M. H., Shariati, M., Abdolahinia, T. & Fotouhi, A. (2012). The distribution of axial length, anterior chamber depth, lens thickness, and vitreous chamber depth in an adult population of Shahroud, Iran. *BioMedCentral Ophthalmology*, **12**, 1-8.
- Heath, G. G. (1956). Components of accommodation. *American Journal of Optometry and Archives of American Academy of Optometry*, **33**, 569-579.
- Hemenger, R. P., Garner, L. F. & Ooi, C. S. (1995). Change with age of the refractive index gradient of the human ocular lens. *Investigative Ophthalmology and Visual Science*, **36**, 703-707.
- Hennessy, R. T. (1975). Instrument myopia. *Journal of Optical Society of America*, **65**, 114-1120.
- Hermans, E., Pouwels, P., Dubbelman, M., Kuijer, J., Van der Heijde, R. & Heethaar, R. (2009). Constant volume of the human lens and decrease in surface area of the capsular bag during accommodation: An MRI and Scheimpflug Study. *Investigative Ophthalmology & Visual Science*, **50**, 281-289.
- Hermans, E. A., Dubbelman, M., van der Heijde, R. & Heethaar, R. (2007). The shape of the human lens nucleus with accommodation. *Journal of Vision*, **7**, 1-10.

- Hill, W., Angeles, R. & Otani, T. (2008). Evaluation of a new IOLMaster algorithm to measure axial length. *Journal of Cataract and Refractive Surgery*, **36**, 920-924.
- Hitzenberger, C. K., Drexler, W. & Dolezal, C. (1993). Measurement of the axial length of cataract eyes by laser Doppler interferometry. *Investigative Ophthalmology & Visual Science*, **34**, 1886-1893.
- Ho, W. C., Wong, O. Y. & Chan, Y. C. (2012). Sign-dependent changes in retinal electrical activity with positive and negative defocus in the human eye. *Vision Research*, **52**, 47-53.
- Hornak, J. P. (2008). The Basics of MRI: an Online Book on magnetic resonance imaging. *Rochester Institute of Technology, Rochester, NY*. Available online at <http://www.cis.rit.edu/htbooks/mri>. Accessed March 1st 2014.
- Horwood, A. M. & Riddell, P. M. (2010). Independent and reciprocal accommodation in anisometropic amblyopia. *Journal of American Association for Pediatric Ophthalmology and Strabismus*, **14**, 447-449.
- Hosny, M., Alio, J. L., Claramonte, P., Attia, W. H. & Perez-Santonja, J. J. (2000). Relationship between anterior chamber depth, refractive state, corneal diameter, and axial length. *Journal of Refractive Surgery*, **16**, 336-340.
- Huang, D., Li, Y. & Radhakrishnan, S. (2004). Optical coherence tomography of the anterior segment of the eye. *Ophthalmology Clinics of North America*, **17**, 1-6.
- Huber, R., Wojtkowski, M. & Fujimoto, J. G. (2006). Fourier Domain Mode Locking (FDML): a new laser operating regime and applications for optical coherence tomography. *Optics Express*, **14**, 3225-3237.
- Irving, E. L., Sivak, J. G. & Callender, M. G. (1992). Refractive plasticity of the developing chick eye. *Ophthalmic and Physiological Optics*, **12**, 448-456.
- Izatt, J. A., Hee, M. R., Schuman, J. S. & Fujimoto, J. G. (1994). Micrometer-scale resolution imaging of the anterior eye in vivo with optical coherence tomography. *Archives of Ophthalmology*, **112**, 1584-1589.
- Jiang, B. C. (1995). Parameters of accommodation and vergence systems and the development of late-onset myopia. *Investigative Ophthalmology and Visual Science*, **36**, 1737-1742.
- Jiang, Z., Shen, M., Xie, R., Xue, A. & Lu, F. (2013). Interocular evaluation of axial length and retinal thickness in people with myopic anisometropia. *Eye & Contact Lens*, **39**, 277-282.

- Jin, J., Hua, W., Jiang, X., Wu, X., Yang, J., Gao, G., Fang, Y., Pei, C., Wang, S., Zhang, J., Tao, L. & Tao, F. (2015). Effect of outdoor activity on myopia onset and progression in school-aged children in northeast china: the sujiatun eye care study. *BMC Ophthalmology*, **15**, 1-11.
- Jones, C. E., Atchison, D. A., Meder, R. & Pope, J. M. (2005). Refractive index distribution and optical properties of the isolated human lens measured using magnetic resonance imaging. *Vision Research*, **45**, 2352-2366.
- Jones, C. E., Atchison, D. A. & Pope, J. M. (2007). Changes in lens dimensions and refractive index with age and accommodation. *Optometry and Vision Science*, **84**, 990-995.
- Jones, C. E. & Pope, J. M. (2004). Measuring optical properties of an eye lens using magnetic resonance imaging. *Magnetic Resonance Imaging*, **22**, 211–220.
- Kadlecova, V., Peleska, M. & Vasko, A. (1958). Dependence on age of the diameter of the pupil in the dark. *Nature*, **182**, 1520-1521.
- Kao, C. Y., Richdale, K., Sinnott, L. T., Grillott, L. E. & Bailey, M. D. (2011). Semiautomatic extraction algorithm for images of the ciliary muscle. *Optometry and Vision Science*, **88**, 275–289.
- Kasthurirangan, S. & A., G. (2005). Characteristics of pupil responses during far-to-near and near-to-far accommodation. . *Ophthalmic and Physiological Optics*, **25**, 328-329.
- Kasthurirangan, S., Markwell, E., Atchison, D. & Pope, J. (2011). MRI study of the changes in crystalline lens shape with accommodation and ageing in humans. *Journal of Vision*, **11**, 1-16.
- Kasthurirangan, S., Markwell, E. L., Atchison, D. A. & Pope, J. M. (2008). In vivo study of changes in refractive index distribution in the human crystalline lens with age and accommodation. *Investigative Ophthalmology and Visual Science*, **49**, 2531-2540.
- Kiernan, D. F., Mieler, W. F. & Hariprasad, S. M. (2010). Spectral-domain optical coherence tomography: a comparison of modern high resolution retinal imaging systems. *American Journal of Ophthalmology*, **149**, 18-31.
- Kinge, B., Milelfart, A. & Jacobsen, G. (1996). Clinical evaluation of the Allergan Humphrey 500 autorefractor and the Nidek AR-1000 autorefractor. *British Journal of Ophthalmology*, **80**, 35-39.
- Klein, B. E., Klein, R. & Moss, S. E. (1998). Correlates of lens thickness: The beaver dam eye study. *Investigative Ophthalmology & Visual Science*, **39**, 1507-1510.
- Kolk, A., Pantke, C., Wiener, E., Plodor, O. & Neff, A. (2005). A novel high-resolution magnetic resonance imaging microscopy coil as an alternative to multislice computed tomography in

postoperative imaging of orbital fractures and computer-based volume measurement. . *Journal of Oral and Maxillofacial Surgery*, **63**, 492-498.

Konstantopoulos, A., Hossain, P. & Anderson, D. F. (2007). Recent advances in ophthalmic anterior segment imaging: a new era for ophthalmic diagnosis? *British Journal of Ophthalmology*, **91**, 551-557.

Koretz, J. F. & Handelman, G. H. (1982). Model of the accommodative mechanism in the human eye. *Vision Research*, **22**, 917-927.

Koretz, J. F., Kaufman, P. L., Neider, M. W. & Goeckner, P. A. (1989). Accommodation and presbyopia in the human eye—aging of the anterior segment. *Vision Research*, **29**, 1685-1692.

Koretz, J. F., Strenk, S. A., Strenk, L. M. & Semmlow, J. L. (2004). Scheimpflug and high-resolution magnetic resonance imaging of the anterior segment: a comparative study. *Journal of the Optical Society of America*, **21**, 346-354.

Kotulak, J. C. & Schor, C. M. (1986). Temporal variations in accommodation during steady-state conditions. *Journal of the Optical Society of America*, **3**, 223-227.

Kotulak, J. C. & Schor, C. M. V. (1987). The effects of optical vergence, contrast, and luminance on the accommodative response to spatially bandpass filtered targets. *Vision Research*, **27**, 1797-1806.

Krumholz, D. M., Fox, R. S. & Ciuffreda, K. J. (1986). Short term changes in tonic accommodation. *Investigative Ophthalmology and Visual Science*, **27**, 552.

Kuchem, M. K., Sinnott, L. T., Kao, C. & Bailey, M. D. (2013). Ciliary muscle thickness in anisometropia. *Optometry and Vision Science*, **90**, 1312-1320.

Kugelberg, U., Zetterstrom, C. & Syren-Noordqvist, S. (1996). Ocular axial length in children with unilateral congenital cataract. *Acta Ophthalmologica Scandinavica*, **74**, 220–223.

Kurian, M., Negalur, N., Das, S., Puttaiah, N. K., Haria, D. J. & S., T. (2016). Biometry with a new swept-source optical coherence tomography biometer: Repeatability and agreement with an optical low-coherence reflectometry device. *Journal of Cataract and Refractive Surgery*, **42**, 577-581.

Kurtev, D. A., Sroimenova, B. D. & Georgiev, M. E. (1990). Diurnal variations in tonic accommodation. *Investigative Ophthalmology and Visual Science*, **31**, 2456-2458.

Lam, A. K., R., C. & Pang, P. C. (2001). The repeatability and accuracy of axial length and anterior chamber depth measurements from the IOLMaster. *Ophthalmic and Physiological Optics*, **21**, 477–83.

- Langaas, T., Riddell, P. M., Svarverud, E., Ystenaes, A. E., Langeeggen, I. & Bruenech, J. R. (2008). Variability of the accommodation response in early onset myopia. *Optometry and Vision Science*, **49**, 4353-4360.
- Langner, S., Martin, H., Terwee, T., Koopmans, S. A., Krüger, P. C., Hosten, N., Schmitz, K. P., Guthoff, R. F. & Stachs, O. (2010). 7.1T MRI to Assess the Anterior Segment of the Eye. *Investigative Ophthalmology and Visual Science*, **51**, 6575-6581.
- Laughton, D. S., Coldrick, B. J., Davies, L. N. & Sheppard, A. L. (2015). A program to analyse optical coherence tomography images of the ciliary muscle. *Contact Lens and Anterior Eye*, **36**, 402-408.
- Laughton, D. S., Sheppard, A. L. & Davies, L. N. (2016). A longitudinal study of accommodative changes in biometry during incipient presbyopia. *Ophthalmic and Physiological Optics*, **36**, 33-42.
- Lempert, P. & Porter, L. (1998). Dysversion of the optic disc and axial length measurements in a presumed amblyopic population *Journal of American Association for Pediatric Ophthalmology and Strabismus*, **2**, 207-213.
- Lewis, H. A., Kao, C. Y., Sinnott, L. T. & Bailey, M. D. (2012). Changes in ciliary muscle thickness during accommodation in children. *Optometry and Vision Science*, **89**, 727-737.
- Li, P., Hu, Y., Xu, Q., Zhang, G. & Mai, C. (2006a). Central corneal thickness in adult Chinese *Journal of Huazhong University of Science and Technology. Medical Science*, **26**, 141-144.
- Li, Y., Shekhar, R. & Huang, D. (2006b). Corneal pachymetry mapping with high-speed optical coherence tomography. *Ophthalmology*, **113**, 792-799.
- Liao, C. C., Chen, L. J., Yu, J. H. & Lin, J. C. (2014). Refractive error change and its association with ocular and general parameters in junior high school students in Taiwan. *Japanese Journal of Ophthalmology*, **58**, 375-80.
- Lim, L. S., Cheung, G. & Lee, S. Y. (2014). Comparison of spectral domain and swept-source optical coherence tomography in pathological myopia. *Eye*, **28**, 488-491.
- Lim, R., Mitchell, P. & Cumming, R., G. (1999). Refractive association with cataract: the Blue Mountain Study. *Ophthalmology and Visual Science*, **40**.
- Lin, L. L., Shih, Y. F. & Lee, Y. C. (1996). Changes in ocular refraction and its components among medical students- a 5-year longitudinal study. *Optometry and Vision Science*, **73**.
- Liney, G. P. (2005). Magnetic Resonance Imaging Physics Lectures. Available online at

http://www.hull.ac.uk/mri/lectures/gpl_page.html Accessed March 1st 2014.

- Logan, N. S., Gilmartin, B., Wildsoet, C. F. & Dunne, M. C. (2004). Posterior retinal contour in adult human anisometropia *Investigative Ophthalmology and Visual Science*, **45**, 2152-2162.
- Logan, N. S., Shah, P., Rudnicka, A. R., Gilmartin, B. & Owen, C. G. (2011). Childhood ethnic differences in ametropia and ocular biometry: the Aston Eye Study. *Ophthalmic and Physiological Optics*, **31**, 550-558.
- Lossing, L. A., Sinnott, L. T., Kao, C., Richdale, K. & Bailey, M. D. (2012). Measuring changes in ciliary muscle thickness with accommodation in young adults. *Optometry and Vision Science*, **89**, 719–726.
- Lutjen-Drecoll, E., Kaufman, P. L., Wasilewski, R., Ting-Li, L. & Croft, M. A. (2010). Morphology and accommodative function of the vitreous zonule in human and monkey eyes. *Investigative Ophthalmology and Visual Science*, **51**, 1554-1564.
- Lutjen, E. (1966). Histometric studies on the ciliary muscle in primates. *Graefes Archiv für klinische und experimentelle Ophthalmologie*, **171**, 121-133.
- Mafee, M. F., Valvassori, G. E. & Becker, M. (2005). Valvassori's Imaging of the Head and Neck. *Second edition. Thieme, New York*, 140-143.
- Maheshwari, R., Sukul, R. R., Gupta, Y., M., G., Phougat, A., Dey, M., Jain, R., Srivastava, G., Bhardwaj, U. & S., D. (2011). Accommodation: its relation to refractive errors, amblyopia and biometric parameters. *Nepal Journal of Ophthalmology*, **3**.
- Mallen, E. A., Kashyap, P. & Hampson, K. M. (2006). Transient axial length change during the accommodation response in young adults. *Investigative Ophthalmology and Vision Science*, **47**, 1251-1254.
- Mallen, E. A. H., Wolffsohn, J. S. W., Gilmartin, B. & Tsujimura, S. (2001). Clinical evaluation of the Shin-Nippon SRW-5000 autorefractor in adults. *Ophthalmic and Physiological Optics*, **21**, 101-107.
- Marg, E. & Morgan, M. W. J. (1949). The pupillary near reflex; the relation of pupillary diameter to accommodation and the various components of convergence *American Academy of Ophthalmology*, **26**, 183-198.
- Marg, E. & Morgan, M. W. J. (1950). Further investigation of the pupillary near reflex; the effect of accommodation, fusional convergence and the proximity factor on pupillary diameter. *American Journal of Optometry and Archives of American Academy of Optometry*, **27**, 215-217.

- McBrien, N. A. & Adams, D. W. (1997). A longitudinal investigation of adult-onset and adult-progression of myopia in an occupational group: refractive and biometric findings. *Investigative Ophthalmology and Vision Science*, **38**, 321-333.
- McBrien, N. A., Jobling, A. L. & Gentle, A. (2009). Biomechanics of the sclera in myopia: extracellular and cellular factors. *Optometry and Vision Science*, **86**, E23-30.
- McFadden, S. A., Howlett, M. H. C. & Mertz, J. R. (2004). Retinoic acid signals the direction of ocular elongation in the guinea pig eye. *Vision Research*, **44**, 643-653.
- McFadden, S. A., Howlett, M. H. C. & J.R., M. (2004). Retinoic acid signals the direction of ocular elongation in the guinea pig eye. *Vision Research*, **44**, 643-653.
- Miege, C. & Denieul, P. (1988). Mean response and oscillation of accommodation for various stimulus vergences in relation to accommodation feedback control. *Ophthalmic and Physiological Optics*, **8**, 165-171.
- Miki, A., Ikuno, Y., Asai, T., Usui, S. & Nishida, K. (2015). Defects of the lamina cribrosa in high myopia and glaucoma. *Plos one*, **10**, 1-12.
- Mitchell, P., Hourihan, F., Sandbach, J. & Wang, J. J. (1999). The relationship between between glaucoma and myopia; the Blue Mountain Eye Study. *Ophthalmic and Physiological Optics*, **106**, 2010-2015.
- Moffat, B. A., Atchison, D. A. & Pope, J. M. (2002a). Age-related changes in refractive index distribution and power of the human lens as measured by magnetic resonance micro imaging *in vitro*. *Vision Research*, **42**, 1683-1693.
- Moffat, B. A., Atchison, D. A. & Pope, J. M. (2002b). Explanation of the lens paradox. *Optometry and Vision Science*, **79**, 148-150.
- Mon-Williams, M., Tresilian, J., Strang, N., Kochhar, P. & Wann, J. (1998). Improving vision: neural compensation for optical defocus. *Proceedings of the Royal Society Biological Sciences*, **265**, 271-277.
- Mora, F., Segovia, G. & del Arco, A. (2007). Aging, plasticity and environmental enrichment: structural changes and neurotransmitter dynamics in several areas of the brain. *Brain Research Reviews*, **55**, 78-88.
- Mori, T., Sugano, Y., Maruku, I. & Sekiryu, T. (2015). Subfoveal choroidal thickness and axial length in preschool children with hyperopic anisometropic amblyopia. *Current Eye Research*, **40**, 954-961.

Moriyama, M., Ohno-Matsui, K., Hayashi, K., Shimada, N., Yoshida, T., Tokoro, T. & I., M. (2011). Topographic analyses of shape of eyes with pathologic myopia by high-resolution three-dimensional magnetic resonance imaging. *Ophthalmology*, **118**, 1626-1637.

Moriyama, M., Ohno-Matsui, K., Modegi, T., Kondo, J., Takahashi, Y., Tomita, M., Tokoro, T. & I., M. (2012). Quantitative analyses of high-resolution 3D MR Images of highly myopic eyes to determine their shapes. . *Investigative Ophthalmology & Visual Science*, **2012**, 4510-4518.

Muftuoglu, O., Hosal, B. M. & Zilefioglu, G. (2009). Ciliary body thickness in unilateral high axial myopia. *Eye*, **23**, 1176-1181.

Murphy, M. R., Randle, R. J. & Williams, B. A. (1977). Diurnal rhythms of visual accommodation and blink responses: Implication for flightdeck visual standards. *Aviation, Space and Environmental Medicine*, **48**, 524.

Mutti , D. O. (2010). Hereditary and environmental contributions to emmetropization and myopia. *Optometry and Visual Science*, **87**, 255-259.

Mutti, D. O., Hayes, J. R., Mitchell, G. L., Jones, L. A., Moeschberger, M. L., Cotter, S. A., Kleinstein, R. N., Manny, R. E., Twelker, J. D. & Zadnik, K. (2007). Refractive error, axial length, and relative peripheral refractive error before and after the onset of myopia. *Investigative Ophthalmology and Visual Science*, **48**, 2510–2519.

Mutti , D. O., Jones, L., Moeschberger, M. L. & Zadnik, K. (2000). AC/A ratio, age, and refractive error in children. *Investigative Ophthalmology and Visual Science*, **41**, 2469–2478.

Mutti, D. O., Mitchell, G. L., Hayes, J. R., Jones, L. A., Moeschberger, M. L., Cotter, S. A., Kleinstein, R. N., Manny, R. E., Twelker, D. J., Zadnik, K. & Group, C. S. (2006). Accommodative lag before and after the onset of myopia. *Investigative Ophthalmology & Visual Science*, **47**, 837-846.

Mutti, D. O., Zadnik, K., Fusaro, R. E., Friedman, N. E., Sholtz, R. I. & Adams, A. J. (1998). Optical and structural development of the crystalline lens in childhood. *Invest Ophthalmol Vis Sci*, **39**, 120-133.

Nakatsuka, C., Hasebe, S., Nonaka, F. & Ohtsuki, H. (2003). Accommodative lag under habitual seeing conditions: comparason between myopic and emmetropic children. *Japanese Journal of Ophthalmology*, **49**, 189-194.

Nakatsuka, C., Hasebe, S., Nonaka, F. & Ohtsuki, H. (2005). Accommodative lag under habitual seeing conditions: comparason between myopic and emmetropic children. *Japanese Journal of Ophthalmology*, **49**, 189-194.

Nemati, B., Dunn, A., Welch, A. J. & Rylander, H. G. (1998). Optical model for light distribution during transscleral cyclophotocoagulation. *Applied Optics*, 764-761.

- Nemati, B., Rylander, H. G. & Welch, A. (1997). Optical properties of conjunctiva, sclera, and the ciliary body and their consequences for transscleral cyclophotocoagulation: erratum. *Applied Optics*, **36**, 416.
- Ni, Y., Liu, X., Lin, Y., Guo, X., Wang, X. & Liu, Y. (2013). Evaluation of corneal changes with accommodation in young and presbyopic populations using pentacam high resolution scheimpflug system. *Clinical and Experimental Ophthalmology*, **41**, 244-250.
- Niesel, P. (1982). Visible changes of the lens with age. *Transactions of the Ophthalmological Societies of the United Kingdom*, **102**, 327–330.
- Nikla, D. L. (2006). The phase relationships between the diurnal rhythms in axial length and choroidal thickness as the association with ocular growth rate in chick eyes. *Journal of Comparative Physiology*, **192**, 399-407.
- Nikla, D. L., Wildsoet, C. & Trollo, D. (2002). Diurnal rhythms in intraocular pressure, axial length, and choroidal thickness in a primate model of eye growth, the common marmoset. *Investigative Ophthalmology and Visual Science*, **43**, 2519–2528.
- Nikla, D. L., Wildsoet, C. & Wallman, J. (1998). Visual influences on diurnal rhythms in ocular length and choroidal thickness in chick eyes. *Experimental Eye Research*, **66**, 163-181.
- Nishida, S. & Mizutani, S. (1992). Quantitative and morphometric studies of age-related changes in human ciliary muscle. *Japanese Journal of Ophthalmology*, **36**, 380-387.
- Niwa, K. & Tokoro, T. (1998). Influence of spatial distribution with blur on fluctuations in accommodation. *Optometry and Vision Science*, **75**, 227-232.
- Nolan, W. P. (2008). Anterior segment imaging: ultrasound biomicroscopy and anterior segment optical coherence tomography. *Current Opinion in Ophthalmology*, **19**, 115-121.
- Nolan, W. P., See, J. L., Chew, P. T. K., Friedman, D. S., Smith, S. D. & Radhakrishnan, S. O. (2007). Detection of primary angle closure glaucoma using anterior segment optical coherence tomography in Asian eyes. *Ophthalmology*, **114**, 33-39.
- Nomura, H., Ando, F., Niino, N., Shimokata, H. & Miyake, Y. (2002). The relationship between age and intraocular pressure in a Japanese population: The influence of central corneal thickness. *Current Eye Research*, **34**, 81-85.
- Norton, T. T., Manny, R. & O'Leary, D. J. (2005). Myopia-global problem, global research. *Optometry and Visual Science*, **82**, 223–225.

- O'Donoghue, L., Kapetanankis, V. V., McClelland, J. F., Logan, N. S., Owen, C. G., Saunders, K. J. & Rudnicka, A. R. (2015). Risk factors for childhood myopia: findings from the NICER study. *Investigative Ophthalmology & Visual Science*, **56**, 1524-1530.
- O'Donoghue, L., McClelland, J. F., Logan, N. S., Rudnicka, A. R., Owen, C. G. & Saunders, K. J. (2013). Profile of anisometropia and aniso-astigmatism in children: prevalence and association with age, ocular biometric measures, and refractive status. *Investigative Ophthalmology & Visual Science*, **54**, 602-608.
- Ohno-Matsui, K., Akiba, M., Modegi, T., Tornita, M., Ishibashi, T., Tokoro, T. & Moriyama, M. (2012). Association between shape of sclera and myopic retinochoroidal lesions in patients with pathologic myopia. *Investigative Ophthalmology & Visual Science*, **53**, 6046-6061.
- Oliveira, C., Tello, C., Liebmann, J. M. & Ritch, R. (2005a). Ciliary body thickness increases with increasing axial myopia. *American Journal of Ophthalmology*, **140**, 324-325.
- Oliveira, C., Tello, C., Liebmann, J. M. & Ritch, R. (2005b). Ciliary body thickness increases with increasing axial myopia. *Am J Ophthalmol.*, **140**, 324-325.
- Orr, J. B., Seidel, Dirk, Day, Mhairi, Gray & Lyle, S. (2015). Is pupil diameter influenced by refractive error? *Investigative Ophthalmology & Visual Science*, **92**, 834-840.
- Ostrin, L. A., Yuzuriha, J. & Wildsoet, C. F. (2015). Refractive error and ocular parameters: comparison of two SD-OCT systems. *Optometry and Vision Science*, **92**, 437-446.
- Owsley, C., McGwin, G., Scilley, K., Meek, G. C., Seker, D. & Dyer, A. (2007). Effect of refractive error correction on health-related quality of life and depression in older nursing home residents. *Archives of Ophthalmology*, **125**, 1471-1477.
- Papastergiou, G., Schmid, G., Riva, C., Mendel, M., RA., S. & Laties, A. (1998). Ocular axial length and choroidal thickness in newly hatched chicks and one-year-old chickens fluctuate in a diurnal pattern that is influenced by visual experience and intraocular pressure changes. *Experimental Eye Research*, **66**, 195-205.
- Pardue, M. T. & Sivak, J. G. (2000). Age-related changes in human ciliary muscle. *Optometry and Vision Science*, **77**, 204-210.
- Park, S. H., Park, K. H., Kim, J. M. & Choi, C. Y. (2010). Relation between axial length and ocular parameters. *Ophthalmologica*, **188**, 188-193.
- Patnaik, B. (1967). A photographic study of accommodative mechanisms: changes in lens nucleus during accommodation. *Investigative Ophthalmology*, **6**, 601-611.

- Pavlin, C. J., Harasiewicz, K. & Foster, F. S. (1992). Ultrasound biomicroscopy of anterior segment structures in normal and glaucomatous eyes. *American Journal of Ophthalmology*, **113**, 381-389.
- Pesudovs, K. & Brennan, N. (1993). Decreased uncorrected vision after a period of distance fixation with spectacle wear. *Optometry and Vision Science*, **70**, 528-531.
- Phillips, J. R. & McBrien, N. A. (2004). Pressure-induced changes in axial eye length of chick and tree shrew: significance of microfibroblasts in the sclera. *Investigative Ophthalmology and Visual Science*, **45**, 758-763.
- Pieroni, C. G., Witkin, A. J. & Ko, T. H. (2006). Ultrahigh resolution optical coherence tomography in non-exudative age related macular degeneration. *British Journal of Ophthalmology*, **26**, 14-20.
- Pierscionek, B. K. & Weale, R. A. (1995). Presbyopia- a maverick of human aging. *Archives of Gerontology and Geriatrics*, **20**, 229-240.
- Polito, A., Del Borello, M., Polini, G., Furlan, F., Isola, M. & Bandello, F. (2006). Diurnal variation in clinically significant diabetic macular edema measured by the stratus OCT. *Retina*, **26**, 14-20.
- Polling, J. R., Loudon, S. E. & Klaver, C. C. (2012). Prevalence of amblyopia and refractive errors in an unscreened population of children. *Optometry and Vision Science*, **89**, 44-49.
- Poyer, J. F., Kaufman, P. L. & C., F. (1993). Age does not affect contractile responses of the isolated rhesus monkey ciliary muscle to muscarinic agonists. *Current Eye Research*, **12**, 413-422.
- Provine, R. R. & Enoch, J. M. (1975). On voluntary ocular accommodation. *Perception and Psychophysics*, **17**, 209-212.
- Pucker, A. D., Sinnott, L. T., Kao, C. Y. & Bailey, M. D. (2013). Region-specific relationships between refractive error and ciliary muscle thickness in children. *Investigative Ophthalmology and Visual Science*, **54**, 4710-4716.
- Radhakrishnan, H., Goldsmith, J. & Westphal, V. (2005). Comparison of optical coherence tomography and ultrasound biomicroscopy for detection of narrow anterior chamber angles. *Archives of Ophthalmology*, **123**, 1053-1059.
- Ramos, J. L. B., Li, Y. & Huang, D. (2009). Clinical and research applications of anterior segment optical coherence tomography – a review. *Clinical and Experimental Ophthalmology*, **37**, 81-89.
- Read, S. A., Buehren, T. & Collins, M. J. (2007). Influence of accommodation on the anterior and posterior cornea. *Journal of Cataract and Refractive Surgery*, **33**, 1877–1885.

- Read, S. A., Collins, M. J. & Iskander, D. R. (2008). Diurnal variation of axial length, intraocular pressure, and anterior eye biometrics. *Investigative Ophthalmology and Visual Science*, **49**, 2911-2918.
- Read, S. A., Collins, M. J., Woodman, E. C. & Cheong, S. (2010). Axial length changes during accommodation in myopes and emmetropes. *Optometry and Vision Science*, **87**, 656-662.
- Reilly, M. & Ravi, N. (2010). A geometric model of ocular accommodation. *Vision Research*, **50**, 330-333.
- Remington, L. A. (2005). *Clinical Anatomy of the Visual System*. Elsevier Butterworth Heinemann. 87-101.
- Richdale, K., Wassenaar, P., Bluestein, K. T. A. A., Christoforidis, J. A., Lanz, T., Knopp, M. V. & Schmalbrock, P. (2009). 7 Tesla MR imaging of the human eye in vivo. *Journal of Magnetic Resonance Imaging*, **30**, 924-932.
- Rodrigues, E. B., Johanson, M. & Penha, F. M. (2012). Anterior segment tomography with the cirrus optical coherence tomography. *Journal of Ophthalmology*, **2012**, 1-5.
- Rohrer, K., Frueh, B. E., Wälti, R., Clemetson, I. A., Tappeiner, C. & Goldblum, D. (2009). Comparison and evaluation of ocular biometry using a new noncontact optical low-coherence reflectometer. *American Academy of Ophthalmology* **10**, 2087-2092.
- Rose, K., Smith, W., Morgan, I. & Mitchell, P. (2001). The increasing prevalence of myopia: implications for myopia. *Clinical and Experimental Optometry*, **29**, 1111-1119.
- Rosenfield, M. & Ciuffreda, K. J. (1991). Effect of surround propinquity on the open-loop accommodative response. *Investigative Ophthalmology and Visual Science*, **32**, 142-147.
- Rosenfield, M., Ciuffreda, K. J., Hung, G. K. & Gilmartin, B. (1993). Tonic accommodation: a review I. Basic aspects. *Ophthalmic and Physiological Optics*, **13**, 266-284.
- Sa, H. S., Kyung, S. E. & Ob, S. Y. (2005). Extraocular muscle imaging in complex strabismus. *Ophthalmic Surgery, Lasers and Imaging*, **36**, 487-493.
- Sakabe, I., Oshika, T., Lim, S. J. & Apple, D. J. (1998). Anterior shift of zonular insertion into the anterior surface of human crystalline lens with age. *Ophthalmology*, **105**, 295-299.
- Santodomingo-Rubido, J., Mallen, E. A. H., Gilmartin, B. & Wolffsohn, J. S. (2002). A new non-contact optical device for ocular biometry. *British Journal of Ophthalmology*, **86**, 458-462.

- Saw, S. M. (2003). A synopsis of the prevalence rates and environmental risk factors for myopia. *Clinical and Experimental Optometry*, **86**, 289-294.
- Schachar, R. A. & Koivula, A. (2008). The stress on the anterior lens surface during human In vivo accommodation. *British Journal of Ophthalmology*, **92**, 348-350.
- Schaeffel, F., Glasser, A. & Howland, H. C. (1988). Accommodation, refractive error, and eye growth in chickens. *Vision Research*, **28**, 639-657.
- Schaeffel, F., Wilhelm, H. & Zrenner, E. (1993). Inter-individual variability in the dynamics of natural accommodation in humans: relation to age and refractive errors. *Journal of Physiology (London)*, **461**, 301-320.
- Schindelin, J., Rueden, C. T., Hiner, M. C. & Eliceiri, K. W. (2015). The ImageJ ecosystem: An open platform for biomedical image analysis. *Molecular Reproduction and Development*, **82**, 518-529.
- Schmid, K. L., Li, Y., Edwards, M. H. & Lew, J. K. (2003). The expandability of the eye in childhood myopia. *Current Eye Research*, **26**, 65-71.
- Schor, C. M., Kotulak, J. C. & Tsuetaki, T. (1986). Adaptation of tonic accommodation reduces accommodative lag and is masked in darkness. *Investigative Ophthalmology & Visual Science*, **27**, 820-827.
- Schultz, K. E., Sinnott, L. T., Mutti, D. O. & Bailey, M. D. (2009). Accommodative fluctuations, lens tension, and ciliary body thickness in children. *Optometry and Vision Science*, **86**, 677-684.
- Seet, B., Wong, T. Y. & Tan, D. T. (2001). Myopia in Singapore: taking a public health approach. *British Journal of Ophthalmology*, **85**, 521-526.
- Seidel, C. L. & Weisbrodt, N. W. (1987). Hypertrophic response in smooth muscle. *Boca Raton, FL: CRC Press*, 199.
- Seidel, D., Gray, L. S. & Heron, G. (2003). Retinotopic accommodation responses in myopia. *Investigative Ophthalmology and Visual Science*, **44**, 1035-1035.
- Seidel, D., Gray, L. S. & Heron, G. (2005). The effect of monocular and binocular viewing on the accommodation response to real targets in emmetropia and myopia. *Optometry and Vision Science*, **82**, 37-48.
- Seidemann, A. & Schaeffel, F. (2003). An evaluation of the lag of accommodation using photorefractometry. *Vision Research*, **43**, 419-430.

- Shammas, H. J. & Shammas, M. C. (2015). Measuring the cataractous lens. *Journal of Cataract and Refractive Surgery*, **41**, 1875–1879.
- Sheppard, A., Evans, C., Singh, K., Wolffsohn, J., Dunne, M. & Davies, L. (2011b). Three-dimensional magnetic resonance imaging of the phakic crystalline lens during accommodation. *Vision and Ophthalmology*, **52**, 3689-3697.
- Sheppard, A. L. & Davies, L. N. (2010a). Clinical evaluation of the Grand Seiko Auto Ref/Keratometer WAM-5500. *Ophthalmic and Physiological Optics*, **30**, 143-151.
- Sheppard, A. L. & Davies, L. N. (2010b). In vivo analysis of ciliary muscle morphologic changes with accommodation and axial ametropia. *Investigative Ophthalmology and Visual Science*, **51**, 6882-6888.
- Sheppard, A. L. & Davies, L. N. (2011). The effect of ageing on in vivo human ciliary muscle morphology and contractility. *Investigative Ophthalmology and Visual Science*, **52**, 1809-1816.
- Shufelt, C., Fraser-Bell, S., Ying-Lai, M., Torres, M. & Varma, R. (2005). Refractive error, ocular biometry, and lens opalescence in an adult population: The Los Angeles Latino Eye Study *Investigative Ophthalmology & Visual Science*, **46**, 4450–4460.
- Simons, K. (2005). Amblyopia characterization, treatment, and prophylaxis. *Surveys in Ophthalmology*, **50**, 123–166.
- Singh, K. D., Logan, N. S. & Gilmartin, B. (2006). Three-dimensional modeling of the human eye based on magnetic resonance imaging. *Investigative Ophthalmology and Visual Science*, **47**, 2272-2279.
- Smith, E. L. & Hung, L. F. (1999). The role of optical defocus in regulating refractive development in infant monkeys. *Vision Research*, **39**, 1415–1435.
- Smith, E. L., Kee, C. S., Ramamirtham, R., Qiao-Grider, Y. & Hung, L. F. (2005). Peripheral vision can influence eye growth and refractive development in infant monkeys. *Investigative Ophthalmology and Visual Science*, **46**, 3956-3972.
- Smith, G. J. M. O. (1983). The accommodative resting states, instrument accommodation and their measurement. *Journal of Modern Optics*, **30**, 347–359.
- Snell, R. S. & Lemp, M. A. (1998). *Clinical Anatomy of the Eye*. Second edition. Blackwell Science (Malden, M. A.) 3-15 and 197-205.
- Solebo, A. L., Cumberland, P. M. & Rahi, J. S. (2015). Whole-population vision screening in children aged 4–5 years to detect amblyopia. *The Lancet*, **385**, 2308-2309.

Sonia, A., Rose, K. A., Gole, G. A., Philip, K., Leone, J. F., French, A. & Mitchell, P. (2013). Prevalence of anisometropia and its association with refractive error and amblyopia in preschool children. *British Journal of Ophthalmology*, **97**, 1095-1099.

Sreenivasan, V., Irving, E. L. & Bobier, W. R. (2011). Effect of near adds on the variability of accommodative response in myopic children. *Ophthalmic and Physiological Optics*, **31**, 145–154.

Srivannaboon, S., Chirapapaisan, C., Chopimai, P. & Loket, S. (2015). Clinical comparison of a new swept-source optical coherence tomography–based optical biometer and a time-domain optical coherence tomography–based optical biometer. *Journal of Cataract and Refractive Surgery*.

Stachs, O., Martin, H., Kirchhoff, A., Stave, J., Terwee, T. & Guthoff, R. (2002). Monitoring accommodative ciliary muscle function using three-dimensional ultrasound. *Graefes Archives of Clinical Experimental Ophthalmology*, **240**, 906-912.

Stark, L. R. & Atchison, D. A. (1997). Pupil size, mean accommodation response and the fluctuations accommodation. *Ophthalmic and Physiological Optics*, **17**, 316-323.

Stone, R. A. & Flitcroft, D. I. (2004). Ocular shape and myopia. *Annals of the Academy of Medicine, Singapore*, **45**, 3380-3386.

Stone, R. A., Quinn, G. E., Francis, E. L., Ying, G. S., Flitcroft, D. I., Parekh, P., Brown, J., Orlow, J. & Schmid, G. (2004). Diurnal axial length fluctuations in human eyes. *Investigative Ophthalmology and Visual Science*, **45**.

Strenk, S. A., Semmlow, J. L., Strenk, L. M., Munoz, P., Gronlund-Jacob, J. & De Marco, J. K. (1999). Age-related changes in human ciliary muscle and lens: a magnetic resonance imaging study. *Investigative Ophthalmology and Visual Science*, **40**, 1162-1169.

Strenk, S. A., Strenk, L. M. & Guo, S. (2010). Magnetic resonance imaging of the anteroposterior position and thickness of the aging, accommodating, phakic and pseudophakic ciliary muscle. *Journal of Cataract and Refractive Surgery*, **36**, 235-241.

Strenk, S. A., Strenk, L. M. & S., G. (2006). Magnetic resonance imaging of aging, accommodating, phakic, and pseudophakic ciliary muscle diameters. *Journal of Cataract and Refractive Surgery*, **32**, 1792–1798.

Strenk, S. A., Strenk, L. M., Semmlow, J. L. & De Marco, J. K. (2004). Magnetic resonance imaging study of the effects of age and accommodation on the human lens cross-sectional area. *Investigative Ophthalmology and Visual Science*, **45**, 539-545.

- Suzuki, S., Suzuki, Y., Iwase, A. & Araie, M. (2005). Corneal thickness in an ophthalmologically normal Japanese population. *Ophthalmology*, **112**, 1327–1336.
- Tamm, E. R., Croft, M. A., Jungkunz, W., Lutjen-Drecoll, E. & Kaufman, P. L. (1992). Age-related loss of ciliary muscle mobility in the rhesus monkey. Role of the choroid. *Archives of Ophthalmology*, **110**, 871-876.
- Tamm, E. R. & Lütjen-Drecoll, E. (1996). Ciliary body. *Microscopy Research and Technique*, **33**, 390-439.
- Tamm, S., Tamm, E. R. & Rohen, J. W. (1992a). Age-related changes of the human ciliary muscle: a quantitative morphometric study. *Mechanisms of Ageing and Development.*, **62**, 209-221
- Tearney, G. J., Brezinski, M. E., Southern, J. F., Bouma, B. E., Hee, M. R. & Fujimoto, J. G. (1995). Determination of the refractive index of highly scattering human tissue by optical coherence tomography. *Optics Letters*, **20**, 2258–2261.
- Thompson, J. R., Woodruff, G., Hiscox, F., Strong, N. & Minshull, C. (1991). The incidence and prevalence of amblyopia detected in childhood. *Public Health*, **105**, 455-462.
- Tian, Y. & Wildsoet, C. (2006). Diurnal fluctuations and developmental changes in ocular dimensions and optical aberrations in young chicks. *Journal of Comparative Physiology*, **192**, 4168-4178.
- Toshida, K., Okuyama, F. & Tokoro, T. (1998). Influences of the accommodative stimulus and aging on the accommodative microfluctuations. *Optometry and Vision Science*, **75**, 221-216.
- van Alphen, G. W. (1986). Choroidal stress and emmetropization. *Vision Research*, **26**, 723-734.
- Van der Heijde, G. L., Beers, A. P. & Dubbelman, M. (1996). Microfluctuations of steady-state accommodation measured with ultrasonography. *Ophthalmic and Physiological Optics*, **16**, 216-221.
- Veneruso, P. E., Ziccardi, L., Magli, G., Falsini, B. & Magli, A. (2014). Short-term effects of vision trainer rehabilitation in patients affected by anisometropic amblyopia: electrofunctional evaluation. *Documenta Ophthalmologica*, **129**, 177-189.
- Vera-Diaz, F., Gwiazda, J., Thorn, F. & Held, R. (2004). Increased accommodation following adaptation to image blur in myopes. *Journal of Vision*, **4**, 1111-1119.
- Verkircharla, P. K., Mathur, A., Mallen, E. A. H., Pope, J. M. & Atchison, D. A. (2012). Eye shape and retinal shape, and their relation to peripheral refraction. *Ophthalmic and Physiological Optics*, **32**, 184-199.

- Vitale, S., Ellwein, L., Cotch, M. F., F.L., F. I. & Sperduto, R. (2008). Prevalence of refractive error in the United States. *Archives of Ophthalmology* **79**, 222-226.
- Vogel, A., Dick, H. B. & Krummenauer, F. (2001). Reproducibility of optical biometry using partial coherence interferometry: intraobserver and interobserver reliability. *Journal of Cataract and Refractive Surgery*, **27**, 1961–1968.
- von Helmholtz, H. (1855). Uber die akkommodation des auges. *Archives of Ophthalmology*, **1**, 1-74.
- Von Noorden, G. K. (1985). Amblyopia a multidisciplinary approach. *Investigative Ophthalmology & Visual Science*, **26**, 1704–1716.
- Walker, T. & Mutti, D. O. (2002). The effect of accommodation on ocular shape. *Optometry and Vision Science*, **79**, 424-430.
- Walline, J. J., Kinney, K. A., Zadnik, K. & Mutti, D. O. (1999). Repeatability and validity of astigmatism measurements. *Journal of Refractive Surgery*, **15**, 23-31.
- Wallman, J., Turkel, J. & J., T. (1978). Extreme myopia produced by modest changes in early visual experience. *Science*, **201**, 1249–1251.
- Wallman, J., Wildsoet, C. & Xu, C. A. (1995). Moving the retina: choroidal modulation of refractive state. *Vision Research*, **35**, 37-50.
- Wang, J. J., Foran, S. & Mitchell, P. (2000). Age-specific prevalence and causes of bilateral and unilateral visual impairment in older Australians: the Blue Mountains Eye Study. *Clinical and Experimental Ophthalmology*, **28**, 268–273.
- Wang, X., Dong, J. & Wu, Q. (2015). Corneal thickness, epithelial thickness and axial length differences in normal and high myopia. *BioMedCentral Ophthalmology* **15**, 1-5.
- Watson, A. B. & Yellott, J. I. (2012). A unified formula for light-adapted pupil size. *Journal of Vision*, **12**, 12.
- Weale, R. A. (1989). Presbyopia towards the end of the 20th century. *Surveys in Ophthalmology*, **34**, 15-30.
- Weale, R. A. (1999). On potential causes of presbyopia. *Vision Research*, **39**, 1263-1272.
- Weale, R. A. (2002). On the age-related prevalence of anisometropia. *Ophthalmic Research*, **34**, 389-392.

- Webber, A. L. & Wood, J. (2005). Amblyopia: prevalence, natural history, functional effects and treatment. *Clinical and Experimental Ophthalmology*, **88**, 365-375.
- Weizhong, L., Zhikuan, Y., Wen, L., Xiang, C. & Jian, G. (2008). A longitudinal study on the relationship between myopia development and near accommodation lag in myopic children. *Ophthalmic and Physiological Optics*, **28**, 57–61.
- Werner, L., Lovisolo, C., Chew, J., Tetz, M. & Müller, M. (2008). Meridional differences in internal dimensions of the anterior segment in human eyes evaluated with 2 imaging systems. *Journal of Cataract and Refractive Surgery*, **34**, 1125-1132.
- Wickremasinghe, S., Foster, P. J., Uranchimeg, D., Lee, P. S., Devereux, J. G. & Alsbirk, P. H. (2004). Ocular biometry and refraction in Mongolian adults. *Investigative Ophthalmology & Visual Science*, **45**, 776–783.
- Wiesel, T. N. & Hubel, D. H. (1963). Single-cell responses in striate cortex of kittens deprived of vision in one eye. *Journal of Neurophysiology*, **26**, 1003–1017.
- Wildsoet, C. & Wallman, J. (1995). Choroidal and scleral mechanisms of compensation for spectacle lenses in chicks. *Vision Research*, **35**, 1175-1194.
- Williams, K. M., Bertelsen, G., Cumberland, P., Wolfram, C., Verhoeven, V. J., Anastasopoulos, E., Buitendijk, G. H. S., Cougnard-Grégoire, A., Creuzot-Garcher, C., Erke, M. E., Hogg, R., Hysi, M., P. , Khawaja, A. P., Korobelnik, J., Ried, J., Vingerling, J. R., Bron, A., Dartigues, J., Fletcher, A., Hofman, A., Kuijpers, R. W. A. M., Luben, R. N. & Hammond, C. J. (2015). Increasing prevalence of myopia in europe and the impact of education. *American Academy of Ophthalmology*, **122**, 1489-1497.
- Wilson, L. B., Quinn, G. E., Ying, G., Francis, E. L., Schmid, G., Lam, A., Orlow, J. & Stone, R. A. (2006). The relation of axial length and intraocular pressure fluctuations in human eyes. *Investigative Ophthalmology and Visual Science*, **47**, 1778-1784.
- Wilson, R. S. (1997). Does the lens diameter increase or decrease during accommodation? Human accommodation studies: a new technique using infra-red retro-illumination video photography and pixel analysis. *Transcripts of the American Optical Society*, **95**, 261-267.
- Winn, B. (2000). Accommodative microfluctuations: a mechanism for steady state control of accommodation. *Stark L ed. Accommodation and Vergence Mechanisms in the Visual System. Boston: Birkhauser Verlag*, 129-140.
- Winn, B., Charman, W. N., Pugh, J. R., Heron, G. & Eadie, A. S. (1989). Perceptual detectability of ocular accommodation microfluctuations. *Journal of the Optical Society of America*, **6**, 459-462.

- Winn, B., Pugh, J. R., Gilmartin, B. & Owens, H. (1990). The frequency characteristics of accommodative microfluctuations for central and peripheral zones of the human crystalline lens. *Vision Research*, **30**, 1093-1099.
- Winn, B., Whitaker, D., Elliott, D. B. & Phillips, N. J. (1994). Factors affecting light-adapted pupil size in normal human subjects. *Investigative Ophthalmology & Visual Science*, **35**, 1132-1137.
- Wirbelauer, C., Gochmann, R. & Pham, D. T. (2005). Imaging of the anterior eye chamber with optical coherence tomography [German]. *Klinische Monatsblätter für Augenheilkunde*, **222**, 856-862.
- Wolffsohn, J. S. (2008). Ophthalmic imaging. In: Eye Essentials (Doshi, S. and Harvey, W., Eds). Butterworth Heinemann Elsevier, Edinburgh.
- Wolffsohn, J. S. & Davies, L. N. (2007). Advances in ocular imaging. *Expert Reviews in Ophthalmology*, **2**, 755-767.
- Wolffsohn, J. S., Gilmartin, B., Thomas, R. & Mallen, E. A. (2003). Refractive error, cognitive demand and nearwork-induced transient myopia. *Current Eye Research*, **467**, 363-370.
- Woodhouse, J. M., Clegg, M., Gunter, H. L., Sanders, D. P., Saunders, K. J., Pakeman, V. H., Parker, M., Fraser, W. I. & Sastry, P. (2000). The effect of age, size of target, and cognitive factors on accommodative responses of children with down syndrome. *Investigative Ophthalmology and Visual Science*, **41**, 2479-2485.
- Woodman, E. C., Read, S. A. & Collins, M. J. (2012). Axial length and choroidal thickness changes accompanying prolonged accommodation in myopes and emmetropes. *Vision Research*, **72**, 34-41.
- Woodman, E. C., Read, S. A., Collins, M. J., Hegarty, K. J., Priddle, S. B., Smith, J. M. & Perro, J. V. (2010). Axial elongation following prolonged near work in myopes and emmetropes. *British Journal of Ophthalmology*, **95**, 652-656.
- Woodman, E. C., Read, S. A., Collins, M. J., Hegarty, K. J., Priddle, S. B., Smith, J. M. & Perro, J. V. (2011). Axial elongation following prolonged near work in myopes and emmetropes. *Br J Ophthalmol*, **95**, 652-656.
- Xiao, O., Morgan, I. G., Ellwein, L. B. & He, M. (2015). Prevalence of amblyopia in school-aged children and variations by age, gender, and ethnicity in a multi-country refractive error study. *Ophthalmology*, **122**, 1924-1931.
- Yaqoob, Z., Wu, J. & Yang, C. (2005). Spectral domain optical coherence tomography: a better OCT imaging strategy. *BioTechniques*, **39**, 6-13.

Yasuda, A. & Yamaguchi, T. (2005). Steepening of corneal curvature with contraction of the ciliary muscle. *Journal of Cataract and Refractive Surgery*, **31**, 1177-1181.

Yasuda, A., Yamaguchi, T. & Ohkoshi, K. (2003). Changes in corneal curvature in accommodation. *Journal of Cataract and Refractive Surgery*, **29**, 1297–2301.

Yun, S., Tearney, G., de Boer, J., Iftimia, N. & Bouma, B. (2003a). High-speed optical frequency-domain imaging. *Optics Express*, **11**, 2953–2963.

Yun, S. H., Boudoux, C., Tearney, G. J. & Bouma, B. E. (2003b). High-speed wavelength-swept semiconductor laser with a polygon-scanner-based wavelength filter. *Optics Express*, **28**, 1981–1983.

Yun, S. H., Boudoux, M. C., Pierce, M. C., de Boer, G. J., Tearney & B.E, B. (2004). Extended-cavity semiconductor wavelength-swept laser for biomedical imaging. . *Photonics Technology Letters* **16**, 293-295.

Zadnik, K., Mutti, D. O., Kim, H. S., Jones, L. A., Qiu, P. H. & Moeschberger, M. L. (1999). Tonic accommodation, age, and refractive error in children. *Investigative Ophthalmology and Visual Science*, **40**, 1050–1060.

Zhao, J., Chen, Z., Zhou, Z., Ding, L. & Zhou, X. (2013). Evaluation of the repeatability of the *Lenstar* and comparison with two other non-contact biometric devices in myopes. *Clinical and Experimental Optometry*, **96**, 92-99.

Zhonga, J., Taoa, A., Xua, J., Jiangb, H., Shaoa, Y., Zhangb, H., Liud, C. & Wanga, J. (2014). Whole eye axial biometry during accommodation using ultra-long scan depth optical coherence tomography. *American Journal of Ophthalmology*, **157**, 1064-1069.

APPENDICES

A1. Ethical approval

Aston University Ethics Committee
Aston University
Aston Triangle
Birmingham
B4 7ET
Telephone +44 (0)121 204 3000
Fax +44 (0)121 204 3696

Chairperson: Ms Nichola Seare

Secretary: Mr John Walter

20th December 2013

Dr Amy Sheppard

School of Life and Health Sciences

Dear Amy

Study Title: 'Ciliary muscle characteristics and accommodative function in emmetropic and myopic eyes'.

REC Reference: Ethics Application 548

Protocol Number:

Confirmation of ethical opinion

On behalf of the Committee, I am pleased to confirm a favourable ethical opinion for the above research on the basis described in the application form, protocol and supporting documentation as revised.

The project is approved until the completion date specified on the form (May 31 2015) provided it is commenced within two years of the date of this letter and you are required to notify the Committee when the project is completed.

Approved documents

The final list of documents reviewed and approved by the Committee is as follows:

Document	Version	Date
University Ethics Application Form	One	07/05/2013
Participant Information Sheet	Version 1.0. Prepared April 2013	07/05/2013
Participant Information Sheet	Version 2.0 October 2013	23/10/2013
Project 548: Resubmission, Word Document	One	23/10/2013
Risk Elimination and Control Form	One	23/10/2013
Participant Information Sheet	Version 3.0 December 2013	04/12/2013
Project 548: Wording for email announcement	Version 3.0	04/12/2013

Statement of compliance

The Committee operates in accordance with the Aston University Ethics policy and procedures:

<http://www1.aston.ac.uk/registry/for-staff/regsandpolicies/ethics-policy-and-procedures/>

Reporting Requirements

The details of the investigation will be placed on file. You should notify the Secretary of the University Ethics Committee of any adverse events which occur in connection with this study and/or which may alter its ethical consideration, and/or any difficulties experienced by the volunteer subjects.

If you intend to make any future protocol amendments these must be approved by the Ethics Committee prior to implementation. You should also seek approval for any extension of the approved completion date.

Membership

The members of the University Ethics Committee present at the meeting are listed below:
Ms Nichola Seare, AHRIC Director, Aston University Dr Robert Morse, Senior Lecturer,
MSc Clinical Sciences, Aston University Mr John Walter, Director of Governance, Aston
University

REC reference: Ethics Application 548

Please quote this number on all correspondence

With the Committee's best wishes for the success of the project

Yours sincerely

A handwritten signature in blue ink that reads "J.G. Walter". The signature is written in a cursive style with a large initial 'J' and 'W'.

Secretary of the Ethics Committee

Email: j.g.walter@aston.ac.uk

A2: Participant information and consent for project 548 (main study)

Participant Information Sheet

Research workers, school and subject area responsible

Dr Amy Sheppard (Lecturer in Optometry and optometrist), Optometry Department, School of Life & Health Sciences, Aston University. a.sheppard@aston.ac.uk

Dr Leon Davies (Reader in Optometry and optometrist), Optometry Department, School of Life & Health Sciences, Aston University. l.n.davies@aston.ac.uk

Miss Richa Saigal (PhD researcher and optometrist), Optometry Department, School of Life & Health Sciences, Aston University. saigalnr@aston.ac.uk

Project Title

Ciliary muscle characteristics and accommodative function in emmetropic and myopic eyes

Invitation

You are being invited to take part in a research study. Before you decide whether you wish to participate, please take the time to read this information sheet about why the research is being done and what it will involve. Furthermore, if you have any questions regarding the study, please do not hesitate to contact any of the researchers involved (email addresses are shown above).

What is the purpose of the study?

To analyse how differences in the size and shape of the ciliary muscle in the eyes affect an individual's ability to focus on near objects, and to gather data on normal ciliary muscle characteristics, and those in amblyopic eyes.

The information collected in this research project will provide an insight into whether changes in ciliary muscle characteristics have an impact on eye focus, and if this may be important in the development of short-sightedness (myopia). A full understanding of why myopia develops in some individuals would be very beneficial in the development of strategies (such as special contact lenses or eye drops) aiming to prevent myopia.

Why have I been chosen to take part?

You have been chosen because you are considered to be a healthy candidate, fitting into the age range we require (18-25 years). Individuals that do not have any eye diseases, or a history of eye problems or health issues that affect the eye (such as diabetes) are invited to participate in this research.

Where will the study take place?

Ophthalmic Research Group laboratories, Vision Sciences, Aston University, Birmingham, B4 7ET

What will happen to me if I take part?

By volunteering to participate in this study, you will be invited to attend the Ophthalmic Research Group's laboratories for a one-off visit lasting around 30-40 minutes. During this visit, a UK-registered optometrist will take various measures from your eyes using a range of validated equipment. All measures are non-invasive, and you will not require any drops during the course of the visit. The following measures will be undertaken:

1. How far down a letter chart you are able to read with each eye (visual acuity).
2. The power of each eye, using an automatic machine (autorefractor). You will be required to look at a target in the distance whilst this measurement is taken.
3. How close to your eye you are able to focus very small print (amplitude of accommodation).
4. The accuracy of your eye's focusing response, using an autorefractor. You will be required to concentrate on targets at different distances in front of your eyes while the machine takes the readings.
5. Imaging the ciliary muscle of the eye; this can be done safely and rapidly using a device called an anterior segment optical coherence tomographer (AS-OCT). The AS-OCT uses a special wavelength of light enabling the ciliary muscle inside the eye to be seen. You will look at targets in different directions whilst the machine takes the images.
6. Measurement of the length of the eye and lens using a biometer device (*Lenstar*). You will be required to concentrate on a small light whilst the readings are taken.

If you are short-sighted, you will be supplied with disposable soft contact lenses to wear during the appointment whilst measurements are taken. The wearing of contact lenses for a short period of time is very unlikely to cause any problems, but we will check the health of your eyes using a microscope before you leave the appointment.

Why have I been chosen to take part?

You have been chosen because you are considered to be a healthy candidate, fitting into the narrow age range the study requires. Individuals that do not have any eye diseases, previous major eye surgery or health issues that affect the eye are invited to participate in this research.

Are there any potential risks in taking part in the study?

There are no known risks involved with the instruments or techniques listed above. Similarly, there are minimal risks if you are to wear soft contact lenses for the duration of the study. All measurements and procedures will be taken in accordance with the manufacturers' guidelines by a GOC (General Optical Council- regulatory body in UK) registered Optometrist. All techniques have been used successfully in previously-published research from our laboratory.

Do I have to take part?

No, you do not have to participate if you do not wish to do so. You are free to withdraw at any time from the project. Your decision to participate (or not) will not influence your ability to participate in any future research, nor will it affect your studies at the university in any way.

Expenses and payments

You will be paid £10 as a thank you for participation in the study

Will my taking part in this study be kept confidential?

Privacy and confidentiality will be carefully protected. Your name will be turned into a code, the details of which will be kept on a separate database which will only be accessed by the investigators. Analysis of data by others, including the internal project examiner, will only be undertaken in the coded format to prevent a breach of confidentiality. We cannot, however, guarantee privacy or confidentiality.

What will happen to the results of the research study?

The researchers aim to publish the results of this project. However, there will be no reference to any individual's performance in any publication. If you wish to receive copies of any publications arising from the data, please let the investigator know, and these can be emailed to you.

Who is organising and funding the research?

The project is being organised and conducted by researchers from the Ophthalmic Research Group at Aston University. The study has been funded by a UK College of Optometrists postgraduate scholarship, for Richa Saigal.

Who has reviewed the study?

The research has been submitted and reviewed by Aston University Research Ethics Committee.

Who do I contact if something goes wrong or I need further information?

Please contact the principal investigator, Dr Amy Sheppard (a.sheppard@aston.ac.uk or 0121 204 4208)

Who do I contact if I wish to make a complaint about the way in which the research is conducted?

If you have any concerns about the way in which the study has been conducted, then you should contact Secretary of the University Research Ethics Committee by email at: j.g.walter@aston.ac.uk or telephone +44(0)121 204 4665.

Patient Identification Number for this study:

CONSENT FORM

Title of Project: Ciliary muscle characteristics and accommodative function in emmetropic and myopic eyes

Name of Researcher:

Please initial box

1. I confirm that I have read and understand the information sheet dated October 2013 (version 2.0) for the above study. I have had the opportunity to consider the information, ask questions, and have had these answered satisfactorily.

2. I understand that my participation is voluntary and that I am free to withdraw at any time, without giving any reason.

3. I understand that relevant sections of any of my data collected during the study may be looked at by responsible individuals from Aston University, where it is relevant to my taking part in this research. I give my permission for these individuals to have access to my data.

4. I agree to take part in the above study.

Name of Participant

Date

Signature

Researcher

Date

Signature

When completed, 1 for participant; 1 for researcher site file

Patient Identification Number for this study:

CONSENT FORM

Title of Project: Ciliary muscle characteristics and accommodative function in emmetropic and myopic eyes

Name of Researcher:

Please initial box

1. I confirm that I have read and understand the information sheet dated October 2013 (version 2.0) for the above study. I have had the opportunity to consider the information, ask questions, and have had these answered satisfactorily.

2. I understand that my participation is voluntary and that I am free to withdraw at any time, without giving any reason, without my medical care or legal rights being affected.

3. I understand that relevant sections of any of my data collected during the study may be looked at by responsible individuals from Aston University, or regulatory authorities, where it is relevant to my taking part in this research. I give my permission for these individuals to have access to my data.

5. I agree to take part in the above study.

Name of Participant Date Signature

Researcher Date Signature

When completed, 1 for participant; 1 for researcher site file

A3: Participant information and consent for project 548 (diurnal study)

Participant Information Sheet

Research workers, school and subject area responsible

Dr Amy Sheppard (Lecturer in Optometry and optometrist), Optometry Department, School of Life & Health Sciences, Aston University. a.sheppard@aston.ac.uk

Dr Leon Davies (Reader in Optometry and optometrist), Optometry Department, School of Life & Health Sciences, Aston University. l.n.davies@aston.ac.uk

Miss Richa Saigal (PhD researcher and optometrist), Optometry Department, School of Life & Health Sciences, Aston University. saigalnr@aston.ac.uk

Project Title

Ciliary muscle characteristics and accommodative function in emmetropic and myopic eyes- diurnal variation in accommodative function

Invitation

You are being invited to take part in a research study. Before you decide whether you wish to participate, please take the time to read this information sheet about why the research is being done and what it will involve. Furthermore, if you have any questions regarding the study, please do not hesitate to contact any of the researchers involved (email addresses are shown above).

What is the purpose of the study?

To analyse whether there are differences in the accuracy of accommodation (focussing) and magnitude of axial length (total eye length) change with accommodation, throughout the day.

Whilst various ocular diurnal (throughout the day) changes are known, very little is known about changes in accommodative function throughout the day, despite the widely researched link between accommodation and myopia (short sightedness). In comparing the differences in axial length change with accommodation between emmetropes (normal sighted individuals) and myopes, it must be determined if, and to what extent any diurnal variation occurs in myopic and emmetropic groups.

Why have I been chosen to take part?

You have been chosen because you are considered to be a healthy candidate, fitting into the age range we require (19-26 years). Individuals that do not have any eye diseases, or a history of eye problems or health issues that affect the eye (such as diabetes) are invited to participate in this research.

Where will the study take place?

Ophthalmic Research Group laboratories, Vision Sciences, Aston University, Birmingham, B4 7ET

What will happen to me if I take part?

By volunteering to participate in this study, you will be invited to attend the Ophthalmic Research Group's laboratories for four visits during the day lasting around 10 minutes each and between the following times: 0800- 0900, 1200 – 1300, 1600- 1700, 2000- 2100. During this visit, a UK-registered optometrist will take various measures from your eyes using a range of validated equipment. All measures are non-invasive, and you will not require any drops during the course of the visit. The following measures will be undertaken:

1. How far down a letter chart you are able to read with each eye (visual acuity).
2. The power of each eye, using an automatic machine (autorefractor). You will be required to look at a target in the distance whilst this measurement is taken.
3. How close to your eye you are able to focus very small print (amplitude of accommodation).
4. The accuracy of your eye's focusing response, using an autorefractor. You will be required to concentrate on targets at different distances in front of your eyes while the machine takes the readings.
5. Measurement of the length of the eye and lens using a biometer device (*Lenstar*). You will be required to concentrate on a small light whilst the readings are taken, and then a letter target.

If you are short-sighted, you will be supplied with disposable soft contact lenses to wear during the appointment whilst measurements are taken. The wearing of contact lenses for a short period of time is very unlikely to cause any problems, but we will check the health of your eyes using a microscope before you leave the appointment.

Why have I been chosen to take part?

You have been chosen because you are considered to be a healthy candidate, fitting into the narrow age range the study requires. Individuals that do not have any eye diseases, previous major eye surgery or health issues that affect the eye are invited to participate in this research.

Are there any potential risks in taking part in the study?

There are no known risks involved with the instruments or techniques listed above. Similarly, there are minimal risks if you are to wear soft contact lenses for the duration of the study. All measurements and procedures will be taken in accordance with the manufacturers' guidelines by a GOC (General Optical Council- regulatory body in UK) registered Optometrist. All techniques have been used successfully in previously-published research from our laboratory.

Do I have to take part?

No, you do not have to participate if you do not wish to do so. You are free to withdraw at any time from the project. Your decision to participate (or not) will not influence your ability to participate in any future research, nor will it affect your studies at the university in any way.

Expenses and payments

You will be paid a £20 amazon voucher as a thank you for participation in the study.

Will my taking part in this study be kept confidential?

Privacy and confidentiality will be carefully protected. Your name will be turned into a code, the details of which will be kept on a separate database which will only be accessed by the investigators. Analysis of data by others, including the internal project examiner, will only be undertaken in the coded format to prevent a breach of confidentiality. We cannot, however, guarantee privacy or confidentiality.

What will happen to the results of the research study?

The researchers aim to publish the results of this project. However, there will be no reference to any individual's performance in any publication. If you wish to receive copies of any publications arising from the data, please let the investigator know, and these can be emailed to you.

Who is organising and funding the research?

The project is being organised and conducted by researchers from the Ophthalmic Research Group at Aston University. The study has been funded by a UK College of Optometrists postgraduate scholarship, for Richa Saigal.

Who has reviewed the study?

The research has been submitted and reviewed by Aston University Research Ethics Committee.

Who do I contact if something goes wrong or I need further information?

Please contact the principal investigator, Dr Amy Sheppard (a.sheppard@aston.ac.uk or 0121 204 4208)

Who do I contact if I wish to make a complaint about the way in which the research is conducted?

If you have any concerns about the way in which the study has been conducted, then you should contact Secretary of the University Research Ethics Committee by email at: j.g.walter@aston.ac.uk or telephone +44(0)121 204 4665.

Patient Identification Number for this study:

CONSENT FORM

Title of Project: Ciliary muscle characteristics and accommodative function in emmetropic and myopic eyes- diurnal variation in accommodative function

Name of Researcher:

Please initial box

1. I confirm that I have read and understand the information sheet dated January 2015 (version 1.0) for the above study. I have had the opportunity to consider the information, ask questions, and have had these answered satisfactorily.

2. I understand that my participation is voluntary and that I am free to withdraw at any time, without giving any reason.

3. I understand that relevant sections of any of my data collected during the study may be looked at by responsible individuals from Aston University, where it is relevant to my taking part in this research. I give my permission for these individuals to have access to my data.

4. I agree to take part in the above study.

Name of Participant

Date

Signature

Researcher

Date

Signature

When completed, 1 for participant; 1 for researcher site file

Patient Identification Number for this study:

CONSENT FORM

Title of Project: Ciliary muscle characteristics and accommodative function in emmetropic and myopic eyes

Name of Researcher:

Please initial box

1. I confirm that I have read and understand the information sheet dated January 2015 (version 1.0) for the above study. I have had the opportunity to consider the information, ask questions, and have had these answered satisfactorily.

2. I understand that my participation is voluntary and that I am free to withdraw at any time, without giving any reason, without my medical care or legal rights being affected.

3. I understand that relevant sections of any of my data collected during the study may be looked at by responsible individuals from Aston University, or regulatory authorities, where it is relevant to my taking part in this research. I give my permission for these individuals to have access to my data.

5. I agree to take part in the above study.

Name of Participant Date Signature

Researcher Date Signature

When completed, 1 for participant; 1 for researcher site file

A4: Participant information and consent for project 543 (amblyopia study)

Participant Information Sheet

Research workers, school and subject area responsible

Dr Amy Sheppard (Lecturer in Optometry and optometrist), Optometry Department, School of Life & Health Sciences, Aston University. a.sheppard@aston.ac.uk

Dr Leon Davies (Reader in Optometry and optometrist), Optometry Department, School of Life & Health Sciences, Aston University. l.n.davies@aston.ac.uk

Miss Richa Saigal (PhD researcher and optometrist), Optometry Department, School of Life & Health Sciences, Aston University. saigalnr@aston.ac.uk

Project Title

Ciliary muscle characteristics in refractive error and amblyopia

Invitation

You are being invited to take part in a research study. Before you decide whether you wish to participate, please take the time to read this information sheet about why the research is being done and what it will involve. Furthermore, if you have any questions regarding the study, please do not hesitate to contact any of the researchers involved (email addresses are shown above).

What is the purpose of the study?

To analyse how differences in the size and shape of the ciliary muscle in the eyes affect an individual's ability to focus on near objects, and to gather data on normal ciliary muscle characteristics, those in amblyopic eyes (lazy eyes) and anisometropic eyes (moderate-large difference in prescription between the eyes). Since amblyopic eyes are known to have reduced vision, it could be predicted that the ciliary muscle in the amblyopic eye could be altered; however, there has been no previous reports of the ciliary muscle in amblyopia, so how the ciliary muscle develops in eyes of amblyopes (those with a lazy eye) is not currently known.

The information collected in this research project will provide an insight into whether changes in ciliary muscle characteristics have an impact on eye focus, and whether the ciliary muscle varies in eyes of amblyopes and anisometropia.

Why have I been chosen to take part?

You have been chosen because you are considered to be a healthy candidate, fitting into the age range we require (18-25 years). Individuals that do not have any eye diseases, or a history of eye problems or health issues that affect the eye (such as diabetes) are invited to participate in this research, along with individuals with a moderate-large difference in prescription between the eyes (anisometropia), or a lazy eye (amblyopia).

Where will the study take place?

Ophthalmic Research Group laboratories, Vision Sciences, Aston University, Birmingham, B4 7ET

What will happen to me if I take part?

By volunteering to participate in this study, you will be invited to attend the Ophthalmic Research Group's laboratories for a one-off visit lasting around 10-12 minutes. During this visit, a UK-registered optometrist will take various measures from your eyes using a range of validated equipment. All measures are non-invasive, and you will not require any drops during the course of the visit. The following measures will be undertaken:

1. How far down a letter chart you are able to read with each eye (visual acuity).
2. The power of each eye, using an automatic machine (autorefractor). You will be required to look at a target in the distance whilst this measurement is taken.
3. Imaging the ciliary muscle of the eye; this can be done safely and rapidly using a device called an anterior segment optical coherence tomographer (AS-OCT). The AS-OCT uses a special wavelength of light enabling the ciliary muscle inside the eye to be seen. You will look at targets in different directions whilst the machine takes the images.
4. Measurement of the length of the eye and lens using a biometer device (*Lenstar*). You will be required to concentrate on a small light whilst the readings are taken.

If you have a prescription, you will be supplied with disposable soft contact lenses to wear during the appointment whilst measurements are taken. The wearing of contact lenses for a short period of time is very unlikely to cause any problems, but we will check the health of your eyes using a microscope before you leave the appointment.

Why have I been chosen to take part?

You have been chosen because you are considered to be a healthy candidate, fitting into the narrow age range the study requires. Individuals that do not have any eye diseases, previous major eye surgery or health issues that affect the eye are invited to participate in this research.

Are there any potential risks in taking part in the study?

There are no known risks involved with the instruments or techniques listed above. Similarly, there are minimal risks if you are to wear soft contact lenses for the duration of the study. All measurements and procedures will be taken in accordance with the manufacturers' guidelines by a GOC (General Optical Council- regulatory body in UK) registered Optometrist. All techniques have been used successfully in previously-published research from our laboratory.

Do I have to take part?

No, you do not have to participate if you do not wish to do so. You are free to withdraw at any time from the project. Your decision to participate (or not) will not influence your ability to participate in any future research, nor will it affect your studies at the university in any way.

Expenses and payments

You will be paid £10 as a thank you for participation in the study

Will my taking part in this study be kept confidential?

Privacy and confidentiality will be carefully protected. Your name will be turned into a code, the details of which will be kept on a separate database which will only be accessed by the investigators. Analysis of data by others, including the internal project examiner, will only be undertaken in the coded format to prevent a breach of confidentiality. We cannot, however, guarantee privacy or confidentiality.

What will happen to the results of the research study?

The researchers aim to publish the results of this project. However, there will be no reference to any individual's performance in any publication. If you wish to receive copies of any publications arising from the data, please let the investigator know, and these can be emailed to you.

Who is organising and funding the research?

The project is being organised and conducted by researchers from the Ophthalmic Research Group at Aston University. The study has been funded by a UK College of Optometrists postgraduate scholarship, for Richa Saigal.

Who has reviewed the study?

The research has been submitted and reviewed by Aston University Research Ethics Committee.

Who do I contact if something goes wrong or I need further information?

Please contact the principal investigator, Dr Amy Sheppard (a.sheppard@aston.ac.uk or 0121 204 4208)

Who do I contact if I wish to make a complaint about the way in which the research is conducted?

If you have any concerns about the way in which the study has been conducted, then you should contact Secretary of the University Research Ethics Committee by email at: j.g.walter@aston.ac.uk or telephone +44(0)121 204 4665.

Patient Identification Number for this study:

CONSENT FORM

Title of Project: Ciliary muscle characteristics in refractive error and amblyopia

Name of Researcher:

Please initial box

1. I confirm that I have read and understand the information sheet dated March 2016 (version 3.0) for the above study. I have had the opportunity to consider the information, ask questions, and have had these answered satisfactorily.

2. I understand that my participation is voluntary and that I am free to withdraw at any time, without giving any reason.

3. I understand that relevant sections of any of my data collected during the study may be looked at by responsible individuals from Aston University, where it is relevant to my taking part in this research. I give my permission for these individuals to have access to my data.

4. I agree to take part in the above study.

Name of Participant Date Signature

Researcher Date Signature

When completed, 1 for participant; 1 for researcher site file

Patient Identification Number for this study:

CONSENT FORM

Title of Project: Ciliary muscle characteristics in refractive error and amblyopia

Name of Researcher:

Please initial box

1. I confirm that I have read and understand the information sheet dated March 2016 (version 3.0) for the above study. I have had the opportunity to consider the information, ask questions, and have had these answered satisfactorily.

2. I understand that my participation is voluntary and that I am free to withdraw at any time, without giving any reason.

3. I understand that relevant sections of any of my data collected during the study may be looked at by responsible individuals from Aston University, where it is relevant to my taking part in this research. I give my permission for these individuals to have access to my data.

4. I agree to take part in the above study.

Name of Participant Date Signature

Researcher Date Signature

When completed, 1 for participant; 1 for researcher site file

